الجمهورية الجزائرية الديمقراطية الشعبية
République algérienne démocratique et populaire
وزارة التعليم العالي والبحث العلمي
Ministère de l'enseignement supérieur et de la recherche scientifique
جامعة العربي التبسي – تبسة
Université Larbi Tebessi – Tébessa
معهد المناجم
Institut des mines
قسم المناجم والجيوتكنولوجيا
Département des mines et de la géotechnologie

MEMOIRE

Présenté en vue de l'obtention d'un diplôme de Master académique

Filière : Génie minier

Option : Géotechnique

On the use of DOE methodology to settlement analysis

Présenté et soutenu par

CHEGROUCHE Ayemen

Devant le jury:

		Grade	Etablissement
Président :	AMRANI Donia	MAA	Université Larbi Tebessi - Tébessa
Encadreur :	BERRAH Yacine	MCB	Université Larbi Tebessi - Tébessa
Examinateurs :	DJELLALI Adel	MCA	Université Larbi Tebessi - Tébessa

Promotion 2020-2021

N°: G.M/……/2021

الجمهورية الجزائرية الديمقراطية الشعبية

République algérienne démocratique et populaire

وزارة التعليم العالي والبحث العلمي

Ministère de l'enseignement supérieur et de la recherche scientifique

جامعة العربي التبسي – تبسة

Université Larbi Tebessi – Tébessa

معهد المناجم

Institut des mines

قسم المناجم والجيوتكنولوجيا

Département des mines et de la géotechnologie

MEMOIRE

Présenté en vue de l'obtention d'un diplôme de Master académique

Filière : Génie minier

Option : Géotechnique

On the use of DOE methodology to settlement analysis

Présenté et soutenu par

CHEGROUCHE Ayemen

Devant le jury :

		Grade	Etablissement
Président :	AMRANI Donia	MAA	Université Larbi Tebessi - Tébessa
Encadreur :	BERRAH Yacine	MCB	Université Larbi Tebessi - Tébessa
Examinateurs :	DJELLALI Adel	MCA	Université Larbi Tebessi - Tébessa

Promotion 2020-2021

الجمهورية الجزائرية الديمقراطية الشعبية
République Algérienne Démocratique et Populaire

Ministère de l'Enseignement Supérieur
et de la Recherche Scientifique
Université Larbi Tebessi – Tébessa
Institut des Mines
Département des Mines et de Géotechnologie

وزارة التعليم العالي و البحث العلمي
جامعة العربي التبسي – تبسة
معهد المناجم
قسم المناجم و الجيوتكنولوجيا

Année universitaire : 2020-2021 Tébessa le : 07/06/2021

Lettre de soutenabilité

Noms et prénoms des étudiants :

1 CHEGROUCHE Ayemen

Niveau : **2ème année Master** Option : Géotechnique

Thème:

On the use of DOE methodology to settlement analysis

Nom et prénom de l'encadreur : BERRAH Yacine

Chapitres réalisés	Signature de l'encadreur
CHAPTER I: Bibliographical research on the compressibility and soils settlement.	Yacine Berrah
Chapter II: Foundations and parameters That affect the Soils compressibility.	
Chapter III: Methods of analysis and calculation of soil settlements.	
Chapter IV: Compressibility index investigations using statistical tools and Design of experiments (DOE)	

الجمهورية الجزائرية الديمقراطية الشعبية
وزارة التعليم العالي والبحث العلمي

مؤسسة التعليم العالي : جامعة العربي التبسي – تبسة

تصريح شرفي
خاص بالالتزام بقواعد النزاهة العلمية لانجاز بحث

أنا الممضي أدناه،

السيد (ة) :شقروش أيمن الصفة : طالب

الحامل لبطاقة التعريف الوطنية رقم : 100725881 و الصادرة بتاريخ: 27/ 04/ 2016
المسجل بمعهد المناجم قسم: المناجم والجيوتكنولوجيا
و المكلف بانجاز أعمال بحث (مذكرة التخرج، **مذكرة ماستر**، مذكرة ماجستير، أطروحة دكتوراه)، عنوانها :

On the use of DOE methodology to settlement analysis

أصرح بشرفي أني ألتزم بمراعاة المعايير العلمية و المنهجية و معايير الأخلاقيات المهنية و النزاهة الأكاديمية المطلوبة في انجاز البحث المذكور أعلاه.

التاريخ:2021/06/06

إمضاء المعني (ة)

الجمهورية الجزائرية الديمقراطية الشعبية

وزارة التعليم العالي و البحث العلمي

جامعة العربي التبسي- تبسة

مقرر رقم: 116 مؤرخ في: 2021/05/20

يتضمن الترخيص بمناقشة مذكرة الماستر

إنّ مدير جامعة العربي التبسي بتبسة،

- بموجب القرار الوزاري رقم 318 و المؤرخ في 05 ماي 2021 المتضمن تعيين السيد "قواسمية عبد الكريم" مديرا لجامعة العربي التبسي - تبسة،

-و بمقتضى المرسوم التنفيذي رقم : 12- 363 مؤرخ في 8 أكتوبر 2012، يعدل و يتمم المرسوم التنفيذي رقم 09 - 08 المؤرخ في : 04 جانفي 2009 و المتضمن إنشاء جامعة العربي التبّسي بتبسة،

-وبمقتضى المرسوم التنفيذي رقم 08-265 المؤرّخ في 17 شعبان عام 1429 الموافق 19 غشت سنة 2008 الذي يحدّد نظام الدراسات للحصول على شهادة الليسانس وشهادة الماستر وشهادة الدّكتوراه، لاسيما المادة 9 منه،

-وبموجب القرار رقم 362 المؤرّخ في 09 جوان 2014 الذي يحدّد كيفيات إعداد ومناقشة مذكّرة الماستر، لاسيما المادة 7 منه،

-وبموجب القرار رقم357 المؤرّخ في 15 جوان 2020، المعدل لملحق القرار رقم 1080 المؤرخ في 13 أكتوبر 2015 والمتضمّن تأهيل ماستر الفروع ذات التسجيل الوطني بعنوان السنة الجامعية 2015-2016 بجامعة تبسة، اختصاص **جيوتقني**.

-وبموجب المقرّر رقم066 المؤرّخ في 2021/05/19 والمتضمّن تعيين لجنة مناقشة مذكّرة الماستر،

-وبعد الاطّلاع على تقرير لجنة مناقشة مذكرة الماستر المؤرّخ في .....

يقرّر ما يأتي:

المادة الأولى: يُرخّصُ للطالب(ة) **أيمن شقروش**، المولود (ة) بتاريخ 1996/07/18 بـ مرسط، بمناقشة مذكّرة الماستر والموسُومة بـ

On the use of DOE methodology to settlement analysis

المادة 2: يكلّف رئيس قسم المناجم والجيوتكنولوجيا بتنفيذ هذا المقرّر الّذي يسلّم نسخة عنه إلى الطّالب المعني بالمناقشة وأعضاء لجنة المناقشة فور توقيعه، وبضمان نشره عبر فضاءات المؤسّسة المادية والرقمية.

المادة 3: تُحفظ نسخة عن هذا المقرّر ضمن الملفّ البيداغوجي للطّالب المعني وينشر في النّشرة الرّسمية لجامعة العربي التبسي.

حُرّر بـ تبسة، في: 2021/05/20

مدير معهد المناجم بالنيابة

المدير عوفي زوبير

عن المدير، وتفويض منه

مدير معهد المناجم

الجمهورية الجزائرية الديمقراطية الشعبية

وزارة التعليم العالي والبحث العلمي

جامعة العربي التبسي- تبسة

مقرر رقم066 مؤرخ في : 2021/05/19

يتضمن تعيين لجنة مناقشة مذكرة الماستر

إنّ مدير جامعة العربي التبسي بتبسة،

- بموجب القرار الوزاري رثم 318 المؤرخ في 05 ماي 2021 المتضمن تعيين السيد "قواسمية عبد الكريم" مديرا لجامعة العربي التبسي - تبسة،

-و بمقتضى المرسوم التنفيذي رقم : 12- 363 مؤرخ في 8 أكتوبر 2012، يعدل و يتمم المرسوم التنفيذي رقم 09 - 08 المؤرخ في : 04 جانفي 2009 و المتضمن إنشاء جامعة العربي التبّسي بتبسة،

-وبمقتضى المرسوم التنفيذي رقم 08-265 المؤرّخ في 17 شعبان عام 1429 الموافق 19 غشت سنة 2008 الذي يحدّد نظام الدراسات للحصول على شهادة الليسانس وشهادة الماستر وشهادة الدّكتوراه، لاسيما المادة 9 منه،

-وبموجب القرار رقم 362 المؤرّخ في 09 جوان 2014 الذي يحدّد كيفيات إعداد ومناقشة مذكّرة الماستر، لاسيما المادتان 10 و11 منه،

-وبموجب القرار رقم357 المؤرّخ في 15 جوان 2020، المعدل لملحق القرار رقم 1080 المؤرخ في 13 أكتوبر 2015 والمتضمّن تأهيل ماستر الفروع ذات التسجيل الوطني بعنوان السنة الجامعية 2015-2016 بجامعة تبسة، اختصاص **جيوتقني**.

-وبعد الاطّلاع على محضر المجلس العلمي لمعهد المناجم المؤرّخ في 2021/05/09،

يقرّر ما يأتي:

المادة الأولى: تُعيَّنُ بموجب هذا المقرّر لجنة مناقشة مذكّرة الماستر المحضَّرة من طرف الطّالب (ة):

أيمن شقروش، المولود (ة) بتاريخ 1996/07/18 بـ مرسط،

والموسُومة بـ

On the use of DOE methodology to settlement analysis

والمسجّل بمعهد المناجم

المادة 2: تتشكّل اللجنة المشار إليها في المادة الأولى من الأعضاء الآتي ذكرهم:

رقم	الاسم واللّقب	الرتبة	مؤسّسة الانتماء	الصّفة
1	ياسين براح	أستاذ محاضر-ب	جامعة العربي التبسي - تبسة	مؤطرا
2	دنيا عمراني	أستاذة مساعدة -أ	جامعة العربي التبسي - تبسة	رئيسة
3	عادل جلالي	أستاذ محاضر-أ	جامعة العربي التبسي - تبسة	مناقشا

المادة 3: يكلّف رئيس قسم المناجم والجيوتكنولوجيا بتنفيذ هذا المقرّر الّذي يُسلّم نسخةً عنه إلى كلّ من الطّالب المعني والمشرف على المذكّرة وأعضاء لجنة المناقشة فور توقيعه.

المادة 4: تحفظ نسخة عن هذا المقرّر في الملفّ البيداغوجي للطالب المعني، وينشر في النّشرة الرّسمية لجامعة العربي التبسي.

حُرّر بـ تبسة، في: 2021/05/19

مدير عن المدير و تفويض منه

مدير معهد المناجم

بهلولي زوبير

Dedication

All the words cannot express the gratitude, the love, the respect

recognition, it is all simply that:

I dedicate this thesis of end of study master 2

To:

To my tender Mother Tozeur: You represent for me the source of

tenderness and the example Of devotion which did not stop encourage me.

You have Done more than a mother can do for her children to follow

The right path in their life and studies.

To My Dearest Father Maammar: No dedication can

express The love, eregard, dedication and respect that I

always have for you.

For you. Nothing in the world is worth the efforts you have

Made day and night for my

My education and my well being

This work and the fruit of your sacrifices that

You have sacrifices you made for my

education and training throughout these years.

To my dear brothers: Takieddine,montassar

To my sisters: Hadjer, sondouss.

To my dear parents-in-law.

To my dear beautiful sisters, my dear brothers-in-law

To my dearest friends: Ala, Ishak, Islem, Issam, Ziad,

Ihab , Anouar ,Haroun, khadidja ,Amina

To Dr. Berrah Yacine: who never stopped encouraging me

And advising me.

This humble dedication cannot express my great

Respect and my deep regard.

To all the members of my promotion.

To all my teachers since my first years of study and the speciality

To all those who are dear to me and whom

I have omitted to mention

Acknowledgement

First of all, I would like to thank God the almighty and merciful, who has given me
the strength and patience to accomplish this modest work.
Then, I would like to express my deep gratitude to my supervisor Dr.Berrah Yacine
Who did me the honor of framing me, for the orientation, the confidence, the patience
which constituted a considerable contribution without which this work would not have been able to be led to the good port.
I would also like to thank the members of the jury for their interest in my work
I would also like to thank the members of the jury for the interest they showed in my work by agreeing to examine my work and to enrich it with their proposals.
Of course, I would never have reached this point without the help and support of my family. Thank you for
for always believing in me, for supporting me in this way.
These thanks would not be complete if I did not mention all the people of the public works laboratory LTPE of Tebessa for their material and moral support.
My gratitude goes to all my family who supported me during this period.
Finally,

I associate to this tribute, all my colleagues and all my friends. May each of them find here the expression of my gratitude

Finally, I would like to thank all those who have helped in any way in the realization of this work

Abstract

Compressibility of fine-grained deposits such as clays and marls in Tebessa valley (N-E of Algeria) is depend on several geotechnical parameters and the main are compression Cc and recompression or swelling Cs indices. in order to avoid wasting time and the number of experiments to obtain the mentioned parameters from oedometer tests, the aim of the present work is to investigate geotechnical parameters that affect the soil compressibility using different approaches. Data set has been collected from a wide range in the studied region and the amount of settlements calculated from the obtained laboratory parameters is validated by numerical modeling with Plaxis and Sigma/w programs. in order to estimate the compression index using indirect methods with an empirical equation for the studied soil, a matrix of the data set has been prepared and analyzed using different statistical approaches. The principal component analysis PCA method used to identify a smaller number of uncorrelated variables, where the first two principal components absorb about 75.04% of the variability, Design of experiments DOE is the proposed approach in this work to obtain the best fit model with regression coefficient of 0.92, the optimal values affecting the soil compressibility has been determined. The process discussed in this research allows to find the best models that describe the studied soil compressibility compared to any other published models as well leads to coasts and time saving in predicting Cc output parameter.

Keywords: compressibility index, geotechnical parameters, principal component analysis PCA, Design of experiments (DOE).

Résumé :

La compressibilité des dépôts à grains fins tels que les argiles et les marnes dans la vallée de la Tébessa (N-E de l'Algérie) dépend de plusieurs paramètres géotechniques et les principaux sont les indices de compression Cc et de recompression ou de gonflement Cs. Afin d'éviter la perte du temps et le nombre d'expériences pour obtenir les paramètres mentionnés à partir d'essais œdométriques, le but du présent travail est d'étudier les paramètres géotechniques qui affectent la compressibilité du sol en utilisant différentes approches. L'ensemble de données a été collecté dans la région étudiée et les valeurs de tassements calculée à partir des paramètres de laboratoire obtenus sont validée par modélisation numérique avec les programmes Plaxis et Sigma/w. Afin d'estimer l'indice de compression en utilisant des méthodes indirectes avec des équations empiriques pour le sol étudié, une matrice de l'ensemble de données a été préparée et analysée en utilisant des approches statistiques différentes. La méthode PCA d'analyse en composantes principales utilisée pour identifier les plus petits nombres de variables non corrélées, où les deux premières composantes principales absorbent environ 75,04 % de la variabilité, le Plan d'expériences DOE est l'approche proposée dans ce travail pour obtenir le meilleur modèle de prédiction avec un coefficient de régression de 0,92 et les valeurs optimales affectant la compressibilité du sol ont été déterminées. Le processus discuté dans cette recherche permet de trouver le meilleur modèle de prédiction de la compressibilité du sol étudiée par rapport à tout autre modèle publié et conduit davantage à un gain de temps dans la prédiction du paramètre de Cc.

Mots clés : Indice de compressibilité Cc, paramètres géotechniques, analyse en composante principale, Plan d’expérience (DOE).

الملخص

تعتمد قابلية ضغط التربة الدقيقة الحبيبات مثل الطين والصلصال في منطقة تبسة شمال شرق الجزائر على العديد من المعلمات الجيوتقنية الرئيسية هي معامل الضغط Cc ومعامل الانتفاخ أو التورم Cs. من أجل تجنب إضاعة الوقت وعدد التجارب للحصول على المعلمات المذكورة من الاختبارات الأودومترية ، فإن الهدف من العمل الحالي هو التحقق من المعلمات الجيوتقنية التي تؤثر على ضغط التربة باستخدام نهج مختلفة. لذلك جمعت مجموعة البيانات من طائفة واسعة في المنطقة المدروسة، كما أن قيم ضغط التربة المتحصل عليها من التجارب المخبرية تم التحقق من صحتها عن طريق النمذجة العددية مع برامج Plaxis و Sigma/w. من أجل تقدير مؤشر الضغط باستخدام أساليب غير مباشرة مع معادلة تجريبية للتربة المدروسة ، تم إعداد مصفوفة لمجموعة البيانات وتحليلها باستخدام نهج إحصائية مختلفة. طريقة تحليل المكون الرئيسي PCA المستخدمة لتحديد عدد أقل من المتغيرات غير المترابطة ، حيث يمتص المكونان الرئيسيان الأولان حوالي 75.04٪ من التباين ، تصميم التجارب DOE هو النهج المقترح في هذا العمل للحصول على أفضل نموذج مناسب مع معامل الترابط 0.91 ، تم تحديد القيم المثلى التي تؤثر على ضغط التربة. العملية التي نوقشت في هذا البحث تسمح بالعثور على أفضل النماذج التي تصف ضغط التربة بالمقارنة مع أي نماذج أخرى نشرت كما يؤدي إلى توفير الوقت في التنبؤ بهذه المعلمة .

الكلمات المفتاحية : معامل ضغط التربة Cc ، المعلمات الجيوتقنية، تحليل المكون الرئيسي، طريقة التصميم التجريبي (DOE).

Summary

Chapter II: Foundations and parameters That affect the Soils compressibility.

Chapter III :Methods of analysis and calculation of soil settlements.

Notations list

S_T	The total settlement
S_i	The immediate settlement
S_c	The consolidation or primary settlement
S_s	The secondary settlement or creep
q	Average pressure applied
B:	Width or diameter of footing
E	Young's modulus of the material measured during a simple compression test or undrained triaxial
μ	Poisson's ratio (0.5 if the deformation is done at constant volume, as it is the case for saturated clays);
Iρ	Coefficient of influence depending on the loaded surface, on the point directly above which one sites and the flexibility of the sole.
A_v	Coefficient of compressibility
M_v	Coefficient of volume compressibility
OCR	Over consolidation ratio
C_V	Coefficient of consolidation
H_{dr}	Average longest drainage path during consolidation.
e_0	Initial void ration of the clay layer
p'_c:	Preconsolidation pressure
h	Thickness of the clay layer
σv_0	Overburden effective pressure at the middle of the clay layer
Cc	Compressibility index
C_s	Swelling index
Cα	Secondary compression index
Δe	Change of void ration
U	Average degree of consolidation
w_L	limit of liquidity
w_n	Natural water content
Ip	plasticity index
e	Void ratio
G_s	Specific gravitiy
γ_w	Water unit weight

γ_d	Dry unit weight
S_t	Sensitivity of the clay
n_0	Porosity
W_0	Optimum water content
DFS	Differential Free Swell
I_s	Shrinkage Index
G_s	Specific Gravity of soil
C_r	The recompression index
S_r	Degree of saturation
σ	Total Stress
γ	Unit weight
Z	Depth
σ'	Effective Stress
u	Pore Water Pressure
γ_{sat}	Saturated unit weight of the soil
μ	Poisson's ratio
I_z	Influence factor depending on the ratio LZ,
q	Bearing capacity
λ_c &λ_d	Are form coefficients
α	A rheological coefficient, depending on the nature, the structure of the soil
B	width (or diameter) of the foundation
E_c, E_d	Are Equivalent pressuremeter modules
PLM	Limit pressure Menard
Pf	Creep pressure
CPT	The cone penetration test
q_c	Being the static cone penetration resistance
C	depth correction factor
C_2	A creep factor
Δz	Thickness of level
SPT	Standard Penetration Test
DMT	Dilatometer Test
NC	Normally consolidated
OC	Over consolidated
n_0 & m_0	Characteristic coefficients of the ground

P	Perimeter of the plate
A	Area of the plate
DCT	Drive cone test
E	Young's Modulus
FEM	Finite element method
PC	Principal Component Analysis
DOE	design of experiment
RSM	response surface methodology
CCD	central composite designs
ANOVA	Analysis of variables
2FI	two factor interaction
VIF	Variance Inflation Factor

Tables List

CHAPTER I

CHAPTER III

CHAPTER IV

Figures List

CHAPTER I

CHAPTER II

CHAPTER III

CHAPTER IV

General introduction

General introduction

Compressibility of sediments and deposits such as clays and marly fine grained soils is the relationship between void ratio and effective stresses due to surcharges transmitted from foundations, if the amount of the settlement is compressibility dependency, compression and recompression index should be defined in sophisticatedly manner with oedometer tests. This later is the best way to obtain the compressibility indices, however the main well known inconvenient of the test long time need to be performed, undisturbed samples required and expensive.

In Tebessa province the problem of settlement is widespread, in some cases its amounts are excessive and can result structural damages to a building frame, or loss of functionality when structures are subjected to differential settlement movements. For this reason, it is aimed from the present master's thesis to study the compressibility in the region of Tebessa using different methods and approaches (Samples and laboratory testing's, data collections, numerical modeling and statistical study). The geotechnical analysis of data by applying the principal components analysis help to groups the parameters into family of groups, the parametric contribution of each group can be analyzed and the main factors affect the compressibility can be determining, the multiple regression analysis methods has been used to avoid the multicollinearity problems and find the best contributed parameters that effectively affect the compressibility of the studied soil.

Finally, it has been focused on our contribution geotechnical engineering in this work by the use of Design of Experiments to analyze the compressibility in Tebessa area.

The present work has been achieved in four chapters, an abstract, a general conclusion and a general conclusion as follows:

The first chapter appear the literature review and discussion of bibliographical research on settlement and compressibility of soils.

The second chapter present an overview and some details on loads and parameters that affect the soils compressibility.

In the third chapter of this memory it has been discussed in detailed the different methods of analysis and calculation of soil settlements and compressibility, also examples are listed using numerical models to analyze and compare the settlement amount in the studied region, besides some investigation such as geological hydrogeological study has been elaborated to define the case study.

The last chapter focus on the use of statistical analysis and design of experiments methods as powerful tools to study engineering properties, parametric contributions and factors affect a process or the relationships between output and input parameters.

Chapter I: Bibliographical research on the compressibility and soils settlement.

I.1 Introduction

Settlements are vertical movements of a soil under an applied load producing a vertical displacement of the substructure, it is one of the most important geotechnical criteria for the security and performance of constructions. An excessive settlement can induce structural damage to the building structure, or the loss of its functionality [1].

Foundation settlements must be estimated with great care for buildings, bridges, towers, power plants, and similar high-cost structures; For engineering structures like fill, embankments, earthen dams, levees, palisades, and supporting walls, a greater margin of error in settlements can generally be tolerated, any structure built on soil is subject to settlement, Settlement is unavoidable and, depending on the situation, some settlement is acceptable. The application of an external load to the soil surface produces on amount of volume change of the soil, this change referred to it is settlement and it is due to compressibility characteristics of the soil [2].

During settlement, the soil passes from a currently body-stressed state to a new state under the effect of the additive load applied, the change in stress due to this additive load produces a time-dependent accumulation of particles that roll, slide, crush, and under elastic deformation. in a boundary region of influence under the stressed area. Settlement is the accumulation of movement in the trend of interested (vertical direction) and is defined as (S_t) or (ΔH) [2].

Compressibility of soils is an important engineering consideration; the oedometer test is used to determine the compressibility characteristics of soils which are typically described using the compression index (C_c), and the coefficient of consolidation (C_v) [3], The compression index is useful for estimating the magnitude of settlement, and the coefficient of consolidation is a rate parameter that is used to determine the time it will take for a given amount of compression to happen. However, oedometric experiments need undisturbed samples and are quite time and money consuming. For this reason, in the past, researchers have established a correlation between compressibility characteristics and index properties [3].

Several researchers have tends to correlate compression index with various index properties in terms of single and multiple regressions (such as liquid limit, plastic limit, plasticity index, water content, void ratio etc.,), but most of these investigations were of regional clays and other mineral soils, these correlations are not generalized and have some limitations due to varying soil properties. Since the presence of soil is

varies from site to site according to geographic region and/or geological origin.

The regional empirical correlations suggested by various researchers on the compression index are resumed on the based on a critical overview. These results may be useful in rapidly finding regional empirical equations for estimating conventional compression as a function of limitations [4].

I.2 The different types of settlement

Settlements can be uniform or different from one point to another depending on the nature of the soil in place.

In unsaturated soils, settlements are almost instantaneous but in saturated soils, they can extend over a few seconds in sandy-gravelly soils, up to several decades in low permeability clays.

To check the conformity of the structures with respect to the safety and service conditions, it is necessary to carry out a settlement calculation [5].

I.2.1 Uniform settlement

Uniformly distributed settlements have little effect on the structure; however, movements can damage services and appurtenances such as water pipes and underpasses [6].

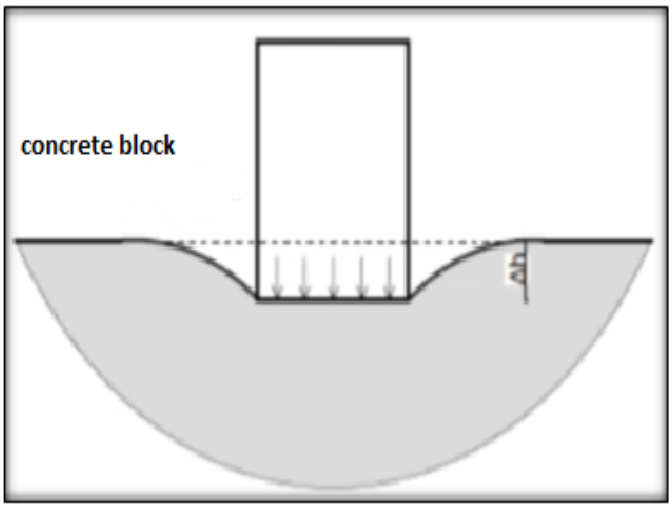

Figure I.1: Uniform settlement [6].

I.2.1 Differential settlements

The differential settlement is a sinking movement of the ground which is not uniform. It can therefore cause dislocations of the masonry such as the appearance of cracks. It is a factor of serious disorder which is most of the time irremediable.

Even when the subsoil is fairly uniform, the differences in unit loads on the foundations can cause very significant differential settlement [6].

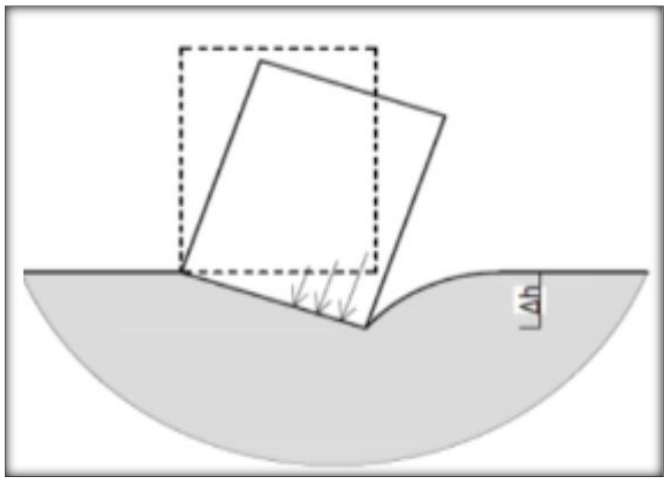

Figure I.2: Differential settlement [6].

Differential settlements can have several origins:

- **Origin linked to loading.**
  - Unequal intensity of charges from one support to another.
  - Non-uniform distribution of loads under a support.
  - Areas of the loaded surfaces different from one support to the other.
- **Origin linked to the supports.**
  - Geometry of the supports (dimensions, depth).
  - Rigidity of the supports.
- **Origin linked to the site.**
  - Variations in the geometric characteristics of the layers.
  - Variability of lithology [6].

I.3 Settlements depending on the type of soil

Settlement can be classified into two types:

I.3.1 Settlement of coarse soils

In coarse-grained soils (sand and gravel), the majority of their properties are associated with their granulometry, the extent of settling of its soils depend on the arrangement and size of particles [7].

Soils with a smaller void index are a priori less compressible than those with the index of voids higher, since their potential volume of voids to be reduced is less. As the stability of coarse-grained soils is ensured by friction and entanglement of particles,

strong vibration caused by earthquakes or by human activity (blasting, driving piles, etc.) can cause settlements [7].

Whatever the source, settlement occurs very quickly in coarse-grained soils. As these are soils with high permeability, water quickly leaves the voids under the pressure of solid particles. Settlement in these soils therefore takes place mainly during construction work [7].

I.3.2 Settlement of fine soils

Fine soils have low permeability, therefore pressure release interstitial is a very slow process, which can extend over a considerable period of time and the evacuation allows the terrain to deform. Thus, settlements in poorly permeable clays can be continuing for months or even years after the application of charges [7].

I.4 Causes of settlement

The causes of settlements are diverse:

- The desiccation of the superficial layers.
- Scouring of the foundation soil following the rupture of buried networks;
- The supply of liquids to areas in the immediate vicinity of the building acts also on the foundation, the soil becomes saturated and loses a large part of its mechanical resistance: load absorption is no longer uniform and leads to differential settlements;
- Unsuitable foundation: the inadequate relationship between the pressure exerted on the ground bedding and ground lift is a frequent cause of settlement [8].
- The presence of compressible or sub-consolidated soils is also a cause of serious disorders.

Settlements are not immediate and occur slowly under the effect of load lowering of the building. Stabilization of settlements may take many years, even decades, for compressible organic soils; Embankments: altered or brought back land loses their bearing capacity; the resulting differential settlements can cause significant damage to the medium or long term [8].

Many other causes can result in damage to buildings, such as landslides and cave-ins, changes in water level due to, for example, the construction of a crawl space; an embankment is created to support a deck; overloading of backfill at the limit of a building, case of a raised ground floor, vibrations produced by road traffic or by machines.

The heterogeneity of the level of consolidation of the different soil layers constituting the foundation of the same building [8].

I.5 Permissible settlements

Table I.1: The values of admissible settlements [9].

Type of movement	Limiting factor	Maximum settlement
Total settlement	Drainage device	15-30 cm
	Access	30-60 cm
	Probability of non-uniform settlement	
	Masonry work	2,5 - 5 cm
	Frames	5 - 10 cm
	fireplaces, silos, rafts	7,5 - 30 cm
Inclination	Stability to overturning	depends on width and height
	Inclination of chimneys and towers	0,004 l
	Rolling gear	0,01 l
	Input storage	0,01 l
	Looms	0.003l
	Turbo generator	0,0002 l
	Crane rails	0,003 l
Differential mouvement	high continuous brick walls	0,0005-0,001 l
	single-storey brick factory cracking walls	0,001-0,002 l
	cracking of plaster walls	0,001 1
	building not reinforced concrete with curtain walls	0,0025-0,004 l
		0,003 l

l: distance between two adjacent columns or two precise points which settle differently. The highest values correspond to regular settlements and the most "tolerant" structures. The lower values are valid for irregular settlements and fragile structures.

The magnitude of absolute settlements is generally not detrimental to structures themselves, but it causes inconvenience to see problems with the elements junction between buildings, especially for pipes (water, gas, sewers), overall settlements can

sometimes be significant without causing major damage. Differential and absolute settlements are considered as admissible when they can be absorbed without inconvenience by the structure [9].

I.5 Settlement components

Virtually all references agree that the total settlement of a foundation is composed of three Components:

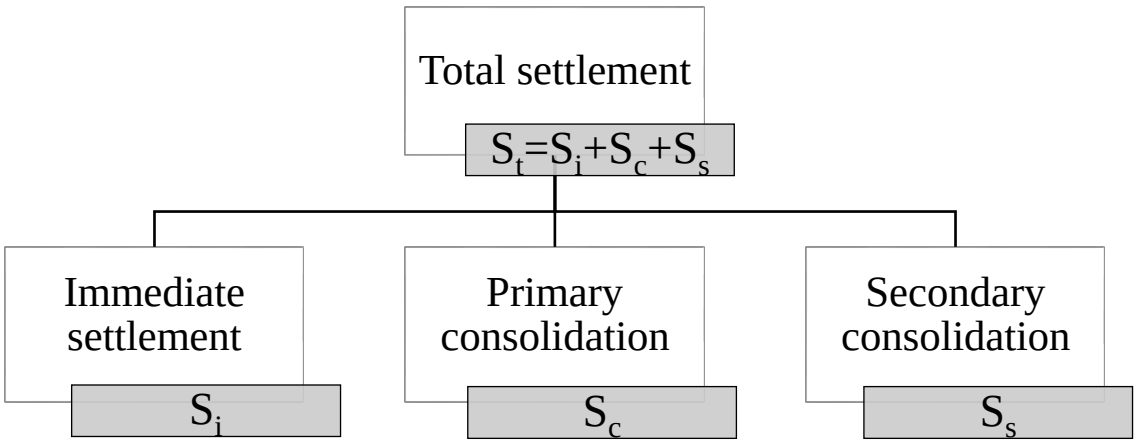

Figure I.3: Settlement components [10].

Where:

S_T : total settlement

Si : immediate settlement

Sc : consolidation or primary settlement

Ss : secondary settlement or creep

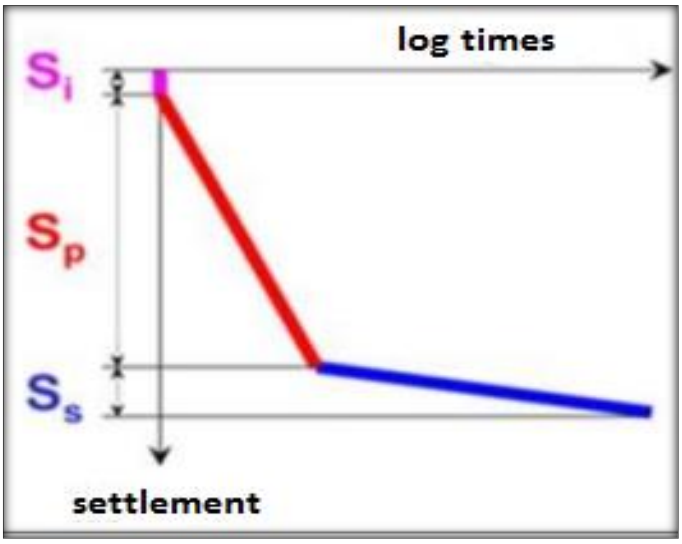

$$ST = Si + Sc + Ss$$

Figure I.4: Settlement versus log times [10].

I.5. 1Immediate Settlement (Si)

Instant settlement occurs before any evacuation of the pore water. It is predominant for unsaturated soils and grainy soils. It corresponds to the «elastic" deformation of the solid skeleton of the soil under the action of overloads.

The overload is transmitted to the grains which deform “instantly»; The expression of this settlement is therefore based on the perfect elastic behavior of the so; it derives from the evaluation of the deformation of a column under an axial load q [10].

$$\mathrm{Si} = \frac{\mathrm{qB}}{\mathrm{E}}(1 - \mathrm{V}^2)\mathrm{I}\rho \qquad (\mathrm{I}.1)$$

q: average pressure applied.

B: width or diameter of footing.

E: Young's modulus of the material measured during a simple compression test or undrained triaxial.

μ: Poisson's ratio (0.5 if the deformation is done at constant volume, as it is the case for saturated clays).

Iρ: coefficient of influence depending on the loaded surface, on the point directly above which one sits and the flexibility of the sole.

The influence factor (Iρ) is affected by a number of parameters, such as the shape of the foundation, its flexibility, the distance from a rigid base, and the embedment depth of the foundation [10].

I.5. 2 Primary Settlements (Consolidation) (S_c)

Primary consolidation corresponds to the departure of water from the soil under the action of overloads. The following mechanical analogy is often used to represent the phenomenon: the soil is represented by a cylinder filled with water and fitted with a piston and of a spring. The spring symbolizes the skeleton of the soil and the water of the cylinder, water interstitial [11].

If an overload $\Delta\sigma$ is applied to the piston (soil), firstly the piston does not move, the overload is taken up by the water; the water pressure increases (we can realize this by measuring the water pressure in the soil). If there is drainage (schematized by a small hole in the piston) the water can flow and the water pressure in the cylinder will gradually dissipate, the piston sinks [11].

At the same time as the water starts, the spring (skeleton of the ground) will therefore take up the overload, which has the effect of deforming it. When the water pressure returns to the initial pressure (zero on the surface), the spring has fully taken

The dimension of the hole in the piston symbolizes the permeability of the ground. The larger the hole (high permeability); the more consolidation will not take place quickly [12].

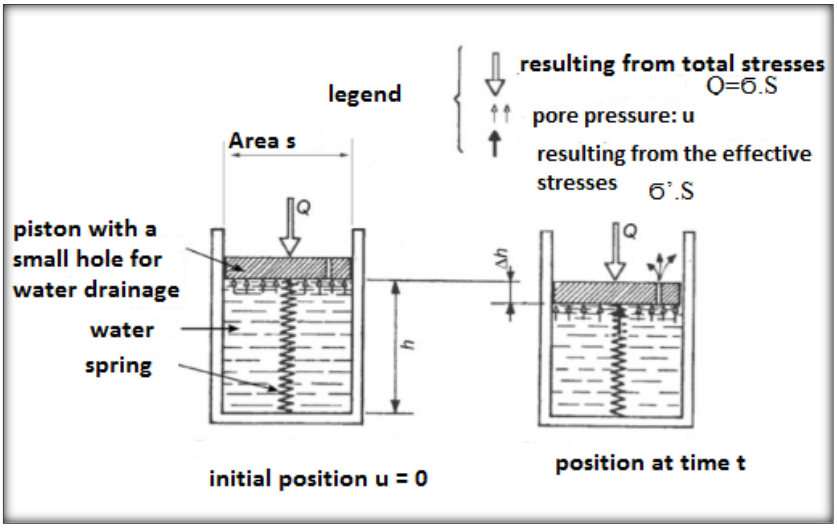

Figure I.5: Rheological model of consolidation [11].

I.5. 3 Secondary Settlements (Creep) (S_s)

The secondary compression settlement corresponds to a deformation of the soil then that the interstitial overpressure has returned to zero. We attribute this deformation

to the gradual change in frictional forces within the material at deformation plastic and the reorientation of the granular structure. [12]

In general, primary consolidation is much higher than compression secondary. This phenomenon can however be important for soils of origin.

Organic and for some silt. We can generally consider that the Secondary compression settlement only appears at the end of consolidation primary and that it varies as a function of the logarithm of time [12].

$$Ss = a(logt - logt1) = a\log\left(\frac{t}{t1}\right) \quad \text{(I.2)}$$

I.6 Consolidation

Consolidation is the process of reducing the volume of soil, in general, it is the reduction of volume due to the displacement of water under a long-term static load. It is produced when stress is applied to a soil, resulting in a tightening of the soil particles and a decrease in its apparent volume. When the stress is eliminated from a consolidated soil, the soil rebounds, regaining some of the volume it had lost during the consolidation process. If the stress is reloaded, the soil will consolidate again along a recompression curve, as defined by the recompression index. The soil from which the load has been eliminated is considered overconsolidated, the highest stress to which it has been subjected being called the preconsolidation stress [13].

The over consolidation ratio or OCR is defined as the highest stress experienced divided by the current stress, a soil which is currently experiencing its highest stress is said to be normally consolidated and to have an OCR of one, a soil could be considered underconsolidated immediately after a new load is applied but before the excess pore water pressure has had time to dissipate [13].

In case of coarse grained soils like sands and gravels, the removal of this pore water is easy since water freely moves from one region to another within these soil types.

However, in case of fine grained soils like silty or clayey soils, consolidation is a time consuming process.

In case of fine grained soil on which a structure is to be built, high water content is not desired as the weight of the structure may cause sinking (consolidation settlement) of the structure in due time, typically the permeability (ability of water to

move through the soil voids) of fine grained soils is low, hence it takes a long time for consolidation process [13].

So two aspects of consolidation settlement are Important:

The rate at which the consolidation is taking place and the total amount of consolidation.

It is very important to note that unlike settlement in sands and other coarse grained soil, consolidation settlement of fine grained soil does not occur immediately. Hence, it is common practice to ensure that the consolidation process is expedited and that most of the consolidation takes place during the various phases of construction. If the soil is such that it has never experienced pressure of the current magnitude in its entire history, it is called a normally loaded soil [13].

The soil is called pre-consolidated (or overconsolidated) if at any time in history, it has been subjected to a pressure equal to or greater than the current pressure applied to it [13].

In case of normally consolidated soils, the consolidation will be greater than that for a pre-consolidated soil. That is because the preconsolidated soil has previously experienced greater or equal pressure and has undergone at least some consolidation under that pressure. So a pre-consolidated soil is preferred over a normally consolidated soil [13].

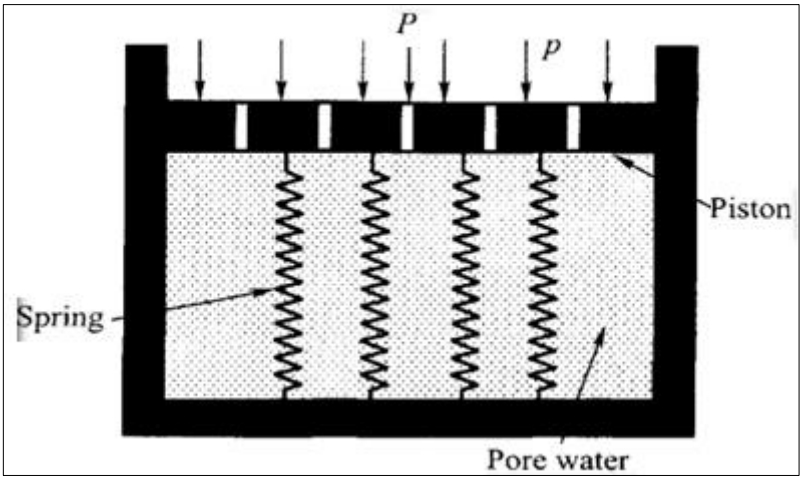

Figure I.6: Mechanical model to explain the process of consolidation [13].

I.7 Soil compressibility

When a saturated clay-water system is subjected to external pressure, the applied pressure is first absorbed by water in the pores, resulting in pore water overpressure [14]

If drainage is permitted, the resulting hydraulic gradients initiate a flow of water out of the clay mass and the mass begins to compress. A portion of the applied stress is transferred to the soil skeleton, which in turn causes a reduction in the excess pore pressure [14].

This process, involving a gradual compression occurring simultaneously with a flow of water out of the mass and with a gradual Consolidation may be due to one or more of the following factors [14]:

1.External static loads from structures.

2.Self-weight of the soil such as recently placed fills.

3.Lowering of the ground water table.

4.Desiccation.

The total compression of saturated clay strata under excess effective pressure may be considered as the sum of:

1.Immediate compression.

2.Primary consolidation.

3.Secondary compression.

The portion of the settlement of a structure which occurs more or less simultaneously with the applied loads is referred to as the initial or immediate settlement.

This settlement is due to the immediate compression of the soil layer under undrained condition and is calculated by assuming the soil mass to behave as an elastic soil [14].

If the rate of compression of the soil layer is controlled solely by the resistance of the flow of water under the induced hydraulic gradients, the process is referred to as primary consolidation.

The portion of the settlement that is due to the primary consolidation is called primary consolidation settlement or compression. At the present time the only theory of practical value for estimating time-dependent settlement due to volume changes, that is under primary consolidation is the one-dimensional theory [14].

The third part of the settlement is due to secondary consolidation or compression of the clay layer. This compression is supposed to start after the primary consolidation ceases that is after the excess pore water pressure approaches zero. It is often assumed that secondary compression proceeds linearly with the logarithm of time. However, a satisfactory treatment of this phenomenon has not been formulated for computing settlement under this category; the transfer of the applied pressure from the pore water to the mineral skeleton is called consolidation [14].

The process opposite to consolidation is called swelling, which involves an increase in the water content due to an increase in the volume of the voids [14].

I.7 Compressibility Parameters

I.7.1 Compression index

Is the rate of change of void ratio (e) with respect to the applied effective pressure (σ') during compression [11].

$$av = \frac{\Delta e}{\Delta \sigma'} = \frac{e1-e2}{\sigma 2-\sigma 1} \qquad \text{(I.3)}$$

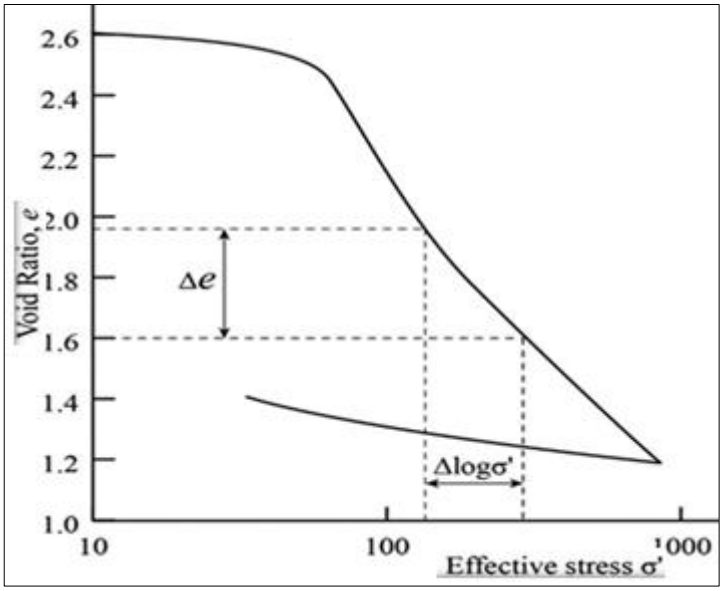

Figure I.7: The compression curve [15]

e_o = initial void ratio.

e_1 = final void ratio.

σ'_o = initial effective stress.

σ'_1 = final effective stress.

$\Delta e = e_o - e_1$.

$\Delta\sigma' = \sigma'_1 - \sigma'_o$

I.7.2 Coefficient of volume compressibility m_v

This parameter is defined as change in volume per unit volume as a ratio with respect to the change in stress. [15]

$$Mv = \left(\frac{av}{1+e0}\right) \quad \text{(I.4)}$$

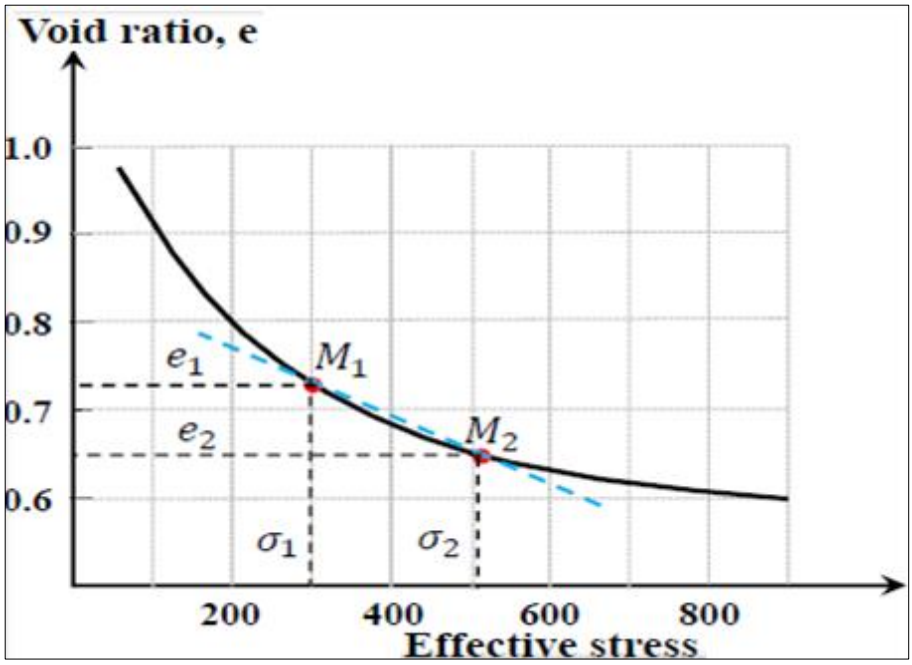

Figure I.8: Determining the Coefficient of volume compressibility. [15]

I.7.2 Pre-consolidation Pressure

Normally consolidated clay, whose present effective overburden pressure is the maximum pressure to which the soil has been subjected in the past. [16]

Over-consolidated, in which the present effective overburden pressure is less than the pressure that the soil has been subjected in the past. The maximum effective past pressure is called the pre-consolidation pressure. [16]

Pre-consolidation pressure can be determined as follow:

1. Establish point a, at which curve has a minimum radius of curvature.
2. Draw a horizontal line ab.
3. Draw the line ac tangent at a.
4. Draw the line ad, which is the bisector of the angle back.
5. Project the straight-line portion gh of the e–log σ’ plot back to intersect line ad at f. The abscissa of point f is the pre-consolidation pressure. [16]

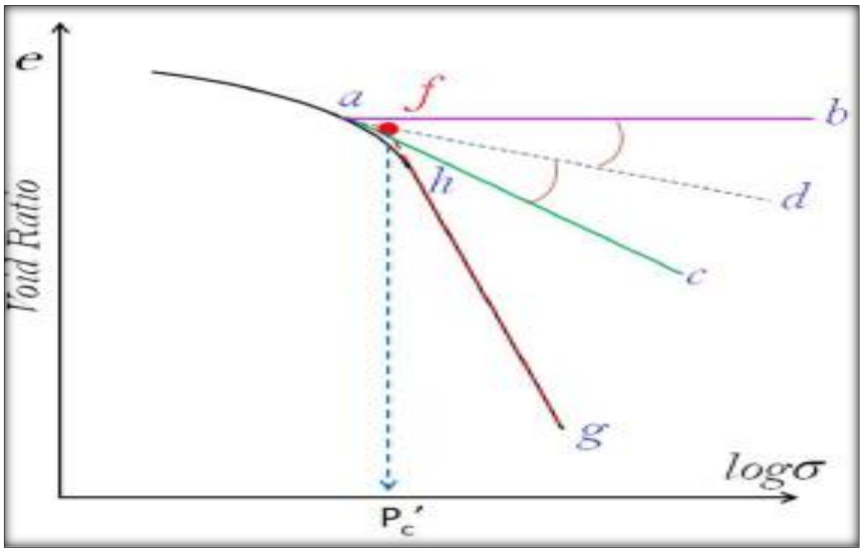

Figure I.9: Determining the Pre-Consolidation Pressure. [16]

The over-consolidation ratio (OCR) for a soil can now be defined as:

$$OCR = \frac{P'C}{\sigma'c} \quad \text{(I.5)}$$

P'_c = pre-consolidation pressure.

σ'_c = present effective vertical pressure.

I.7.3 Coefficient of consolidation C_v

The rate of consolidation settlement is estimated using the Coefficient of consolidation C_v, this parameter is determined for each load increment in the test. [17]

The coefficient of consolidation (C_v) can be determined by the (Casagrande) Logarithm-of-Time and by (Taylor) Square –Root of Time Methods. [17]

I.7.3.1 Logarithm –of – time Method

The following construction is needed to determine C_v:

1. Extend the straight line portions of primary and secondary consolidations to intersect at A.

The ordinate of A is representing by d100 - that is, the deformation at the end of 100% primary consolidation. [17]

2. The initial curved portion on the plot of deformation versus log t is approximated to be a parabola on the natural scale. Select times t1 and t2 on the curved portion such that t2 = 4 t1. Let the difference of specimen deformation during time (t2 – t1) be equal to x

3. Draw a horizontal line DE such that the vertical distance BD is equal to x.

The deformation corresponding to the line DE is d_0 (that is deformation at 0% consolidation.

4. The ordinate of point F on the consolidation curve represent the deformation at 50% primary consolidation and its abscissa represent the corresponding time (t_{50}). [17]

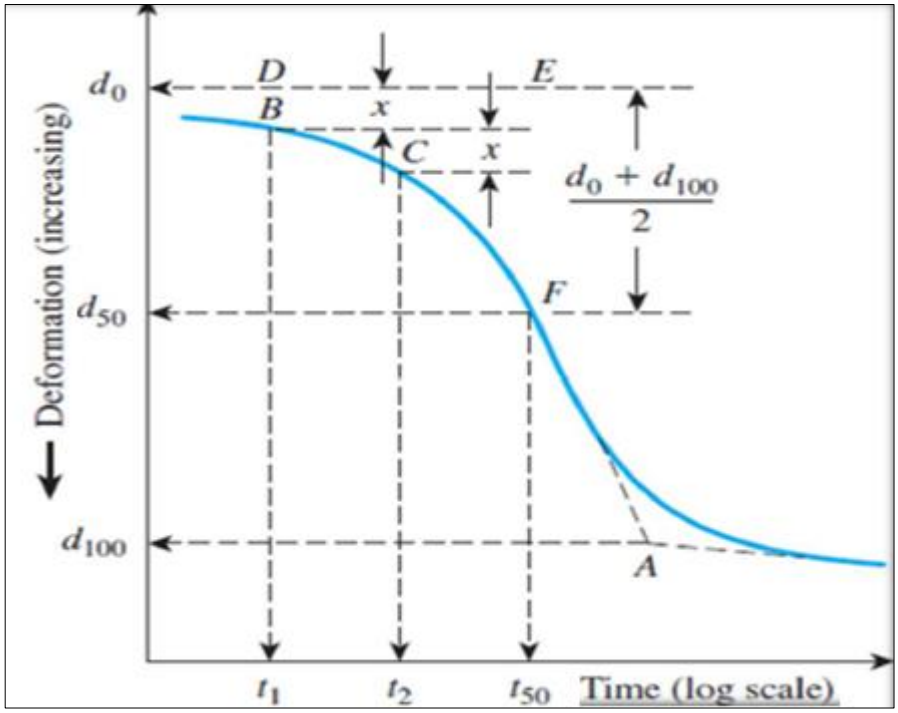

Figure I.10: Logarithm –of– time Method. [17]

5. For 50% average degree of consolidation T_v =0.197, so:

$$Cv = \frac{0{,}197\ H^2 dr}{t50} \qquad \text{(I.6)}$$

Where:

H_{dr} = average longest drainage path during consolidation.

For specimen drained on only one side, H_{dr} equals the average height of the specimen during consolidation. [17]

I.7.3.2 Square-Root-of-Time Method (Taylor)

Plot a deformation against the square root of time.

1. Draw a line AB through the early portion of the curve.

2. Draw a line AC such that OC = 1.15 OB.

The abscissa of point D, which is the intersection of AC and the consolidation curve, gives the square root of time for 90% consolidation. [18]

$$Cv = \frac{0{,}848\ H^2 dr}{t90} \qquad \text{(I.7)}$$

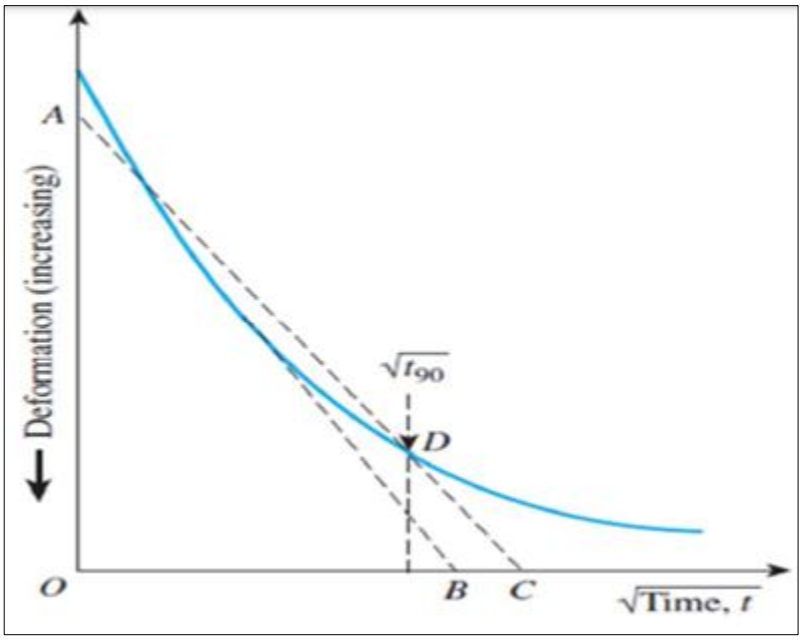

Figure I.11: Square-Root-of-Time Method (Taylor) [18]

I.8 Consolidated Settlement

I.8 .1 Primary consolidations

For normally consolidated clay [18]:

$$S = \frac{Cc\ h}{(1+e0)} \log \frac{(\text{ɛ}'v0+\Delta\text{ɛ}v))}{\text{ɛ}'v0} \quad \text{(I.8)}$$

For over consolidated clay with: $\text{ɛ}'v0 + \Delta\text{ɛ}v \leq p'c$

$$S = \frac{Cs\ h}{(1+e0)} \log \frac{(\text{ɛ}'v0+\Delta\text{ɛ}v))}{\text{ɛ}'v0} \quad \text{(I.9)}$$

Where:

C_c= compression index.

C_s=swelling index.

For over consolidated clay with: $\text{ɛ}'v0 \leq p'c \leq \text{ɛ}'v0 + \Delta\text{ɛ}v$. [18]:

$$S = \frac{Cs\ h}{(1+e0)} \log\left(\frac{p'c)}{\text{ɛ}'v0}\right) + \frac{Cc\ h}{(1+e0)} \log\left(\frac{(\text{ɛ}'v0+\Delta\text{ɛ}v))}{p'c}\right) \quad \text{(I.10)}$$

Where:

e_0=initial void ration of the clay layer.

p'_c= pre-consolidation pressure.

h= thickness of the clay layer.

σ_{v0}= Overburden effective pressure at the middle of the clay layer.

I.8 .2 Secondary Consolidations

At the end of primary consolidation (i.e., after the complete dissipation of excess pores water pressure) some settlement is observed that is due to the plastic adjustment of soil fabrics. This stage of consolidation is called secondary consolidation.

A plot of deformation against the logarithm of time during secondary consolidation is practically linear as shown in Figure I.10. [18]

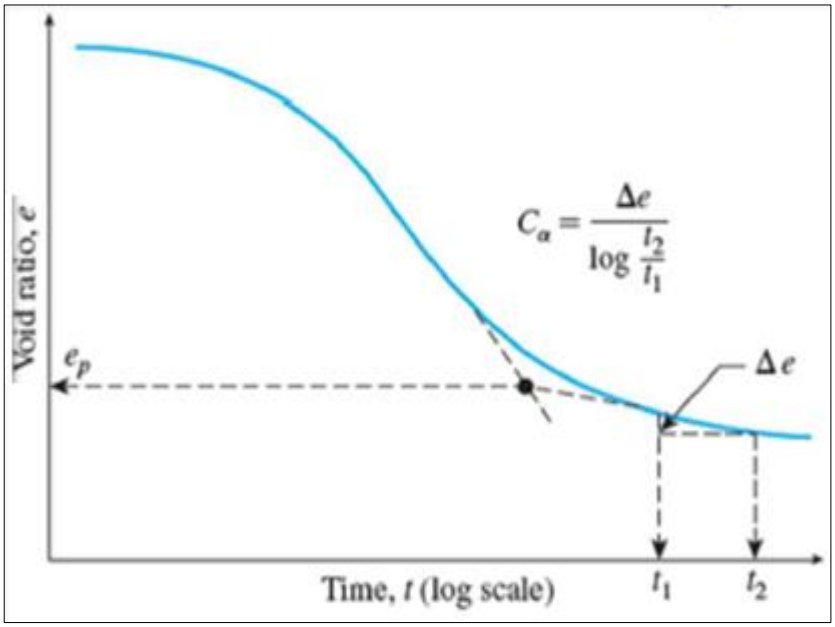

Figure I.12: Deformation against the logarithm of time. [18]

The secondary compression index can be defined as:

$$C\alpha = \frac{\Delta e}{(log\ t2 - log\ t1)} \quad \text{(I.11)}$$

Where:

Cα= secondary compression index.

Δe= change of void ration.

t_1 and t_2 =time.

The magnitude of the secondary consolidation can be calculated as:

$$Scs = \frac{C'\alpha\ h}{\log\left(\frac{t2}{t1}\right)} \quad \text{(I.12)}$$

Where:

$$C'\alpha = \frac{C\alpha}{(1+ep)} \quad \text{(I.12.a)}$$

e_p = void ratio at the end of primary consolidation.

h=thickness of the clay layer .

Secondary consolidation settlement is more important in the case of all organic and highly compressible inorganic soils, in overconsolidated inorganic clays, the secondary Compression index is very small and of less practical significance. [18]

I.9 Time rate of consolidation

The time rate of consolidation based on the following assumptions [18]:

1 -The soil is homogeneous and fully saturated.

2 -There is a unique relationship, independent of time, between void ratio and effective stress

3 -The solid particles and water are incompressible.

4 -Compression and flow is one-dimensional (vertical).

5 -Strains in the soil are relatively small.

6 -Darcy's law is valid at all hydraulic gradients.

7-The coefficient of permeability and volume compressibility remain constant throughout the process. [18]

I.9.1 Degree of consolidation

The average degree of consolidation for the entire depth of the clay layer at any time t can be expressed as [18]:

$$U = \left(\frac{St}{Sf}\right) = 1 - \left(\frac{1}{2Hdr}\right) = \int_0^{2Hdr} Uz\, dz \qquad \text{(I.13)}$$

Where:

U= average degree of consolidation.

S_f=final settlement of the layer from primary consolidation.

S_t=settlement of the layer at time t.

I.10 Empirical equations developed by various researchers

In literature, several correlations have been proposed for soil compressibility characteristics such as compression index C_c with index properties in terms of single and multiple regressions using liquid limit, natural water content, initial void ratio plasticity index, specific gravity, void ratio at liquid limit, and several other properties of soil (example $Cc = f(w_L, w_n, I_p, e, G_s, \gamma w, \gamma d$ max, DFS). [19]

The summarized empirical equations are presented in Table I.2 to Table I.7 based on the critical overview. The empirical equations developed by various researchers are

summarized as per the region/conditions of applicability and theses equations are as follows [19]:

Table I.2: Compression index equations with function of liquid limit

$$C_c = f(w_L)$$

Eq. No.	Empirical Equations	Reference	Region/Conditions of Applicability
1.	$Cc = 0.007\ (Wl - 10)$	Skempton [20]	Remoulded clays, (Normally consolidated, St < 1.5)
2	$Cc = 0.01\ (Wl - 12)$	Murayama et al. [21]	Osaka alluvial clays
3	$Cc = 0.013\ (Wl - 13.5)$	Yamagutshi [22]	All clays
4	$Cc = 0.013\ Wl$	Kyushu Branch of JSSMFE[23]	Ariake clay
5	$Cc = 0.014\ (Wl - 20)$	Taniguchi et al. [24]	Ishikari clay
6	$Cc = 0.0046(\mathrm{Wl} - 9)$	Cozzolino [25]	Brazilian clays
7	$Cc = 0.004\ (Wl - 10)$	Taniguchi [26]	Rumoi clay
8	$Cc = 0.017\ (Wl - 20)$	Shouka [27]	All clays
9	$Cc = 0.009\ (Wl - 10)$	Terzaghi & Peck [28]	Normally consolidated, (Moderately sensitive, St < 5)
10	$Cc = 0.0083(Wl - 9)$	Schofield and Wroth [29]	Various clays
11	$Cc = 0.0051(Wl^2 + 0.1328Wl - 6.412)$	Beverly [30]	Blake-Bahama Outer Ridge Area deep-sediments
12	$Cc = 0.0046(Wl - 9)$	Azzouz et. al. [31]	Brazilian clay, (Moderately Overconsolidated)
13	$Cc = 0.006\ (\mathrm{Wl} - 9)$	Azzouz et al. [31]	All clays with wL< 100%
14	$Cc = 0.0092(\mathrm{Wl} - 13)$	Mayne (1980) [32]	Various clays
15	$Cc = 0.008\ (\mathrm{Wl} - 10)$	Burghignoli & Scarpelli [33]	Italian soft clays
16	$Cc = 0.0046(\mathrm{Wl} - 9)$	Bowles [34]	Brazilian clays; (Moderately overconsolidated)
17	$Cc = (0.01\ \mathrm{Wl} - 0.063)$	Hirata et al. [35]	Natural soils (cohesive)
18	$Cc = 0.063\ (\mathrm{Wl} - 10)$	Abdrabbo & Mahmoud	Egyptian clay

		[36]	
19	$Cc = 0.009\ (\mathrm{Wl} - 8)$	Tsuchida [37]	Osaka Bay clay
20	$Cc = 0.008(Wl - 12)$	Sridharan & Nagaraj [38]	All clays
21	$Cc = 0.006\ (Wl + 1), R^2 = 0{,}509$	Lav & Ansal [39]	Soil in Turkey
22	$Cc = 0.011\ (Wl - 6.36)$	Yoon et al. [40]	Marine costal clays, Korea
23	$Cc = 0.0061(Wl - 0.0024),$ $R^2 = 0.8435$	Solanki and Desai [41]	Alluvial deposits, Surat, India
24	$Cc = 0.0046(Wl - 1.39)$	Arpan & Sujit [42]	Soil in NIT Agartala campus and Howrah, India
25	$Cc = 0.0055(Wl - 1.8364)\ ,$ $R^2 = 0.970$	Vinod and Bindu [43]	Remoulded, highly plastic, marine clays, Kerala, India
26	$Cc = 0.014\ Wl - 0.168)$	Park and Lee [44]	Soils in Korea
27	$Cc = 0.5217(\ Wl - 1.3)$	Widodo & Abdelazim [45]	Soil in Supadio Airport in Pondianak
28	$Cc = 0.01706(Wl - 1.29),$ $R^2 = 0.349$	Widodo & Abdelazim [45]	Pontianak Soft Clay
29	$Cc = 0.026(Wl - 0.536)$ $R^2 = 0.939$	Nesamatha and Arumairaj [46]	Remoulded clay sample, Coimbatore, India
30	$Cc = 0.0067(Wl - 0.0364)$ $, R^2 = 94.0$	Kumar et al. [47]	Black cotton soil. red soil and yellow soil, Bhopal, India
31	$Cc = 0.001\ (Wl - 0.013)\ ,$ $R^2 = 0.863$	Shiva and Darga Kumar [48]	Hyderabad, Andhra Pradesh (A.P.), India

Table I.3: Compression index equations with function of plasticity index; $C_c = f\ I(p)$

Eq. No.	**Empirical Equations**	**Reference**	**Region/ Conditions of Applicability**

1.	$Cc = 0.02 + 0.014\ (I\ p\ )$	Nacci et al. [49]	North Atlantic clay
2.	$Cc = 1.325(Ip)$	Wroth and Wood [50]	Remoulded clays
3.	$Cc = Ip\ /74$	Wroth and Wood [50]	All clays
4	$Cc = 1.325(Ip)$	Koppula [51]	Remoulded clays
5	$Cc = 0.104(Ip) + 0.46$	Nakase et al. [52]	Best for (I_P<50%)
6	$Cc = 0.007(Is + 18)$	Sridharan and Nagaraj [38]	Remoulded clays
7	$Cc = 0.014(Ip + 3.6)$	Sridharan and Nagaraj [38]	Remoulded clays
8	$Cc = 0.014(Ip) + 0.165$	Yoon et al. [40]	Busan clay, Korea
9	$Cc = 0.0082\ IP + 0.0915,$ $R^2 = 0.7862$	Solanki and Desai [41]	Alluvial deposits, Surat, India
10	$Cc = 0.0086(IP + 24.2674),$ $R^2 = 0.970$	Vinod and Bindu [43]	Remoulded, highly plastic, marine clays, Kerala, India
11	$Cc = 0.0055(Is + 21.2364),$ $R^2 = 0.977$	Vinod and Bindu [43]	Remoulded, highly plastic, marine clays, Kerala, India
12	$Cc = 0.0058(IP - 13.76)$	Arpan and Sujit [42]	Soil of NIT Agartala campus and Howrah, India
13	$Cc = 0.0082IP + 0.0475$	Jain et al. [53]	Various river valley projects, India
14	$Cc = 0.026IP - 1.152,$ $R^2 = 0.777$	Nesamatha and Arumairaj [46]	Remoulded clay sample, Coimbatore, India

Table I.4: Compression index equations with function of natural moisture content

$C_c = f\ (w_n)$

Eq. No.	Empirical Equations	Reference	Region/ Conditions of Applicability
1.	$Cc = 0.0001766wn^2 + 0.00593wn - 0.135$	Peck and Reed [54]	Chicago subsoils
2.	$Cc = 0.0054(2.6wn - 35)$	Nishida (1956) [56]	Undisturbed clays

3.	$Cc = 0.0102(wn - 9.15)$	Hough [56]	Inorganic cohesive soil: silt, silty clay
4	$Cc = 0.0115wn$	Moran & Rutledge [72]	Soft clays
5	$Cc = 0.01wn$	Osterberg [57]	Chicago clay, (Normally consolidated, St<1.5)
6	$Cc = 0.01(wn - 5)$	Azzouz et. al. [58]	USA and Greece Clay
7	$Cc = 0.01(wn - 7.549)$	Herrero [59]	All clays
8	$C\,c = 0.01\,wn$	Koppula [51]	Chicago and Alberta clays, (Normally consolidated, S_t < 1.5)
9	$Cc = 0.0102(wn - 9.15)$	Serajuddin [60]	Alluvial clay and silt in Bangladesh
10	$Cc = 0.0115wn$	Bowles [26]	Organic silt and clays; (Normally consolidated, S_t < 1.5)
11	$Cc = 0.115wn$	Bowles [26]	Organic silt and clays, (Normally consolidated, St<1.5)
12	$Cc = 0.0066wn$	Abdrabbo & Mahmoud [36]	Egyptian clays with (20% < w_n < 140%)
13	$C\,c = 1.235l\,wnn - 5.65,$ $R^2 = 0.803$	Lav & Ansal [39]	Soil in Turkey
14	$Cc = 0.479l\,wn - 1.367, R2 = 0.784$	Lav & Ansal [39]	Soil in Turkey
15	$Cc = 0.012wn - 0.1,$ $R2 = 0.758$	Lav & Ansal [39]	Soil in Turkey
16	$Cc = 0.01(wn + 2.83)$	Yoon et al. (2004) [40]	Busan clay
17	$Cc = 0.0091wn + 0.0522,$ $R^2 = 0.77$	Solanki and Desai [41]	Alluvial deposits, Surat, India
18	$Cc = 0.0072(wn - 12.625)$ $R^2 = 0{,}878$	Vinod and Bindu [43]	Remoulded, highly plastic, marine clays, Kerala, India
19	$Cc = 0.013wn - 0.115$	Park and Lee [40]	Soils in Korea
20	$Cc = 0.0102(wn + 11.57),$ $R^2 = 0.238$	Widodo & Abdelazim [45]	Pontianak Soft Clay
21	$Cc = 0.0074wn - 0.007$	Kalantary & Afshin [61]	clayey soils, Mazandaran, Iran
22	$Cc = 0.5217(wn + 11.57)$	Widodo & Abdelazim [45]	Soil in Supadio Airport in Pondianak, Indonesia
23	$Cc = 0.0136wn + 0.0156,$	Sari & Firmansyah,	Surabaya Soft Soil,

	$R^2 = 0.4871$	[63]	Indonesia (w_n= 0-150%; Ip = 0-70%)
24	$Cc = 0.0141wn + 0.0078$, $R^2 = 0.4913$	Sari & Firmansyah, [63]	Surabaya Soft Soil, Indonesia (w_n = 0-150%; Ip = 0-120%)
25	$Cc = 0.0143wn - 0.0165$, $R^2 = 0.5102$	Sari & Firmansyah, [63]	Surabaya Soft Soil, Indonesia (w_n = 0-100%; Ip = 0-70%)
26	$Cc = 0.0327wn - 0.3819$ $R^2 = 0.5265$	Sari & Firmansyah, [63]	Surabaya Soft Soil, Indonesia (w_n = 0%-30%)
27	$Cc = 0.0179wn - 0.1005$ $R^2 = 0.5341$	Sari & Firmansyah, [63]	Surabaya Soft Soil, Indonesia (w_n = 30%-50%)
28	$Cc = 0.0137wn + 0.0034$ $R^2 = 0.4980$	Sari & Firmansyah, [63]	Surabaya Soft Soil, Indonesia (w_n = 50%-70%)
29	$Cc = 0.014(wn - 22.7)$ $R^2 = 0.858$	Bryan et al. [64]	Irish soft soils

Table I.5: Compression index equations with function of void ratio; $C_c = f(e)$

Eq. No.	Empirical Equations	Reference	Region/ Conditions of Applicability
1.	$Cc = 0.54(en - 0.35)$	Nishida [55]	All clays; Normally consolidated, S_t<1.5
2.	$C\,c = 1.15\,(e - eo\,)$	Nishida [55]	All clays (Normally consolidated, St<1.5)
3.	$Cc = 0.29(eo - 0.27)$	Hough [56]	Inorganic silty sand-silty clay; Overconsolidated
4	$Cc = 0.35(eo - 0.5)$	Hough [56]	Organic soils
5	$Cc = 0.156eo + 0.0107$	Hough [56]	Cohesive soil, silt, clay, silty clay and inorganic soil
6	$Cc = 0.4049(eo - 0.3216)$	Hough [56]	Inorganic cohesive soil: silt, silty clay
7	$Cc = 0.256 + 0.43(eo - 0.84)$	Cozzolino, [24]	Motley clays: Sao Paulo, Brazil
8	$Cc = 1.21 + 1.055(eo - 1.87)$	Cozzolino, [24]	Lowland of Santos, Brazil
9	$Cc = 0.246 + 0.43(eo - 0.25)$	Cozzolino, [24]	Motley clays, Brazil
10	$Cc = 0.75(eo - 0.5)$	Nishida [55]	For low plasticity
11	$Cc = 1.21 + 1.005(eo - 1.87)$	Azzouz et. al. [30]	Motley Clays from Sao Paulo City

12	$Cc = 0.208eo + 0.0083$	Azzouz et. al. [30]	Chicago clay
13	$Cc = 0.4(eo - 0.25)$	Azzouz et. al. [30]	Clay in USA and Greece
14	$Cc = 0.3(eo - 0.27)$	Herrero [59]	All soil types
15	$Cc = 0.2343\, eL$	Nagaraj and Srinivasa Murthy [63]	All remoulded normally consolidated clays
16	$Cc = 0.75(eo - 0.5)$	Bowles [26]	Soils with low plasticity; (Moderately sensitive, S_t < 5)
17	$Cc = 1.21 + 1.055(eo - 1.87)$	Bowles [26]	Motley clays from Sao Paulo clay; (Highly sensitive, S_t>5)
18	$Cc = 0.208(eo - 0.0083)$	Bowles [26]	Chicago clays; (Moderately Overconsolidated)
19	$Cc = 0.156eo + 0.0107$	Bowles [26]	All clays; (Moderately Overconsolidated)
20	$Cc = 0.256(eL - 0.04)$	Burland [66]	Reconstituted clay
21	$Cc = 0.302(e0 - ep) + 0.064$	Koumoto and park (1998) [44]	Remoulded natural clays
22	$Cc = e0/(371.747 - 4.275e0))$	Koumoto and park [44]	Remoulded natural clays
23	$Cc = 0.4e0 - 0.1,$ $R^2 = 0.765$	Lav & Ansal [39]	Soil in Turkey
24	$Cc = 0.485l\,en\,0 + 0.329,$ $R^2 = 0.785$	Lav & Ansal [39]	Soil in Turkey
25	$l\,Cnc = 1.272l\,en\,0 - 1.282,$ $R^2 = 0.817$	Lav & Ansal [39]	Soil in Turkey
26	$Cc = 0.39(e0 - 0.13)$	Yoon et al. (2004) [40]	Busan clay , Korea
27	$Cc = 0.4066e0 - 0.0415, R2 = 0.7223$	Solanki and Desai [41]	Alluvial deposits, Surat, India
28	$Cc = 0.2875\,(e0 - 0.5082),$ $R2 = 0.903$	Vinod and Bindu [43]	Remoulded, highly plastic, marine clays, Kerala, India
29	$Cc = 0.2001\,(eL + 0.0755),$ $R^2 = 0.955$	Vinod and Bindu [43]	Remoulded, highly plastic, marine clays, Kerala, India
30	$Cc = 0.49e0 - 0.11$	Park and Lee (2011) [44]	Republic of Korea
31	$Cc = 0.3608e0 - 0.0713$	Kalantary & Afshin [61]	Clayey soils, Mazandaran, Iran
32	$Cc = 0.5217(e0 - 0.20)$	Widodo & Abdelazim [62]	Soil in Supadio Airport in Pondianak, Indonesia
33	$Cc = 0.6787e0 - 0.1933,$ $R^2 = 0.5643$	Sari & Firmansyah, [63]	Surabaya Soft Soil, Indonesia (w_n = 30%-50%)
34	$Cc = 0.58e0 - 0.1428, R^2 = 0.4996$	Sari & Firmansyah, [63]	Surabaya Soft Soil, Indonesia, (w_n = 50%-70%)

Table I.6: Compression index equations with function of dry unit weight, DFS, optimum moisture content $C_c = f(\gamma_d)$, $f(DFS)$, $f(W_0)$

Eq. No.	Empirical Equations	Reference	Region/ Conditions of Applicability
$Cc = f(\gamma d)$			
1.	$C_c = 0.5(\gamma_w/\gamma_d)_{2.4}$	Herrero [59	All soil types
2.	$C_c = 0.5(\gamma_{w/}\gamma_{d2\ 1.2})$	Herrero [59]	Soil systems of all complexities and types
3.	$Cc = 0.618 - 0.975\gamma d$	Lav & Ansal [39]	Soil in Turkey
4	$Cc = 0.7045(\gamma w/\gamma d - 0.4711)$ $R^2 = 0.869$	Vinod & Bindu [43]	Remoulded, highly plastic, marine clays, Kerala, India
$Cc = f(DFS)$			
5	$Cc = 0.0029(DFS) + 0.1837$	Kumar et al. [47]	Black cotton soil. red soil and
	$R^2 = 0.88$		yellow soil, Bhopal, India
$Cc = f(W0)$			
6	$Cc = 0.0404(w0) - 0.3024$	Kumar et al. [47]	Black cotton soil. red soil and yellow soil, Bhopal, India

Table I.7: Compression index equations with function of multiple variables; Cc = $f(w_L, wn, e\ Io, p, Gs, \gamma_d, \gamma w, \gamma_d\ max, DFS)$

Eq. No.	Empirical Equations	Reference	Region/ Conditions of Applicability
1.	$Cc = 0.37(e0 + 0.003wL - 0.0004wn - 0.34)$	Azzouz et. al. [30]	Clays: Greece, parts of USA
2.	$Cc = 0.048(e0 + 0.001wn - 0.25)$	Azzouz et. al [30]	Clays: Greece, parts of USA
3.	$Cc = -0.156 + 0.41e0 + 0.00058wn$	Azzouz et. al. [30]	Clay in USA and Greece
4	$Cc = 0.37(e0 + 0.003wL - 0.34)$	Azzouz et. al. [30]	Clay in USA and Greece
5	$Cc = 0.5IpGs$	Wroth and Wood [50]	All remoulded normally consolidated clays

6	$Cc = 0.185Gs(\gamma w/\gamma d)2 - 0.144$	Herrero [59	All soil types
7	$Cc = 0.009wn + 0.005wL$	Koppula (1981) [51	All clays
8	$Cc = 0.2343(wL/100)Gs$	Nagaraj & Murthy [65]	Normally Consolidated clays
9	$Cc = 0.009wn + 0.002wL - 0.10$	Nagaraj and Murthy [65]	Normally Consolidated clays
10	$Cc = -0.156 + 0.411e0 + 0.00058wL$	Al-Khafaji and Andersland [70]	All Clays
11	$Cc = 0.007wL + 0.0001wn2 - 0.18$	Kosasih et al. [69]	Surabaya clay based from lab testing
12	$Cc = 0.006wL + 0.13e02 - 0.13$	Kosasih et al. [69]	Surabaya clay based from lab testing
13	$Cc = -0.194e0 + 0.0098wL - 0.0025Ip - 0.256$	Yoon et al. [40]	Busan clay, Korea
14	$Cc' = 0.0022wL + 0.0478$, $R^2 = 0.9063$	Solanki & Desai [41]	Alluvial deposits, Surat, India
15	$Cc' = 0.0029Ip + 0.0833$, $R^2 = 0.8579$	Solanki & Desai (2008) [41]	Alluvial deposits, Surat, India
16	$Cc' = 0.0035wn + 0.0631$, $R2 = 0.6735$	Solanki & Desai [41]	Alluvial deposits, Surat, India
17	$Cc = 0.002(Is * G + 65.35)$, $R^2 = 0.969$	Vinod & Bindu [43]	Remoulded, highly plastic, marine clays, Kerala, India
18	$Cc = 0.002(Ip * G + 110.55)$ $R^2 = 0.963$	Vinod & Bindu [43]	Remoulded, highly plastic, marine clays, Kerala, India
19	$Cc = 0.2926(wL/100) * Gs$	Park and Lee [44]	Soils in Korea
20	$Cc = 0.002wL + 0.0025Ip - 0.005$	Amardeep & Shahid, [70]	Different Indian hydropower projects
21	$Cc = 0.7331 + 0.4152e0 - 0.00134wn - 0.3167Gs + 0.0007wL$	Kalantary & Afshin (2012) [71]	Clayey soils, Mazandaran, Iran.
22	$Cc = 6.23wn + 0.115wL, R2 = 0.5099$	Sari & Firmansyah, [63]	Surabaya Soft Soil, Indonesia (w_n = 0-100%; Ip = 0-70%)
23	$Cc = 0.4044(e0 + 0.01wn) - 0.0795$, $R2 = 0.5024$	Sari & Firmansyah, (2013) [63]	Surabaya Soft Soil, Indonesia (w_n = 0-100%; Ip = 0-70%)

24	$Cc = 1.0941(0.123e0 + 0.01wn) - 0.0415,$ $R^2 = 0.5101$	Sari & Firmansyah, [63]	Surabaya Soft Soil, Indonesia, (w_n = 0-100%; Ip = 0-70%)
25	$Cc = 0.2867(1.567e0 + 0.01wn) - 0.0843,$ $R^2 = 0.5001$	Sari & Firmansyah, [63]	Surabaya Soft Soil, Indonesia (w_n = 0-100%; Ip = 0-70%)
26	$Cc/1 + e0 = 0.1905[ln\ wn - 3.03],$ $R^2 = 0.623$	Bryan et al. [64]	Irish soft soils
27	$Cc/1 + e0 = 0.173[ln\ wl - 3.01],$ $R^2 = 0.602$	Bryan et al. [64]	Irish soft soils
28	$Cc = 0.0128(wL) - 0.008(Ip) - 0.1423,$ $R^2 = 0.92$	Kumar et al. [47]	Black cotton soil. red soil and yellow soil, Bhopal, India
29	$Cc = 0.0149(wL) - 0.0092(Ip) - 0.00671(w0),$ $-0.10692(\rho dmax) + 0.0554$ $R^2 = 0.95$	Kumar et al. [47]	Black cotton soil. red soil and yellow soil, Bhopal, India
30	$Cc = 0.0122\ (wL) - 0.0069\ (I\ p + w0) - 0.061\ (\rho dmax\ ) + 0.0004\ (DFS) + 0.0451$ $R^2 = 0.94$	Kumar et al. [47]	Black cotton soil. red soil and yellow soil, Bhopal, India

I.11 Conclusion

Soil settlement is a very important phenomenon in the geotechnical field, in this chapter I have described this phenomenon in detail by starting with their types, causes, components, parameters.

Besides, I have mentioned the different correlation equations used by the research to explain the effect of physical parameters on compressibility using a function of simple and multiple regressions of soil parameters such as liquid limit (w_L), plasticity index (I_p), natural water content (w_n), void ratio (e_0), dry unit weight (γ_d), differential free swell (DFS), water content (w), specific gravity (G_s), this equation describes the effects of soil parameters on compressibility index (Cc).

Chapter II: Foundations and parameters That affect the Soils compressibility.

II.1 Introduction

Site investigation and estimation of soil settlement characteristics are essential parts of a geotechnical design process, geotechnical engineers must determine the average values and Variability of soil properties, when soil is subjected to an increase in compressive stress due to foundation load, the resulting soil compression is known as settlement of the foundation; in situ testing is important in geotechnical engineering, as simple laboratory tests may not be reliable while more complicated laboratory testing can be time consuming and costly. [73]

One of in situ testing methods is the Standard Penetration Test (SPT) that is used to identify soil type and stratigraphy along with being a relative measure of strength. [73]; the results of in situ test reveal the bearing capacity and settlement characteristics of the soil used to determine the type of foundation required to effectively carry structural load without bearing capacity failure and/or excessive settlement. [74]

Foundation design and construction are two basic requirements of any earth retaining structure, which transfers its load to the underlying earth's crust. The materials that constitute the earth's crust are arbitrarily divided into two types, i.e. soil and rock, which are the main structural materials and in reality, there is no clear distinction between them. Soils and sites are so variable that it is not practicable to formulate any hard and fast rules. [75]

In order to demonstrate the effect of soil properties on compressibility several researchers have done many empirical correlations between C_c and physicals and mechanicals properties that it is easier to determine with precision and at a much lower cost. [76]

II.2 The foundations

A structure essentially consists of two parts, namely the super structure which is above the plinth level and the substructure which is below the plinth level, the substructure or foundation is the part of structures that is usually placed below the surface of the ground to transmit the load from the superstructure to the underlying soil or rock. [77]

Footings are those parts of the foundation which resting directly on the soil, support specific portion of building and distributed building loads directly to the soil.

The most efficient footing and foundation system is that transmit building loads mostly to the soil without exceeding the bearing capacity of the soil; all soil compress noticeably when loaded and because the supported structure to settle. If soil of sufficient bearing capacity lies immediately below the structure, then the load can be spread by footings as shown below. [77]

II.2.1 Requirements for Foundations

Loads must be carried by a foundation system would include the dead load of the building and live loads of its occupants and contents, foundation system must resist lateral loads from both ground pressure and wind, and provide anchorage for the building superstructure against uplift and racking force. [78]

The most critical factor in determine the foundation system of building is the type and bearing capacity of the soil to which the building loads are distributed. (Adequate safety). [78]

-Small settlements (Total and differential settlement).

-Construction problems (stability of excavation bottom heave ground water problems)

-Economical requirement. [78]

II.2.2 Characteristics of foundations

-Distribution of loads

-Foundation helps to distribute the loads of super-structure to a large of the soil.

-Therefore, the intensity of load at its base does not exceed the safe bearing capacity of the soil. [79]

-In the case of deep foundations, the super imposed loads are transmitted either through end bearing or both by side friction & end bearing.

-Stability against sliding & overturning

-Foundation imparts lateral stability to the super structure by anchoring it to the ground

-It increases the stability against sliding & overturning due to horizontal forces to wind, earthquake, etc. [79]

-Minimize differential settlement

-Foundation distributes the super-imposed loads evenly on the sub-soil, even in the case of non-uniform loads. [79]

-This can be achieved by constructing combined footing or raft foundation.

-Safe against undermining

Foundation provides safety against scouring or undermining by flood water or burrowing animals. [79]

-Minimize distress against soil movement

-Distress or failure due to expansion or contraction of the sub-soil due to moisture variation in clayey & black cotton soils are minimized by the provision of special type foundations.

II.2.3 Classification of foundations

Foundations are classified as shallow and deep foundations based on the depth at which the load is transmitted to the underlying and / or surrounding soil by the foundation.

If the forces are transferred to the surface of the ground, the foundations will be said to be Shallow; if the efforts are postponed in depth, it will be deep foundations. [80]

II.2.3.1 Shallow foundations

Depth of foundation is less than or equal to width. It transfers the superimposed load to the soil at a level close to the lowest floor of the building. [81]

These types of foundations are so called because they are placed at a shallow depth (relative to their dimensions) beneath the soil surface. Their depth may range from the top soil surface to about 3 times their breadth (about 6 meters).

They include footings (spread and combined), and soil retaining structures (retaining walls, sheet piles, excavations and reinforced earth), There are several others of course different types of shallow foundation are [81]:

– Spread footing.

– Combined footing.

– Strap footing.

– Mat foundation.

a) Spread footing or pad foundation

Spread footing is the one which supports either one column or one wall. It is divided into following types:

- Single footing for a column.
- Stepped footing for a column.
- Wall footing without step.
-Stepped footing for wall.

-Grillage foundation. [81]

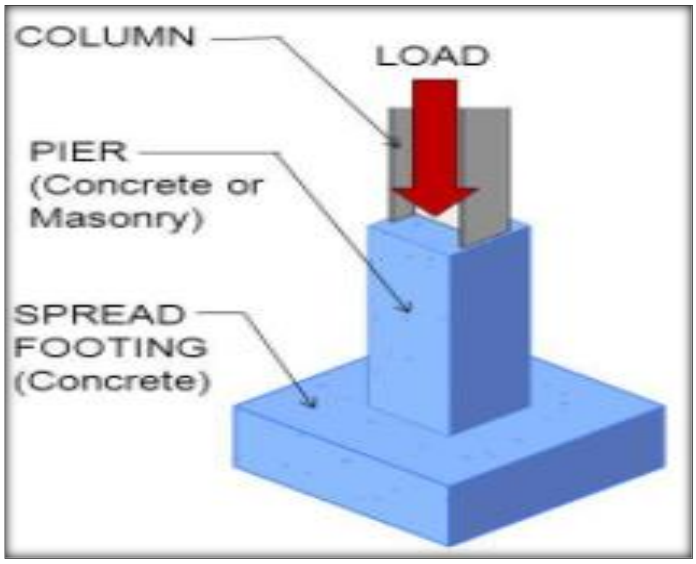

Figure II.1: Spread footing. [81]

b) Strap footings

Independent footing of two columns are connected by a beam. [81]

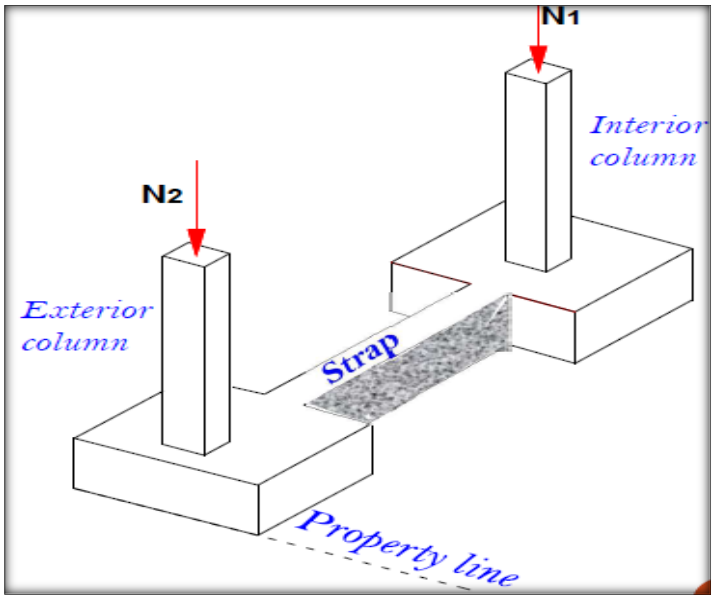

Figure II.2: Strap footing. [81]

c) Combined footing

A spread footing which supports two or more columns is termed as combined footing type of combined footings.

- Rectangular combined footing.

-Trapezoidal combined footings.

- Combined column wall footings. [74]

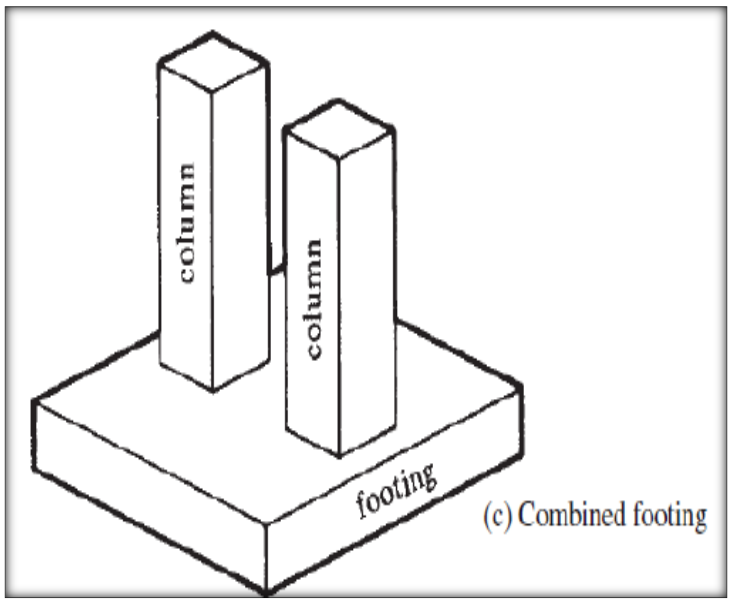

Figure II.3: Combined footing. [82]

d) Mat (Raft) foundation

A raft foundation is a combined footing that covers the entire area beneath a structure and support all the walls and columns.

- Use of mat foundation. [82]

- When an allowable soil pressure is low the building loads are heavy mat foundation is economical to use.

- Use to reduce settlement.

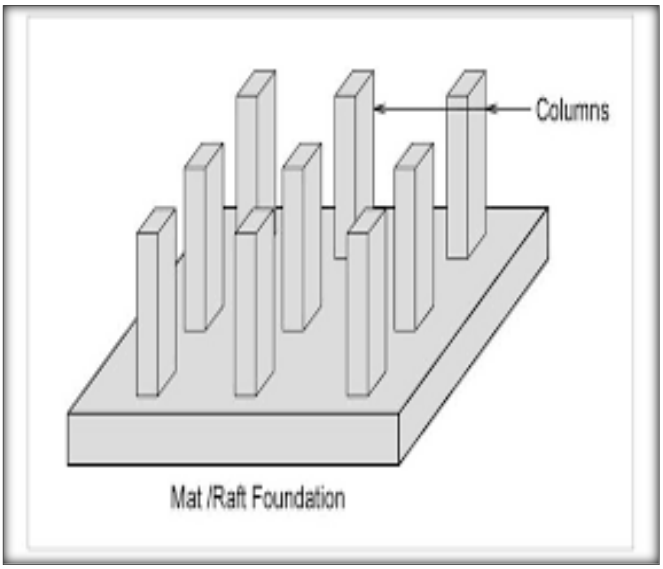

Figure II.4: Raft foundation. [82]

II.2.3.2 Deep foundation

Deep foundations are those in which the depth of the foundation is very large in comparison to its width. They transfer the super imposed load to the soil at a level that is at a great distance from the lowest. [83]

Types of deep foundations

-Pile foundation.

- Pier foundation.

- Well or caisson foundation.

a) Pile foundation

Pile foundation is that type of deep foundation in which loads are taken to low level by means of vertical members which may be timber, concrete or steel. [84]

Pile foundation is used were:

- Soil condition is very poor.

- Water table is high.

- Area with heavy loads.

-Compressive soil.

- To ensure stability and durability.

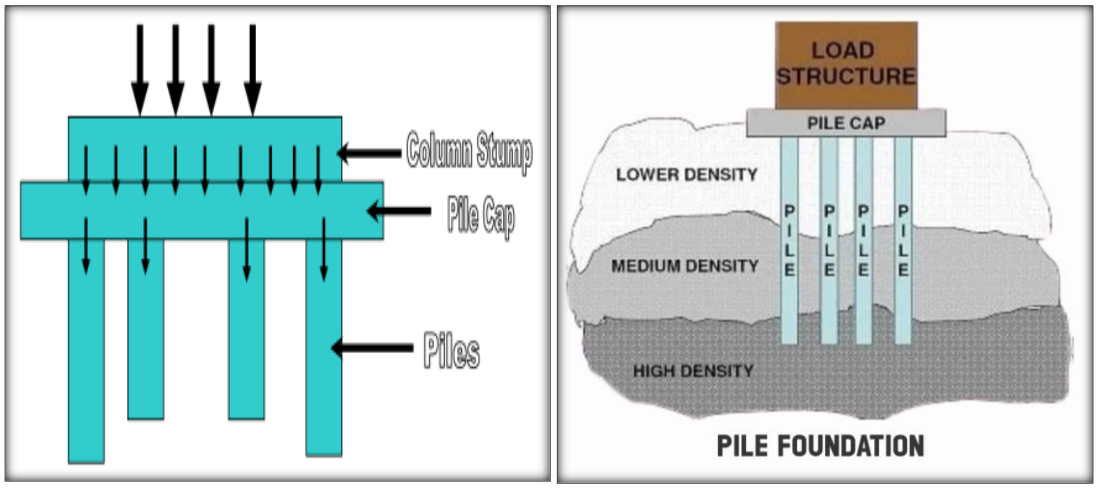

Figure II.5: Pile foundation. [84]

b) Pier foundation

A pier foundation is a collection of large diameter cylindrical columns to support the superstructure and transfer large super-imposed loads to the firm strata below. It stood several feet above the ground. It is also known as "post foundation". [84]

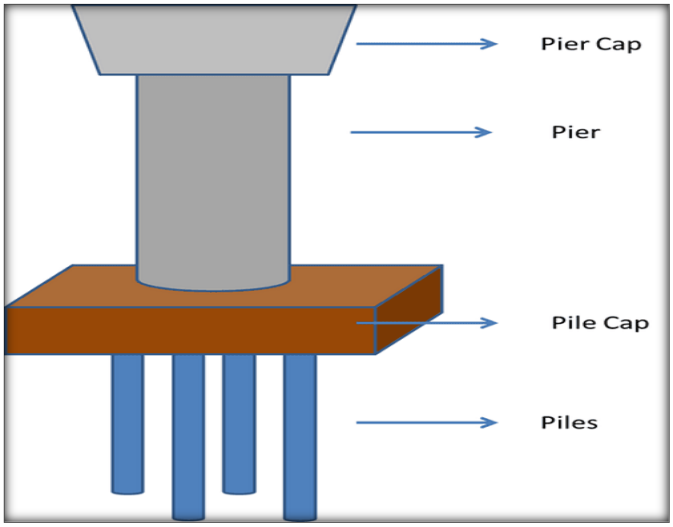

Figure II.6: Pier foundation [84]

c) well or caisson foundation

Well foundation is the water tight box structure of wood/ RCC/steel and mostly used in the foundation of the bridges.

– Purpose: to develop an enclosure below for plumb and provide access shaft to reach a deep tunnel transmitting the loads to hard bearing strata.

– Types of well foundations (Caissons):

- Box caissons
- Well foundation or open caissons- single, double or cylindrical
- Pneumatic caissons. [84]

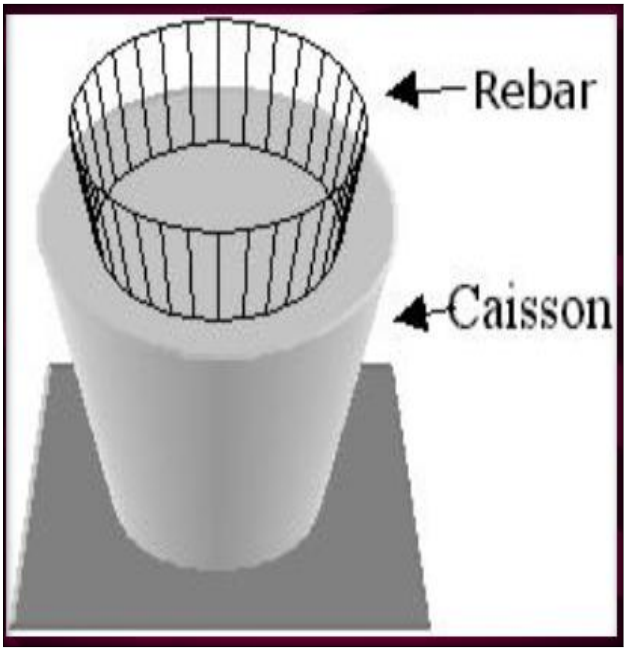

Figure II.7: Well foundation. [84]

II.3. Settlements in shallow foundation

The load applied on a footing changes the stress state of the soil below the footing.

This stress change may produce a time-dependent accumulation of elastic compression, distortion, or consolidation of the soil beneath the footing. This is often termed foundation settlement. [85]

True elastic deformation consists of a very small portion of the settlement while the major components of the settlement are due to a change of void ratio, particle rearrangement, or crushing. Therefore, very little of the settlement will be recovered even if the applied load is removed. [85]

II.3.1 On cohesionless soils

Settlements of structures on cohesionless soils such as sand take place immediately as the foundation loading is imposed on them. Because of the difficulty of sampling these soils, there are no practicable laboratory procedures for determining their compressibility characteristics. [86]

Consequently, settlement of cohesionless soil deposits may be estimated by a semi empirical method based on the results of static cone or dynamic penetration test or plate load tests. The relevant Indian Standards may be followed. [86]

II.3.2 On cohesive soils

In the case of clay layers, the total settlement should be computed by adding the immediate and consolidation settlements together. The two cases as given below are considered for estimation of settlements of foundation on cohesive soils.

-Clay layer sandwiched between cohesionless soil layers or between a cohesionless soils layer at top and rock at bottom.

- Clay layer resting on cohesionless soil layer or rock. [87]

II.4 Settlements in deep foundation

II.4.1 In cohesionless soils

The settlement of a single pile in cohesionless soils can be reliably estimated by pile load test. The settlement of a friction pile group in cohesionless soils is expected to be less than the observed settlement of a test pile (driven alone, not a pile in the group) as the soil between the piles is compacted by displacement due to pile driving. It can reasonably be assumed that the settlement of a pile group in cohesionless soils will be

equal to the settlement of a well foundation having a depth and base equal to the overall dimensions of the pile group estimated. [88]

II.4.2 In cohesive soils

The pile group may be replaced by an equivalent foundation for which the settlement may be computed.

Pile Foundation in Erratic Deposits: In variable erratic soil deposits, if the variation occurs over distances greater than half the width of foundation, settlement analysis should be based on the worst and the best conditions and if the variation occurs over distances lesser than half the width of the foundation, the settlement analysis should be based on worst and average condition. [89]

II.5 Effect of different parameters on the compressibility and settlement

The compressibility of a soil is the relationship between the effective stresses applied to the soil and the volume change which is induced by the stress. It may be described as being the inverse of stiffness, as soils with a high stiffness generally have low compressibility's while soils with low values for the stiffness are generally highly compressible.

This may also be seen directly from expression (14) in which the compressibility λ is defined as the inverse of the modulus number m:

$$\lambda = \frac{1}{m} \qquad \text{(II.1)}$$

A compressibility index Cc can be found from λ as in expression

$$Cc = \lambda \, ln\, 10 \qquad \text{(II.2)}$$

The compressibility characteristics of compacted cohesionless materials are primarily influenced by the same factors that influence the shear strength, namely, the mineralogical composition, size and gradation of the particles, shape of the particles, void ratio and confining pressure. [90]

In general, the compressibility decreases with increasing gradation, decreasing as-compacted void ratio, decreasing angularity, and increasing confining pressure.

The mineralogy of the individual particles contributes to the compressibility characteristics by influencing other properties such as the size, shape, cleavage planes, elasticity, etc., of the particles. [90]

Compression tests on sand-mica mixtures showed that compressibility increases as the percentage of plate - shaped particles increases.so different investigation on micaceous sands and silts also indicated that the compressibility is significantly affected by the percentage of mica that is present in the material. [91]

The presence of plate-like particles, such as mica, produces two effects that influence the compressibility, first the surface properties of these layer-latticed minerals are probably smoother than the massive- shaped minerals and therefore can be more easily densified. Second, the introduction of these flat particles produces a decrease in the compacted density which also contributes to an increase in compressibility.

Several data have presented to indicate that decreasing grain-sized material will exhibit increasing compressibility. These data are for samples with mean diameter from 0. 51 to 1.00 mm. [92]

Using the same method of compaction, the initial void ratio increases with decreasing grain size; however, the initial relative density increases with decreasing grain size.

Therefore, at a constant relative density, the increase in compressibility would be even more pronounced than indicated.

The influence of relative density on compressibility is similar to the effect of relative density on shear strength; that is, increasing relative densities for a given material will cause decreasing compressibility. [92]

The compressibility increases with increasing initial void ratio. These data also indicate that the compressibility increases for a given initial void ratio as the void ratio between the maximum and minimum states increases; these increasing compressibility are due to the properties of the material such as grain shape and grain-size distribution. [92]

II.5.1 Compressibility characteristics of compacted cohesive materials

The compressibility characteristics of cohesive materials are significantly influenced by soil type, molding water content, dry density, degree of saturation, and the compaction method. The amount of compressibility for a given range of pressure is influenced by the combined effect of these factors.

In general, the compressibility increases with increasing liquid limit, increasing molding water content, decreasing dry density, increasing degree of saturation, and

compaction procedures that produce large shearing strains during the compaction process. [93]

It is evident, therefore, that the compressibility characteristics of cohesive soils are much more complicated than the compressibility characteristics of cohesionless materials whose behavior is controlled primarily by the relative density and gradation characteristics.

Furthermore, the time rate of compression is an important factor in cohesive soils, whereas in cohesionless materials the rate of compression is generally rapid enough to eliminate the consideration of time rate of compression. The influence of these various factors will be discussed in the following sections. [93]

In general, it appears that the compressibility will increase for a soil compacted by static, vibratory, impact, and kneading compaction methods, in that order. That is, the statically compacted specimens should be less compressible than the specimens that are compacted using kneading methods for the same water content and dry density on the wet side of optimum; however, on the dry side of optimum the compressibility should be approximately the same regardless of the compaction method used. [93]

II.5.2 Effect of saturation on compressibility

The previous section dealt with samples that were tested in the as-compacted state or samples that were saturated prior to testing. In the field, however, the material is generally compacted and then saturation may occur at a later stage when a confining pressure will exist on the material. [94]

The effect of saturation of the material under various confining pressures has been studied to explain the change in vacuum ratio which can be quite large and may in fact be of the same order of magnitude of the change in void ratio which occurs during high pressure increased applied from the outside. [94]

For soils that appear to be subject to this collapse phenomenon it appears that increased compaction which produces a decrease in the void ratio will significantly aid in reducing the amount of void ratio decrease that, will occur upon saturation of the material. The amount of collapse may also be reduced by increasing the degree of saturation of the material during the compaction process; however, this increase in degree of saturation and/or water content will lead to greater compressibility caused by external pressures. [94]

II.5.3 Correlation of Soil type with compressibility

The compressibility of a soil is an important parameter in terms of determining the expected consolidation and settlements of the soil. As such, it is interesting to see

how it relates to other properties of the soil.

It is necessary to determine the compressibility parameters of soils such as the compression index (C_c) and the recompression index (C_r) for safe and economic design of geotechnical engineering structures, in order to calculate the consolidation settlement of normally consolidated and over-consolidated saturated fine-grained soils, the compressibility parameters are determined by means of laboratory oedometer test on undisturbed samples based on Terzaghi's consolidation theory, these parameters can be influenced from the quality of samples used in the tests. [95]

The presence of relationships between the compressibility parameters and the basic soil properties has been investigated from past to present.

These studies are generally focused on relationships between the compression index and physical properties of the soils such as the dry unit weight (γ_d), wet unit weight (γ_h), fine fraction(F_f), degree of saturation (S_r), the initial void ratio (e_0), natural water content (W), liquid limit (W_L), and plasticity index (I_p), specific density specific (G_s). [95]

The researches show that the physical parameters of soils have a significant effect on compressibility parameters of soil.

In literature, the given regression equations to predict the compressibility parameters generally divided into two groups; connected with state variables such as void ratio and water content and connected with intrinsic variables such as liquid limit and plasticity index. [95]

The relations between the compression index Cc and the physical parameters presented in empirical equations that give good correlation coefficients values mean that there is a strong correlation between the compression index and soil parameters.

Many Researchers have proposed equations between the compressibility index (C_c) and Physicals parameters such as (γ_d, I_p, w_L, I_p, W_n ,e_0 ...), which gives a good correlation . [95]

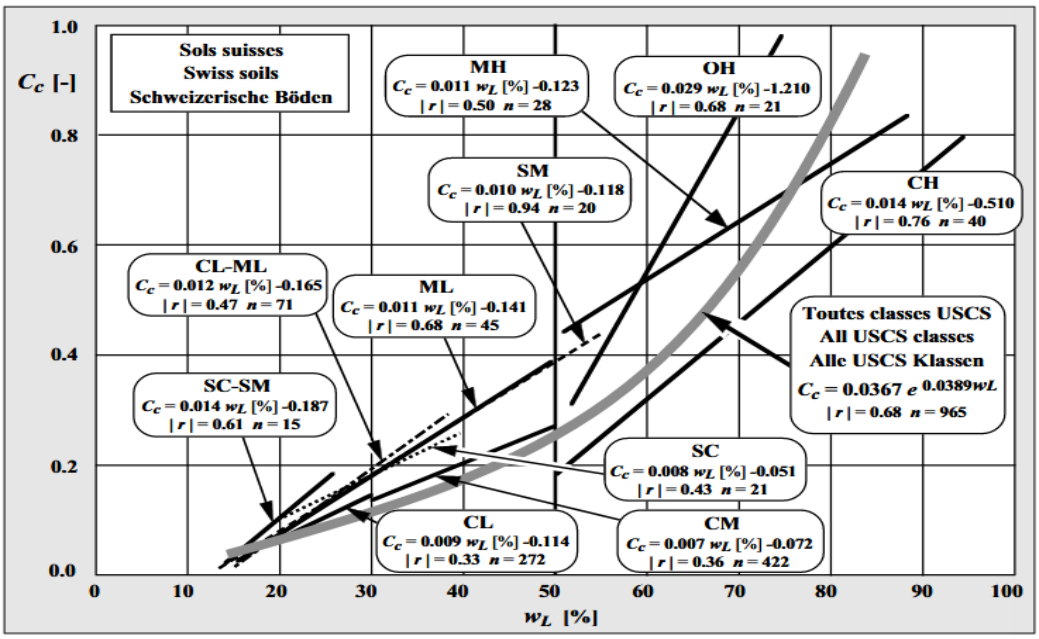

Figure II.8: Correlations between the compression Cc index and the liquidity limit w_L [96]

So we can say that there is a good correlation between them , the same thing for the other parameters like the plasticity index I_p ,the void ratio e_0 and the water content w_n .[95]

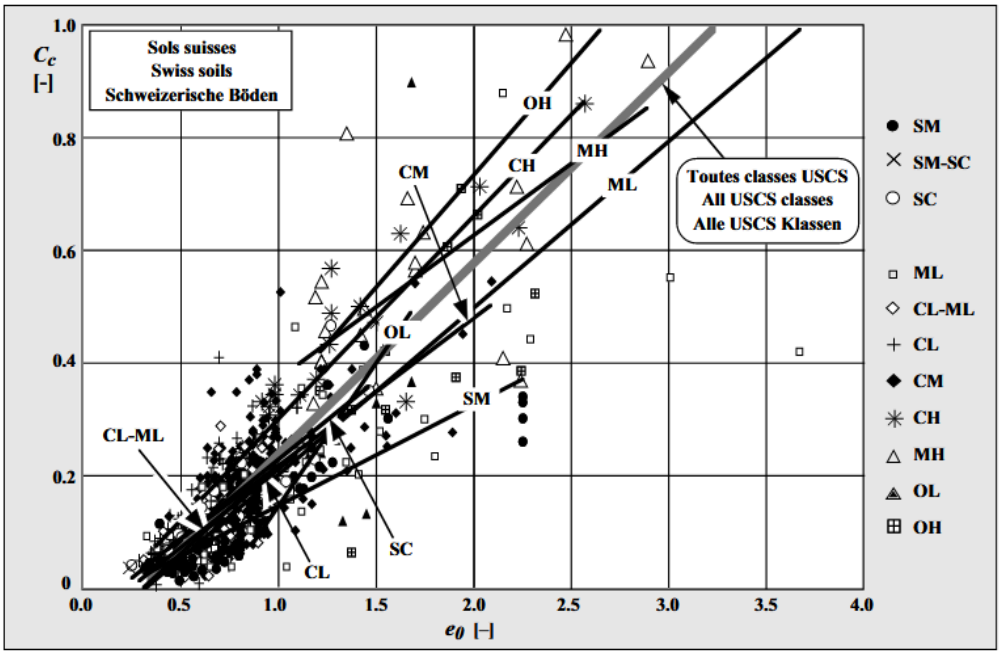

Figure II.9: Correlations between Cc and the void ratio e_0 . [96]

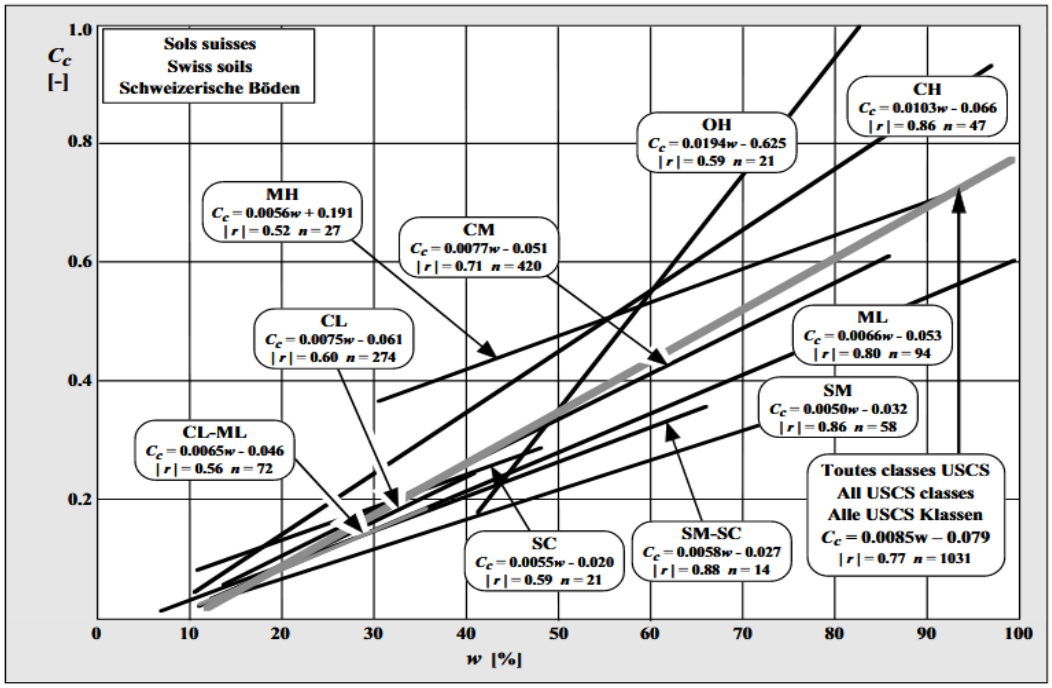

Figure II.10: Correlations between Cc and the water content w. [96]

The mechanical parameters such as the coefficient of swelling C_s, the pressure of pre-consolidation P_c have an important influence on the coefficient of compressibility which is very necessary in the study of settlement.

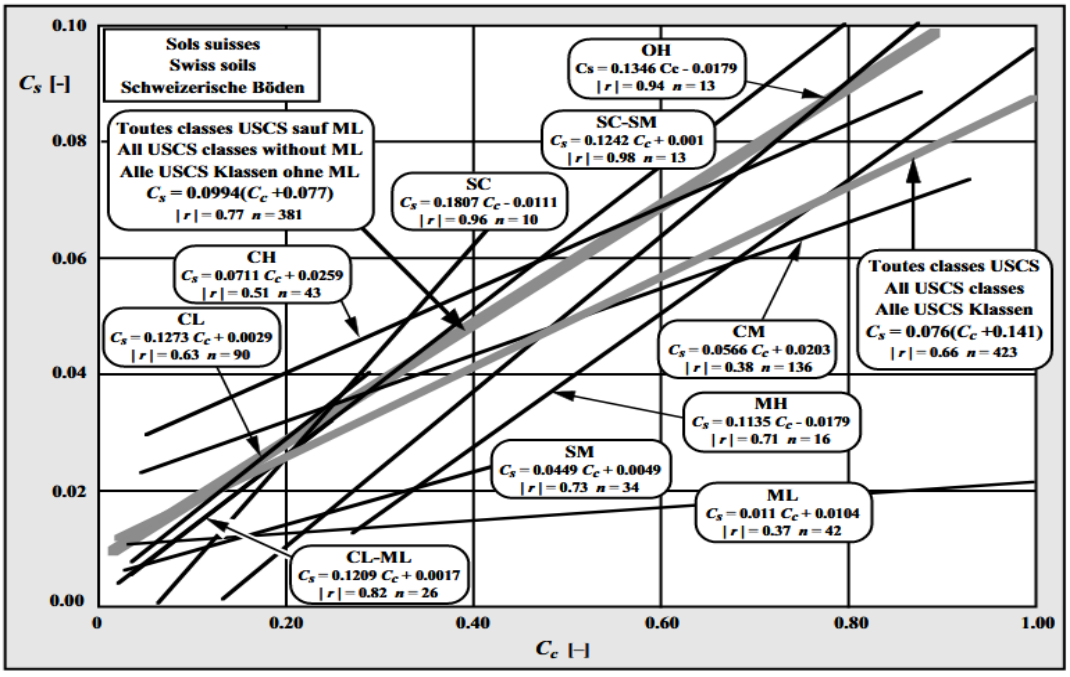

Figure II.11: Correlations between the compression C_c index and the swelling index C_s. [96]

Empirical equations that give good correlation coefficients values mean that there is a strong correlation between the compression index and soil parameters proposed and this means that they can be used with high accurately to predict the soil compression index.

Equations with multiple index properties to obtain C_c parameter, these are slightly better than equations obtained from simple regression analysis. [96]

II.6 Conclusion

A foundation is the element of an architectural structure which connects it to the ground, and transfers loads from the structure to the ground. Foundations are generally considered shallow or deep.

The main objectives of foundation design are to ensure that the structural loads are transmitted to the subsoil safely, economically and without any unacceptable movement during the construction period and throughout the anticipated life of the building or structure.

The choice of foundation type depending on the soil profile, size, and load of the structure, engineer's thing different kinds of foundation.

We conclude that soil compressibility is affected by several soils parameters such as mineralogical composition, particle size and gradation, particle geometry, void ratio, and confining pressure.

Compressibility can be related to index properties (parameters) of clay soils such as initial void rate (e_0), liquid limit (W_L), and natural water content (W_n), and dry unit weight (γ_d), degree of saturation (S_r), wet unit weight (γ_h), fine fraction (F_f) by a statistical tool to study the relationships between the dependent variable and the independent variables

Chapter III: Methods of analysis and calculation of soil settlements.

III.1 Introduction

Before starting the computation of settlement, it is necessary to specify certain data. When the ground is overloaded, it deforms. This deformation can be divided into three types for better analysis, only the instantaneous deformation which exerts the elastic properties of the soil is the elastic settlement. [97]

The so-called primary consolidation, until the pore pressure generated by the overload can be dissipated by any substance: the water flowing to the zero pressure zones is lost. This type will lead to settling after a longer or shorter time. Finally, the second consolidation corresponds to the rearrangement of the soil particles under the residual load and constitutes a settlement.

Usually, elastic settlement will be the foundation of the foundation. On the other hand, the so-called basic fusion will be based on rafts. In general, the secondary consolidation is very insensitive, except on very soft layers of greater thickness or on very heavy foundations. [97]

Before proceeding with the calculation of settlement, it is necessary to understand the distribution of the stress exerted by the overload on the soil surface. Whether the medium is viscous or powdery, this distribution is very consistent with the elastic theory proposed by boussinesq. [98]

III.2 Stress due to self-weight

The vertical stress on element A can be determined simply from the mass of the overlying material. If represents the unit weight of the soil, the vertical stress is [99]:

$$\sigma = \gamma z \qquad \text{(III.1)}$$

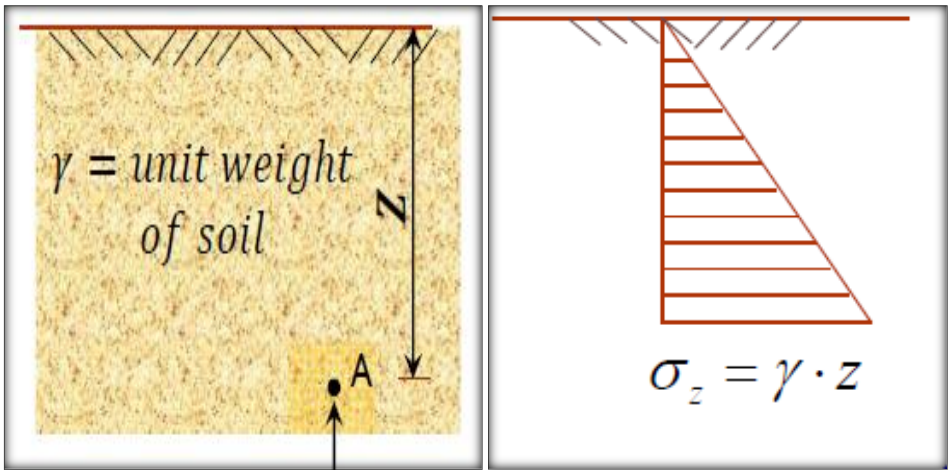

Figure III.1: Variation of stresses with depth. [99]

III.2 .1 Stresses in a layered deposit

The stresses in a deposit consisting of layers of soil having different densities may be determined as [100]:

$$\sigma z = \gamma 1 z 1 + \gamma 2 z 2 + \cdots \ldots + \gamma n z n = \sum_{i=1}^{n} \gamma i z i \qquad \text{(III.2)}$$

Vertical stress at depth z1

$$\sigma z1 = \gamma 1 z 1$$

Vertical stress at depth z2

$$\sigma z2 = \gamma 2 z 2$$

Vertical stress at depth z3

$$\sigma z3 = \gamma 3 z 3$$

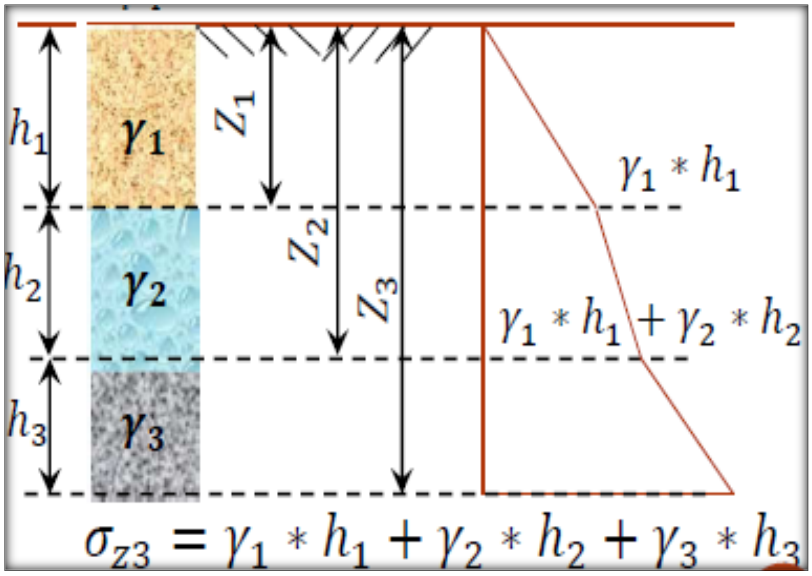

Figure III.2: Stresses in many layers. [100]

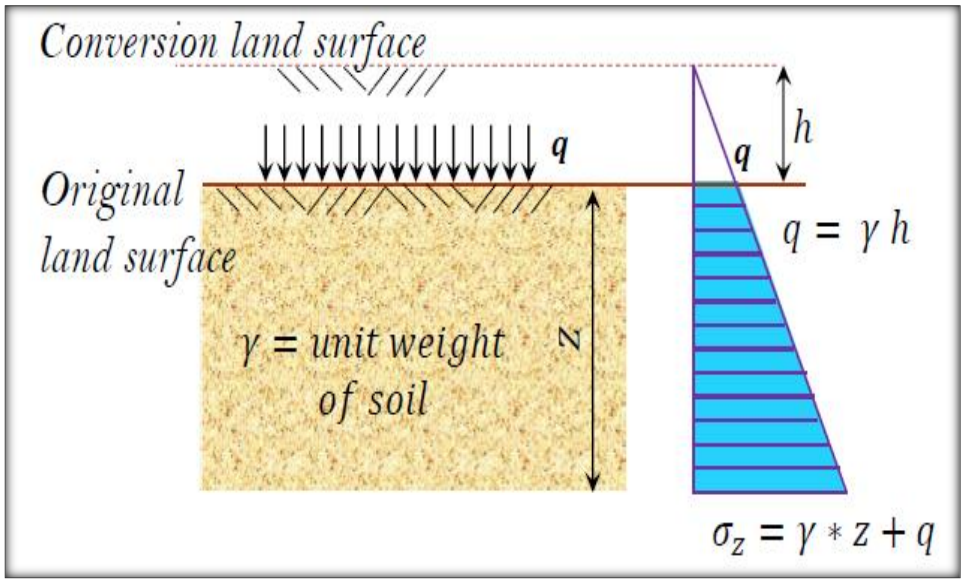

Figure III.3: Uniform overload on infinite land surface. [100]

III.2 .2 Vertical stresses

Vertical stresses due to self-weight increase with depth, there are 3 types of geostatic stresses [101]:

a. Total Stress, σ total.

b. Effective Stress, σ'.

c. Pore Water Pressure, u.

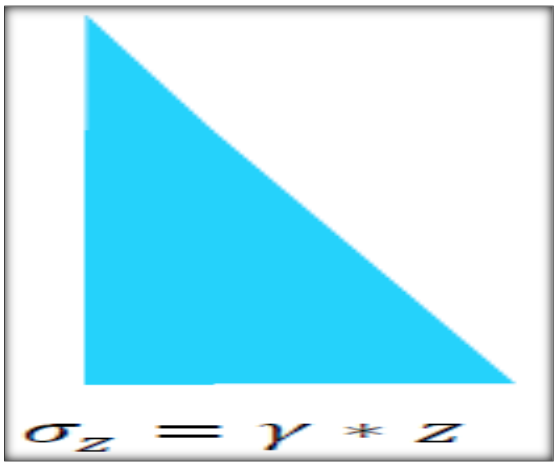

Figure III .4: Vertical stresses. [101]

III.2 .2.1 Total vertical stress

Consider a soil mass having a horizontal surface and with the water table at surface level. The total vertical stress at depth z is equal to the weight of all material (solids + water) per unit area above that depth, i.e. [101]

$$6\,z\,totale = \gamma sat * z \quad \text{(III.3)}$$

III.2 .2.2 Pore water pressure

The pore water pressure at any depth will be hydrostatic since the void space between the solid particles is continuous, therefore at depth z:

$$\mu = \gamma w * z \quad \text{(III.4)}$$

III.2 .2.3Effective vertical stress due to self-weight of soil

The pressure transmitted through grain to grain at the contact points through a soil mass is termed as effective pressure.

The difference between the total stress ($\sigma_{z\ totale}$) and the pore pressure (u) in a saturated soil has been defined by Terzaghi as the effective stress (σ'_z) [101]:

$$6'\,z = 6\,z\,totale - \mu \quad \text{(III.5)}$$

III.2 .3 Stresses in saturated Soil

If water is seeping, the effective stress at any point in a soil mass will differ from that in the static case.

It will increase or decrease, depending on the direction of seepage, the increasing in effective pressure due to the flow of water through the pores of the soil is known as seepage pressure. [101]

III.2 .3 .1 Stresses in saturated soil without seepage

A column of saturated soil mass with no seepage of water in any direction, the total stress at the elevation of point A can be obtained from the saturated unit weight of the soil and the unit weight of water above it. [102]

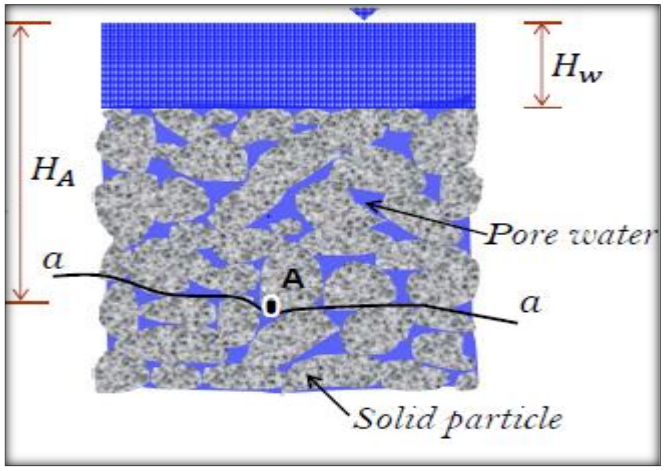

Figure III .5: Stresses in Saturated Soil without Seepage [103]

$$6\,z = \gamma w + (HA - H)\gamma sat \quad \text{(III.6)}$$

Where:

$б_z$= totale stress at the elevation of point A.

γ_{sat} = satured unit weight of the soil.

H_A=distance between point A and the water table.

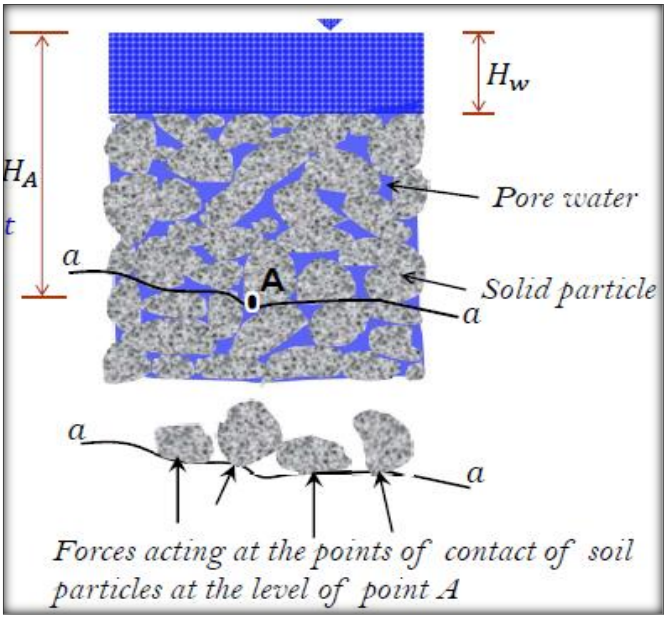

Figure III.6: Forces acting on soil in point A [103]

III.3 Stress due to a concentrated load

Individual column footings or wheel loads may be replaced by equivalent point loads provided that the stresses are to be calculated at points sufficiently far from the point of application of the point load.

Vertical stress due to a concentrated load [103]:

• Boussinesq's Formula.

• Wastergaard Formula.

III.3.1 Determination of the stresses due to an overload (Boussinesq's Formula)

Determining the deformation of the soil requires understanding the constitutive laws of the soil. The constitutive laws which reproduce the behavior of soils are complex; this is why the determination of the stress is generally separated from the determination of the strain.

In order to determine the stress due to the overload, one generally assumes a homogeneous and isotropic elastic soil. It is an acceptable assumption to determine the vertical component of the underground stress (far from the case of the horizontal stress) the calculation of the additional stress of non-heavy elastic medium is established by BOUSSINESQ [104].

III.3.2 Case of a point load

Consider an elastic medium, not heavy, homogeneous and isotropic, whose upper part is limited by an infinite horizontal plane, and is subjected to an isolated vertical force P. Boussinesq must prove that the direction of the stress applied to the horizontal facet centered on M is OM (O: the point of application of the force P), and that the expression of the component perpendicular to the facet is:

The Boussinesq method uses the theory of elasticity to calculate the vertical stress under a point load in a homogeneous, semi-infinite half space [105]:

$$\sigma L = \frac{3P}{2\pi.Z^2}\sin^5\theta \qquad \text{(III.7)}$$

Equation shows that the vertical stress is directly proportional to the load inversely proportional to the depth squared, and Proportional to some function of the ratio(r/z); it should be noted that the expression for z is independent of elastic modulus (E) and Poisson's ratio (μ), i.e. stress increase with depth is a function of geometry only To compute the stresses under a distributed load, the Boussinesq solution is integrated over the area of the footing. [105]

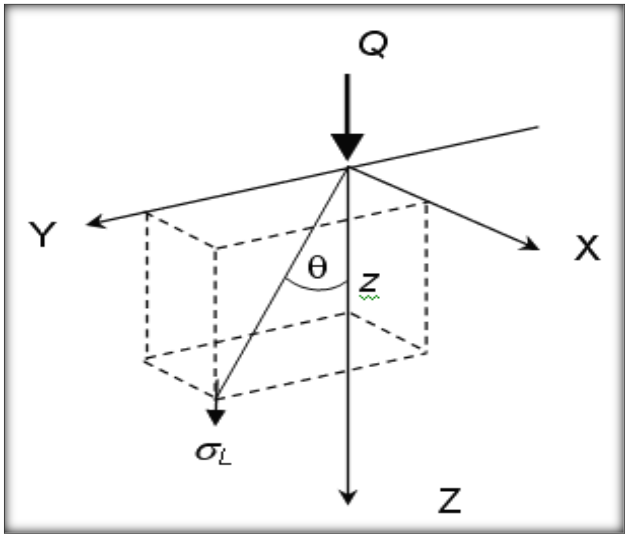

Figure III.7: Point load [105].

III.3.3 Case of a soil with a uniformly loaded horizontal surface

The vertical stress distribution on a horizontal plane at depth of z below the ground surface. [106]

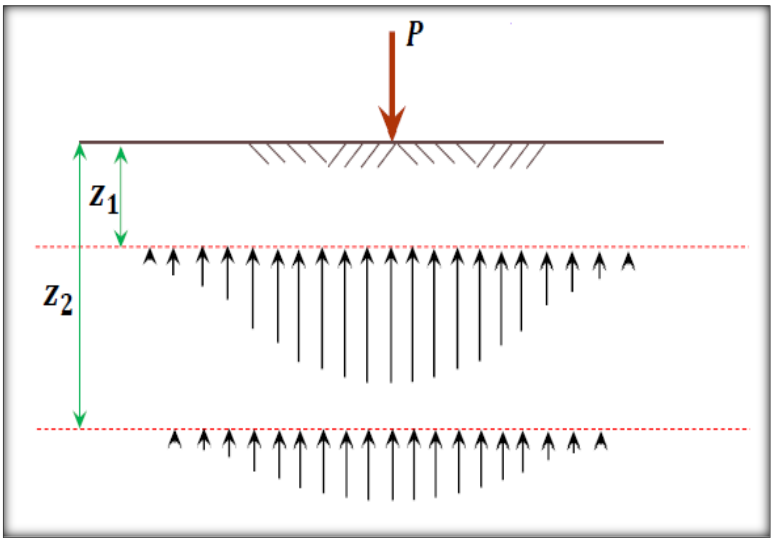

Figure III.8: Uniformly loaded horizontal surface. [106]

III.3.4 Distribution on a vertical plane

The vertical stress distribution on a vertical plane at a distance of r from the point load [106]:

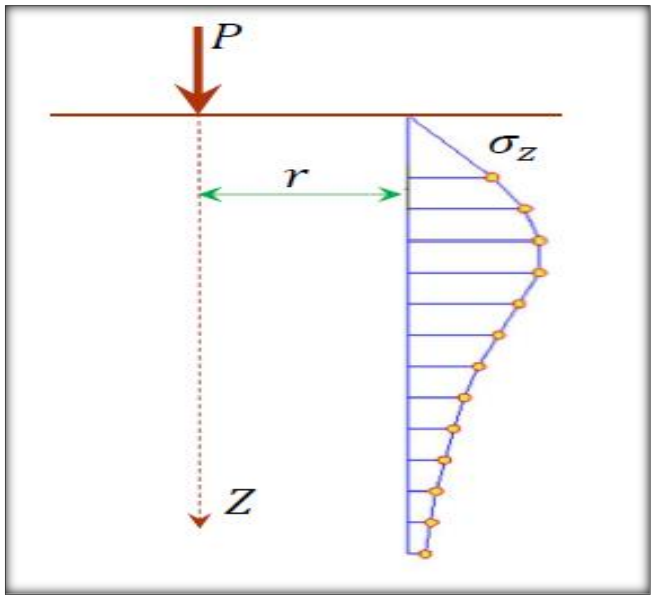

Figure III.9: Stress on vertical plane. [106]

III.3.5 Stress isobars

An isobar is a line which connects all points of equal stress below the ground surface in other words, an isobar is a stress contour. [106]

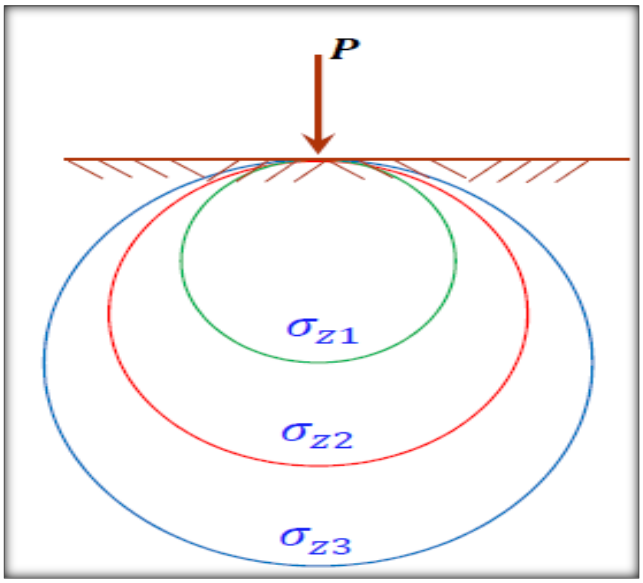

Figure III.10: Stress isobars. [106]

III.4 Determination of the stresses due to an overload (Westergaard Formula)

Westergaard proposed a formula for the computation of vertical stress σ_z by a point load, P at the surface as [107]:

$$6z = (p\ a)/(2\pi z^2[a^2 + \left(\frac{r}{z}\right)^2]^{\frac{3}{2}} \quad \text{(III.8)}$$

$$a = \sqrt{(1-2\mu)/(2-2\mu)} \quad \text{(III.8.a)}$$

In which μ is Poisson's ratio

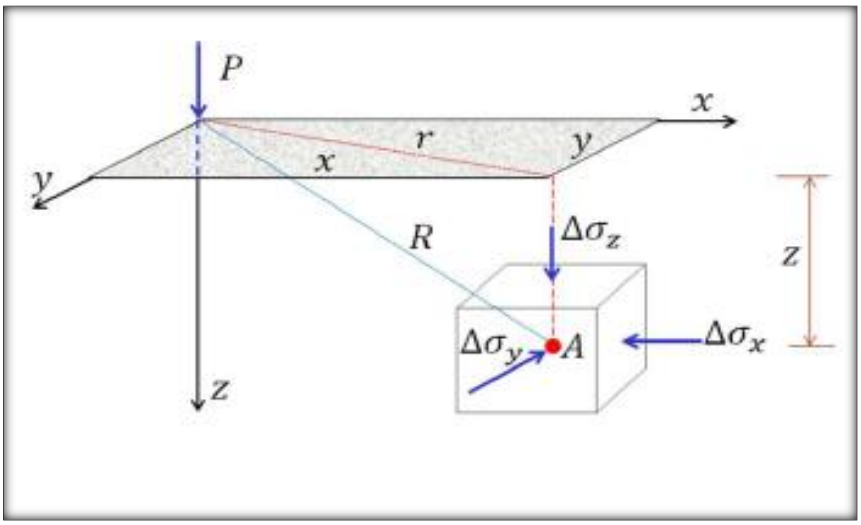

Figure III.11: Determination vertical stress by Westergaard. [107]

III.4 .1 Stress below a Line Load

The vertical stress increase due to line load, inside the soil mass can be determined by using the principles of the theory of elasticity. [107]:

$$6z = \left(\frac{2qz3}{\pi(x^2+z^2)^2}\right) \qquad \text{(III.9)}$$

This equation can be rewritten as:

$$\frac{\frac{6z}{q}}{z} = \frac{2}{\pi\left[1+\left(\frac{x}{z}\right)^2\right]^2} \qquad \text{(III.9.a)}$$

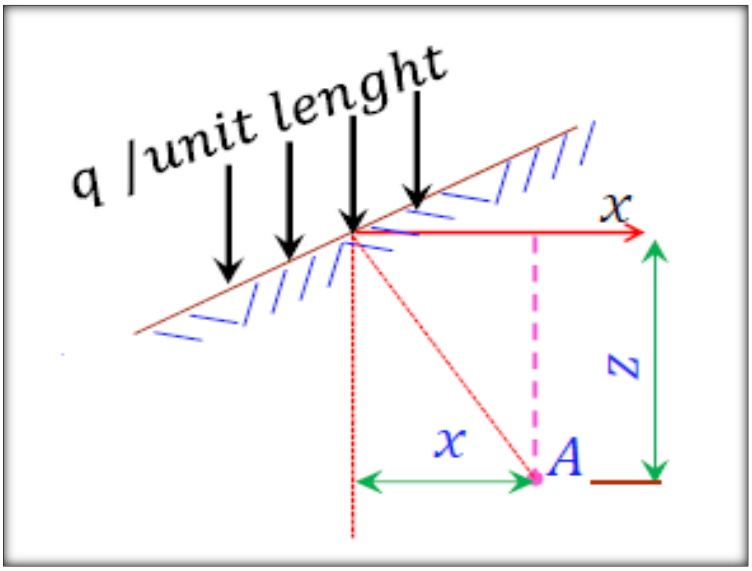

Figure III.12: Stress below a Line Load. [107]

III.4 .2 Vertical stress caused by a horizontal line load

The vertical stress increase (σ_z) at point A in the soil mass caused by a horizontal line load can be given as [108]:

$$6z = \frac{2q\,x\,z^2}{\pi(x^2+z^2)^2} \qquad \text{(III.10)}$$

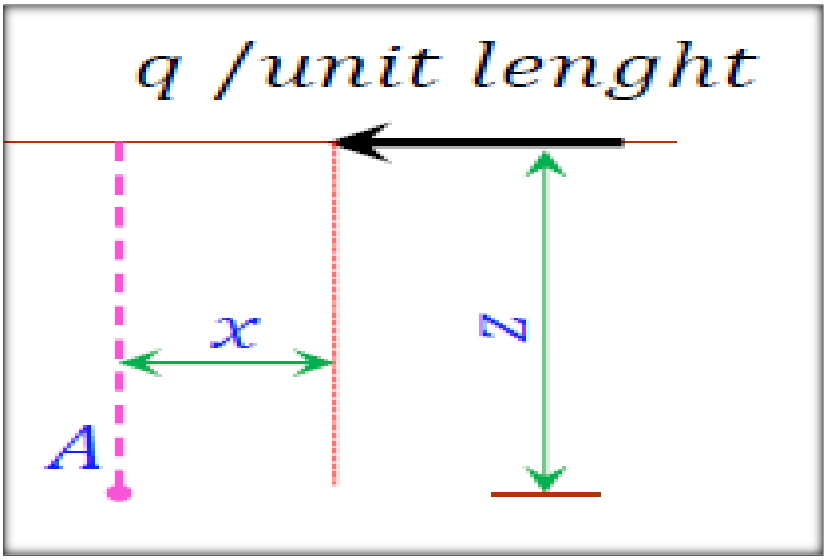

Figure III.13: Vertical Stress caused by a horizontal line load.

[108]

III.4 .3 Vertical stress caused by a strip load

The term strip loading will be used to indicate a loading that has a finite width along the x axis but an infinite length along the y axis.

The fundamental equation for the vertical stress increase at a point in a soil mass as the result of a line load can be used to determine the vertical stress at a point caused by a flexible strip load of width B.

Vertical stress at point A can be determined by equation [109]:

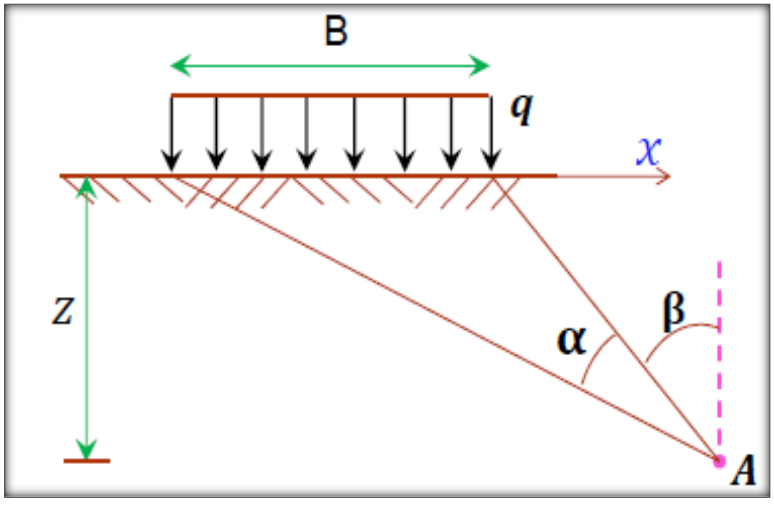

Figure III.14: Vertical Stress caused by a strip load. [109]

$$6z = (\frac{q0}{\pi})[(\alpha + sin\alpha \cos(\alpha + 2\beta)] \qquad \text{(III.11)}$$

III.4 .4 Vertical stresses due to embankment loading

The vertical stress increase in the soil mass due to an embankment of height H may be expressed as [110]:

$$6z = \left(\frac{q0}{\pi}\right)\left[\left(\frac{a+b}{a}\right)(\alpha 1 + \alpha 2) - \left(\frac{b}{a}\right)(\alpha 2)\right] \quad \text{(III.12)}$$

Where:

$q_0 = \gamma_h$

γ= unit weight of embankment soil.

H= height of embankment.

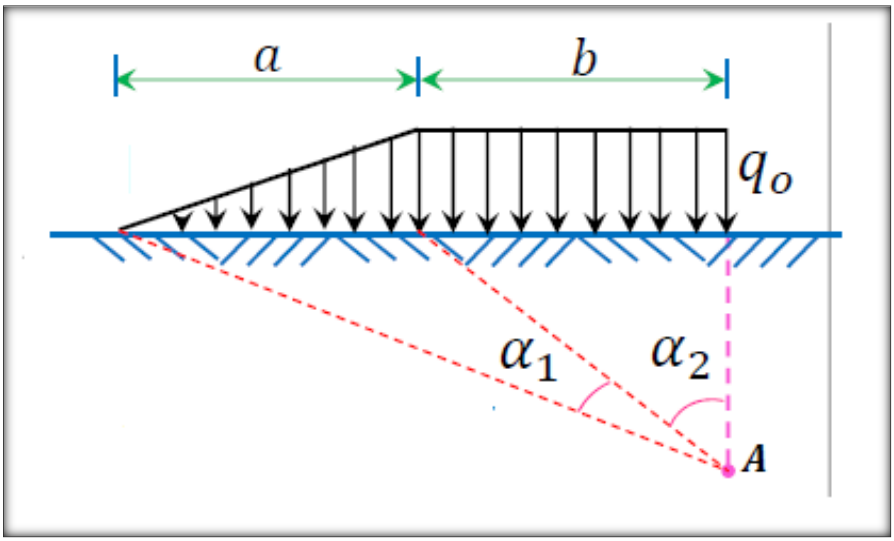

Figure III.15: Vertical Stresses Due to Embankment Loading. [110]

III.4 .5 Vertical stresses due to a uniformly loaded circular area

1- Under the center: The increase in the vertical stress (σz) at depth z (point A) under the center of a circular area of diameter D = 2R carrying a uniform pressure q is given by[110]:

$$6z = q[1 - \frac{1}{\left[\left(\frac{R}{z}\right)^2 + 1\right]}^{\frac{3}{2}} \quad \text{(III.13)}$$

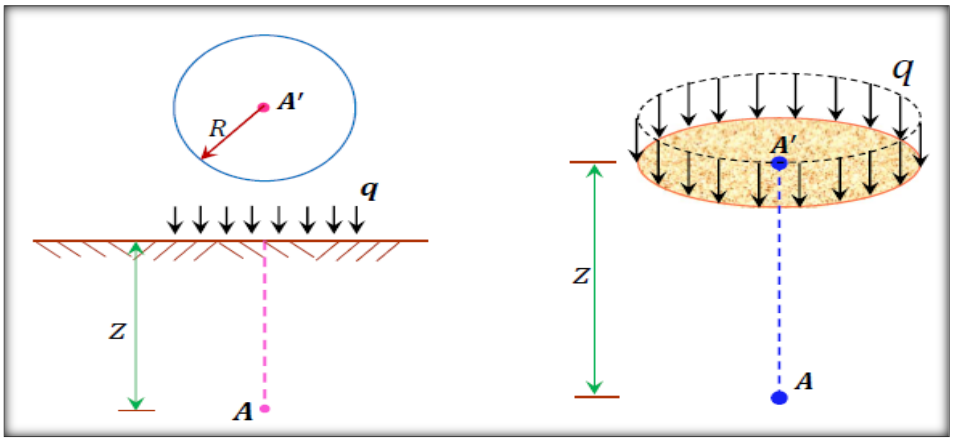

Figure III.16: Vertical Stresses due to a uniformly loaded circular area. [110]

2- At any point: The increase in the vertical stress (σ_z) at any point located at a depth z at any distance r from the center of the loaded area can be given:

$$6z = q(A' + B') \qquad \text{(III.13.a)}$$

Where A' and B' are functions of Z/R and r/R.

III.4 .6 Vertical Stress Caused by a Rectangular loaded area

The increase in the vertical stress (σ_z) at depth z under a corner of a rectangular area of dimensions B = m z and L = n z carrying a uniform pressure q is given by[110]:

Where:

$$6z = q0\ Iz \qquad \text{(III.14)}$$

I_z: influence factor depending on the ratio $\left(\frac{L}{Z}\right), \left(\frac{B}{Z}\right)$.

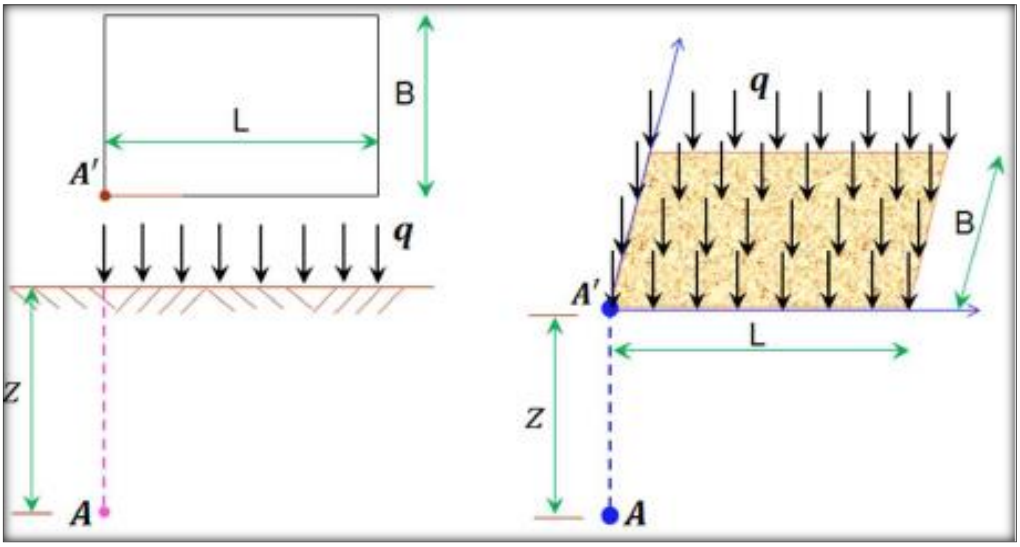

Figure III.17: Vertical Stress Caused by a Rectangular loaded area. [110]

$$Iz = \left(\frac{1}{4\pi}\right)\left[\frac{2mn\sqrt{m^2+n^2+1}}{m^2+n^2+m^2n^2+1}\right)\left[\frac{m^2+n^2+2}{m^2+n^2+1}\right] + tan^{-1}\frac{((2mn\sqrt{m^2+n^2+1})}{[(m^2+n^2-m^2n^2+1))} \quad \text{(III.15)}$$

The increase in the stress at any point below a rectangular loaded area can be found by dividing the area into four rectangles. The point A' is the corner common to all four rectangles. [110]

$$\sigma zA = \sigma z1 + \sigma z2 + \sigma z3 + \sigma z4 \quad \text{(III.16)}$$

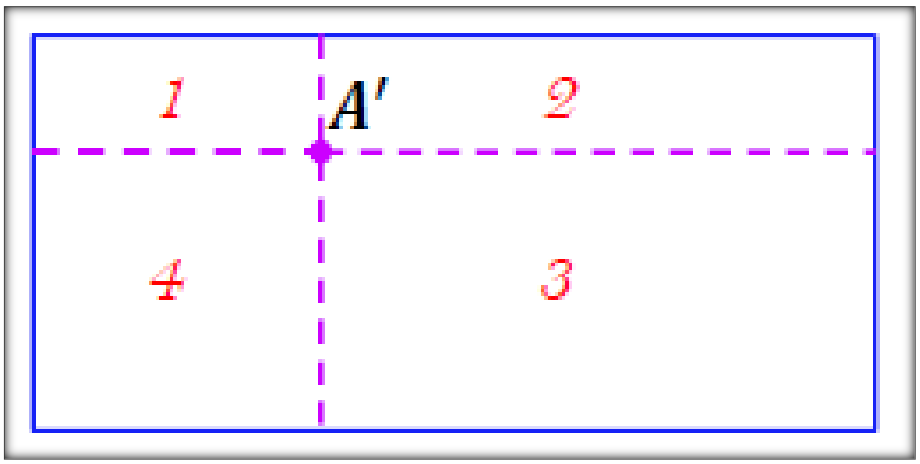

Figure III.18: Increase of stress below a rectangular loaded area. [110]

III.5 Calculation of settlement by the oedometric method

An oedometer test is a kind of geotechnical investigation performed in geotechnical engineering that measures a soil's consolidation properties.

Oedometer tests are performed by applying different loads to a soil sample and measuring the deformation response. The results from these tests are used to predict how a soil in the field will deform in response to a change in effective stress.

The compressibility of a soil is often measured in a laboratory by an oedometer or consolidometer, as shown in Figure III.18 in which the cylindrical soil sample is confined inside a ring in order to prevent lateral strain, Porous stones are placed on both sides of the soil to permit escape of water. [111]

The vertical load is applied to the soil in one of a variety of ways such as by application of weights to a hanger, by means of weights applied through a lever system to the top of the soil or by means of air pressure applied to a piston.

The amount of vertical compression experienced by the soil as a result of the application of load is measured by means of a dial gauge or a displacement transducer.

The conventional testing technique, which is described in most books on soil testing, consists of applying successive increments of load and observing the deflection after each increment until the movement ceases. [111]

In a saturated sample of soil, the application of the vertical load results in the development of a pore pressure (equal to the vertical stress applied) within the soil, this pore pressure gradually dissipates as water is expelled from the soil through the porous stones, movement of the soil continues until the pore pressure has fully dissipated.

Soil deflection continuing until approx. 24 hr. [111]

Figure III.19: Oedometer apparatus. [111]

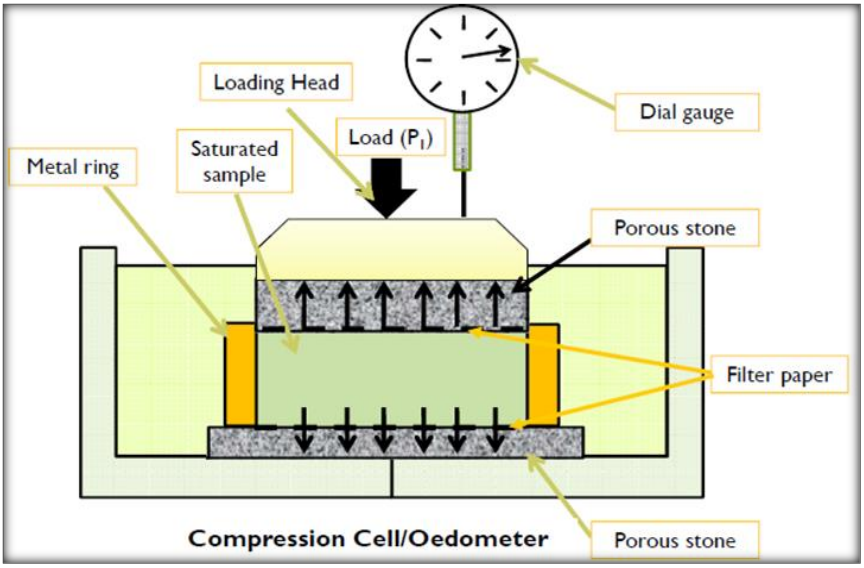

Figure III.20: Oedometer components. [111]

III.5.1 Types of oedometer

The major experimental difficulty with the oedometer test is side friction: shear stresses develop along the cylindrical surface of the specimen as vertical strains occur.

The presence of side friction disturbs the state of strain and prevents some of the axial force from reaching bottom portions of the specimen.

- To minimize the effect of these side friction forces the thickness-diameter ratio of the specimen is kept as small as practicable.
- Use of the oedometer with the floating ring container also helps to minimize the effects of side friction.
- Many attempts have been made to minimize side friction through the use of lubricants and plastic liner sheets.
- In a fixed ring oedometer the friction gradually decreases to zero towards the bottom.
- A floating ring oedometer has the plane of zero friction (i.e. the neutral plane) at the middle of the sample because the sample is compressed from both sides. [111]

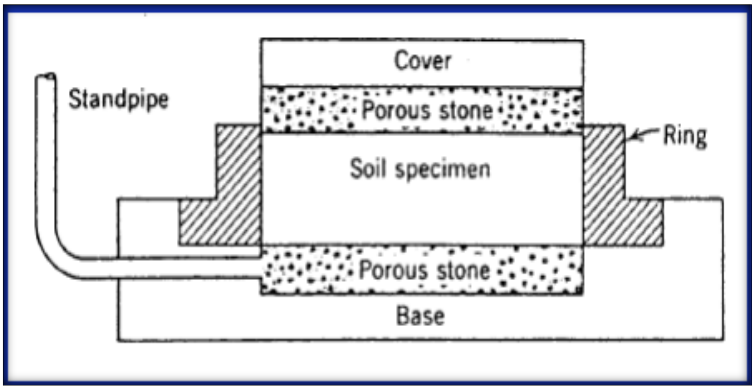

Figure III.21: Oedometer with Fixed ring. [111]

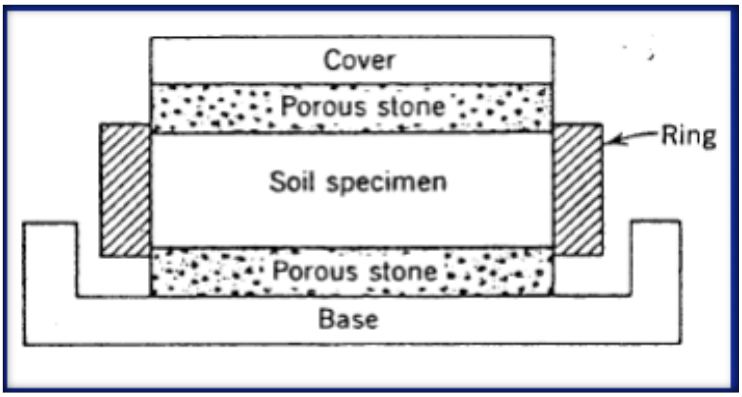

Figure III.22: Oedometer with Floating ring. [111]

III.5.2 Testing procedure

The typical testing procedure consists of the following steps:

- Position the dial gauge (or electronic instrument).
- Measure weight, height, diameter of the confining ring.
- Measure height (H) and diameter (D) of aluminum sample.
- Trim specimen into the confining ring.
- Take water content measurement from the trimmings.
- Weigh soil sample and confining ring.
- Soak porous stones and filter papers.
- Place the consolidation cell in the loading frame and adjust height. The loading beam should be almost horizontal.
- Take initial reading (R_i – reading will be subtracted from all measurements).
- Place seating load.
- Add water to the reservoir.

The load is maintained for a period of 24 hours (in certain clays the required time is 48 hours) during which the soil consolidates with drainage from the porous stones. Afterwards, the applied load is increased incrementally by doubling the applied stress at each stage. [112]

The number of the load stages and the maximum stress applied depends on the stress range of interest, during the loading process, water is provided into the cell so that the specimen remains fully saturated.

At each loading stage, readings of deformation are taken systematically to develop a time-settlement curve. That is, after the application of each load, the deformation is measured at 6, 15, and 30 seconds, then at 1, 2, 4, 8, 16, 30 min and at 1, 2, 4, 8 and 24 hours, respectively. [112]

When the maximum load is reached, and possibly in a load increment in between, an unloading stage is introduced that may be conducted in one or multiple steps; typically, the load is reduced by a factor of 4 at each step. When the test is completed, the final height of the sample and its water content are measured. [112]

III.5.3 Oedometric compressibility curve

For clay soils, which are the most compressible in general, the relationship between the effective vertical stress and the void index obtained in oedometric tests is bilinear in semi-logarithmic coordinates.

This oedometric compressibility curve makes it possible to define the three parameters which make it possible to calculate the test amplitudes in the oedometric method, namely:

- The compression index C_c,
- The swelling (or recompression) index C_s;
- The pressure of pre-consolidation (consolidation) σ'_p.

For the entire test on the trace the oedometric curve, volume variation or more precisely variation of the void index and as a function of the decimal logarithm of the stress (Figure III.22).

By simplifying, we obtain a first straight line with a slight slope and a second straight line with a much higher slope. [112]

The intersection of the 2 lines is the maximum preconsolidation stress that the soil has known in its history (this is the largest effective vertical stress applied to the soil in its history). This test allows to know the initial state of the soil (σ'_{v0} and e_0).

- If the current effective stress σ'_{v0} is less than the preconsolidation stress σ'_p, in this case the soil is overconsolidated;
- If the current effective stress $\sigma'v_0$ is equal to or greater than the preconsolidation stress σ'p, the soil is normally consolidated.

The slopes of the two (02) straight lines C_s and C_c account for the compressibility of the soil respectively in the overconsolidated domain and in the normally consolidated domain. [112]

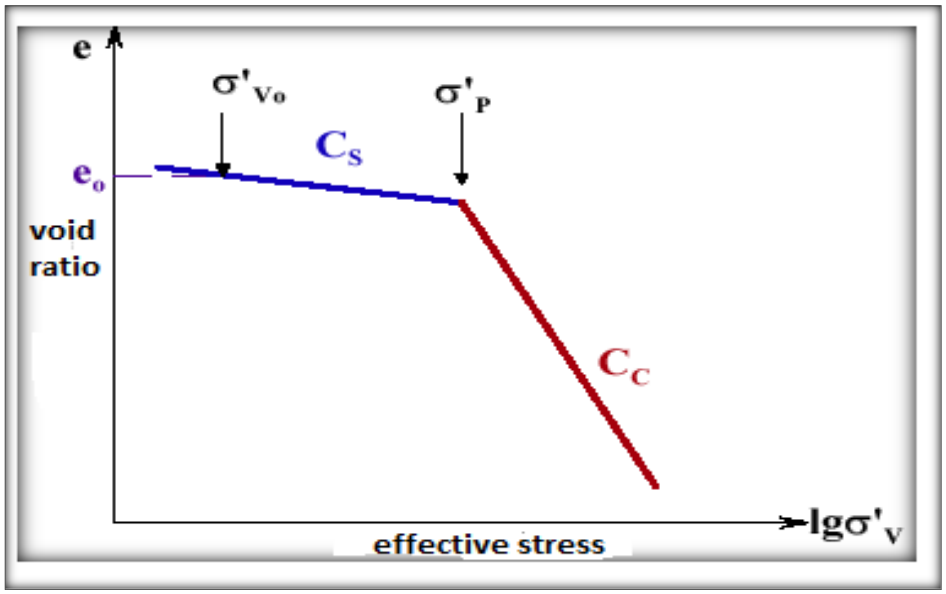

Figure III.23: Oedometric compressibility curve. [112]

Knowing the effective vertical stress $\sigma'v_0$ and the corresponding initial void index e_0; we calculate the variation of the void index by one of the formulas:

$$e = e0 - Cs \log\left(\frac{\sigma'vf}{\sigma'v0}\right) \quad \text{(III.17)}$$

$$e = e0 - Cc \log\left(\frac{\sigma'vf}{\sigma'v0}\right) \quad \text{(III.17.a)}$$

$$e = e0 - Cs \log\left(\frac{\sigma'vf}{\sigma'v0}\right) - Cc \log\left(\frac{\sigma'vf}{\sigma'v0}\right) \quad \text{(III.17.b)}$$

Depending on the position of σ'_{v0}, σ'_{vf} and σ'_{p}.

The calculation of the settlements of a point on the ground surface is carried out in two stages:

1. Determination of the variation with the depth of the effective vertical stresses under the point considered;
2. Calculation of the surface settlement by integration of the elementary settlements given by the oedometric formula:

$$S = \Delta H = \int \varepsilon\, v\, dz = \int \frac{\Delta e}{(1+e)} dz \quad \text{(III.18)}$$

In the current case where the soil mass is considered as a stack of homogeneous layers, the vertical stresses are calculated in the middle of each layer and the following formulais used for the calculation of the settlement of the layer, of initial thickness H_0 .

$$S = \Delta H = \frac{\Delta e}{(1+e0)} H0 = \left[\frac{H0}{1+e0}\right)\left[Cslog\ \left(\frac{\sigma'p}{\sigma'v0}\right) + Cclog\frac{\sigma'vf}{\sigma'p}\right] \quad \text{(III.19)}$$

For certain structures built on clay soils, a long-term settlement, known as creep, is added to the oedometric settlement.

It is suggested to use the following procedure for the computation of settlements by the oedometric method. [112]

Step 01: Define the geometry of the problem and the points whose settlement will be calculated (point P in Figure III.23). Determine the points located in the middle of the layers vertically to these points (points A, B, C, and D under point P, in Figure III.23).

Step 02: Calculate the increase in vertical stress at the chosen points, using the appropriate abacus.

Step 03: Calculate the settlement of each layer at the chosen points. $s(layer) = \Delta H(layer) = f\left(sol, \Delta\sigma_v^{'}\right)$

Step 04: Add the settlements of the layers to obtain the settlement at the surface. .

$$s(total) = \Delta H(total) = \sum_{layers} \Delta H(layer)$$

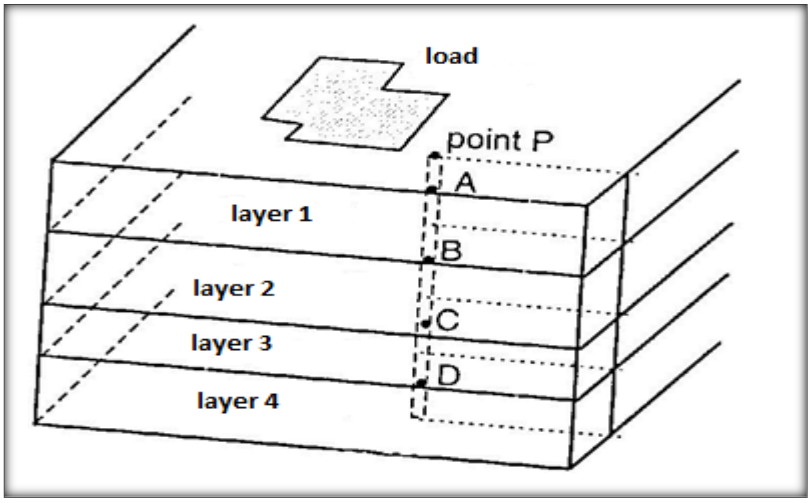

Figure III.24: Calculation principle of settlement. [112]

III.6 Calculation of settlement by the pressiometric method

The test was invented by Kögler in the 1930s, but only took off today under the leadership of Menard in 1955.

The principle of the test consists of radially expanding, in a borehole previously carried out, a cylindrical probe, and measuring the relationship between the pressures applied to the ground and the displacement of the wall of the probe.

Among the information that can be deduced directly from this test, we note in particular the pressuremeter modulus EM, the limit pressure PLM, and the creep pressure P_f.

This test for recognizing the soil in place is associated with a method for calculating the foundations. Superficial or deep. It is used to assess the bearing capacity of foundations and induced settlements. [113]

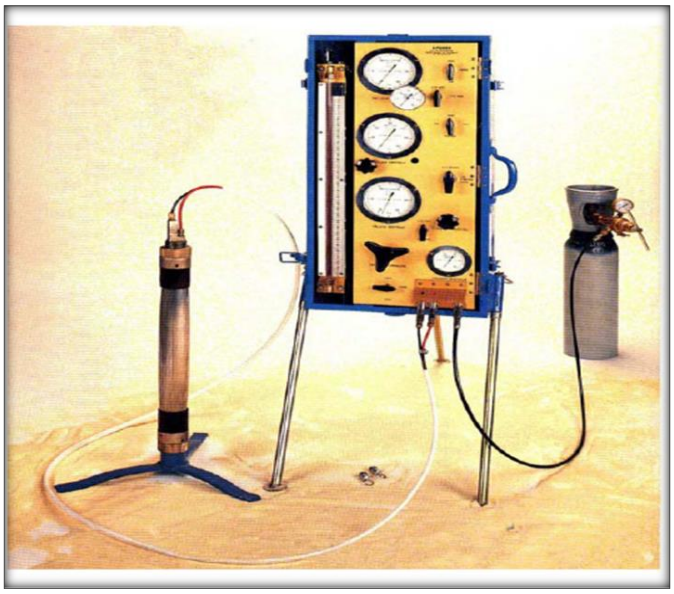

Figure III.25: The pressure Metter test. [113]

The pressuremeter is used in Algeria for dimensioning the foundations of buildings and structures; it is a soil loading test that measures in place both a deformability characteristic, the pressuremeter modulus, and a soil resistance characteristic, the limiting pressure. These two characteristics are usually used directly to determine the allowable stress (ELU) and settlement of foundations (SLS) using charts or rules of thumb. [114]

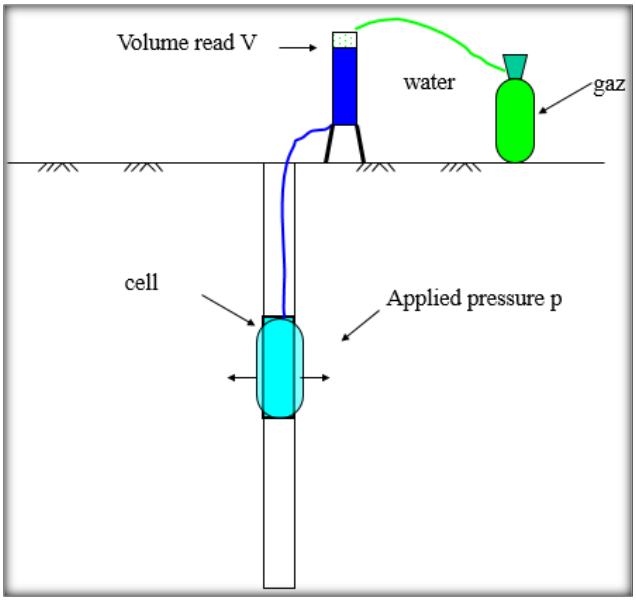

Figure III.26: Principle of the test. [114]

It is an in situ test during which the soil behavior is observed up to failure of expanded cylindrical cavity induced by a flexible cell expandable subjected to increased water pressure.

The pressuremeter test is designed to be used both to calculate the bearing capacity and the estimation of settlement. Indeed, punching the ground by a foundation (in particular rigid) corresponds to the lateral expansion of the pressuremeter probe.

Although these two stresses are different in the direction where the soil is requested, they have the common point to produce shearing by which the soil reaches failure. Due to be performed in any soil type (sand, clay, etc. ...), regardless of its state (saturated, wet or dry), the pressuremeter characteristics, at least obtained with the device most commonly used (PMT), inform the behavior of the mixture "solid skeleton and water" without testing the saturation of the soil. [114]

The method of calculating settlements from the Menard pressuremeter is the calculation method originally proposed by Menard.

The pressuremeter module (EM) is a deviatoric module, particularly suitable for calculating the settlement of foundations for which the deviatoric stress field is preponderant, namely the "narrow" foundations, such as the footings of buildings and structures. [114]

The settlement formula is given by Equation (III.20):

$$S = Sc + Sd = \frac{\alpha 9}{9\,Ec}\lambda cB + \frac{2\,q}{(9Ed)}B0\left(\frac{\lambda dB}{B0}\right)^{\alpha} \qquad \text{(III.20)}$$

Where:

q is bearing capacity

λ_c et λ_d are form coefficients, given in Table III.1.

α is rheological coefficient, depending on the nature, the structure of the soil (or the rock) and the time, given in Table III.2

B is width (or diameter) of the foundation.

B_0 is reference dimension equal to 0.60 m.

E_c and E_d are Equivalent pressuremeter modules in the volume zone and the deviator zone, respectively. [114]

Table III.1: Values λ_c and λ_d . [114]

L/B	circle	square	2	3	5	20
λ_c	1	1.10	1.20	1.30	1.40	1.50
λ_d	1	1.12	1.53	1.78	2.14	2.64

Table III.2: Rheological coefficient α for clays silts and sands. [114]

Nature of the soil	Clay		Silt		Sand	
Soil condition	E_M/P_{lim}	α	E_M/P_{lim}	α	E_M/P_{lim}	α
Overconsolidated or very tight	>16	1	>14	2/3	>12	1/2
Normaly consolidated or tight	9-16	2/3	8-14	½	7-12	1/3
Underconsolidated and remolded or loose	7-9	2/3	5-8	½	5-7	1/3

Figure III.27 shows the soil layers taken into account in the weighting of pressuremeter modules (EM) for Equations (III.21)

The E_c module is that of layer 1. The (E_d) module is calculated with the following weights[114]:

$$\left(\frac{1}{Ed}\right) = \left(\frac{0.25}{E1}\right) + \left(\frac{0.3}{E2}\right) + \left(\frac{0.25}{E3.5}\right) + \left(\frac{0.1}{(E6\text{à }8}\right) + \left(\frac{0.1}{E9\text{à}16}\right) \quad \text{(III.21)}$$

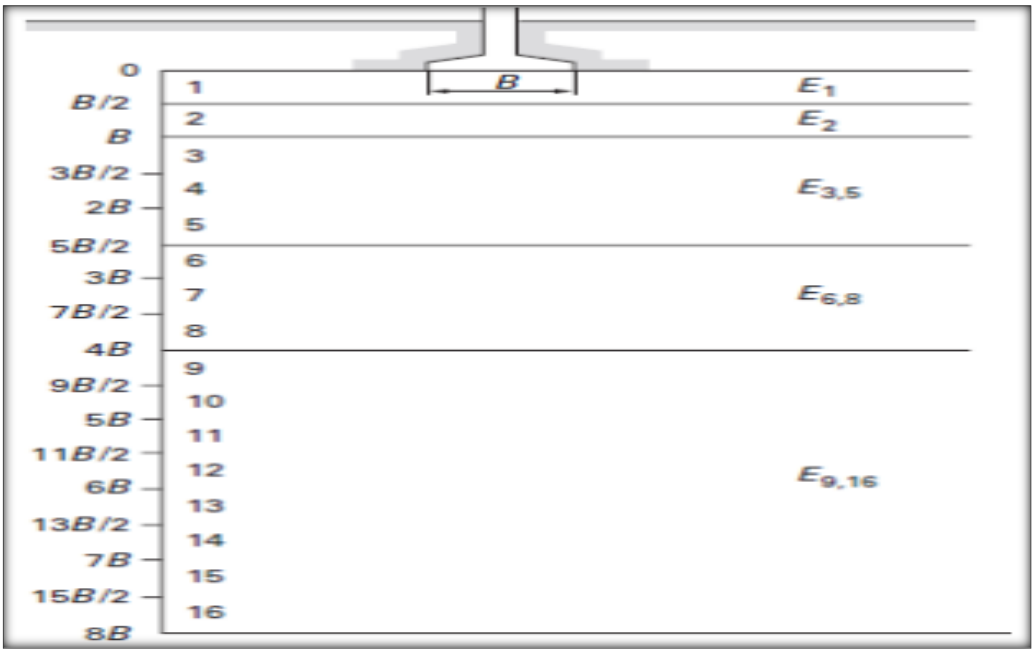

Figure III.27: Weighting diagram of pressuremeter modules. [114]

III.6 Static penetration test (CPT) method

The cone penetration test (CPT) has also been used extensively in the past to estimate settlement of shallow foundations on granular soils. Most of the approaches based on the results of the CPT rely on the tip resistance values obtained from the test.

A description of the mechanics of the CPT is presented in Appendix B along with a brief discussion regarding the differences between mechanical and electrical cones.

In this section, several methods for estimating settlement using CPT results which have been presented in the literature are described. [115]:

The process of defining the calculation method is based on a multitude of approximations (interpretation of the oedometric loading curve, adjustment, and statistical analysis), which requires a calibration of the formulas obtained compared to the conventional method based on the oedometric test. This operation was carried out by launching the computation of settlement by the two methods of three foundations stuck at 1.5 m in relation to the natural ground and having the slenderness L / B = 1,2 and 10. [115]:

The case studies are those used to develop the penetrometric method It was noted that the ratio $\frac{scoed}{scCPT}$ decreases from 1.48 for L / B = 1 to 1.24 for L / B = 10, whatever the vertical pressure applied to the foundation. The settling coefficient of the settlement thus decreases slightly with the slenderness L / B, but can take an average value of 1.35 with a coefficient of variation of 9%, which indicates a rather low dispersion.

Finally, we can reformulate the calculation equation for the one-dimensional consolidation settlement s_c of a slice of the soil, H_0 thick and subjected to a final effective stress σ_v 'from the CPT test, taking this calibration into account [115]:

$$sc = 0{,}6 \left(\frac{H0}{(qc/(\sigma v0\prime)}\right) F(\sigma v') \qquad \text{(III.22)}$$

Is the normalized static penetrometer resistance, and F (σ_v') is adopted as a function of vertical stress distribution, given by:

$$F(\sigma' v) = \frac{\frac{\Delta' \sigma v}{\sigma' v0}}{1+\left(d\frac{\Delta \sigma' v}{\sigma v0}\right)}. \qquad \text{(III.23)}$$

Figure III.28 illustrates the variation of the function F and is used in practice as an abacus for the graphical evaluation of F as a function of the relative variation of the stresses. [115]:

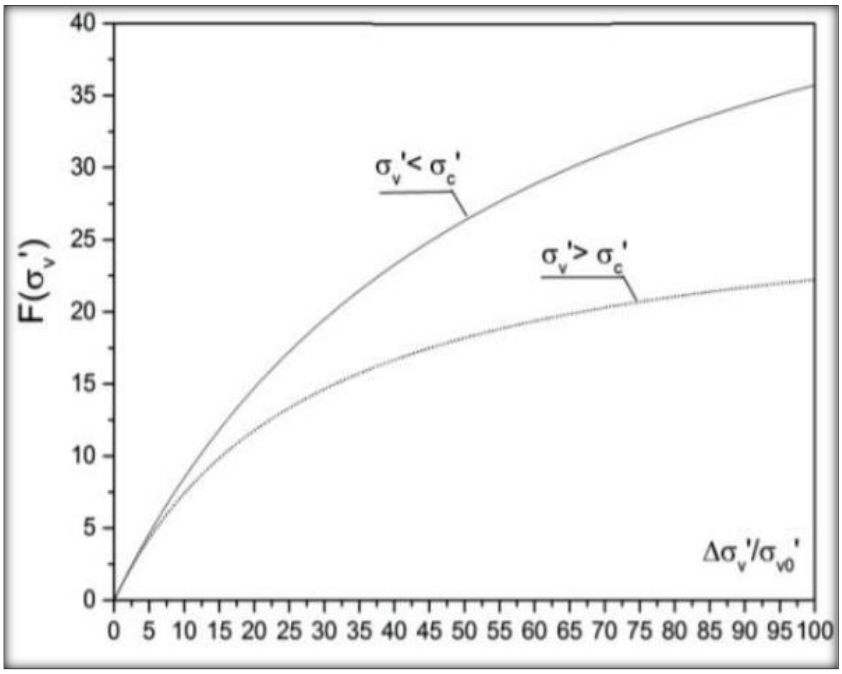

Figure III.28: Abacus of the function F (σ_v '). [115]

III.6.1 Settlement computation methods

The cone resistance (i.e. without the use of friction jacket) is used for computing the settlement of & footing.

The cone resistance shall be corrected for the dead weight of the cone and sounding rods in use Based on static cone penetration test data, there are two methods in use for the estimation of settlement of a footing [116]:

(1) De-Beer and Marten's method.

(2) Schmertmann's method. [116]

III.6.1.1 De-Beer and Marten's method

Are proposed a settlement calculation method based on the semi-empirical Terzaghi-Buishman formula in the following form:

$$Si = \left(\frac{Hi}{c}\right) \log e \left(\frac{pi+\Delta pi}{pi}\right) \quad \text{(III.24)}$$

S_i: Settlement of a Layer of sand of thickness H_i.

Δp_i= averagement increase in vertical stress in a layer due to footing load.

p_i= mean effective overburden pressure for the layer.

C= a constant of compressibility which is related to static cone resistance by the equation $C = 1.5 \left(\frac{qc}{Pi}\right)$.

q_c =being the static cone penetration resistance.

P_i = versus depth curve is broken into several parts each having approximately same values of q_c.

The average cone resistance of each layer is taken for calculating the constant of compressibility, P_i and ΔP_i values at the middle of each layer are representative to that layer. [116]

III.6.1.2 Schmertmann's method

Has proposed a semi-empirical equation based on the similarity of the shape of the deformation distribution in sand under a footing to that of an elastic medium idealizing the distribution of the deformation influence factor I_z in the form of a triangle to a depth of 2B under the footing for a square (B is the width of the footing) and 48 for a long footing (I≥10 B). [116]

The deformation within each layer is considered as: $I_z = p/E_z$

Where:

I_z is a deformation influence factor.

Thus:

$$S = C1\ C2\ \Delta P\ \sum \left(\frac{Iz}{qc}\right) \Delta z \quad \text{(III.25)}$$

Where:

C1 is a depth correction factor

C2 is a creep factor to be taken as follow:

$$C1 = 1 - 0{,}5 \left(\frac{\sigma' v0}{\Delta p}\right) \geq 0{,}5 \quad \text{(III.25.a)}$$

$$C2 = 1 + 0{,}2 \log 10(10t) \quad \text{(III.25.b)}$$

σ'_{v0}= effective in situ overburden pressure at foundation level .

Δ_P = net loading intensity at foundation level.

T= time in years from load application.

X= 2, 5 for a square foundation.

X= 3, 5 for a long foundation.

Δ_z= thickness of level.

B= width of the footing.

I_z= (the strain influence factor) should be taken are given in eq (41):

$$Izp = 0{,}5 + 0{,}1 \left(\frac{\Delta P}{\sigma' vp}\right) \quad \text{(III.26)}$$

Where:

σ'_{vp} = effective vertical stress at the depth where the peak occurs, that is, at a depth if B/2 and B respectively for a square and a long footing.

The cone resistance diagram is divided into layers of approximately equal or representative values of q_c.

The settlement in each layer resulting from the loading intensity ΔP is then calculated using the values of E and I_z appropriate to each layer

The sum of settlement in each layer is then corrected for the depth factor and creep factor using eq (III.25.a) and (III.25.b) respectively. [116]

III.7 Standard penetration test

The use of the Standard Penetration Test to estimate the settlement of shallow foundations on granular soils is deeply seated within the practice of geotechnical engineering. The authors feel confident in suggesting that this test has been and remains to be the most often used tool to make such estimates. This is in part due to the fact that the test is widely available, easily understood, and low cost even though the test is subject to wide variations in procedures and results despite being standardized by ASTM, However the test remains the most commonly used in situ test in practice. [117]

Most of the methods will present in this section are considered empirical. That is, they rely on either a direct correlation between the average N blow count value (either corrected or uncorrected) and observed settlement, or the blow count value is used to obtain an intermediate design parameter, the correlation of which is based on observations. [117]

III.7.1 Terzaghi and Peck (1948, 1967)

This method is based primarily on shallow foundation bearing capacity charts developed using the bearing capacity equations presented by Meyerhof (1956).

The charts are used to obtain the allowable bearing capacity (although the F.S. used is not stated) for different footing widths and SPT blow counts values with the maximum settlement not greater than25 mm (1 in.) and a differential settlement not greater than 19 mm (3/4 in.) at a given allowable bearing capacity.

According to Terzaghi and Peck, square and continuous footings of the same width show similar settlement behavior for the same soil and loading intensity. [117]
Settlement is given as:

$$S = \left(\frac{8q}{N}\right)(Cw\ Cd) \qquad (for\ B \leq 4ft) \tag{III.27}$$

$$S = (12q/N)[B/(B+1)]^2\ Cw\ Cd\ \ (for\ B > 4ft) \tag{III.27.a}$$

$$S = \left(\frac{12q}{N}\right) Cw\ Cd \qquad (for\ raft\ ) \tag{III.27.b}$$

These expressions can also be stated in generale form as:

S=settlement (in inches).

q =net footing stress (in tsf).

N=uncorrected (field) blow counts.

B=footing width (in ft).

C_w=water correction.

C_w =2-(W/2B)≤ 2 for surface footing .

C_w =2-0,5 (D/B)≤ 2 for fully submerged .

Embedded footing W≤D.

C_d= embedded correction.

C_d =1-0, 25 (D/B).

Where:

W = depth of water table (in ft.).

D = footing depth (in ft.).

The uncorrected SPT blow count data are used in calculating settlement, however, if the sand is dense, saturated and very fine or silty (e.g., abundant fines content), it was recommended that the blow count should be corrected according to[117]:

$$N0 = 15 + 0{,}5\ (N - 15)\ for\ N > 15 \tag{III.28}$$

The correction for water table applies to cases where ground water is at or above the base of the footing (complete submerged case). For partial submergence (water

located between D and D+B) a correction factor is given for surface footings (no embedment) only. In common practice, the water correction is often omitted from the settlement estimates using this method since the method is generally considered to be overly conservative. [117]

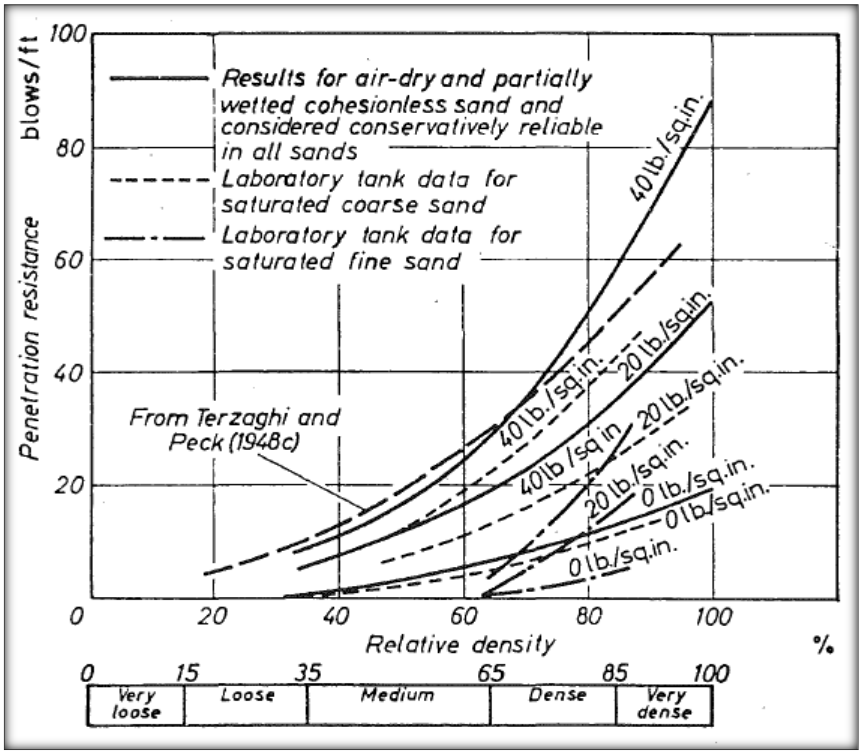

Figure III.29: SPT Correction. [117]

III.8 Dilatometer test

Marchetti (1980) suggested that the Dilatometer Modulus, could be used to estimate the One-dimensional constrained modulus, and provided an empirical approach to estimating Settlement; this was also shown by Schmertmann (1981) to be a reasonable approach as evaluating soil stiffness. . [118]

The DMT has proven especially useful for rapid and economical preliminary estimates of settlements of shallow foundations and has been used in a number of different soils; each DMT produces a predicted modulus value at a particular point in the foundation soil, and at the particular effective stress condition existing at that point at that true. [118]

The engineer can calculate this condition by computing total vertical overburden pressure and the equilibrium water pressure at each point. All soil modulus values are effective stress dependent to varying degrees on vertical and horizontal pre-stress magnitudes, cementation, etc. In some problems it may be advisable to adjust the DMT

determined modulus values to better match the vertical stress changes imposed by the structure involved during its construction and service life as outlined. [118]

III.8.1 Schmertmann method (1986)

Schmertmann (1986) recommended a procedure to estimate footing settlements based on the work by Janbu (1963, 1985) in which it was pointed out that among other things, using a simple modulus concept could significantly simplify the understanding and calculation of consolidation settlements.

Janbu suggested using the following equation of calculate consolidation settlement:

$$S = \sum \left(\frac{\Delta\sigma' v}{Mihi}\right) \qquad \text{(III.29)}$$

Where:

s = settlement.

h =the thickness of each "i" soil layer or sublayer.

i =the ith layer in a total of n layers (total thickness of H).

M =the applicable vertical dimension modulus of compressibility in the "i" the soil layer.

$\Delta\sigma'_v$= effective stress increase at the mid-height of each "i" layer that produces the settlement.

The first term in brackets in Equation (44) computes the vertical strain, which is then multiplied by the layer thickness to obtain the consolidation settlement for that layer, and all such layers are then summarized to give the total settlement.

The step-by-step procedure presented by Schmertmann is presented below.

III.8.2 Method A - ordinary method

I. Perform a DMT sounding at each settlement analysis location and determine profiles of M through the soil layers of interest.

2. Divide the compressible soils into layers and/or sublayers of similar soil type and stiffness.

3. Determine the average M value from the DMT results for each layer and sub layer in 2.

4. Calculate the vertical stress increase $\Delta\sigma_v$ at the mid-height of each layer and sublayer in 2 using any suitable method to calculate the vertical stress increase.

5. Calculate the 1-D settlement of each later or sub layer using the following equation:

Settlement= (stress increase x thickness)/ (modulus): $\Delta\sigma_v$ H/M

6. Obtain the total settlement by adding all the contributions from the layers and sublayers in step 5.

7. Make corrections to the settlement calculated in step 6, as appropriate and using DMT experience with similar soils and loadings. [118]

III.8.3 Method B - Special Method

This method includes the extra steps 4.1 to 4.5, the soil purpose of which is to adjust M to the average vertical effective stress during the loading that produces the settlement of interest.

4.1. Calculate the initial effective overburden stress σ_d at the mid-height of each layer and sublayer in step 1.

4.2 Determine the average $p_{'c}$ and ad' value from the DMT results for each layer and sublayer in step 24.3 Compare (σ_d' vs. $\sigma_{'0}$ (the effective overburden pressure at the time of the structure loading may not be the same as at the time of the DMT because of excavation, surcharge, dewatering, etc.)

4.4 Compare pc' and ($\sigma_{0'} + \Delta\sigma_v$) and decide on which of the following cases applies to each layer or sublayer.

a. All virgin compression: use M for the normally consolidated (NC) case.

b. All recompression: use M for the OC case.

c. The stress increase spans part recompression and part virgin compression: use M from step 4.5 below.

4.5 Make adjustments to the average M values in step 3, as needed.

Schmertmann reported the results of 16 comparisons using this technique and field observations.

The range in the ratio of DMT predicted/measured was 2.2 to 0.7 with an overall mean of about 1.1, corrections to the settlement computation to account for three-dimensional effects, secondary compression, aging, structural rigidity, etc. still should be applied as the engineer feels necessary. [118]

III.8.4 Leonards and Frost (1988)

A modification to the Schmertmann (1970) method for predicting settlement of shallow foundations on granular soils using the results of the CPT was presented by Leonard and Frost (1988) for use with the DMT.

This method acknowledges the effects of overconsolidation on reducing the compressibility of soil and suggests evaluating the preconsolidation stress so that settlements in both the reload and virgin loading range may be evaluated. The step-by-step procedure as presented by Leonard’s and Frost (1988) is as follows:

1. Perform DMT and CPT soundings at appropriate locations through soil layers of interest.

2. Divide the soil profile into layers with similar characteristics for settlement calculations.

3. Determine the average q_c/σ'_{v0} ratio and K0 value for each layer.

4. Determine K (OC) according to:

$$K(OC) = 0.376 + 0.095\,K0 - 0.0017\left(\frac{qc}{\sigma' v0}\right) \quad \text{(III.30)}$$

5. Using the chart prepared by Marchetti (1985) from the Durgunoglu and Mitchell (1975) equations, determine $\phi_{ps.}$

6. Calculate the value of ϕax from:

ϕax = ϕps - [(ϕps - 32°)/3)].

7. Determine OCR from:

$$\text{OCR} = \left[\frac{\text{K(OC)}}{1-\sin\phi}\right](1-\sin\phi)^{\frac{1}{0{,}8\sin\phi}} \quad \text{(III.31)}$$

8. Calculate the initial vertical effective stress at the center of the layer.

9. Determine the preconsolidation pressure at the test elevation as:

10. Determine the stress increment at the center of the layer due to the applied load.

II. Determine the final stress at the center of the layer as:

$$\sigma' f = \sigma' v0 + \Delta\sigma' \quad \text{(III.32)}$$

12. Determine that portion of the load increment that will be in the OC range R, (OC) and in the NC range R (NC) as:

$$Rz(OC) = \frac{P'c - \sigma' v0}{\sigma' f - \sigma' vo} \quad \text{(III.33)}$$

$$Rz(NC) = \frac{\sigma' f - P'c}{\sigma' f - \sigma' v0} \quad \text{(III.33.a)}$$

13. Determine the average E0 value for the layer.

14. Determine the strain influence factor I_z for the layer from Schmertmann's approximation).

15. Calculate the settlement for the layer from [118]:

$$S = c1qnet \sum_0^D Iz\Delta z \frac{Rz(OC)}{Ez(OC)} + \frac{Rz(NC)}{(Ez(NC)]} \quad \text{(III.34)}$$

III.8 Plate load test

The use of the plate load test has in the past been an attractive approach to predicting the settlement of shallow footings on granular soils, largely because the plate acts as a prototype.

Foundation and load is applied in the same direction as anticipated by the foundation. In order for the results of a plate load test to be useful in predicting settlements the test must be performed on soil which is representative of that to be stressed by the foundation, which means that the surface where the plate test is to be performed must be undisturbed and that the soil throughout the zone of influence of the plate and the foundation is the same.

However, since the stiffness of granular soils is related to the stress level in the ground (i.e. modulus is stress dependent) errors maybe associated with evaluating stiffness from small plate tests (typically 0.3m) and then extrapolating the results to larger footings. [119]

III.8.1 Barata method (1973)

Barata also pointed out that the expression for settlement of plates on granular soils was Severely limited in application and that in many cases the results obtained from this extrapolation would be in error. It was suggested that an expression based on the concepts suggested by Housel (1929) and Burmister (1947) would be of more general applicability.

According to Housel (1929) the settlement of a square plate with side B = 2b on the surface of the ground is given as [119]:

$$S = n0 + m0\left(\frac{P}{A}\right) \qquad \text{(III.35)}$$

Where:

s = settlement.

n0 & m0 = characteristic coefficients of the ground.

P =perimeter of the plate.

A= area of the plate.

III.9 Drive cone test

The use of an impact driven point in the form of a cone penetrometer has frequently been suggested as an expedient substitute for the Standard Penetration Test

Farren (1963) had suggested that the test could be used to predict the settlement of footings on granular soils. In this case, a cone tip of 50mm (2in.) diameter with an apex angle of 60° was used.

Comparisons made at two sites indicated that the blow count values obtained by the drive cone (over a distance of 0.3m (1ft.)) were equivalent to SPT blow count values over the same zone.

The obvious advantages of the drive cone are increased frequency of test data and expedience in deployment and execution of the test; The use of the drive cone test is well documented for sand deposits as well as in gravelly materials

Charts have been presented providing a comparison between SPT's and DCT's and in some cases allowable bearing capacity charts for shallow foundations on granular soils have been developed based on the results of DCT's

Parrent (1963) suggested the following approach could be used to calculate settlements based on the elastic approach presented by Terzaghi (1943) [120]:

$$S = KqB\left[\frac{1-\mu^2}{E}\right] \qquad \text{(III.36)}$$

Where:

s = settlement.

K = a constant depending on the position where settlement is desired.

q = applied footing stress.

2B =width of the footing.

μ = Poisson's ratio.

E =Young's Modulus.

It was further suggested that μ and E could be assumed constant provided that the applied stress did not exceed about 1/3 to 1/2 of the ultimate bearing capacity (with FS = 2 to 3). Based on back calculation of load-settlement curves presented by Terzaghi and Peck (1948) for different values of SPT penetration resistance, Parrent suggested [120]:

$$\frac{E}{1-\mu^2} = 15{,}000\ N\ (Psf) \qquad \text{(III.37)}$$

Where:

N = SPT or DCT blow count.

III.10 Finite element method

The FEM consists of replacing the physical structure to be studied by a finite number of discrete elements or components that represent a mesh. These elements are linked together by a number of points called nodes. We first consider the behavior of each independent part, and then we assemble these parts in such a way that we ensure the balance of forces and the compatibility of the actual displacement of the structure as a continuous object.

The FEM is extremely powerful because it allows the correct study of continuous structures with geometric properties and complicated load conditions. It requires a large number of calculations which, because of their repetitive nature, adapt perfectly to digital programming.

The finite element method is theoretically the most efficient because it allows the modeling of complex geotechnical problems.

It requires:

- ✓ The definition of the geometry of the problem, so that the boundaries of the calculation do not influence the results.
- ✓ The choice of a law of soil behavior, of type Mohr- Coulomb, Cam- Clay, etc.
- ✓ The characteristics of structures and interface elements to introduce soil interaction structures and hydraulic conditions.
- ✓ The initial state of interstitial stresses and pressures.

It allows:

- Perform flow calculations.
- Simulate all phases of the project.
- To take into account the variations of the characteristics: structures, soil layers.
- The planned outputs for the works
- The movement of the structures.
- The internal solicitations of the works.

And for the soils:

- ❖ The movement of the ground.
- ❖ The deformations of the ground.
- ❖ Total and effective stresses in the soil.
- ❖ The interstitial pressures.

The main software used is:

a) GEO-SLOPE.

b) PLAXIS 2D software. [121]

III.10.1 Definition of plaxis software

Plaxis is the leading geotechnical finite element software designed to perform deformation and stability analyses for various types of geotechnical applications .

The program uses a convenient graphical interface that allows users to quickly generate a geometric model and a finite element mesh based on the vertical cross-section of the structure to be studied.

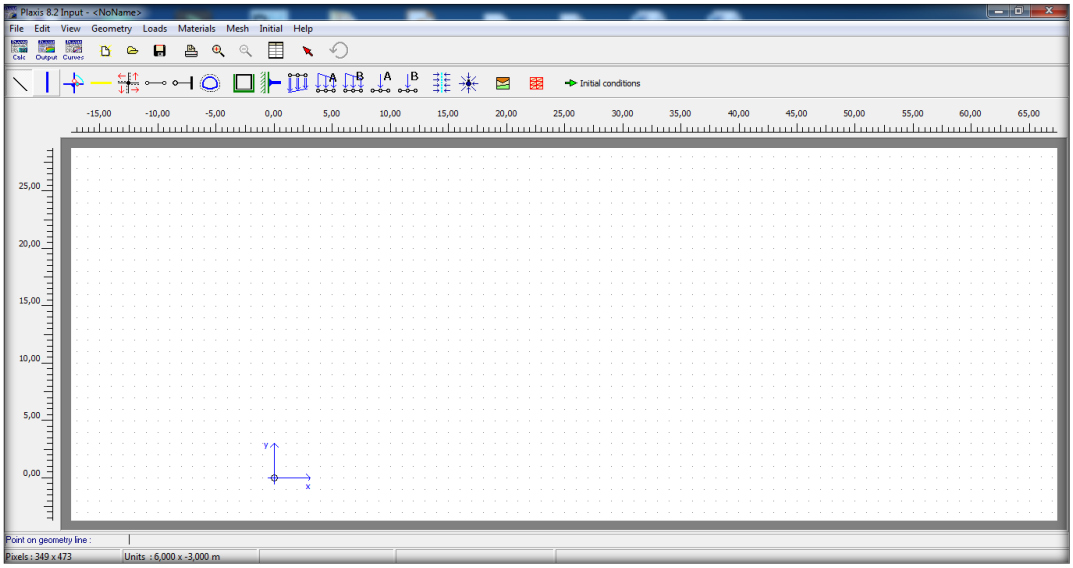

Figure III.30: Main window of the data entry program (Input).

III.10.2 Numerical modeling

In the context of the construction of access embankments at the level of PK 3+680 at PK 4+240 at the avoidance of the wilaya of Tebessa.

The fill is made in a layer of silty and marly clay , the Plaxis software allowed us to obtain an estimate of the deformations that are produced in soil layers. The results are modeling in plane deformation.

The settlement value obtained by the analytical settlement calculation is :

$$\Delta hi = \frac{Cc\ h}{(1+e0)} \log \frac{(\sigma 0+\Delta \sigma))}{\sigma 0} \qquad \text{(III.38)}$$

($\sigma = \sigma_c$ for over consolidated soils)

($\sigma = \sigma_0$ for normally under consolidated soils)

With :

Settlement expressed in (cm)

H : Height of the considered layer in (cm)

e0 : Void index corresponding to σ_0.

σ0 : Effective stress of the soil at point z

z : Point where the settlement is calculated

z : Difference in stress due to the loading.

σ c : Stress of preconsolidation of layer.

Survey: 1 PK 03+680

Table III.3: Different parameters for settlement calculation.

Depth (m)	Hi m	Zi (m)	Cc	σc (Kpa)	σ_0	e_0	$\Delta\sigma$	$\sigma_0 + \Delta\sigma$	Δh_i
7.00 – 17.00	7.00	10.50	0.215	200	200	0,42	76,7	283	13.70 cm

Settlement equal to **13.70 cm.**

III.10.3 The modelling approach with Plaxis

I represent here the path and main steps of a calculation under Plaxis:

a- Geometry

The first step under Plaxis is the definition of geometry.

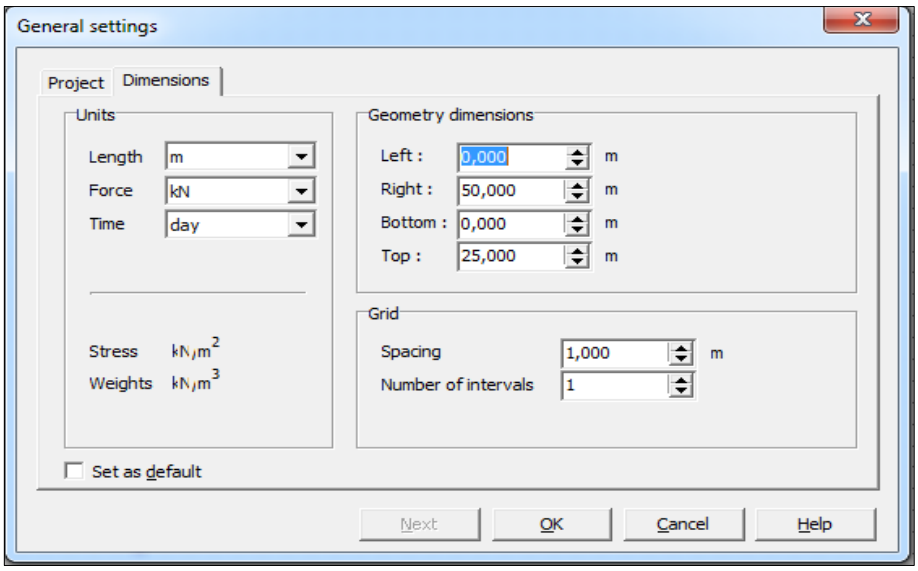

Figure III.31: Definition of geometry.

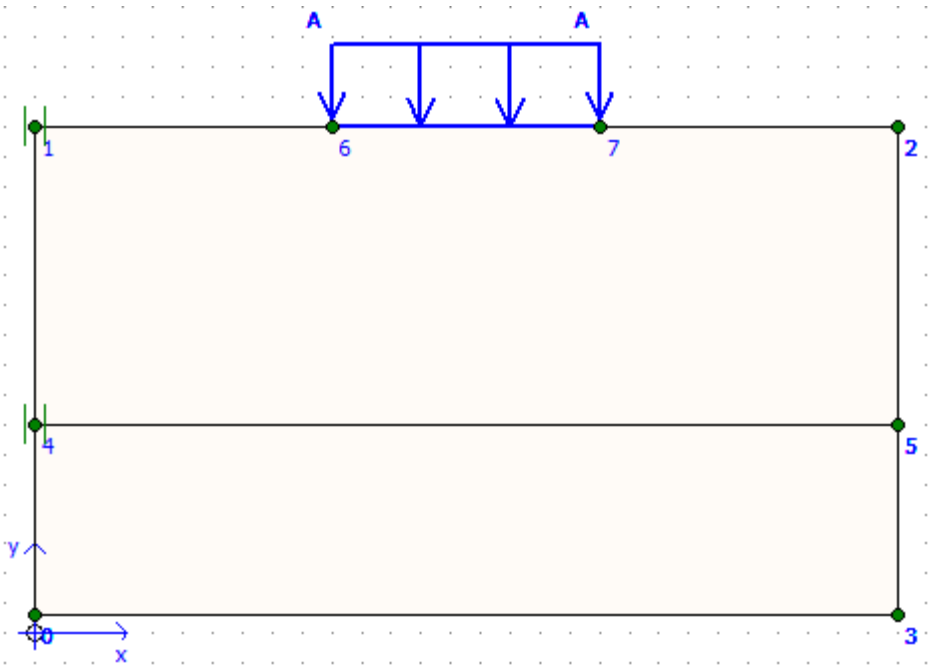

Figure III.32: The geometry model.

b- boundary conditions

if geometry is defined, the boundary conditions must be entered , the displacements and stresses imposed on the outer limits of the geometry.

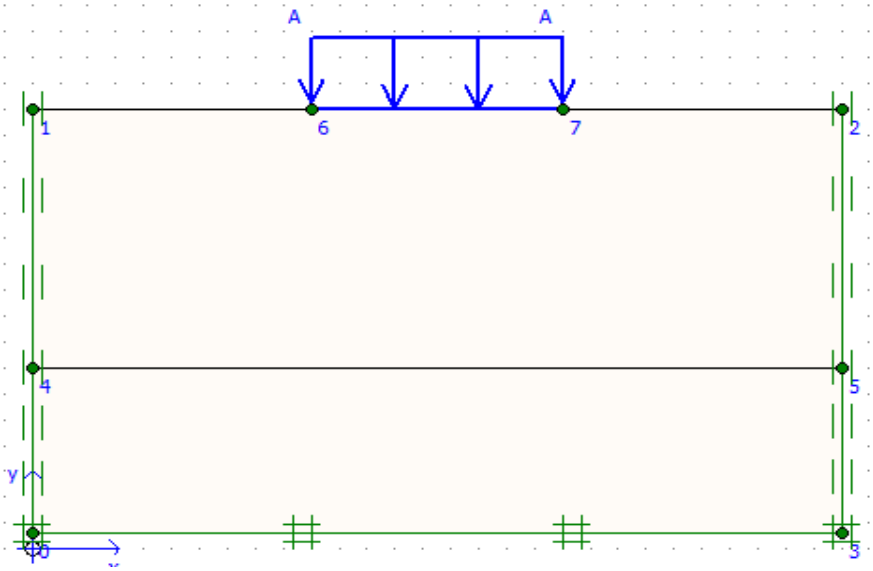

Figure III.33: Boundary conditions.

C-Definition of material parameters

Next, the different properties of the different materials should be defined according to their type (soil and interface, plate, anchorage, geogrid, etc....), behaviour model and different parameters to define it. For soils, in addition to the definition of mechanical characteristics, their interfaces with other types of elements can be

parameters, it is also necessary to define the hydraulic behaviour of the soil (drain, undrainer or non-porous).

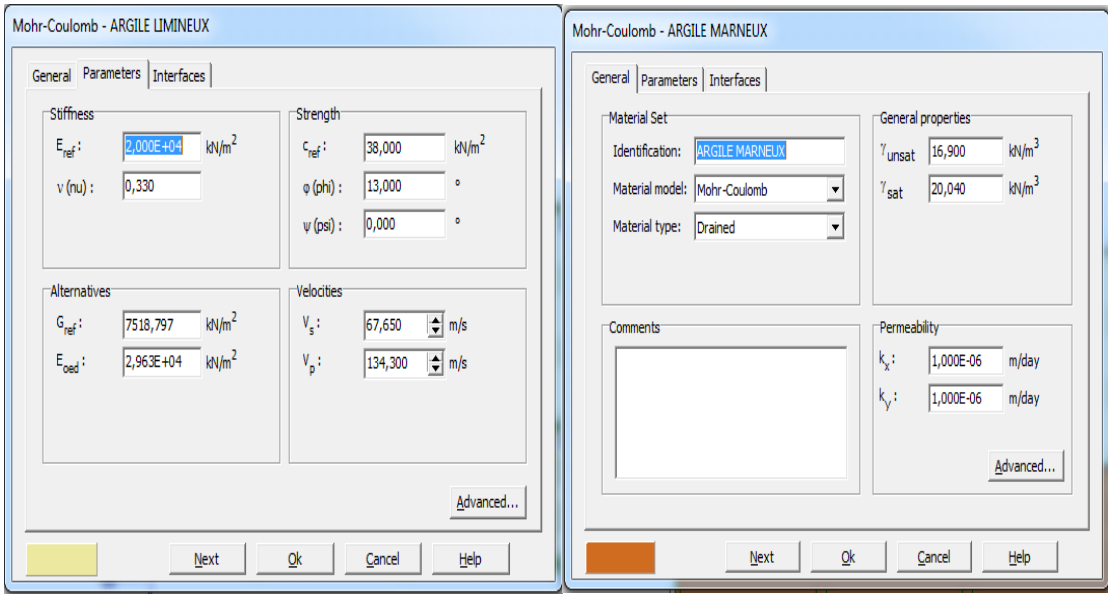

Figure III.34: Definition of materials setting.

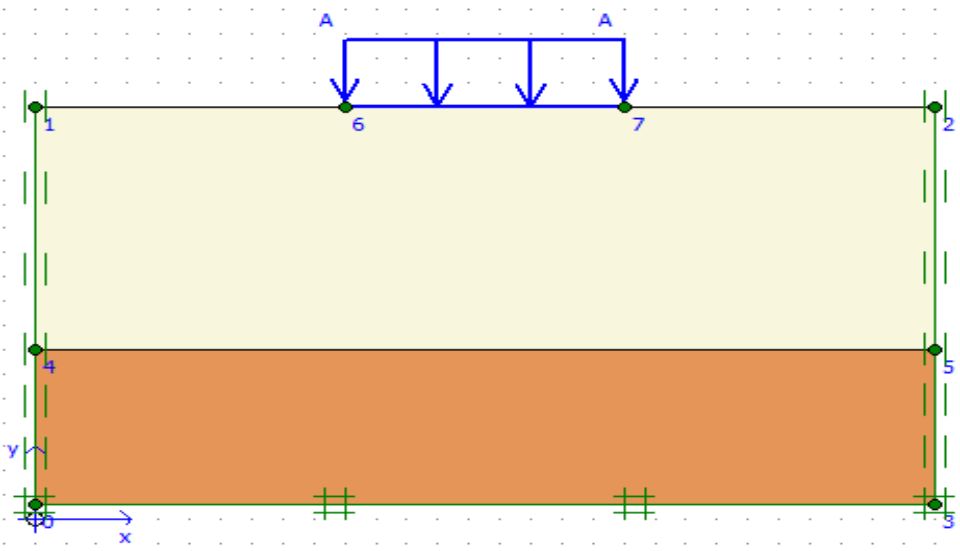

Figure III.35: Laying materials.

d-Mesh

The mesh is generated automatically, which is a strong point of Plaxis. The operator can set the fineness of the mesh between different options (very coarse, coarse, medium, fine, very fine.

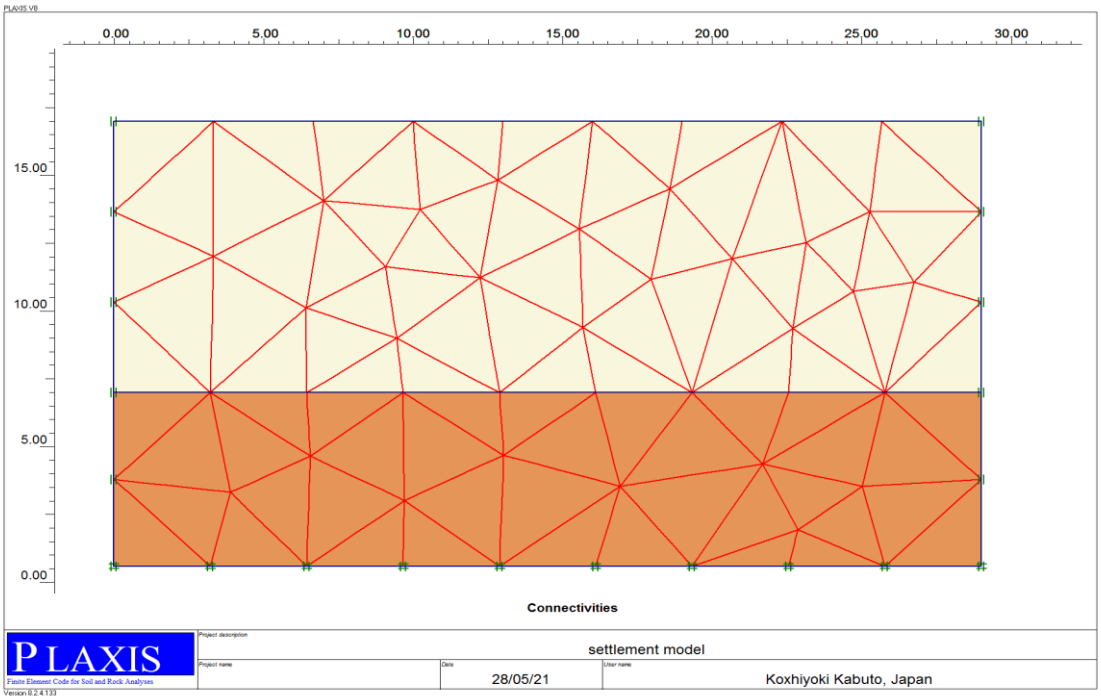

Figure III.36: The mesh.

e- Initial conditions

The initial conditions are defined in two distinct steps:

The first is called «Initiale pore pressure» to define a layer level initial groundwater (if necessary), and generate the corresponding interstitial pressures.

The second window allows to generate the initial constraints inside the massif .

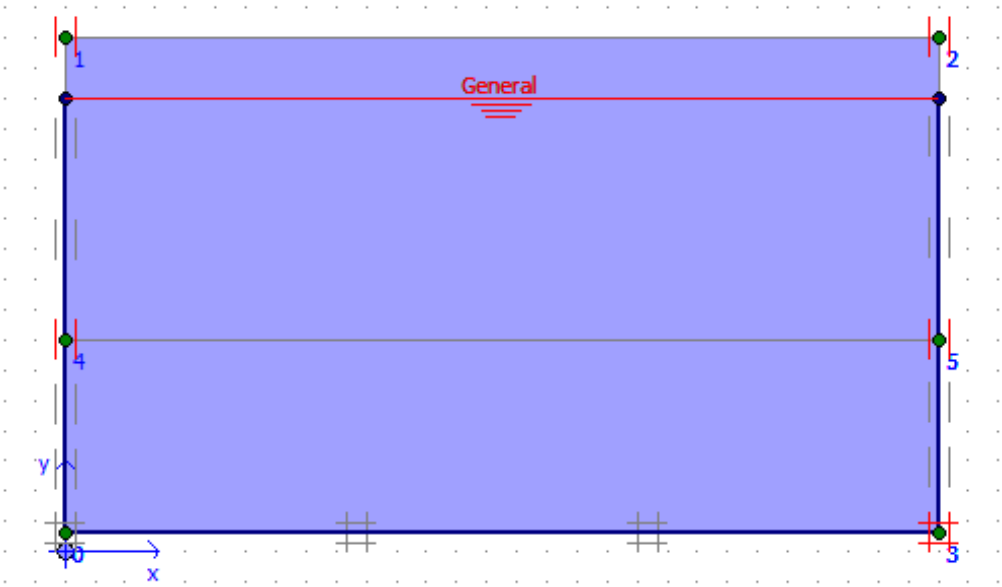

Figure III.37: Initial conditions step.

f- Calculation phases

After having carried out all these settings, the calculations can be accessed by the button “Calculation”. The Plaxis “Input” interface closes and gives way to a new interface: "Calculation". A phase 0 is already calculated, this phase corresponds to the initial state of the structure. This interface defines the phasing of the construction.

The model will be solved following the detailed phases as follows:

Phase 0

initial stress state is given by $\sigma v = \gamma z$, $\sigma h = K_0 \gamma z$

Phase 1

1. Select Plastic Calculation from the General tab.
2. Set the number of additional steps to 250 on the tab page Parameters.
3. Select Staged Construction as the load entry in the settings, then click Define.
4. Activate the soil layers and click update.

Phase 2

1. Select consolidation for the calculation type in the General tab.
2. Set the number of additional steps to 250 on the tab page Parameters.
3. Select Staged Construction as the load entry in the settings, then click Define.

Phase 3

1. activate "Distributed Load System A" in the selects items window and give its values then click update

After the definition phases of the calculation phases, and before starting the calculation, it is possible to select points to draw stress-displacement curves and constraint paths.

g-Start of calculations

We can then start the calculation of the different steps, during this one a window information appears gave the evolution of the calculation.

h-Displaying Results

The main results of a finite element calculation are the nodes and constraints at stress points. To see these results, it is you need to go to the «Output» menu.

You can get the deformed mesh under the consolidation, and you get the total ground displacement is **142.27×10^{-3} m.**

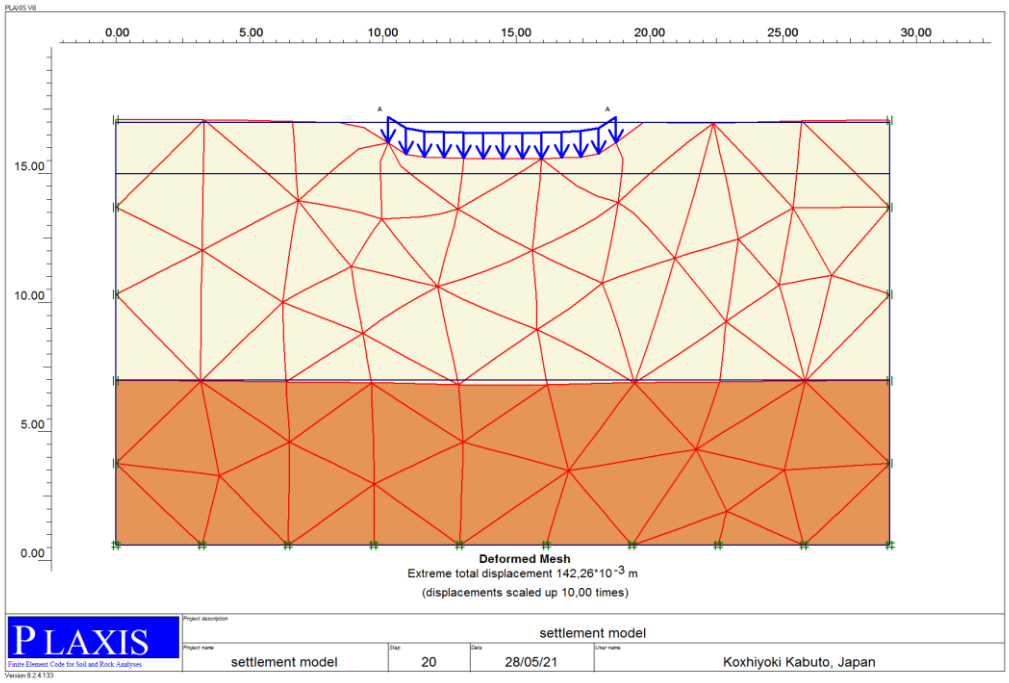

Figure III.38: Deformed mesh .

Click on «deformation» and define the different values of the displacements(vertical or call also settlement, horizontal displacement and displacements totals).

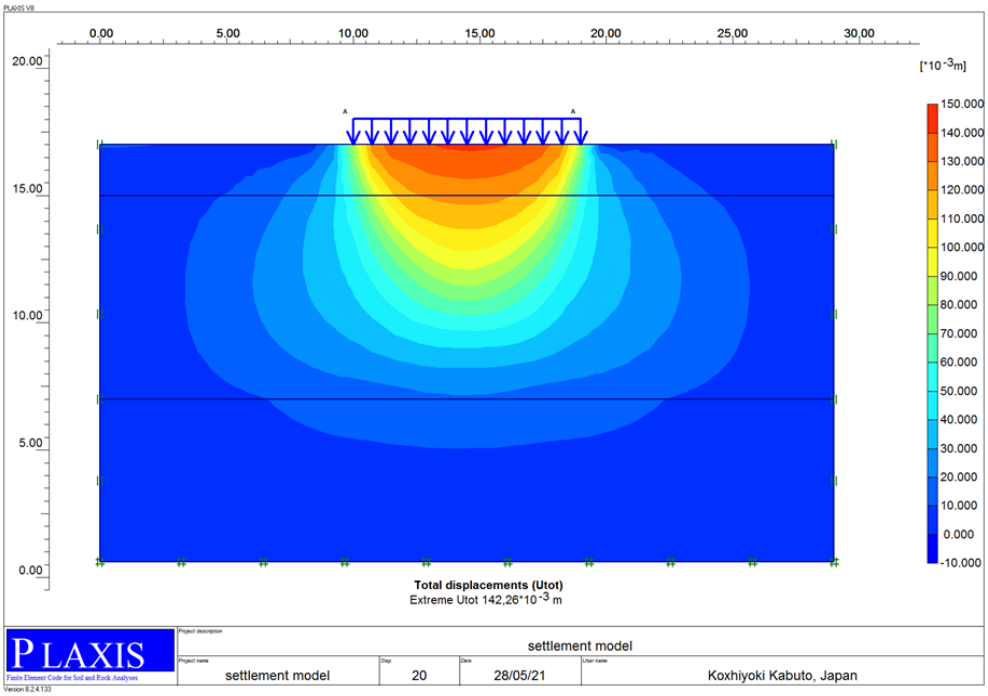

Figure III.39: Total displacements.

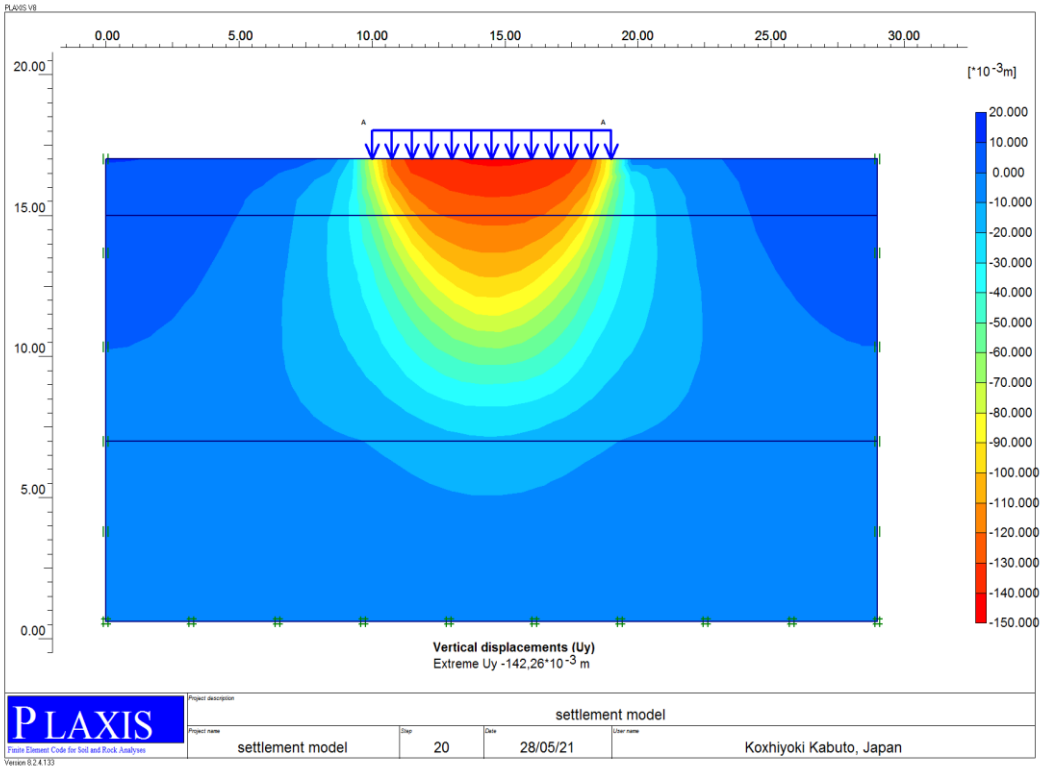

Figure III.40: Vertical displacements.

III.10.4 The modeling approach with Geoslope "sigma w "

SIGMA/W is a finite element software product that can be used to perform stress and deformation analyses of earth structures. Its comprehensive formulation makes it possible to analyze both simple and highly complex problems. For example, you can perform a simple linear elastic deformation analysis or a highly sophisticated nonlinear elastic-plastic effective stress analysis. When coupled with other GEOSLOPE software products, it can also model the pore-water pressure generation and dissipation in a soil structure in response to external loads using either a fully coupled or un-coupled formulation.

SIGMA/W has application in the analysis and design for geotechnical, civil, and mining engineering projects.

The following steps represent the itinerary for the calculation of the settlement by SIGMA /W

Step 1: selected the type and parameters of analysis;

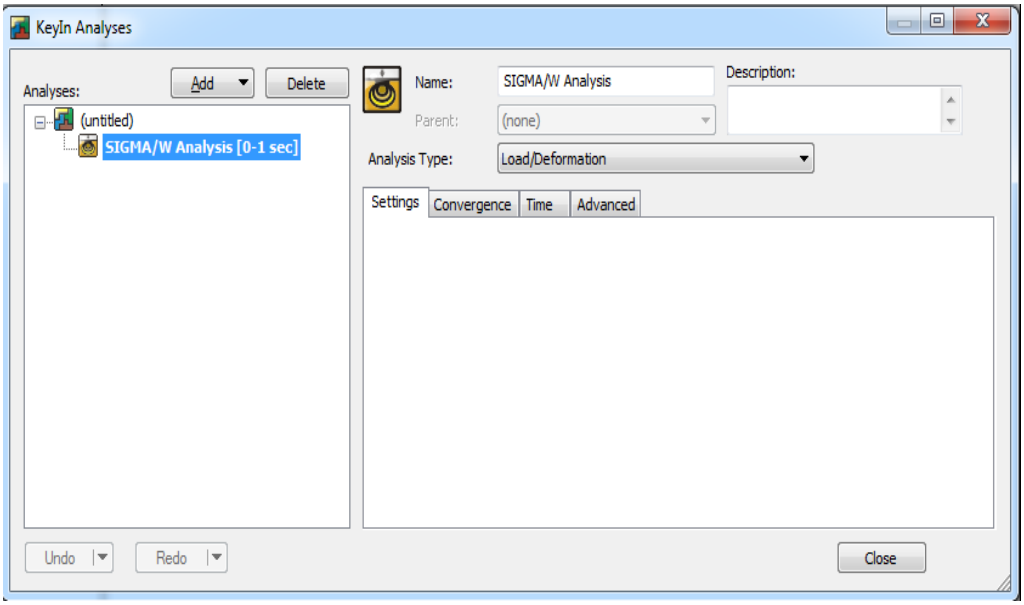

Figure III.41: Select parameters and type of analysis.

Step 2: define units and scale;

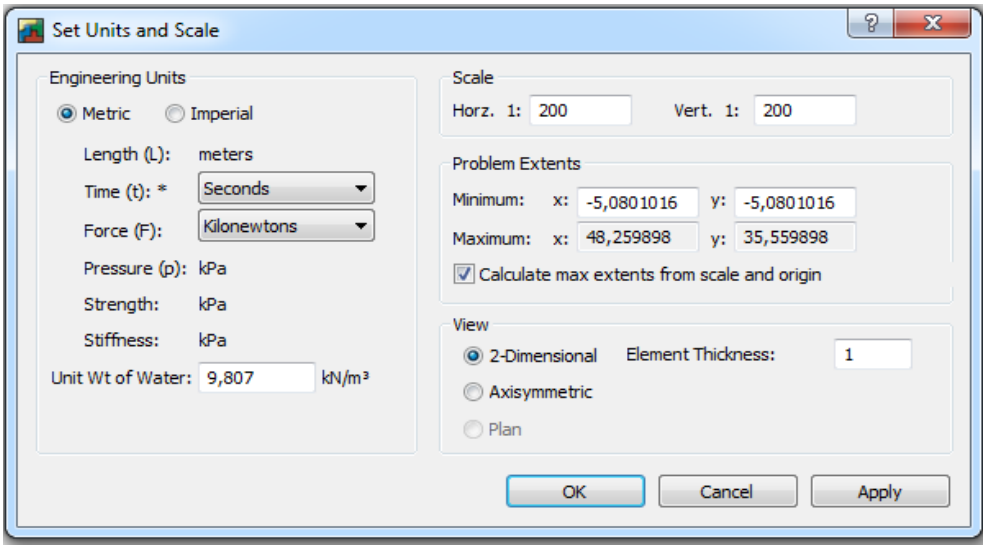

Figure III.42: Setting of units and workspace.

Step 3: Draw the geometries and meshing of the regions and input materials from each region.

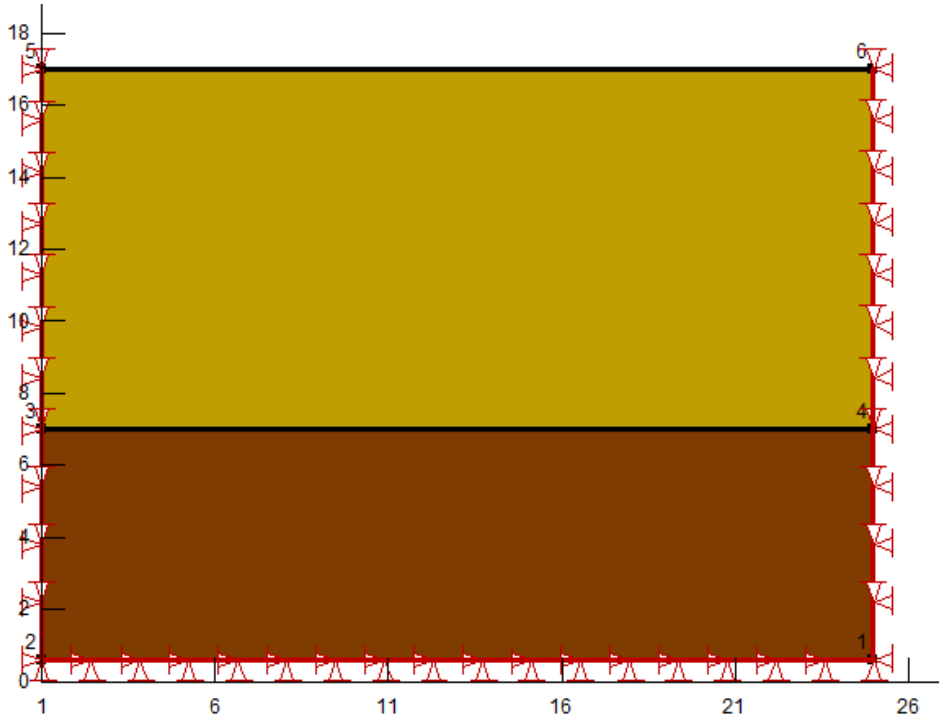

Figure III.43: The geometry of model with mesh.

Step 4: Plot boundary conditions;

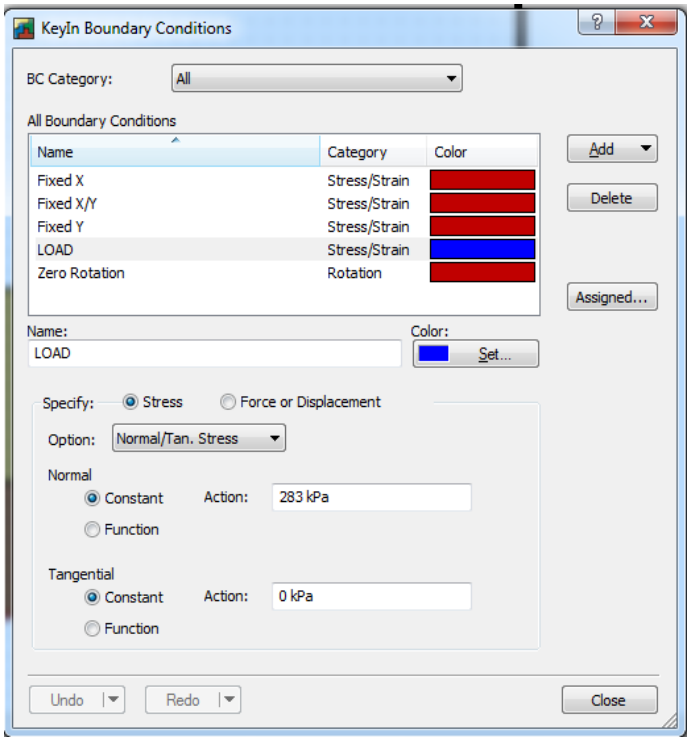

Figure III.44: Enter the load value.

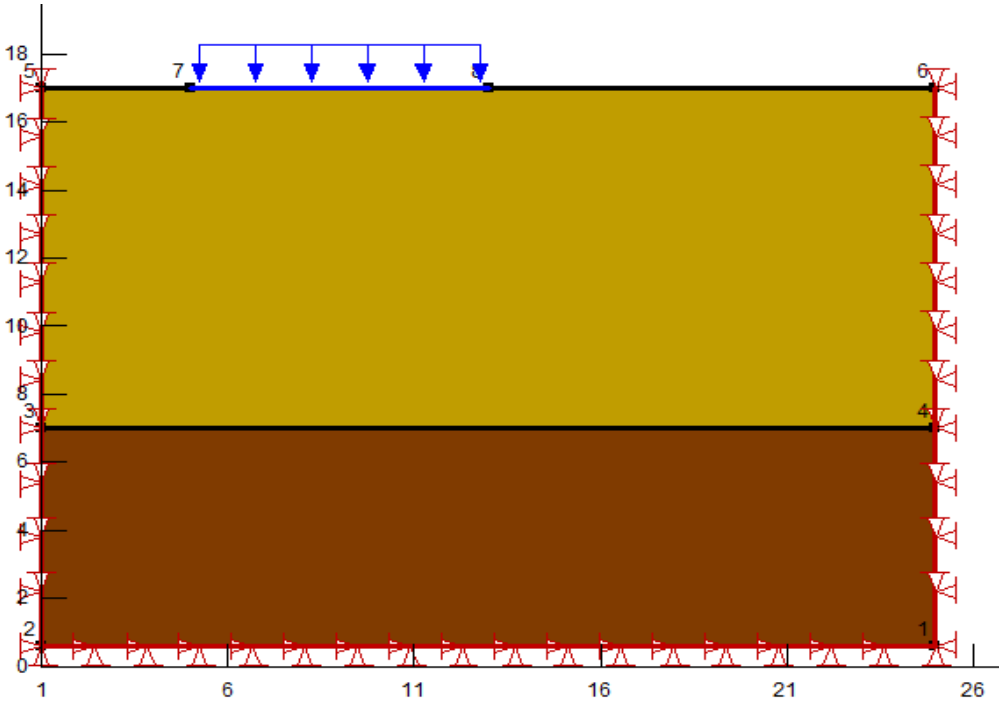

Figure III.45: Drawing the boundary condition.

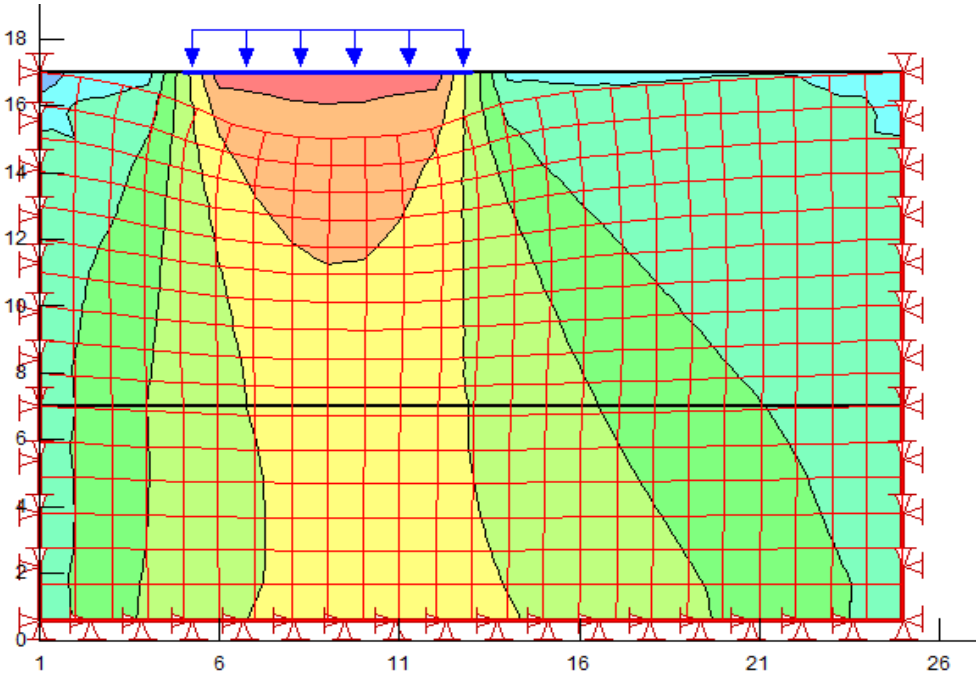

Figure III.46: Displaying the result.

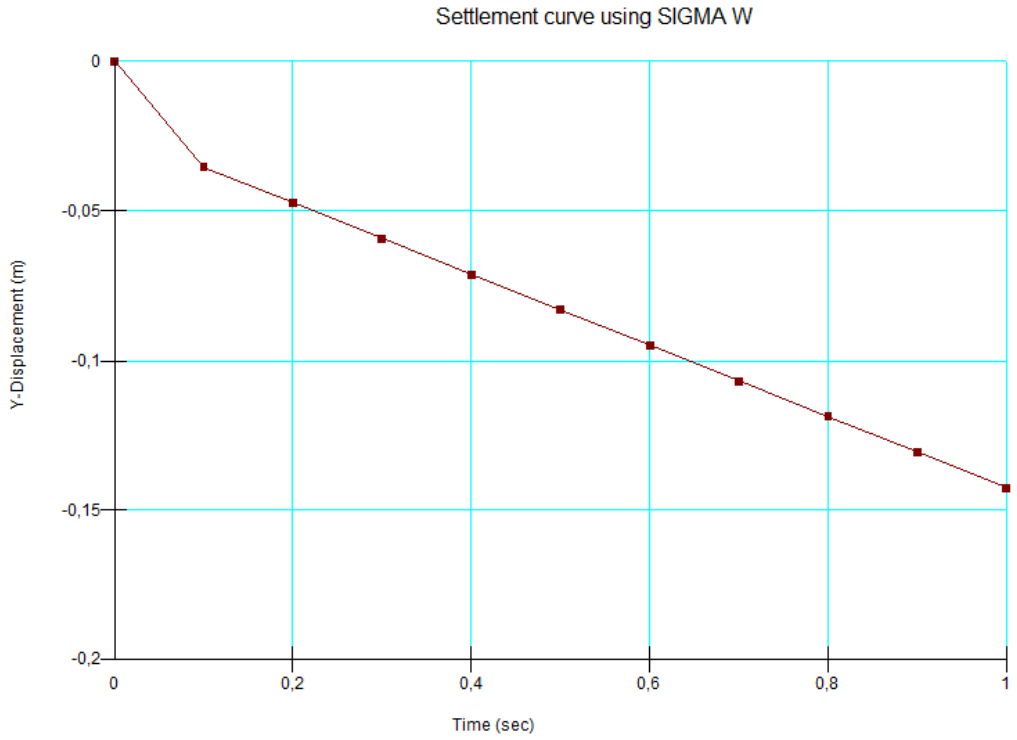

Figure III.47: Curve of displacement as a function of time.

Table III.4: comparison between numerical and analytical methods for the calculation of settlements.

Settlement value by analytical calculation	**Settlement value by numerical calculation by plaxis**	**Settlement value by numerical calculation by Geoslope 'sigma w'**
Δh (cm)	Δh (cm)	Δh (cm)
13,7	14,2	14,26

The use of the finite element method in the calculation of the settlement allows us to note that the values found by the numerical calculation (plaxis 2D and Geoslope "SIGMA/W") are equivalent to 14.2 cm.

These values obtained by the numerical calculation are equivalent to those determined by the analytical calculation, thus it may be concluded that the settlement computation was determined by several methods either numerical or analytical.

III.11. Conclusion

Settlement is a reduction in the volume of the subsoil following an increase in effective stress. It is the sum of the "elastic" compression and the deformation due to consolidation.

The term "settlement" is normally used for deformation resulting from the combined effect of load transfer, increase in effective stress and creep under long-term conditions. The amount of deformation for a given contact stress depends on the stress distribution in the affected soil mass relative to the existing stress (the imposed change in effective stress) and the compressibility of the soil layer. The change in effective stress is the difference between the initial (original) effective stress and the final effective stress.

The calculation of settlement can be done using different methods, among the methods used is the oedometer test which is the most important test in the geotechnical field because from this test we can find parameters which help in the settlement computation.

Moreover, there are various in-situ methods which are used in settlement calculation such as Pressuremeter Test, Standard Penetration Test SPT, Conical Penetration Test (CPT), Drive Cone Test, Dilatometer Test and Plate Load Test.

Thus, all of the above methods are used in settlement calculations, but they are less important than the oedometer test.

A finite element approach is suggested in the calculation of settlements, in order to have a reference result with which to refine the settlement analysis and to compare with the results of other methods, therefore, I make a model aims to explain how the finite element method 'plaxis' and geoslope is used to calculate settlements and I compare the value found with that of the oedometer test.

Finally, the computation of settlements is established by several methods according to the importance of this phenomenon in the geotechnical field.

III.12. Geological and hydroclimatological overview of the study area

III.12.1 Geological overview

The plain of Tebessa has an extensive surface of flat relief surrounded by mountains. It is composed of filling materials derived from erosion of the reliefs surrounding areas enclosing mainly recent formations composed mainly of Clays, silts, sands and gravel of Mi-Pliocene to Quaternary age Figure III.49).

Generally, the materials become coarser from the center of the plain outwards. Near the outer margin, the dominant fractions in detritic sediments are Table-shaped limestone fragments of different sizes.

Going further towards the center, the percentage of the finer fraction increases to the detriment of the coarser fraction. Parts of the plain, such as the north of the city, consist of fine-grained and weathered marl formations.

This waterproof lithology led to the formation of a large swamp whose area derives its name Merdja

III.12.2 Geographical situation

The study area belonging to the wilaya of Tebessa is located in the east of the Algerian-Tunisian border, this is a collapse basin surrounded by mountains altitude varying from 800m to 1600m.

The city of Tebessa is limited to the North by Souk ahras, to the South by the city of Oued, to the East by the Algerian-Tunisian border and to the West by the two wilayas Oum el-bouaghi and Khenchella (Figure III.48).

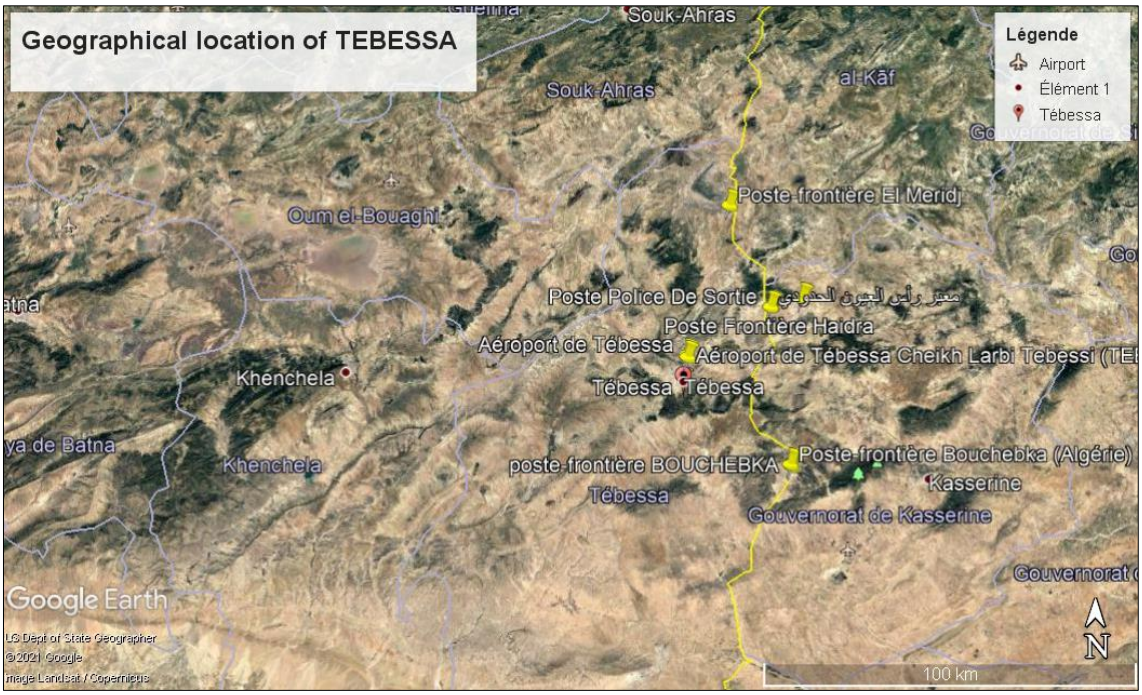

Figure III.48: Geographical location of the study area (google earth).

III.12.3 Geological Survey

Geological study is essential if the nature and distribution of the formations composed mainly of clays and marls are to be determined, since they are the main materials affected by compressibility.

The Tebessa region is part of the Nord-aurèsiènne Aboriginal structure (Aurès Nememcha) of the Saharan atlas). [123]

The geological map (Figure III.49) shows the distribution and structure of the different lithology in the region. It is composed mainly by:

- Diapiric triasic formation dislocating overlying formations at the Djebel Djebissa.
- Carbonate formations represented by large layers of marl from Cretaceous to Tertiary ages. Some of these formations are observable at the borders of the plain of Tebessa.
- A large Mio-Plio-Quaternary alluvial deposit which lies in conflict with previous formations and thus forms the filling of the depression, currently the plain.

This formation is observable especially at the foot of the hilly terrain .

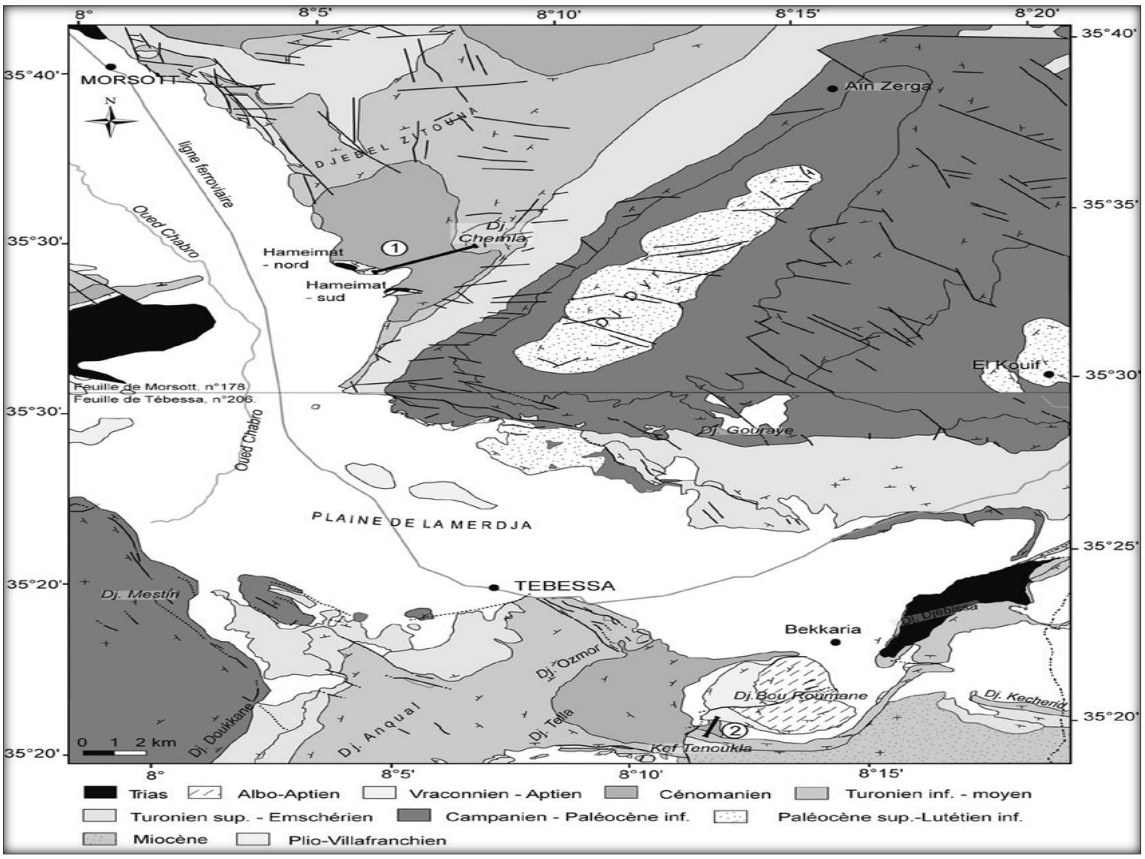

Figure III.49: Schematic section of the geological formations of the Tebessa region. [123]

III.13. Lithostratigraphy of the Tebessa region

The study of the stratigraphy of the Tebessa region is essentially based on the research work of several authors. [123]

III.13.1. Secondary

A. The Triassic

In the region of Tebessa, the Trias outcrops in the form of extrusions on a large extended north of El Hammamet and south of Tebessa to Dj Djebissa.

It generally occupies the heart of anticline structures [124], with reefs at its apex at the Aptien and Albien rivers. It consists mainly of gypsum, marl, dolomites and rock debris of different kinds.

B. Lower and Middle Cretaceous

B.1. Aptian

It is formed by banks of limestone with Orbitolines, often brechic with dolomitic or calcium cement. In the southern part of Dj. Belkfif, this limestone is included in the diapiric Trias, with a thickness of more than 100 m.

B.2. Albian

It outcrops near Dj. Bouroumane where it is formed by limestones in thick brown banks on a thickness of 90 m. These foundations form a large part of the average slopes of the west side of Bouroumane. This floor is not in the study area, perhaps because of the increased diapirism during this period, however according to the last article of there exists near Dj.Belkfif

B.3. Vraconien

It is well developed in the area of Bouroumane and it probably exists deep in the ditch of Hammamet.This floor is characterized by a set of limestone and marl limestone gray in patches, containing footprints of Ammonites.

C. Upper Cretaceous

C.1. Cenomanien

It outcrops in the northwest part of the moat of Hammamet to the east of Dj.Essen, in the form of blue violet marl interspersed with lumachelles.

C.2. Turonian

It is subdivided into two parts, the lower Turonian and the upper Turonian. The base of Lower Turonia is represented by greyish marls and limestones, of which the thickness is of the order of 60 m.

The summit of the lower Turonian is represented by Beige limestones that make up the cliffs of Dj.Essen; Dj.Belkfif, kef Daheche, Dj. Tella (Ozmor chain).

Upper Turonian is in grey marl, alternating with green marls with a thickness of about150 m.

C.3. Emscherian (Santonian and Coniacian)

It is a thick and monotonous series of marls grey or green, containing lumachellic limestone levels at the top over a thickness of 250 m.

C.4. Campanian

Campanian (lower and upper) is characterized by a series of mannes grises having a thickness of 200 m. The middle Campanian present in the relief a new cornice between that of Turonien and Maestrichtien, it passes noticeably to the marly formations that make the passage between Campanien Superior and Maestrichtien lower.

C.5. Maestrichtien

The lower Maestrichtien is represented by scree at the foot of the reliefs. The upper Maestrichtien is a powerful formation of white massive limestone with numerous

Inocerames footprints. Their thickness is of the order80 to 100 m, but reaches 200 m southwest of Youkous (Hammamet).

III.13.2 Tertiary

A. The Paleocene

Its base has marls analogous to those of the superior Maestrichtien which is interspersed with from phosphate layers to higher levels.

B. The Eocene

Limestones with flint and others with Nummulites characterize the lower and middle Eocene, meadows perimeters of the Tébessa region. Their power is 200 meters.

C. The Miocene

The deposits of the lower and middle Miocene are based transgressively on the ancient formations (Albien-Sénonien and even on the Triassic). It is a powerful accumulation of marls and sandstones. [124]

At their base, miocene formations consist of conglomerates containing elements of various limestone, grey flint, ferruginous pebbles and elements borrowed from the Triassic, evidence of diapiric activity. Flint remodeling, renowned of Y presian age at the base of the Miocene testifies to the existence of an Eocene sea where deposits marine sedimentation during the Eocene and Lower to Middle Miocene. Sedimentation at the end of the Miocene indicates the beginning of a regression phase, the average power of the Miocene in the study area is 150 m. [125]

III.13.3. The Quaternary

Quaternary deposits are of continental origin and are distributed in parts and cover important surfaces (current plains and valleys). They are formed of limestone crusts, scree silts, pebbles and puffs. The power of the Quaternary ranges from 10 to 30 m [125]. Lithological formations that can be distinguished are the current formations, the old formations and the Plio- Quaternary.

III.13 Tectonic and structural descriptions of the Tebessa region

In structural terms, the area in question occupies two geotectonic regions which are distinguished by the age of their pleated base and by the peculiarity of their structure (Figure III.50).

They are hypercinian platforms (North and center of the territory) and antecambrian (South) divided by the Atlasic North Fault (Saharan Flexure).

The territory of the Tebessa region is covered by large synclinal structures and anticline steering NE-SW. These structures are clearly visible especially on the Cheria plateau and Dj Dyr.

In the El Ma-Labiod area, deeper structures are covered by the Miocene continental; they are therefore anterior to the Miocene and to the phase of distension caused the collapse of the Tebessa-Morsott plain which is much further north behind Bekkaria.

If one considers the grounds of the Morsott map, it is difficult to determine the age of the folds; the only tertiary deposits, posterior to the emersion Eocene, sublittoraux attributed to the Tortonian are located in the heart of Dj Dyr's synclinal, where they overcome without apparent discordance of the limestone of Lower Lutheran.

However, to the east of El Kouif, between the leaf boundary and the Tunisian border, the same sands of the lower Miocene are unconformable on Eocene limestones or Paleocene marls.

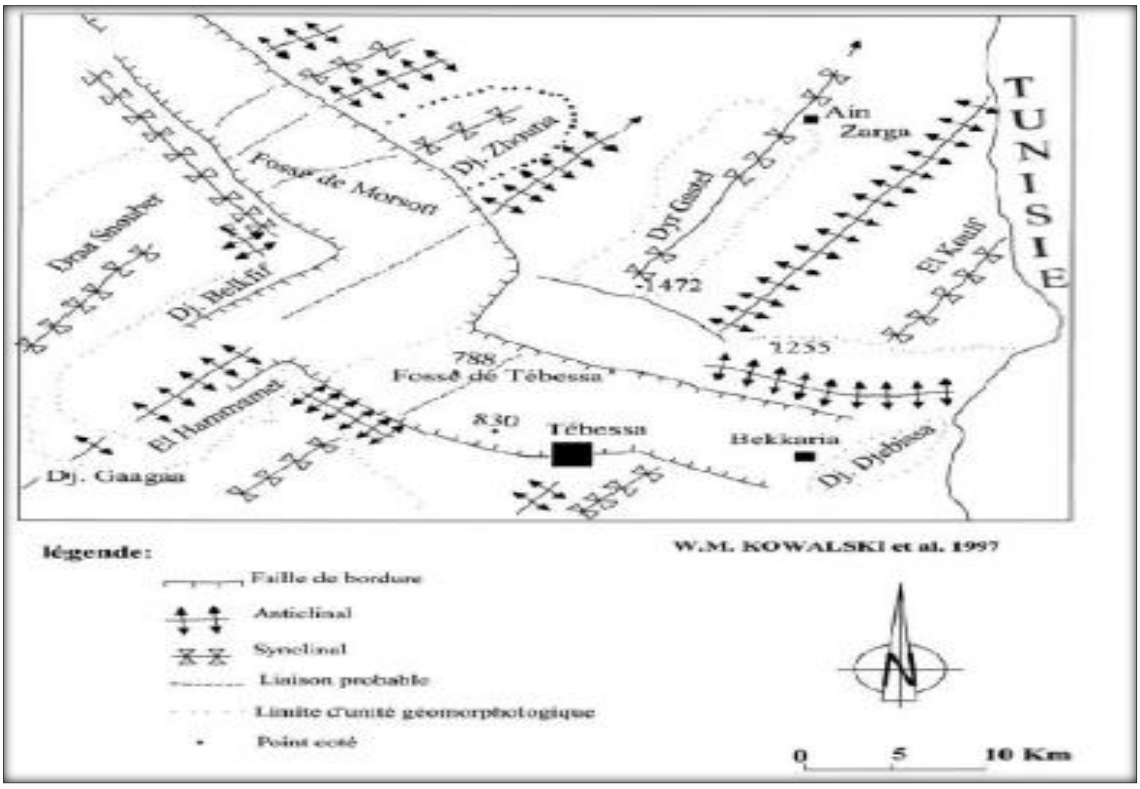

Figure III.50: Tectonic sketch of the Tebessa region. [126]

Further north (leaves Boukhadra and Dj Ouenza, as well as Dj Mesloula) [125-126], the Miocene is discordant about all terms of the series Cretaceous (Tebessa leaf) we also note, the Miocene discordant on the terms of the Cretaceous. The folding of the

region is therefore posterior to the Lower Lutheran and prior to the Miocene and is, no doubt, responsible for the emergence of the Middle Eocene [127].

A major steering accident NE-SW seems to cut and unhook the plain of Tebessa, this is a reverse fault. The compartment SE overlaps the compartment NW; this is clearly visible to Dj Chemela between Morsott-Tebessa.

The SW continuation of this accident seems to be drowning in depth under the anticline of Cheria. On the edge of the plateau, it mainly affects Turonian and does not seem to pass up to the limestone of the Maestrichtien. This stacking of structures towards the depth is organized with a reduction of the radius of curvature and beyond a certain depth by the formation of a fault especially when the levels become competent at the level of the Turonian limestones. Upwards, this accident subsides in the marls of the Coniacian, Santonian and Campanian. This is how the maestrichtien of Chéria is not affected.

The axis of the large structures, at a dip towards the SW, the highest point of the region is at the SW of the synclinal of Dj Dyr with 1472 m.

The summits of the limestone reliefs of altitudes from 1000 to 1500m, represent the evidence of an old erosion surface, almost flat but slightly left, culminating at Dj Dyr's South Point (from this point on, it slopes steadily towards the North and perpendicular to this direction, towards N-W and S-W).

This erosion surface, practically not deformed, is posterior to the folds and In particular, post-Miocene lower continental tangential compression: The sandy or conglomerate formations of this stage constitute, in fact, some peaks of the same altitudes as those of the older surrounding formations that determine this surface. It is also prior to the formation of the Morsott Ditch which intersects it clearly.

III.14 Local surface geology

Figure III.51from the soil map is used to describe "soil" surface formations the following distribution is poorly distinguished:

1. The dominance, according to this map is for calcium soils generally have marl and marl-limestone, or marly clays
2. limestone is present with distribution throughout the region
3. alluvial substances

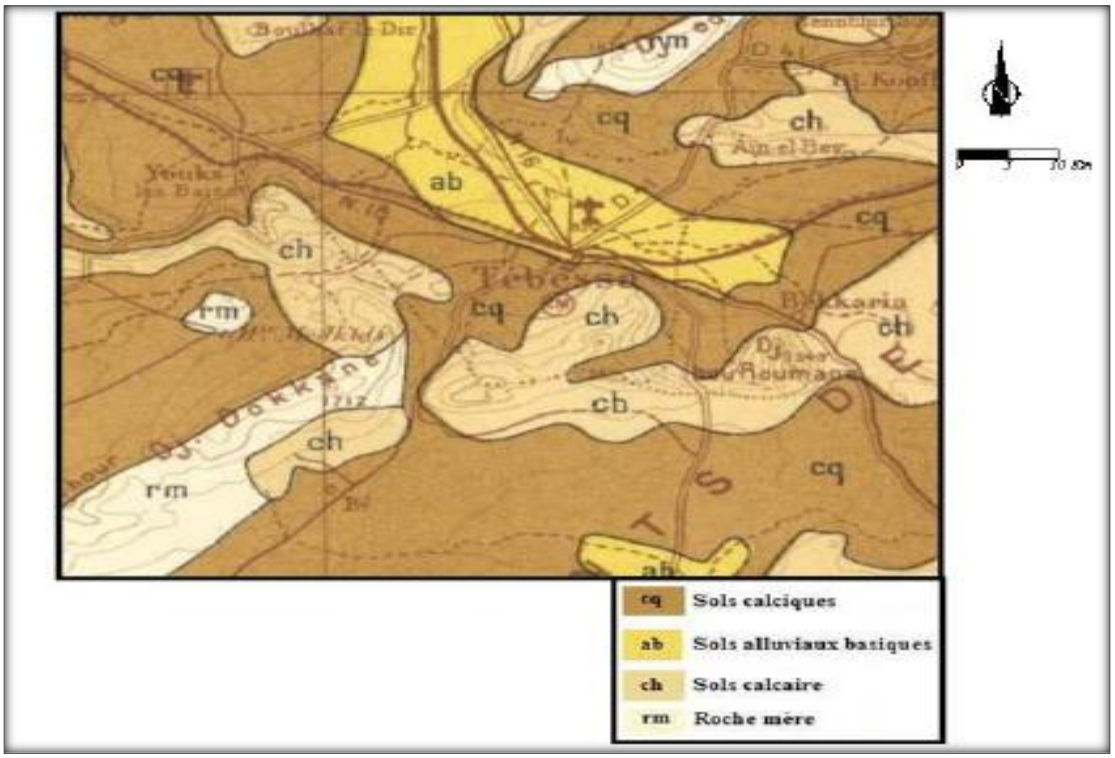

Figure III.51: Extract from the soil map of Tebessa Scale: 1/50.000. [128]

III.15 Conclusion

The survey of the different geological environments in the region identifies areas with clay and marl primary formations from a lithostratigraphic description of the ages existing in the region. Among these formations we quote the lower Mæstrichtian formed essentially by gray marls and marl-limestone, Paleogene with clay and gypsum formations, Pliocene characterized by the abundance of red clays, alluvial formations Presence of clays, stony clays, sand and silt deposits

Thus the consultation of geological maps and sections from the core boreholes made at the level of the studied region affirms the existence of clay and clay marl formations at shallow depths that despite their heterogeneity at the metric scale, they can be considered homogeneous across the study area.

Degradation clay and marl formations directly produce fine plastic soils that can change in volume as a result of the change in their water state, this mechanism cause short- or long-term terrain instability problems.

III.15 Hydrogeological overview

III.15.1 Hydrogeological conditions of the Tebessa plain

The plain of Tebessa contains three levels of water (p1, p2 & p3), these levels are captured either by domestic wells case of level p1 or by drilling, the case of the other

two remaining. Since the levels p2 and p3 aquifers are deep enough to make negligible the influence of groundwater on the water state of fine surface soil formations, in this part of the study, the piezometry of the domestic wells capturing level p1 and the boundary conditions at the scale of the plain will be treated.

III.15.2 Boundary conditions and underground inputs

Starting from the regional hydrogeological context (Figure III.52), we note the following facts:

-The eastern (northern) border is formed by the red clayey formations of the Trias.

-The southern (southern) border of Bekkaria to Ain Chabro presents a series complete stratigraphic of the lower Aptian to the middle Maestrichtien.

-The northern border: the contact between the filling and the Cretaceous-Eocene formations of the border is made by fault.

The hydrogeological limit is constituted by the faulty base lower maestrichtien limestone that gives several sources of overflow.

-Western border: has a watertight boundary with the exception of contact with limestone of the Turonian Djebel Belkfif whose hanging is directed towards the quaternary filling.

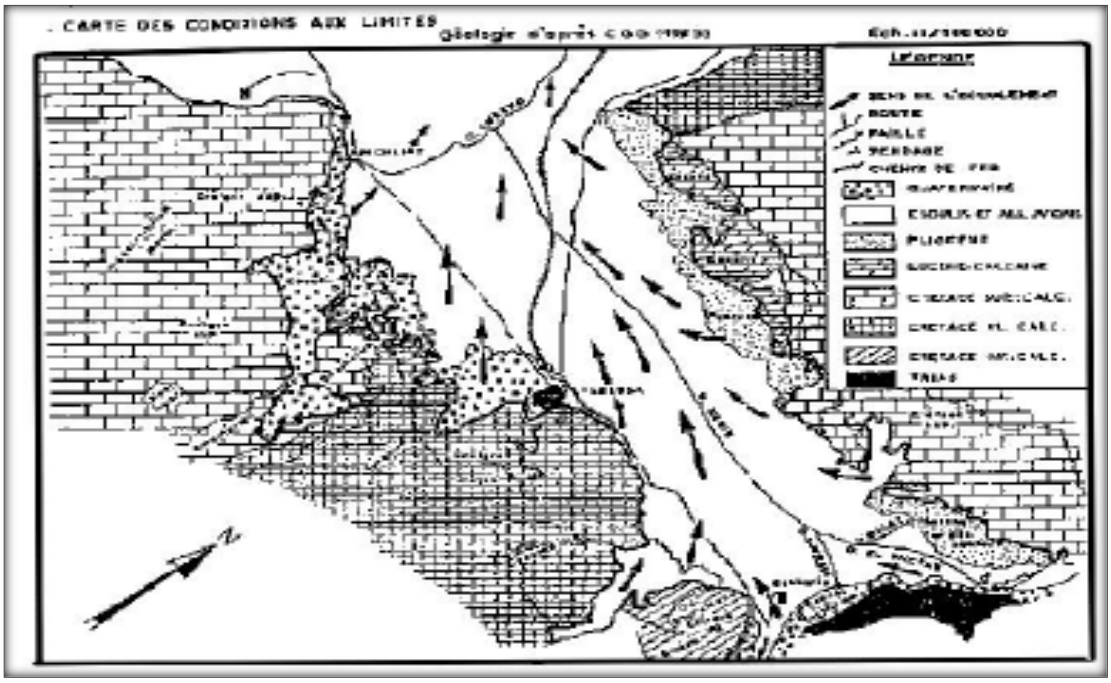

Figure III.52: Map of boundary conditions. [127]

Hydraulic exchanges are characterized by a mixed relationship between Wadi Kebir and the table. In addition, the changes in faces revealed by the geophysical study plotting the discontinuity of levels P1, P2 & P3, cause an overflow of the layer in the

area of Tebessa. Areas with elevated substratum make it possible to rise from the level of the subterranean layer even to the surface (Figure III.53), case of the Merdja

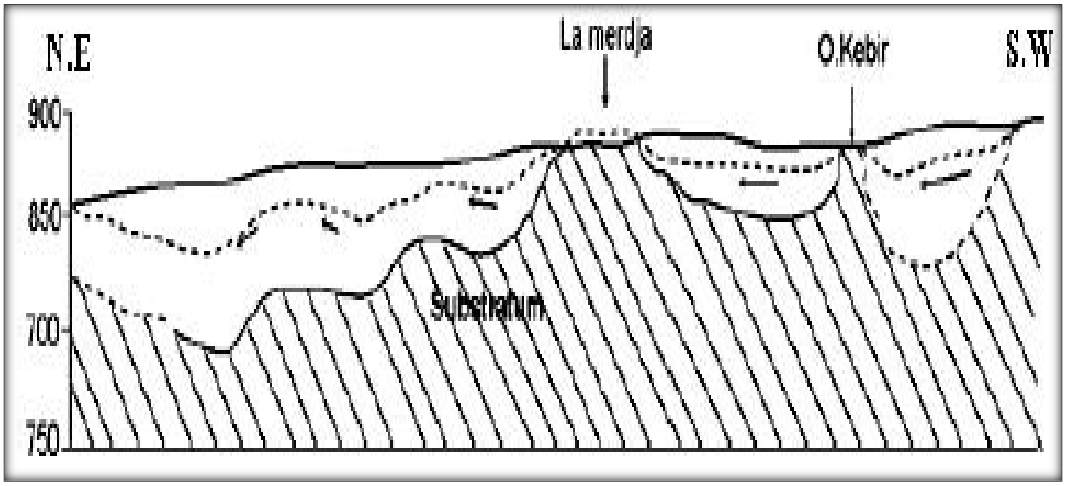

Figure III.53: Schematic profile of the evolution of piezometry and Substratum Of the Tebessa Aquifer. [127]

III.15. 3 Piezometry of domestic wells

The piezometric map (Figure III.54) made during the month of March [128] is based on water table static level measurements on 28 domestic wells.

This map shows an irregular piezometric surface where groundwater flow is directed SE-NW in agreement with the surface flow where the morphology of the surface shows an elevation of the Bekkaria region with an altitude of 900m compared to the other regions (Tebessa and Ain Chabro 800m).

The isopieze curves are concentric in the Tebessa area resulting from the pumping effect of the wells.

Similarly, the western zone shows fluctuations in the piezometric curves with the lowest pressure values indicating an area of groundwater drainage through the Wadi Chabro.

The drainage of the entire aquifer is carried out mainly by Oued El Kebir and its tributaries; it is compensated by a supply from the limestone borders located in the southern and northern part of the region.

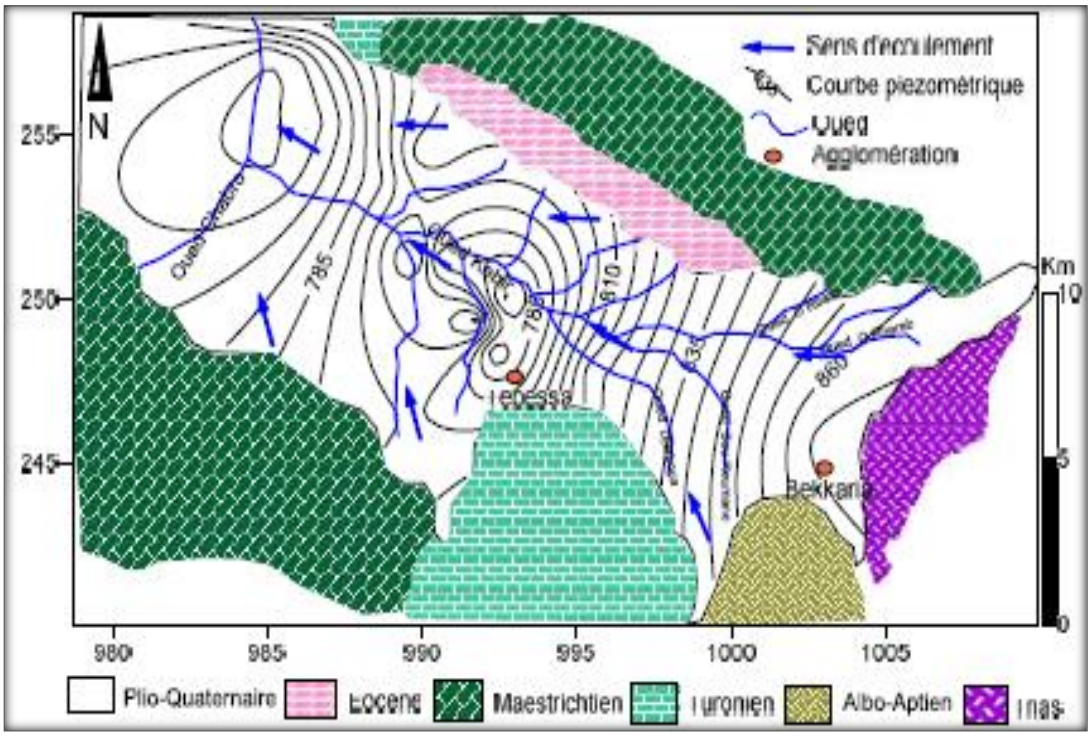

Figure III.54: Piezometric map of the Tebessa water table, March 2015. [128]

III.15.4 Conclusion

An overview of the hydrological and hydrogeological state indicates the abundant existence of water, especially in the Tebessa sector:

- overflow of the groundwater in the Tebessa sector;
- Hydraulic exchanges through a mixed relationship between Wadi Kebir and the aquifer;
- Supply and inflow of water from shallow surface limestone with a hanging down towards the plain.

A continuous contact of these waters with the fine soils especially clay of our area study contributes to a wetting of the clays which, despite being waterproof, can adsorb quantities of water that effectively contribute to their swelling (retention coefficient high specific). The drying up of these waters or their loss by drainage or evaporation during periods of drought makes the reverse phenomenon of shrinkage.

III.16 Climatological overview

III.16.1 Introduction

The phenomenon of compressibility of a clay soil cannot be studied without taking into account the hydroclimatic data of the region.

The greatest depths of seasonal moisture change are reached in regions where seasonal climate change is greater, i.e. long periods of drought followed by excessive

rainfall. Temperature conditions ambient directly influence the depth of seasonal variations in humidity:

During the cold seasons, moisture is accumulated in the warmer lows of the atmosphere, then dissipates into the depths.

The reverse occurs during warm seasons. For moderate and semi-arid climates, seasonal moisture variations reach depths of 3.00 - 3.60 m. In a classical methodological context, our hydroclimatological study is based on the exploitation of climatic data from the Tebessa weather station of coordinates: X=991.2m, Y=247.2m, Z=890m. And this for a period of 40 years (1972 to 2012).

III.16.2 Type of climate

Algeria, because of its geographical location, is divided into three zones:

The first with Mediterranean climate in the north, the second with climate semi-arid towards the interior of the country (highlands) and finally an arid climate that characterizes the great Sahara.

The Tebessa study area is part of the semi-arid area known by hot and hot summer's dry and cold and humid winters. This is how these very different variations of the hydroclimatic parameters greatly influence the phenomenon of swelling-withdrawal of clay formations on the surface.

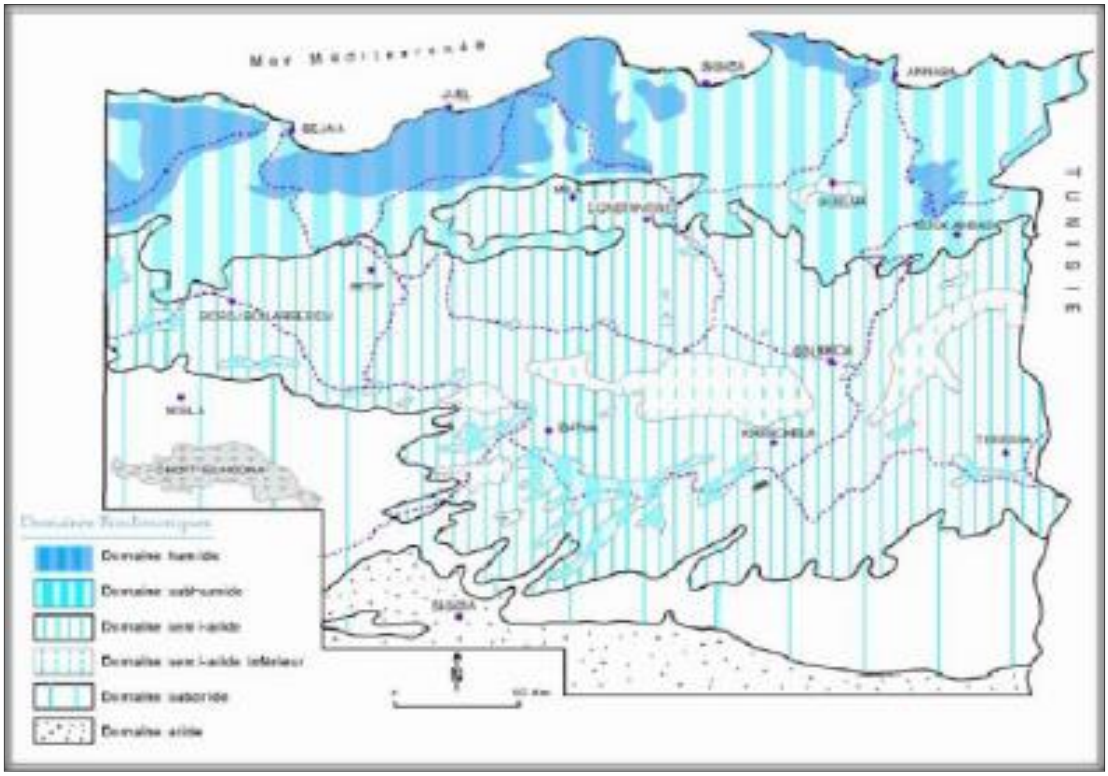

Figure III.55: Simplified map of bioclimatic zones in Eastern Algeria. [131]

III.16. 3 Conclusion

The hydroclimatic study revealed the participation of the water quantities of precipitation to feed surface water courses as well as groundwater especially in January, February and March. During the months when the rainfall is lower than the monthly average, the water supply is compensated by the increase in humidity.

When the potential evapotranspiration loses all the quantity of surface water and subsurface (easily usable reserves) the withdrawal of clays comes into action especially in summer time.

During this period of drought, the reduction in the volume of clays makes appear desiccation cracks in characteristic polygonal shape and prepare the clay surfaces to a new cycle of swelling during torrential precipitation and thunderstorms known especially in summer.

Chapter IV: Compressibility index investigations using statistical tools and Design of experiments (DOE).

IV.1 Introduction

Principal Component Analysis (PCA) is a powerful statistical technique for variable reduction, it used when variables are highly correlated; PCA becomes an essential tool for multivariate data analysis and unsupervised dimension reduction.

The first principal component of the transformation is the linear combination of the original variables with the largest variance; the second principal component is the linear combination of the original variables with the second largest variance and orthogonal to the first principal component.

In many data sets, the first several principal components contribute most of the variance in the original data set, so that the rest can be disregarded with minimal loss of the variance for dimension reduction of the data. [132]

IV.2 Basic Concept

The areas of variance in the data are those where the elements can be best discriminated and where the main underlying phenomena can be observed. [133]

- Areas of greatest "significance "in the data
- If two items or dimensions are highly correlated or dependent
- They are likely to represent highly related phenomena
- If they tell us about the same underlying variance in the data, it is reasonable to combine them to form a single measure.

So we want to combine the related variables and focus on the uncorrelated or independent variables, especially those for which the observations have high variance.

- We want a smaller set of variables that explain most of the variance in the original data, in a more compact and insightful form. [133]

IV.3 Principal components analysis (PCA)

IV.3.1 Mathematical model for principle component analysis (PCA)

Principal component analysis is a statistical tool used to analyze data sets, The central idea of principal component analysis (PCA) is to reduce the dimensionality of a data set consisting of a large number of interrelated variables, while retaining as much of the variation present in the data set as possible [134].

The mathematics behind principal component analysis is statistical and revolves around standard deviation, eigenvalues and eigenvectors.

The whole subject of statistics is based on the idea that you have a large data set and you want to analyze that set in terms of the relationships between individual points in that data set [135].

This is achieved by transforming a new set of variables, the principal components (PCs), which are uncorrelated and are ordered such that the former retain most of the variation present in all of the original variables. [136]

IV.3.2 Principal Component analysis classification

PCA is widely used in the field of image processing feature reduction, feature extraction, anomaly detection, classification and pattern recognition,The following section presents some examples studies combines PCA with classification methods to improve the performance of these methods

A hybrid approach to increase the face recognition accuracy using a combination of Wavelet, PCA, and Neural Networks. They apply a combination of wavelet transform and PCA [137].

Researchers made a different attempt; they presented a comparison between several classification algorithms with feature extraction on a real dataset.

Analysis (PCA) has been used for feature extraction with different values of the ratio R, evaluated and compared using four different types of classifiers on two real benchmark data sets. They reached to the result that feature extraction is especially effective for classification algorithms that do not have any inherent feature selections or feature extraction build in, such as the nearest neighbor methods or some types of neural network. [138]

Recently, a study on the use of PCA and support vector machine classification for heart disease prediction system has been conducted. The main objective of their work is to develop an effective heart disease prediction system using feature extraction and SVM classifier that can be used to predict the onset of the disease. [139]

IV.3.3 PCA for feature reduction

Is one of the most fundamental tools of dimensionality reduction for extracting effective features from high dimensional vectors of input data [140-141].

Dimensionality Reduction is broadly categorized as Feature Selection where a subgroup of all the features is selected and Feature Extraction where the existing features are combined and a new subset of the combinations is created.

Principal Components Analysis (PCA) is one of the common techniques used under Feature Extraction. PCA uses a signal based representation criterion where the purpose of feature extraction is to represent the samples accurately in a lower dimensional space whereas the alternate technique, Linear Discriminant Analysis (LDA) deploys a classification based approach. PCA performs dimensionality reduction whilst maintaining maximum feasible arbitrariness in the high dimensional space.

It can be seen as a data visualization method since high dimensional datasets can be condensed to a lower dimension (2D OR 3D) and then plotted using graphs or visualized using charts [142].

There is a study using principal component analysis (PCA) for dimensionality reduction in an anomaly detection model [12], the major drawback of PCA is that it does not account for class distributability, as it does not take into account the class label of the feature vector. [143]

PCA just performs a coordinate rotation that aligns the coordinate axes transformed earlier, along the directions of maximum variance.

There is no assurance that the directions of maximum variance will comprise of features worthy enough for discrimination [144].

IV.3.4 PCA for anomaly detection

An anomaly discovery method that combines distributed tracking and principal component analysis (PCA), this method has been shown empirically to be effective in highly aggregated networks, i.e., those with a limited number of large nodes and at coarse time scales [145].

Different researchers are attempting to apply the well-known PCA method to real-world anomaly detection. [146], they found that direct application of the PCA method results in poor performance in terms of ROC curves; they studied the problem and discovered that the main source of the problem is the bias due to the correlation of the prediction error terms. After a detailed theoretical analysis, it appears that the correct framework is not the classical PCA but rather the Karhunen-Loeve expansion. They presented the KL expansion and provided a Galerkin method to develop a predictive model. This method was then applied to the Switch network data traces and we showed that a significant improvement is obtained when temporal correlation is taken into account.

An online oversampling principal component analysis (PCA) algorithm to handle interactive visualization of anomalies, their algorithm uses mixture models and the EM algorithm for anomaly detection, but their ideas can be generalized to anomaly detection in other probabilistic settings. [147]

IV.3.5 Advantages and limitations

PCA's key advantages are its low noise sensitivity, the decreased requirements for capacity and memory, and increased efficiency given the processes taking place in a smaller dimension; the complete advantages of PCA are listed below:

1) Lack of redundancy of data given the orthogonal components

2) Reduced complexity in images' grouping with the use of PCA

3) Smaller database representation since only the trainee images are stored in the form of their projections on a reduced basis.

4) Reduction of noise since the maximum variation basis is chosen and so the small variations in the background are ignored automatically. [148]

Table IV.1: The features of PCA [149].

Feature	Principal component analysis
Discrimination between classes	PCA manages the entire data for the principal components analysis without taking into consideration the fundamental class structure
Applications	PCA applications in the significant fields of criminal investigation are beneficial
Computation for large datasets	PCA does not require large Computations
Direction of maximum discrimination	The directions of the maximum discrimination is not the same as the directions of maximum variance as it is not required to utilize the class information such as the within class scatter and between class scatter

Focus	PCA examines the directions that have widest variations
Supervised learning technique	PCA is an unsupervised technique
Well distributed classes in small datasets	PCA is not as powerful as other methods.

Two key disadvantages of PCA are:

1) The covariance matrix is difficult to be evaluated in an accurate manner.

2) Even the simplest invariance could not be captured by the PCA unless the training data explicitly provides this information [150].

IV.4 Introduction

Deposits of fine-grained soils in Tebessa valley North-East of Algeria consist in majority of clayey and marls geological formations are widespread and elongated through the province, many surface settlements and differential movements occur under increased loadings or also can results from the shrinkage swelling of the clayey soils [151]. Consolidation settlement occurs in saturated or near-saturated fine-grained soil due to volume change caused by load-induced squeezing out of water from the pore spaces over a relatively long period of time and is followed by secondary compression. [152]

Total settlements can vary over an area due to variations in loading, soil characteristics, and thickness of compressible layers. The differential settlement movements affect structures foundations stability, building can be devastating by floor cracks and interior walls, non-uniform settling of doors and windows, bulging walls and sunken slabs are often considered as the adverse effects of differential settlement.

Compressibility hazard is, this semi-arid region is composed in major parts of clayey and clayey-shales geological formations, the fine grained materials show large vertical displacements and converted with in this compressible soil a large force is generated within clayey; the knowledge of compressibility index is very important it helps in the design of all shallow projects, underground structures and deep excavation.

The amount of compressibility maybe estimated directly or indirectly; using the laboratory tests corresponds to the first manner estimations, compressible soil was also the main cause of the observed damage to different structures at the study area due to the high intensity generated within the clayey formations in a flat [153], compressible

hazard has become a serious problem. Several formulas have been established in order to predict the compressibility index and potential using simple geotechnical parameters. Recently, the compressibility behavior of soils has been studied using more sophisticated modeling techniques such as dimensional analysis [154-155].

The present study relied on the combination of statistical tools [156-158], and approaches to evaluate and predict the compressibility index parameter from the correlation of physical and mechanical parameters such as the water content, the dry density, plasticity index, the clay content and the pre-consolidation pressure.

The principal component analysis (PCA) and the multiple regressions were used for the studied soil data to derive the model that allows the evaluation of the compressibility index (C_c) [159]; Therefore, many aspects of statistical analyses like the type of regression, the models and results interpretations, and the determination of whether the used methods are feasible and how well the best model fits, were all included in this work. Since the compression index was to be associated with the design of structures, measurement of this amount with direct or indirect methods assumes importance. It has been reported that values of compressibility and collapse potential were found to vary dramatically.

Most of direct methods for determination of the compressibility index are made in the laboratory oedometer tests [160-161], such tests are very expensive and take a long time. In the present research work it is aimed to use the data set collected from our research collaborator, the public works laboratory of Tebessa (LTPE of Tebessa), it is montioned also that the amounts of compressibility and the pre-consolidation pressure are measured in the oedometer test using procedure of the AFNOR standards [162],The test is initially for the study of the soil compressibility, it also allows the measures of the compressibility parameters (C_c).

Our aim from this research work is to save time, costs and serve the public works laboratory with a rapid way to predict this property of compressible clayey soil; we proceeded to estimate the compressibility index by the use of the indirect methods. As first step we proceed at the different analysis using full factorial design, then the principal component analysis has been investigated and finally a combination with regression analysis were detailed to show the feasibility of the use of regression tools in estimating engineering compressibility index properties of compressible soils.

Experimental studies on compressible soils show that the compressibility percentage of soils increase in proportion to their unit weights, the liquid limits, the water contents, plasticity index, void ratio and the pre-consolidation pressures, It takes into consideration from all the measured parameters or calculated in laboratory tests; which are physical parameters (dry unit weight $\boldsymbol{\gamma_d}(\mathrm{kN/m^3})$, water content $\boldsymbol{w}$ (%), plasticity index $\boldsymbol{I_p}$(%) and liquid limit $\boldsymbol{W_L}$(%) the fine fraction $\boldsymbol{F_f}$(%) that present the percent of fines under 80µm, and mechanical parameters the pre-consolidation pressure $\boldsymbol{P_c}$(kPa).

IV.5 Methods and materials

IV.5.1 General statistical parametric analysis

Principal component analysis (PCA) is a multivariate statistical procedure that can be used to identify factors (correlated subsets of variables) in large data sets. This statistical method appears useful for scientists investigating soil processes, but it has received little attention. Reported applications of principal component analysis share a common fault--subjective, user-specified analytical options apparently are not recognized, for they are not discussed. [163]

Principal component analysis and common factor analysis ordinarily begin with the correlation matrix and are mathematically similar in many respects. The methods share the common goals of:

1)attempting to summarize intercorrelations among the variables,

2) Reducing a large number of variables to a smaller number of factors.

The major difference in the two methods is the variance that is targeted for explanation, PCA attempts to account for all of the variance in the data set, as represented by the 1.0 values in the diagonal of the correlation matrix. Common factor analysis attempts to account for only that variance that is common to the variables sampled. For example, the shared variance for a given variable is often represented by the squared multiple correlation, R^2, between the jth variable and the rest of the variables. Clearly R^2 is less than or equal to 1.0.

The focus on only that portion of the variance that is shared by the variables led to the phrase "common factor analysis". Detailed discussion is beyond the scope of this paper.

With (PCA) technique we can reduce the number of variables and eliminate the

relations among input variables by developing a set of new variables that are linear functions of the original variables. This set will retain properties of the original ones, provided that the number of new variables will not exceed the original number. That is, if the original number of variables is $\boldsymbol{p}$ and the number of new variables is $\boldsymbol{m}$, then $\boldsymbol{m \leq p}$ [164].

The number of variables m is chosen components to sufficiently explain the variation of the data, descriptive analysis of all data sets taken from was performed by classical statistics, determining the minimum and maximum values and calculating the values of mean and the standard deviation presented on Table IV.2

Table IV.2: Summary statistics Summary statistics of 118 analyzed data of the studied soil [154]

Variable	Observations	Obs. with missing data	Obs. without missing data	Minimum	Maximum	Mean	Std. deviation
γd (kN/m3)	118	0	118	14,100	20,200	16,951	1,273
γh (kN/m3)	118	0	118	17,300	21,900	19,733	1,022
W %	118	0	118	8,430	32,300	19,292	4,502
FF <0,08mm	118	0	118	61,200	98,500	88,297	9,662
WL %	118	0	118	33,000	83,000	52,568	10,304
IP%	118	0	118	16,000	60,000	33,686	8,079
e0	118	0	118	0,355	1,066	0,653	0,144
Cs	118	0	118	0,005	0,184	0,065	0,039
Cc	118	0	118	0,012	0,427	0,194	0,103
Pc(KPA)	118	0	118	12,000	360,000	178,292	53,330
Gs	118	0	118	2,657	2,790	2,709	0,024
Sr	118	0	118	52,000	100,000	81,669	11,493

In this first step statistical tests were carried out to take a general overview and screening as much as parameters that known have any relationships with the coefficient of compressibility (C_c) of any clayey soil. These variables are chosen as independent variables as pre-consolidation pressure ($\boldsymbol{P_c}$), dry density ($\boldsymbol{\gamma_d}$), water content ($\boldsymbol{w}$) plasticity index ($\boldsymbol{I_P}$), liquid limit ($\boldsymbol{w_L}$)**,** and the fine fraction ($\boldsymbol{ff}$) in % < 80µm, ,wet density (γ_h),swelling coefficient ($\mathbf{C_s}$), void ratio ($\mathbf{e_0}$), degree of saturation ($\mathbf{S_r}$), density of solid grains ($\mathbf{G_s}$)

IV.5.2 The use of different literature empirical models

From all models published in literature as mentioned in the following figures IV.9, it is clear that the maximum and best fitted model than can describe the goodness of fit of the compressibility index of the studied soil region is the model of (Azzouz et Al, Wroth & Wood, koppula, Khafadji, Nagaraj, Vinod).

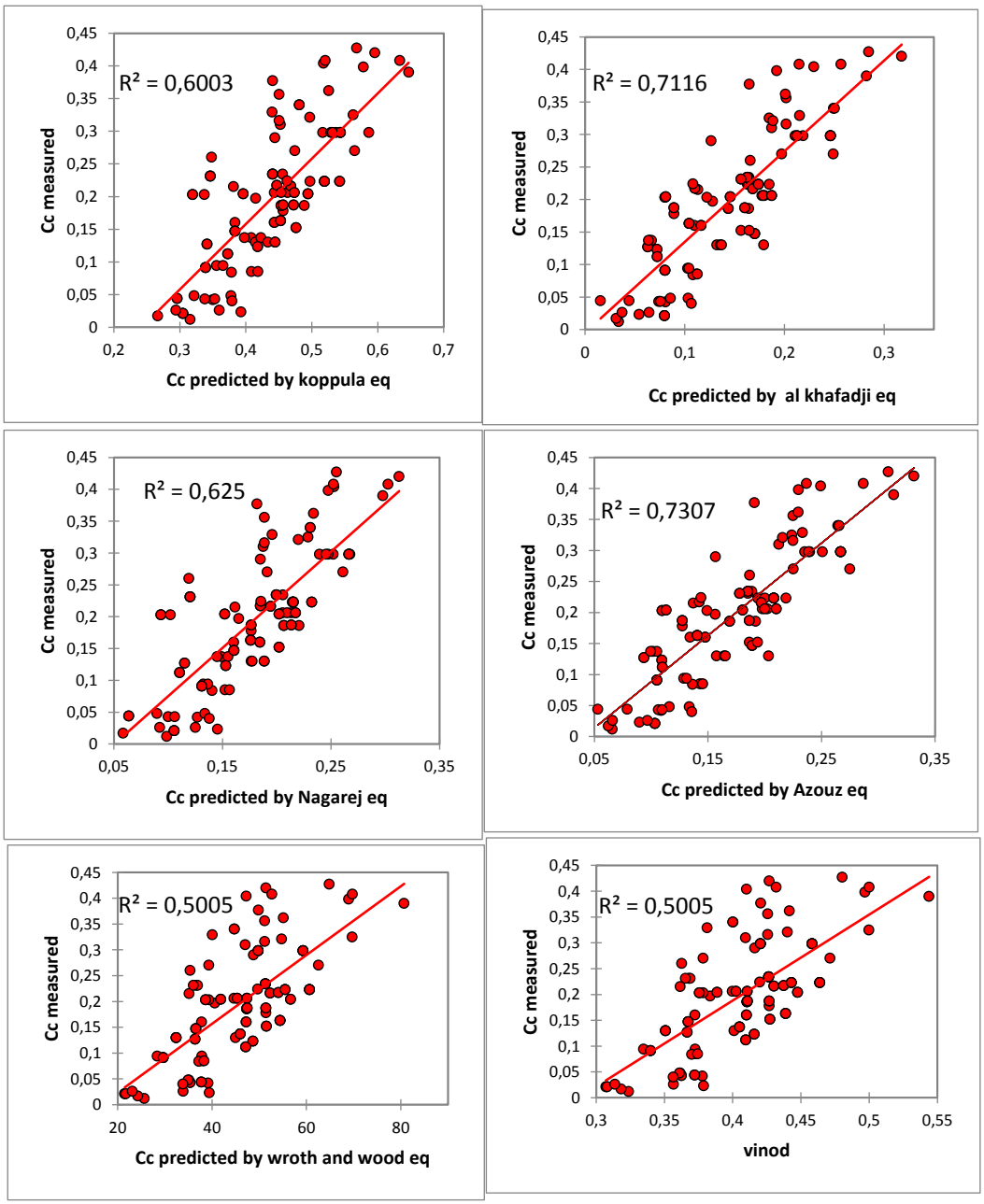

Figure IV.1: Compressibility index (Cc) measured vs predicted using different published equations

IV.5.3 Statistical Data analysis of the collected samples in Tebessa province

Table IV.3: PCA correlation matrix

Variables	γd (KN/m3)	γh (KN/m3)	W %	Ff <0,08mm	WL %	IP%	e0	Cs	Cc	Pc(kPA)	Gs	Sr
γd (KN/m3)	**1**	0,8489	-0,786	-0,3718	-0,483	-0,468	-0,871	-0,648	-0,711	0,0765	0,1683	0,0128
γh (KN/m3)	0,8489	**1**	-0,584	-0,2581	-0,379	-0,352	-0,803	-0,618	-0,685	0,0811	0,1531	0,3012
W %	-0,7866	-0,5846	**1**	0,4297	0,4600	0,4756	0,8341	0,6603	0,6751	0,0758	-0,039	0,4807
Ff <0,08mm	-0,3718	-0,2581	0,4297	**1**	0,3665	0,5025	0,3993	0,4778	0,5418	0,1203	0,1416	0,1793
WL %	-0,4835	-0,3795	0,4600	0,3665	**1**	0,9381	0,4541	0,6702	0,5957	0,0902	0,0775	0,1561
IP%	-0,4682	-0,3523	0,4756	0,5025	0,9381	**1**	0,4588	0,7026	0,6541	0,1841	0,0902	0,1920
e0	-0,8717	-0,8036	0,8341	0,3993	0,4541	0,4588	**1**	0,6886	0,8123	-0,0229	-0,049	0,0117
Cs	-0,6480	-0,6185	0,6603	0,4778	0,6702	0,7026	0,6886	**1**	0,8453	0,0214	-0,0766	0,0997
Cc	-0,7113	-0,6850	0,6751	0,5418	0,5957	0,6541	0,8123	0,8453	**1**	0,1011	-0,054	0,0145
Pc(kPA)	0,0765	0,0811	0,0758	0,1203	0,0902	0,1841	-0,022	0,0214	0,1011	**1**	-0,055	0,2152
Gs	0,1683	0,1531	-0,039	0,1416	0,0775	0,0902	-0,049	-0,076	-0,054	-0,0558	**1**	0,0795
Sr	0,0128	0,3012	0,4807	0,1793	0,1561	0,1920	0,0117	0,0997	0,0145	0,2152	0,0795	**1**

The first result to look at is the correlation matrix. We can see right away that γ_d has an important regression with γ_h (R^2 =0,84), also they are negatively correlated with some parameters like water content w, limit of liquidity W_L, plasticity index Ip, void ratio e_0, swelling index C_s, and compression index C_c, but we can also see that has a low correlation with the rest of parameter (P_c, G_s, S_r), These latter variables could have been removed without effect on the quality of the results

The next table and the corresponding chart are related to a mathematical object, the eigenvalues, which reflect the quality of the projection from the N-dimensional initial table (N=12 in this example) to a lower number of dimensions. In this example, we can see that the first eigenvalue equals 5,8795 and represents 48,99% of the total variability. This means that if we represent the data on only one axis, we will still be able to see % of the total variability of the data.

Each eigenvalue corresponds to a factor, and each factor to a one dimension. A factor is a linear combination of the initial variables, and all the factors are un-correlated (r=0). The eigenvalues and the corresponding factors are sorted by descending order of how much of the initial variability they represent (converted to %).

Ideally, the first two or three eigenvalues will correspond to a high % of the variance, ensuring us that the maps based on the first two or three factors are a good quality projection of the initial multi-dimensional table.

In this example, the first two factors allow us to represent 63, 56 % of the initial variability of the data. This is a good result, but we'll have to be careful when we interpret the maps as some information might be hidden in the next factors.

One notes that there are four components with eigenvalues greater than or equal to 1.0 and that together they account for 81,68 % of the variability in the original data ,it is safe to only retain two components, the first and second principal components are a result of the linear combination of the twelve studied variables and both explained 48,99 % and 14,56 % of the variance, respectively, the others components as shown on the Table IV.4 the values in bold correspond for each variable to the factor for which the squared cosine is the largest.

Table IV.4: Eigenvalue and accumulated proportion of principal component analysis of data samples

	F1	F2	F3	F4	F5	F6	F7	F8	F9	F10	F11	F12
Eigenvalue	5,879	1,748	1,154	1,019	0,800	0,631	0,342	0,167	0,095	0,080	0,042	0,0305
Variability (%)	48,99	14,56	9,622	8,496	6,675	5,308	2,856	1,394	0,799	0,668	0,357	0,2545
Cumulative %	48,99	63,56	73,18	81,685	88,360	93,669	96,526	97,920	98,719	99,388	99,745	100,000

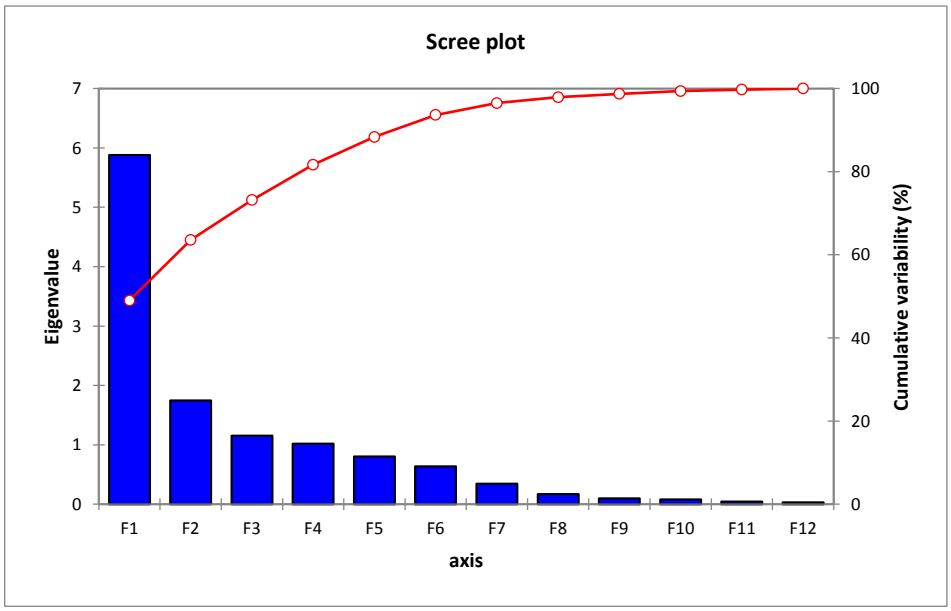

Figure IV.2: Scree plot of the data

Table IV.5: Squared cosines of the variables

	F1	F2	F3	F4	F5	F6	F7	F8	F9	F10	F11	F12
γd (kN/m3)	**0,677**	0,094	0,020	0,019	0,018	0,007	0,103	0,046	0,011	0,001	0,003	0,001
γh (kN/m3)	**0,650**	0,238	0,002	0,000	0,026	0,007	0,003	0,000	0,043	0,030	0,000	0,000
W %	**0,745**	0,006	0,085	0,125	0,002	0,004	0,000	0,004	0,000	0,004	0,006	0,018
FF <0,08mm	0,343	0,109	0,042	0,000	0,030	**0,459**	0,015	0,000	0,002	0,000	0,000	0,000
WL %	**0,562**	0,091	0,072	0,063	0,115	0,042	0,019	0,006	0,007	0,007	0,016	0,001
IP%	**0,653**	0,097	0,047	0,069	0,067	0,007	0,016	0,000	0,010	0,007	0,024	0,001
e0	**0,802**	0,053	0,007	0,035	0,023	0,004	0,003	0,049	0,000	0,013	0,000	0,012
Cs	**0,792**	0,000	0,001	0,004	0,025	0,001	0,107	0,053	0,007	0,009	0,002	0,001
Cc	**0,844**	0,003	0,001	0,010	0,004	0,005	0,074	0,002	0,029	0,016	0,011	0,001
Pc(KPA)	0,017	0,243	0,153	**0,295**	0,267	0,023	0,000	0,000	0,001	0,001	0,000	0,000
Gs	0,002	0,149	**0,502**	0,119	0,161	0,064	0,002	0,002	0,000	0,000	0,000	0,000
Sr	0,018	**0,552**	0,180	0,199	0,029	0,002	0,000	0,000	0,003	0,011	0,002	0,003

According to Factor Loadings Correlations between variables and factors, and the Eigenvalue vectors (Figure IV.3, Table IV.6) the variables with negative contribution are on the factors F1, F2 respectively, ((γ_d), ((γ_h) (e_0) (C_c) (G_s) the other factors represented by (w) (Ff <0,08mm) (w_L) (I_P) (C_s) (P_c) (S_r) have a positive contribution in this analysis, it is important to note the high and strong correlation between the parameter ((w_L) (I_P)), also the good correlation between (C_c) and ((e_0), (C_s), (I_P)), this is because this method take into account neither the position of points in space, neither the degrees of similarity between the parameters.

Table IV.6: Factor loadings correlations between variables and factors.

	F1	F2	F3	F4	F5	F6	F7	F8	F9	F10	F11	F12
γd (KN/m3)	-0,86	0,33	0,14	-0,10	-0,03	0,07	0,23	-0,04	0,02	0,21	0,009	0,023
γh (KN/m3)	-0,76	0,53	-0,01	0,02	-0,14	0,13	0,09	-0,20	-0,15	-0,11	-0,01	0,007
W %	0,83	0,08	-0,40	0,30	-0,02	-0,09	-0,02	-0,00	-0,07	0,05	0,007	0,126
Ff<0,08mm	0,577	0,323	0,127	0,113	0,351	0,616	-0,16	0,030	-0,01	0,028	-0,02	-0,04
WL %	0,731	0,341	0,343	-0,22	-0,33	-0,15	-0,15	-0,02	-0,00	0,045	-0,13	0,003
IP%	0,757	0,423	0,319	-0,25	-0,20	-0,03	-0,10	-0,03	0,00	-0,00	0,153	0,003
e0	0,885	-0,26	-0,13	0,170	0,129	-0,11	0,010	-0,20	-0,09	0,099	0,008	-0,09
Cs	0,877	0,036	0,087	-0,09	-0,11	0,084	0,365	0,206	-0,12	-0,01	-0,00	-0,02
Cc	0,906	-0,04	0,055	-0,08	0,120	0,078	0,282	-0,17	0,165	-0,07	-0,02	0,032
Pc(kPA)	0,06	0,47	-0,33	-0,55	0,527	-0,25	-0,01	0,030	-0,02	-0,01	-0,01	-0,04
Gs	-0,05	0,38	0,54	0,568	0,345	-0,32	0,048	0,038	0,001	-0,02	-0,01	-0,02
Sr	0,13	0,70	-0,53	0,32	-0,24	-0,00	0,02	0,05	0,11	-0,03	-0,09	-0,06

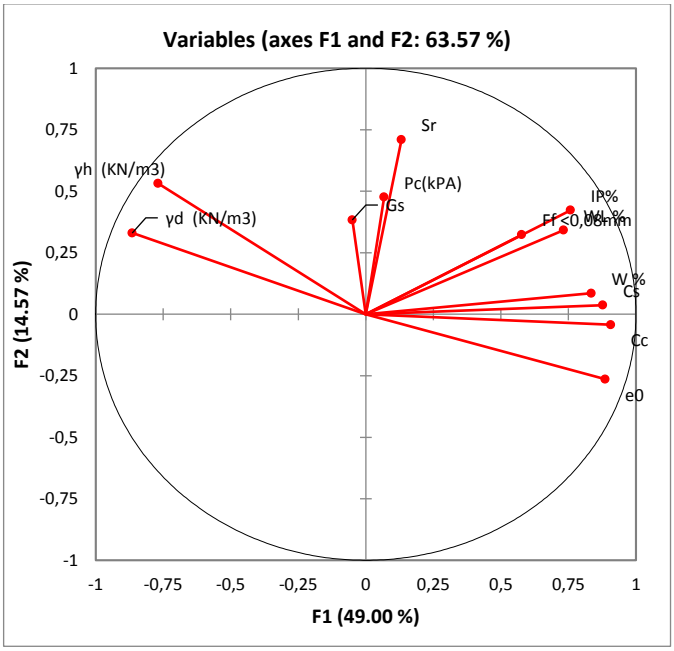

Figure IV.3: The circle of correlation of variables

The first map is called the correlation circle (below on axes F1 and F2). It shows a projection of the initial variables in the factors space. When two variables are far from the center, then, if they are: Close to each other, they are significantly positively correlated (r close to 1); If they are orthogonal, they are not correlated (r close to 0); If they are on the opposite side of the center, then they are significantly negatively correlated (r close to -1).

When the variables are close to the center, some information is carried on other axes, and that any interpretation might be hazardous. For example, we might be tempted to interpret a correlation between Cc and Sr, although, in fact, there is none. This can be confirmed either by looking at the correlation matrix or by looking at the correlation circle on axes F1 and F3.

The first component was negatively correlated with the variable (γ_d (kN/m^3) and (γ_h (kN/m^3), barely negative with the (G_s) and positively with the other variables (Figure IV.11). Thus, the effect of the variation factor of the variable (γ_d (kN/m^3) led to a reduction of its values while the values of other variables increased. This component can be interpreted as a response related to the initial soil proprieties and the standard AFNOR procedure applied to obtain the compressibility value, according to [165], the compressibility without applying any load to a specimen depends mainly on moisture content and on dry density when a certain load is applied, while the compressibility in constant volume method depends on dry density [166], showed that the fine grained and

clayey soil need long time to complete compression process. Time is also function of permeability, thickness of layer, initial moisture content and dry density.

We not that total of the parameters is inversely correlated with density. The effect of soil water w% content is clearly distinguished on the figure IV.3 with negative contribution on axis F2 and show inverse correlation with the total of parameters

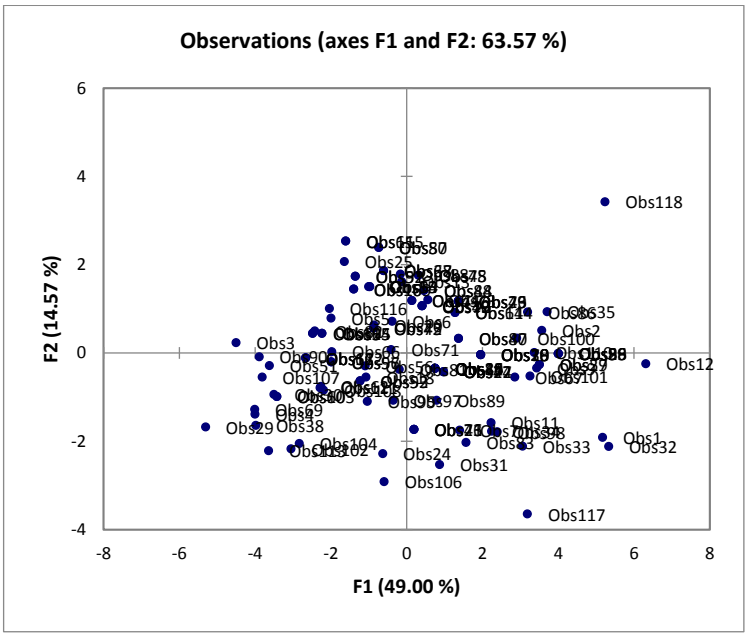

Figure IV.4: First factorial plane (F1F2) of individuals

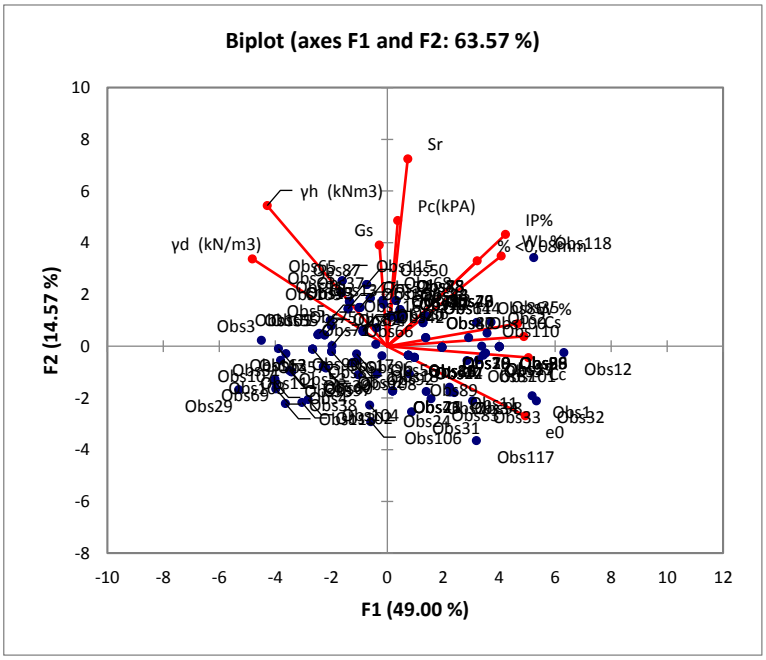

Figure IV.5: The Biplot show of analyzed parameters and individuals in the (F1F2) plane.

IV.5.4 multicollinearity study

Variables are said to be multicolinear if there is a linear relationship between them. It is an extension of the simple case of collinearity between two variables. For example, for three variables X_1, X_2, X_3, we will say that they are multicolinear if we can write:

$$X1 = aX2 + bX3 \quad \text{(IV.1)}$$

where: a and b are two real numbers.

Multicollinearity is a problem in regression analysis that occurs when independent variables are highly correlated.

The relationship between the independent variables and the dependent variables is distorted by the very strong relationship between the independent variables [167], leading to the likelihood that our interpretation of relationships will be incorrect.

In the worst case, if the variables are perfectly correlated, the regression cannot be computed.

Multicollinearity is detected by examining the tolerance for each independent variable. Tolerance is the amount of variability in one independent variable that is no explained by the other independent variables.

Tolerance values less than 0.10 indicate collinearity, if we discover collinearity in the regression output, we should reject the interpretation of the relationships as false until the issue is resolved.

The tolerance for each of the models is $(1\text{-}R^2)$. It is used in several methods (linear regression, logistic regression, discriminant factor analysis) as a filter criterion for variables. If a variable has a tolerance lower than a fixed threshold (the tolerance is calculated by taking into account the variables already used in the model), it is not allowed to enter the model because its contribution is negligible and it would risk causing digital problems.

Sightings, the VIF or Variance Inflation Factor which is equal to the inverse of the tolerance, Multicollinearity can be resolved by combining the highly correlated variables through principal component analysis, or omitting a variable from the analysis, the PCA leads to obtain the eight highly correlated parameters as shown on the correlation circle Figure IV.6 and the scree plot Figure IV.7 display the number of factors retain in an exploratory factor analysis (FA) or principal components to keep in

a principal which the first two factors represent 75.04% of the initial variability in the data.

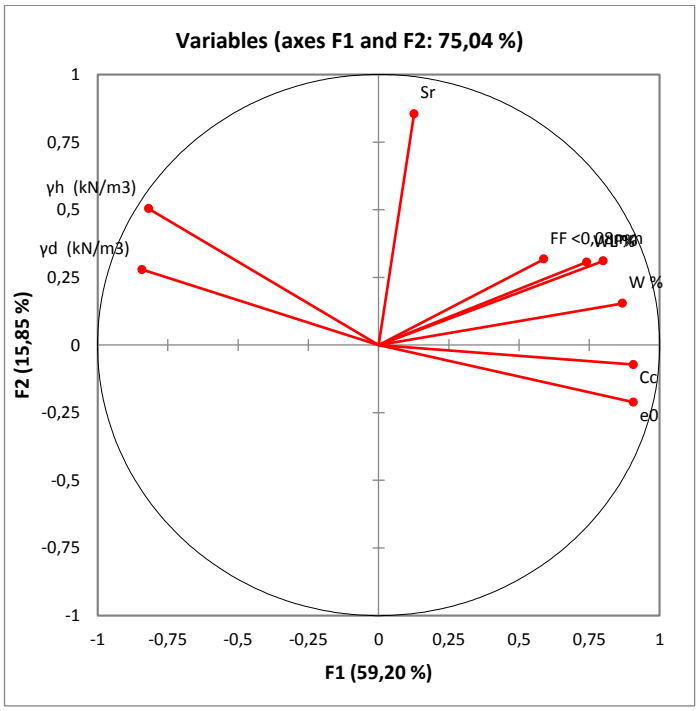

Figure IV.6: The correlation circle

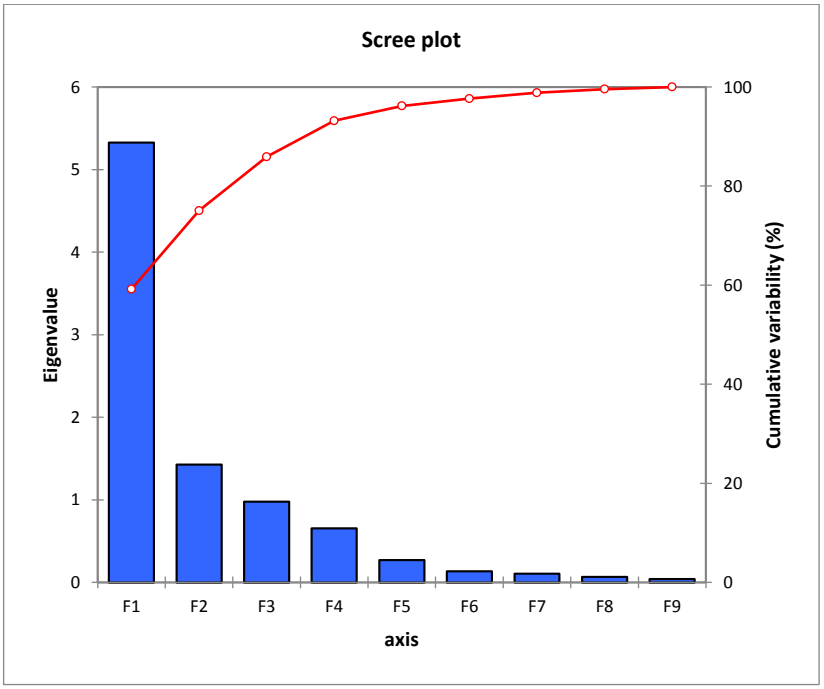

Figure IV.7: Scree plot of data

It is concluded that the contributed parameters are (γ_d,γ_h);(S_r); (F_f <0,08mm,W_L,I_P, W);(Cc,e_0). [168]

Table IV.7: Multicolinearity statistics

	γd (kN/m3)	γh (kN/m3)	W %	FF <0,08mm	WL %	IP%	e0	Sr
Tolerance	0,212	0,155	0,068	0,666	0,157	0,134	0,095	0,234
VIF	4,725	6,458	14,693	1,502	6,353	7,483	10,520	4,276

IV.5.5 Agglomerative hierarchical clustering (Dendrogram) AHC

The chart below is the dendrogram. It represents how the algorithm works to group the observations, then the subgroups of observations. As you can see, the algorithm has successfully grouped all the observations, the dotted line represents the automatic truncation, leading to five groups.

So, the AHC identify groups of observations with similar characteristics (e.g. the different parameters (γ_d, γ_h, W, I_P….), individuals in the same group are the most alike possible, in this case the data is classified into three classes based on the parameters, we can see this in the graph Figure IV.8 and on the Table Table IV. 8 below.

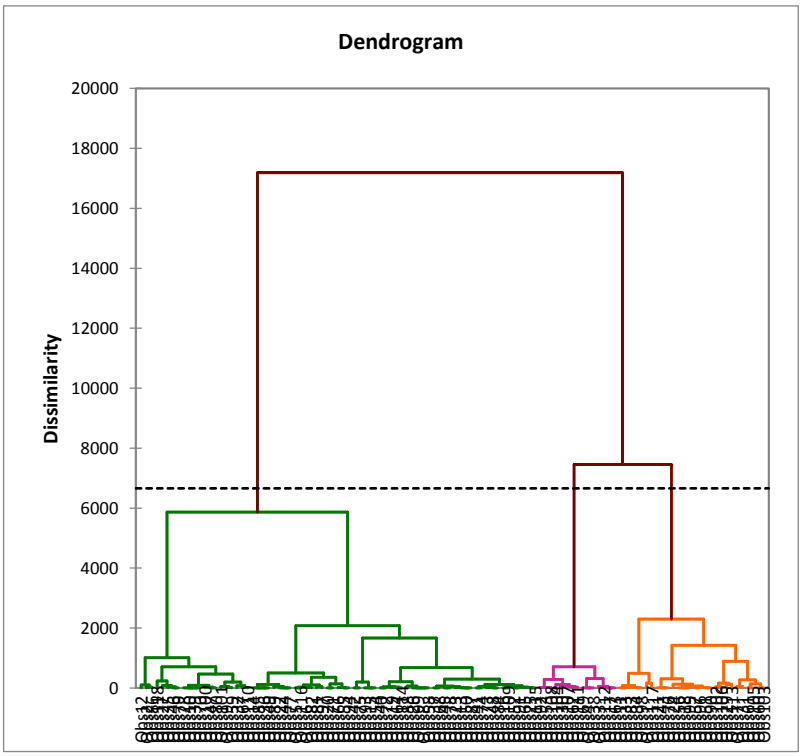

Figure IV.8: Dendrogram

Table IV.8: Class centroids

Class	γd (kN/m3)	γh (kN/m3)	W %	FF <0,08mm	WL %	IP%	e0	Sr
1	17,007	19,400	16,089	86,497	47,607	30,143	0,649	64,643
2	16,755	19,713	21,017	92,422	56,813	37,280	0,677	87,373
3	17,827	20,453	16,651	71,028	40,600	22,333	0,540	84,933

IV.5.6 Multiple regression analysis and results discussion

Multiple regression analysis [169], was considered to derive an equation that can be used to predict the compressibility index from known soil physical and mechanical properties.

The use of multiple regression analysis is very useful in reducing the number of variables contributed in the compressible soil phenomenon, variables are reduced to the minimum factor which adequately explains the variation in compressibility properties of the studied soils. Trials were carried out to correlate the compressibility index to a combination of variables.

Table IV.9: Different models proposed for the prediction of the compressibility index by the use of multiple regression analysis

	Goodness of fit statistics:								
Equation of the model:	ANOVA								
1 variable	R^2	Ad. R^2	Se	F	P v	VIF			
Cc = -0,19+0,59*e0	***0,68***	0,68	0,052	250,29	< 0,0001	6,92			
Cc = 4,6315E-02+2,29*Cs	***0,74***	0,74	0,046	339,82	< 0,0001				
2 variables									
Cc = 0,67-4,053E-02*γd +4,01E-03*WL	***0,59***	0,58	*0,066*	83,002	< 0.0001	1,25			
Cc = 0,57-3,47E-02*γd +6,30E-03*IP	***0,64***	0,63	*0,064*	103,44	< 0.0001	1,35			
Cc = -0,14-2,23E-03*γd +0,57*e0	***0,68***	0,67	*0,089*	124,21	< 0.0001	2,92			
Cc = 0,38-0,018*γd +1,91*Cs	***0,77***	0,77	*0,056*	200,54	< 0.0001	1,64			
Cc = 0,94-4,76E-02*γh +9,92E-03*W	***0,67***	0,66	*0,069*	116,75	< 0.0001	1,68			
Cc = 1,14-6,49E-02*γh +3,71E-03*FF <0,08mm	***0,66***	0,66	*0,056*	116,18	< 0.0001	1,10			
Cc = 1,168-5,90E-02*γh +3,65E-03*WL	***0,66***	0,65	*0,062*	114,26	< 0.0001	1,25			
Cc = 1,04-5,32E-02*γh +5,85E-03*IP	***0,72***	0,71	*0,056*	147,93	< 0.0001	1,30			

Cc = 0,25-1,90E-02*γh +0,48*e0	***0,69***	0,68	*0,094*	130,39	< 0.0001	3,32			
Cc = 0,70-0,03*γh +1,74*Cs	***0,80***	0,79	*0,055*	229,65	< 0.0001	1,79			
Cc = -0,209+0,01*W +5,59E-03*IP	***0,66***	0,66	*0,064*	116,32	< 0.0001	1,46			
Cc = -0,19+1,83E-03*W +0,54*e0	***0,68***	0,67	*0,103*	125,00	< 0.0001	3,91			
Cc = -2,81E-02+5,35E-03*W +1,84*Cs	***0,77***	0,76	*0,064*	194,47	< 0.0001	2,07			
Cc = 7,11E-02+2,05E-02*W -3,33E-03*Sr	***0,65***	0,64	*0,061*	107,08	< 0.0001	1,22			
Cc = -0,373+2,57E-03*FF <0,08mm+0,52*e0	***0,73***	0,72	*0,053*	156,56	< 0.0001	1,20			
Cc = -9,26E-02+1,72E-03*FF <0,08mm+2,08*Cs	***0,76***	0,76	*0,051*	187,68	< 0.0001	1,30			
Cc = -0,273+2,78E-03*WL +0,49*e0	***0,74***	0,73	*0,055*	164,28	< 0.0001	1,34			
Cc = 2,30E-02+5,71E-04*WL +2,19*Cs	***0,74***	0,74	*0,064*	169,96	< 0.0001	1,90			
Cc = -0,25+4,76E-03*IP+0,44*e0	***0,78***	0,77	*0,052*	205,01	< 0.0001	1,42			
Cc = -9,68E-02+0,30*e0+1,47*Cs	***0,82***	0,82	*0,057*	273,64	< 0.0001	2,16			

3 variables											
Cc = 1,04-3,84E-03*γd -4,96E-02*γh +5,76E-03*IP	***0,72***	0,71	*0,058*	98,10	< 0.0001	3,20	3,09	1,37			
Cc = 0,70-3,37E-03*γd -2,84E-02*γh +1,72*Cs	***0,80***	0,79	*0,057*	152,29	< 0.0001	3,15	3,42	1,86			
Cc = 0,72-4,67E-02*γh +7,42E-03*W +2,76E-03*FF <0,08mm	***0,72***	0,71	*0,054*	99,63	< 0.0001	1,69	1,90	1,24			
Cc = 0,72-4,17E-02*γh +7,61E-03*W +2,743E-03*WL %	***0,72***	0,71	*0,058*	99,66	< 0.0001	1,75	1,87	1,38			
Cc = 0,70-3,99E-02*γh +6,29E-03*W +4,68E-03*IP	***0,75***	0,75	*0,056*	119,25	< 0.0001	1,75	1,97	1,52			
Cc = 0,35-2,33E-02*γh +3,55E-03*W +0,35*e0	***0,70***	0,69	*0,149*	88,47	< 0.0001	3,64	4,30	8,46			
Cc = 0,57-2,73E-02*γh +3,28E-03*W +1,54*Cs	***0,80***	0,80	*0,063*	160,67	< 0.0001	1,97	2,29	2,43			
Cc = -0,37+7,57E-07*W +2,57E-03*FF <0,08mm+0,52*e0	***0,73***	0,72	*0,096*	103,47	< 0.0001	4,05	1,24	3,93			
Cc = -0,13+4,74E-03*W +1,45E-03*FF <0,08mm+1,72*Cs	***0,78***	0,78	*0,064*	139,29	< 0.0001	2,12	1,33	2,23			
Cc = -0,12+1,77E-02*W +2,83E-03*FF <0,08mm-3,30E-03*Sr	***0,70***	0,69	*0,056*	91,75	< 0.0001	1,47	1,24	1,22			
Cc = -0,39+1,96E-03*FF <0,08mm+2,26E-03*WL +0,45*e0	***0,76***	0,76	*0,054*	124,93	< 0.0001	1,29	1,44	1,44			
Cc = -0,10+1,68E-03*FF <0,08mm+3,16E-04*WL +2,03*Cs	***0,76***	0,76	*0,065*	124,38	< 0.0001	1,33	1,94	2,09			
Cc = -0,23-1,82E-03*WL +6,86E-03*IP+0,44*e0	***0,78***	0,78	*0,051*	140,00	< 0.0001	5,97	6,30	1,42			
Cc = 2,86E-02-2,58E-03*WL %+5,14E-03*IP%+1,98*Cs	***0,77***	0,76	*0,065*	128,17	< 0.0001	6,01	6,71	2,14			
Cc = -0,14+2,15E-03*IP+0,29*e0+1,16*Cs	***0,84***	0,83	*0,067*	199,00	< 0.0001	2,13	2,16	3,24			

Cc = -0,27+4,58E-03*IP+0,45*e0+1,23E-04*Pc	***0,78***	0,77	*0,044*	138,16	< 0.0001	1,48	1,44	1,04			
Cc = 0,28+4,83E-03*IP+0,44*e0-0,20*Gs	***0,78***	0,77	*0,043*	137,18	< 0.0001	1,43	1,43	1,01			
Cc = -0,20+4,98E-03*IP+0,44*e0-6,76E-04*Sr	***0,78***	0,78	*0,044*	139,92	< 0.0001	1,47	1,43	1,03			
Cc = -0,13+0,30*e0+1,45*Cs+1,94E-04*Pc	***0,83***	0,83	*0,038*	192,21	< 0.0001	2,17	2,17	1,00			
Cc = -0,21+0,29*e0+1,48*Cs+4,30E-02*Gs	***0,82***	0,82	*0,039*	180,96	< 0.0001	2,16	2,17	1,00			
Cc = -0,04+0,29*e0+1,51*Cs-6,08E-04*Sr	***0,83***	0,82	*0,038*	186,65	< 0.0001	2,17	2,20	1,02			
Cc = -0,161+2,29*Cs+1,54E-04*Pc+6,65E-02*Gs	***0,75***	0,74	*0,046*	114,64	< 0.0001	1,00	1,00	1,00			
Cc = 8,98E-02+2,32*Cs+2,03E-04*Pc-1,00E-03*Sr	***0,76***	0,75	*0,047*	122,03	< 0.0001	1,01	1,05	1,06			
4 variables											
Cc = 0,61+1,56E-02*γd -5,05E-02*γh +8,13E-03*W +4,71E-03*IP	***0,76***	0,75	*0,056*	92,81	< 0.0001	4,46	3,09	2,74	1,52		
Cc = 0,540+5,99E-03*γd -3,16E-02*γh +4,08E-03*W +1,52*Cs	***0,81***	0,80	*0,064*	120,38	< 0.0001	4,54	3,53	3,30	2,47		
Cc = 0,61-4,07E-02*γh +5,42E-03*W +1,67E-03*FF <0,08mm+3,85E-03*IP	***0,77***	0,76	0,059	97,55	< 0.0001	1,75	2,05	1,44	1,76		
Cc = 0,48-2,88E-02*γh +2,47E-03*W +1,66E-03*FF <0,08mm+1,38*Cs	***0,82***	0.81	0,063	134,77	< 0.0001	1,99	2,36	1,34	2,63		
Cc = -0,39-9,49E-04*W +2,00E-03*FF <0,08mm+2,29E-03*WL +0,47*e0	***0,76***	0,75	0,091	93,09	< 0.0001	4,10	1,32	1,46	4,03		
Cc = -0,17+1,52E-02*W +2,14E-03*FF <0,08mm+2,65E-03*WL -3,15E-03*Sr	***0,75***	0,74	0,051	87,59	< 0.0001	1,73	1,32	1,43	1,23		
Cc = -0,31+1,21E-03*FF <0,08mm-1,40E-03*WL +5,76E-03*IP+0,43*e0	***0,79***	0,78	0,051	109,72	< 0.0001	1,47	6,17	7,15	1,47		
Cc = -0,11-2,38E-03*WL +4,80E-03*IP+0,29*e0+1,20*Cs	***0,84***	0,84	0,066	158,92	< 0.0001	6,02	6,72	2,16	3,27		
c = -0,18-1,81E-03*WL +7,07E-03*IP+0,44*e0-6,73E-04*Sr	***0,79***	0,78	0,043	107,51	< 0.0001	5,97	6,35	1,43	1,03		
Cc = -8,79E-02+2,36E-03*IP+0,28*e0+1,17*Cs-7,64E-04*Sr	***0,84***	0,84	0,037	155,93	< 0.0001	2,17	2,18	3,25	1,04		
Cc = 0,52+1,53E-02*γd -	***0,78***	0,77	0,058	81,07	<	4,46	3,09	2,83	1,44	1,76	

0,05*γh +7,23E-03*W +1,66E-03*FF <0,08mm+3,89E-03*IP					0.0001						
Cc = 0,44+6,9E-03*γd -3,39E-02*γh +3,38E-03*W +1,68E-03*FF <0,08mm+1,35*Cs	***0,82***	0,82	0,064	108,06	< 0.0001	4,55	3,56	3,35	1,34	2,68	
Cc Cc = 0,63-0,04*γh +5,40E-03*W +1,59E-03*FF <0,08mm-9,22E-04*WL +4,97E-03*IP	***0,77***	0,76	0,12	77,96	< 0.0001	1,76	2,05	1.03	6,15	7,33	
Cc = 0,47-2,89E-02*γh +2,47E-03*W +1,61E-03*FF <0,08mm+3,74E-04*WL %+1,31*Cs	***0,82***	0,82	0.072	107,40	< 0.0001	1,99	2,36	1,37	1,94	3,45	
Cc = -0,31-2,13E-03*W +1,261E-03*FF <0,08mm-1,49E-03*WL +5,99E-03*IP+0,48*e0	***0,79***	0,78	0,085	88,12	< 0.0001	4,19	1,48	6,20	7,30	4,03	
Cc = -0,10+1,42E-02*W +1,52E-03*FF <0,08mm-5,03E-04*WL +5,03E-03*IP-3,06E-03*Sr	***0,77***	0,76	0,049	78,17	< 0.0001	1,81	1,48	6,15	7,32	1,23	
Cc = -0,17+8,76E-04*FF <0,08mm-2,06E-03*WL +4,07E-03*IP+0,28*e0+1,16*Cs	***0,85***	0,84	0,065	130,59	< 0.0001	1,48	6,24	7,45	2,18	3,31	
Cc = 0,34+1,33E-03*FF <0,08mm-1,23E-03*WL +5,59E-03*IP+0,42*e0-0,24*Gs	***0,79***	0,78	0,043	88,70	< 0.0001	1,51	6,27	7,20	1,50		
Cc = -0,26+1,34E-03*FF <0,08mm-1,34E-03*WL +5,88E-03*IP+0,42*e0-7,898E-04*Sr	***0,80***	0,79	0,043	91,06	< 0.0001	1,49	6,17	7,16	1,48	1,05	
6 variables											
Cc = 0,54+1,60E-02*γd -5,18E-02*γh +7,29E-03*W +1,57E-03*FF <0,08mm-1,11E-03*WL +5,24E-03*IP	***0,78***	0,77	0,119	67,74	< 0.0001	4,49	3,11	2,83	4.79	1,48	6,19
Cc = 0,43+7,182E-03*γd -0,034*γh +3,42E-03*W +1,63E-03*FF <0,08mm+4,07E-04*WL +1,28*Cs	***0,82***	0,82	0,073	89,78	< 0.0001	4,56	3,57	3,35	1,37	1,95	3,53
Cc = 7,60E-02-1,70E-02*γh -7,83E-04*W +1,38E-03*FF <0,08mm-1,37E-03*WL +5,61E-03*IP+0,35*e0	***0,80***	0,79	0,123	76,31	< 0.0001	3,75	4,65	1,50	6,22	7,42	8,61
7 variables											
Cc = 1,55E-02+1,42E-02*γd -2,75E-02*γh +1,08E-03*W +1,36E-03*FF <0,08mm-1,52E-03*WL +5,83E-03*IP+0,34*e0	***0,81***	0,80	0,121	67,74	< 0.0001	4,51	5,33	5,63	1,50	6,26	7,46	8,65
Cc = 0,45+9,23E-03*γd -3,55E-02*γh +3,39E-03*W +1,20E-03*FF <0,08mm-1,88E-03*WL +3,86E-03*IP+1,195*Cs	***0,84***	0,83	0,072	83,21	< 0.0001	4,62	3,58	3,35	1,50	6,30	7,59	3,63

Cc = 0,56+1,55E-02*γd -5,29E-02*γh +7,134E-03*W +1,55E-03*FF <0,08mm-1,01E-03*WL +4,98E-03*IP+1,10E-04*Pc	***0,78***	0,77	0,045	58,43	< 0.0001	4,50	3,15	2,85	1,48	6,23	7,54	1,07
Cc = 0,157+1,95E-02*γd -3,25E-02*γh +0,01*W +1,53E-03*FF <0,08mm-9,09E-04*WL +5,24E-03*IP-2,03E-03*Sr	***0,80***	0,78	0,079	62,89	< 0.0001	4,62	5,63	6,94	1,48	6,22	7,38	3,51
Cc = -6,28E-03-7,22E-03*γh -3,387E-03*W +1,02E-03*FF <0,08mm-2,18E-03*WL +4,29E-03*IP+0,32*e0+1,196*Cs	***0,86***	0,85	0,066	98,18	< 0.0001	3,92	4,87	1,52	6,34	7,61	8,64	3,54
Cc = 3,65E-03-1,186E-02*γh +1,67E-03*W +1,39E-03*FF <0,08mm-1,23E-03*WL +5,53E-03*IP+0,31*e0-7,12E-04*Sr	***0,80***	0,79	0,084	65,46	< 0.0001	5,44	12,12	1,50	6,33	7,45	10,29	4,08
Cc = -0,19-4,43E-03*W +9,20E-04*FF <0,08mm-2,16E-03*WL +4,06E-03*IP+0,39*e0+1,25*Cs+1,55E-04*Pc	***0,86***	0,85	0,036	101,40	< 0.0001	4,36	1,50	6,32	7,69	4,49	3,41	1,07

Notations:

C_c: compressibility index

γ_d : dry unit weight in kN / m^3

γ_h: wet unit weight in kN / m^3

W: water content in %

F_F <0,08mm: fraction fine in %

W_L: liquidity limit in %

I_P: plasticity index in %

e_0: void ratio

S_r: degree of saturation in %

Gs: soil specific gravity

The linear model exhibit test of hypothesis involved the significance testing of regression, also the coefficients of individual regression, The Figure IV.9 show the different indicating of the residual plot when the strong correlation between each variable for all statistical models, single or multiple linear regressions, satisfactorily fulfilled the F-test as shown on Table IV.9 and the standardized coefficient as shown by Figure IV.10.

The coefficient of determination (R^2) has been used as a global statistic to assess the fit of the model. However, this value will increase when a regressor is added. The R^2 for the obtained model is 0.87 and the equation can be written on the following form:

$$Cc = -0{,}0246 + 0{,}0092 * \gamma d - 0{,}0095 * \gamma h + 0{,}0003 * W + 0{,}001 * FF - 0{,}00192 * WL + 0{,}0039 * IP + 0{,}285 * e0 + 1{,}15 * Cs + 0{,}0001 * Pc - 0{,}0365 * Gs - 0{,}0008 * Sr \quad \text{(IV.2)}$$

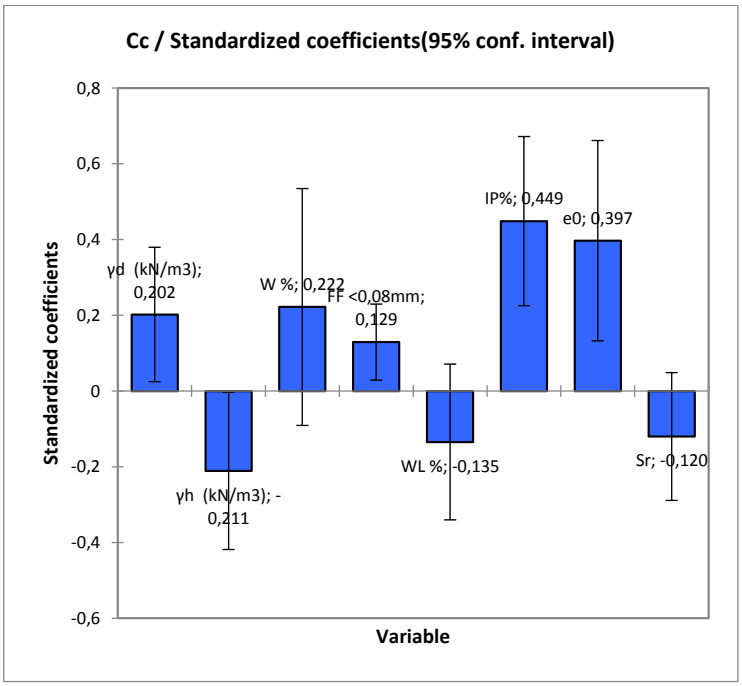

Figure IV.9: Standardized coefficients (C_c)

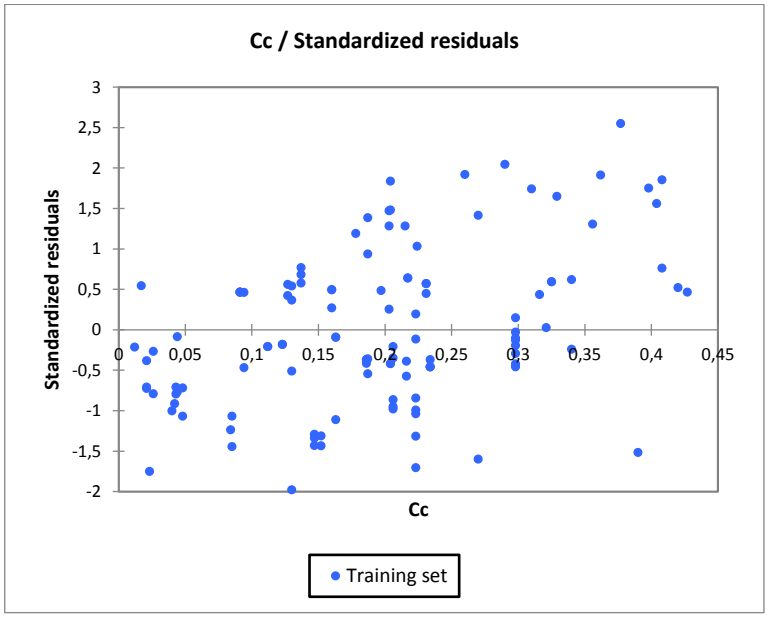

Figure IV.10: Standardized residuals

Scatter plot are a simple way to visualize the association between two quantitative variables, in this example, the different graph of different parameters depending on the compression index (C_c) represent a better look, this is due to the existence of regression between the compressibility index and the other parameters (γ_d, γ_h,w,I_p, W_l,S_r,e_0……)

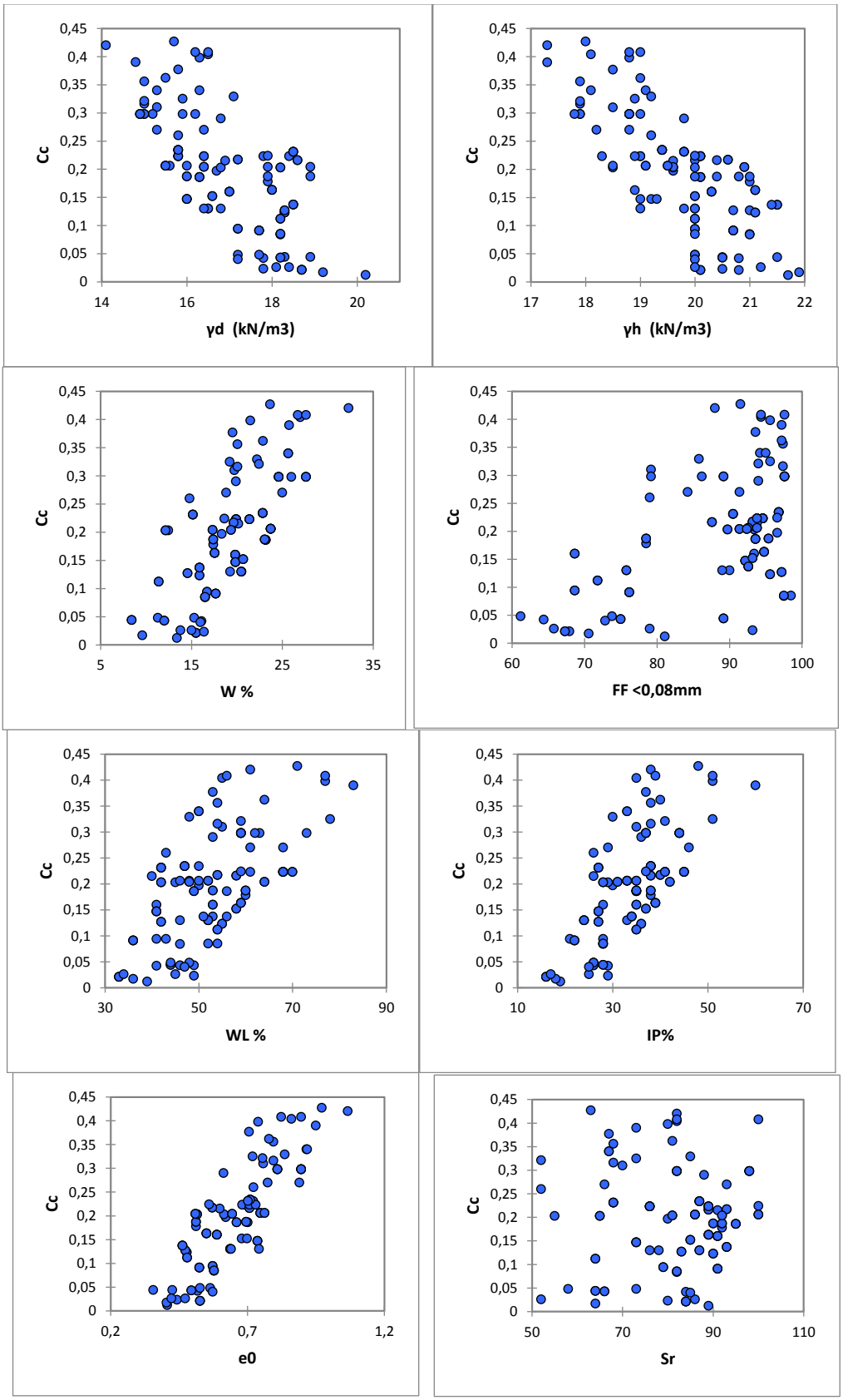

Figure IV.11: Scatter plots of different parameters according to compressibility index (C_c)

It can be concluded that the compressibility index is linearly related to γ_d , γ_h, w, F_F <0,08mm ,W_L ,I_P,e_0, C_s ,S_r ,Testing of individual regression coefficient requires that at least one of the variables contributes significantly to the model. It has been observed that the γ_h γ_d,w, F_F <0,08mm, I_P, e_0, w_L S_r, imply a significant contribution according to the standard, and the P-value was less than 0.05 (Table IV.9)

The coefficients of variables lie in the range of 95% confidence level. The overall test indicated that the variables fulfilled the requirements of the t-test and F-test.

Simple routine is needed to effectuate tests that can be performed on disturbed engineered samples to achieve the same purposes. The empirical models obtained in the present study use 118 data samples compiled from different geotechnical tests for all parameters appears primarily related to prediction of coefficient of compressibility from index properties of soils.

Sometimes, the empirical models proposed cannot be applied appropriately to all soils due to different soil conditions and testing procedures. It was hoped that the final model would be acceptable and generalized, Figure IV.12 shows the best fit correlation between predicted and measured compression index.

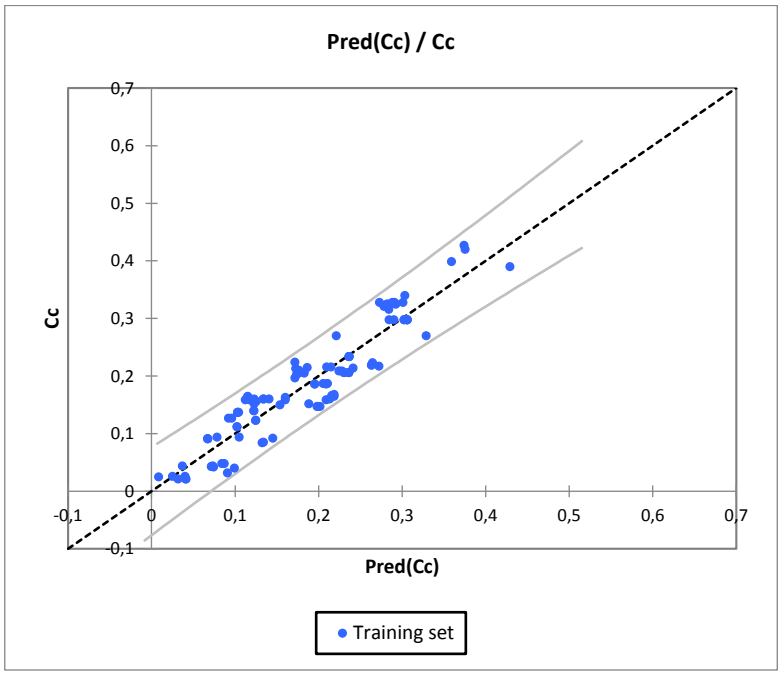

Figure IV.12: Measured compressibility (C_c Experimental) vs. predicted compressibility (C_c Theoretical) values of settlement

IV.6 Introduction

The term experiment is defined as the systematic procedure carried out under controlled conditions in order to discover an unknown effect, to test or establish a hypothesis, or to illustrate a known effect. When analyzing a process, experiments are often used to evaluate which process inputs have a significant impact on the process output, and what the target level of those inputs should be to achieve a desired result (output). Experiments can be designed in many different ways to collect this information.

Design of Experiments (DOE) mathematical methodology used for planning and conducting experiments as well as analyzing and interpreting data obtained from the experiments. It is a branch of applied statistics that is used for conducting scientific studies of a system, process or product in which input variables (Xs) were manipulated to investigate its effects on measured response variable (Y).

Experimental design can be used at the point of greatest leverage to reduce design costs by speeding up the design process, reducing late engineering design changes, and reducing product material and labor complexity. Designed Experiments are also powerful tools to achieve manufacturing cost savings by minimizing process variation and reducing rework, scrap, and the need for inspection [170].

IV.6.1 Components of experimental design

There are three aspects of the process that are analyzed by a design of experiment:

-Factors or inputs to the process, factors can be classified as either controllable or uncontrollable variables

-Levels or settings of each factor in the study

-Response or output of the experiment [171]

IV.6.2 The main uses of DOE

Design of experiment is multipurpose tool that can be used in various situations for identification of important input factors (input variable) and how they are related to the outputs (response variable).

Therefore, DOE mainly uses "hard tools" as it was reported in [172], In addition, DOE is basically regression analysis that can be used in various situations. Commonly used design types are the following [173]:

1. Comparison: this is one factor among multiple comparisons to select the best option that uses t–test, Z–test, or F–test.

2. Variable screening: these are usually two level factorial designs intended to select important factors (variables) among many that affect performances of a system, process, or product.

3. Transfer function identification: if important input variables are identified, the relationship between the input variables and output variable can be used for further performance exploration of the system, process or product via transfer function.

4. Robust design: deals with reduction of variation in the system, process or product without elimination of its causes. Robust design was pioneered by Dr. Genichi Taguchi who made system robust against noise (environmental and uncontrollable factors are considered as noise).

5. System Optimization: the transfer function can be used for optimization by moving the experiment to optimum setting of the variables by using the response surface methodology (RSM)

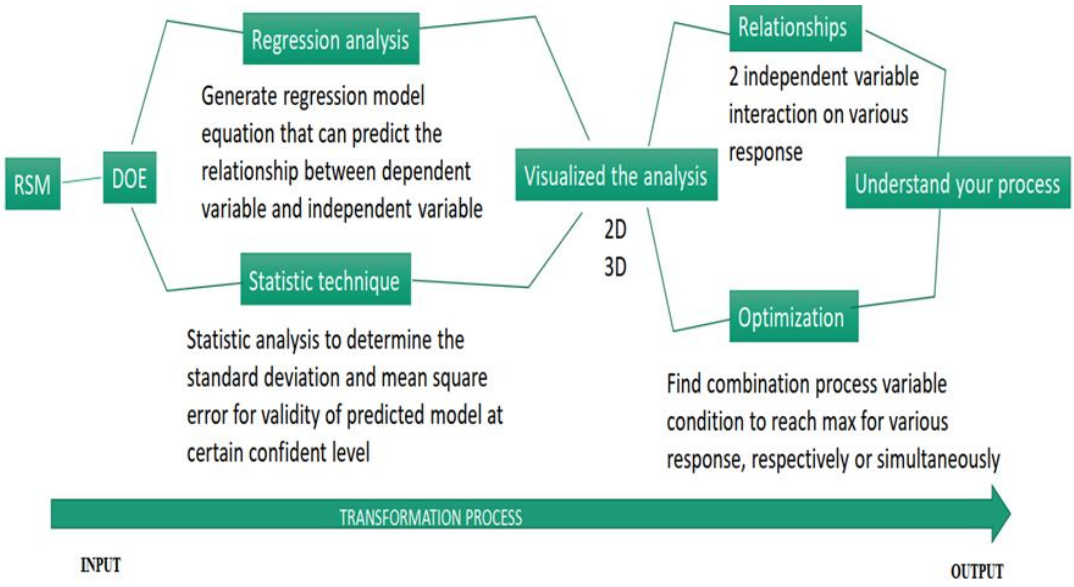

Figure IV.13: Design of experiments steps [173]

IV.6.3 General settings

Compressibility index can be directly determined for any fine-grained soils by conventional methods such as consolidation tests or indirectly by correlation to other soil parameters. Direct laboratory methods are characterized by high accuracy, but

require long time and effort at the same. In geotechnical engineering, many empirical relationships and correlations between physical and soil properties have been widely used by several researchers [174-179], Each of these proposed correlations has been applied on a specific soil and the results were acceptable within specific ranges only.

The consolidation properties of soil are very important in engineering and designs construction where (C_c) compression index and (C_s) are the main used parameters to determine the settlement occurs due to structures loads [180-187] ,these indices can be obtained directly in the laboratory by consolidation tests on soil sample while on the other hand there are many relationships between compression index to other geotechnical parameters and due to the importance of this parameter, many researchers developed a numerous empirical method to predict the compression index of a soil based on their physical properties such as densities, Atterberg limits, initial void ratio and natural water content, [188-191]

In literature different approaches and methodology has been investigated to estimate compression index using soil properties; such as artificial neural network technique, genetic programming, artificial intelligence, regression methods and general basic statistical analysis methods, to predict compression index using the soil properties [192-197].

The present work aims to investigate geotechnical parametric effects on the compressibility of clayey and fine-grained soils, where samples are collected from several locations in TEBESSA province north-east of Algeria using the Design of Experiment method (DOE). The detail in this research work provides theoretical and practical considerations for implementation of Design of Experiments (DOE) in geological and geotechnical engineering

Recently, DOE has been used in the rational development and optimization of analytical methods, it becomes extremely important to advance knowledge in the natural and social sciences and engineering. But it remains limited in use to the geological research domain [198].

The compressibility indices C_c and C_s was identified as two crucial parameters to estimate settlements in soil, where the compression index C_c is mostly used to estimate compressibility settlement of the normally consolidated soils for the most collected samples, physical soil parameters provide the principal geotechnical characterization and can help in estimating the compression index using mathematical correlations.

In this review the principal and application of different screening designs, such as two-level full factorial; and optimization designs, such as central composite designs (CCD) illustrates the principles and applications of design of experiments (DOE) in geotechnical engineering and soil compressibility characterization. In this research, compressibility behavior of soil was studied using oedometer test.

Compression index is one of the soil parameters that are required for calculation of foundation settlements, however, the determination of compression index is expensive, cumbersome, time consuming and required a lot of experience for obtaining undisturbed soil samples from the field. In order to mitigate these complexities, equations have been developed by many researchers in the past to predict compression index using index properties of soil which are relatively easier to conduct in the laboratory.

In order to determine the effect of the reported parameters for the study region allow detailed analysis using the experiment design and the parametric optimization process with Response Surface Methodology (RSM), each parameter influences on the compressibility index have been studied according to the different literature focuses on the indirect estimation of the settlement amount based on compressibility indices.

All data collected in the studied prone area allows the ability of detailed analysis using design of experiment and parametric optimization process with response surface methodology (RSM), the factors which have an influence on the compressibility gives equations of best fit and the models necessary to better understand, the main objective is the optimization of the response by the use of maximizing or minimizing the output or input factors in the RSM method, the best models obtained here are compared to different published model to see the validity and effectiveness of RSM in geoscience modeling.

In this memory, the linear regression model has been built to predict the compression index for the studied area soil depending with physical properties. The results of all the proposed parameters were subject to the statistical analysis in order to evaluation the geotechnical properties and empirical correlations for these parameters.

The design of experiments models are classical statistical models whose objective is find out if certain factors influence a variable of interest, or if there is influence of some factor in term of quantity.

The methodology of design of experiments is based on experimentation. It's known that if an experiment is repeated, under indistinguishable conditions, the results show some variability. If the experimentation is done in a laboratory where most of the causes of variability are highly controlled, experimental error will be small and there will be little variation in the results of the experiment. But if it is experienced in industrial processes or administrative variability will be greater in most cases.

The objective of the design of experiments is to study whether when using a certain treatment there is an improvement in the process or not. To do this, you must experiment by applying the treatment and not applying it. If the experimental variability is large, only the influence of the use of the treatment when it produces large changes in relation to the observation error.

The methodology of the design of experiments studies how to vary the usual conditions

conducting an empirical process to increase the probability of detecting significant changes in the response; in this way a greater knowledge of the behavior is obtained of the process of interest.

For the design of experiments methodology to be effective it is essential that the experiment is well designed.

An experiment is performed for one of the following reasons:

- Determine the main causes of variation in the response.

-Find the experimental conditions with which an extreme value is achieved in the variable of interest or response.

- Compare the responses at different levels of observation of controlled variables.

- Obtain a statistical-mathematical model that allows making predictions of responses future.

Our work consists in studying a very important phenomenon in the geotechnical field which is the compressibility of soils based on compression index to use it in measuring the settlement of soils. Therefore, to better understand the phenomenon it is necessary to link it with the parameters which have a direct influence and from which we can see and study this phenomenon from the compressibility index.

We take the different physical input parameters (dry unit weight γ_d (kN / m^3), wet density γ_h (kN / m^3), water content w (%), fine fraction f_f (%), limit of liquidity w_L (%), plasticity index I_p (%), void ratio and degree of saturation (S_r), depending on the

compressibility index (C_c) that considers as output parameter as illustrated in Figure IV.14.

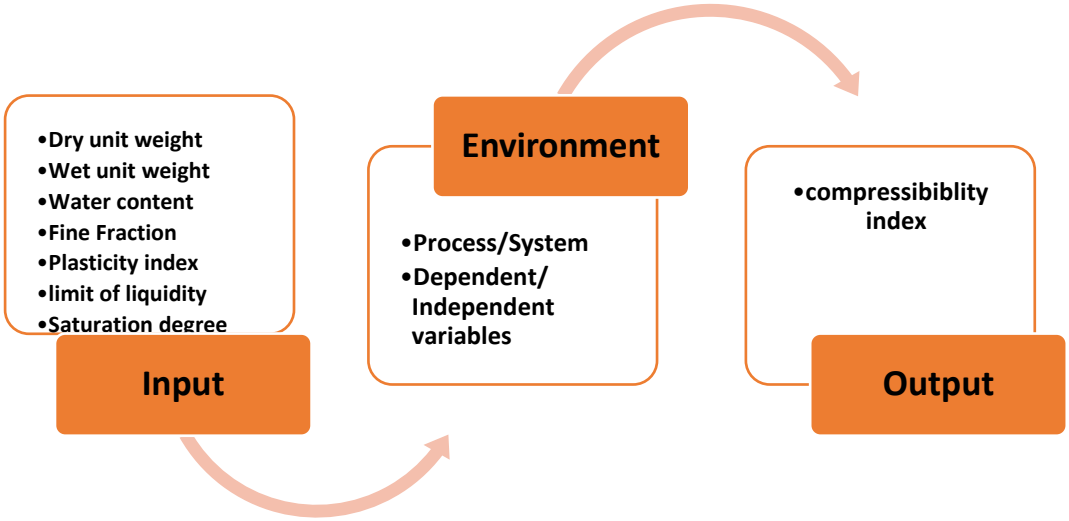

Figure IV.14: Design of Experiments organigram visualization

The properties of soil consolidation are very important in engineering designs. In general, compression index (C_c) can be obtained directly in the laboratory by consolidation tests on the different soils while on the other hand there are relationships between compression index with another geotechnical properties and due to the importance of this parameter to predict the rate of settlement, many researchers developed a numerous empirical methods to predict the compression index of a soil based on their physical properties such as (dry unit weight $\boldsymbol{\gamma_d}$($\mathbf{kN/m^3}$), wet unit weight $\boldsymbol{\gamma_h}$($\mathbf{kN/m^3}$) water content $\mathbf{w}$ (%),fine fraction $\mathbf{F_f}$ (%) , Liquidity limits $\mathbf{W_L}$ (%), plasticity index $\mathbf{I_p}$(%), void ratio $\mathbf{e_0}$, Saturation degree $\mathbf{S_r}$(%) **[199–201].**

The Tebessa area (Algeria) is the case study of the present work, in point, the weathered geological facies in this arid region has primarily created cover soils in a large basin with very plastic behavior. However, compressible soils exist and well identified litigation and reports high difficulties to infrastructure stability.

In the present research the concept of design of experiments (DOE) has been introduced to study the compressibility behavior of the clayey soils **[202-203]**.

with about 118 samples collected and tested in soil mechanics laboratory identification (LTPE).

IV.6.4 Material and methods

In the present study, an attempt has been made to estimate compressibility index (C_c) as a function of basic soil properties since their determination is comparatively easy

Soil samples of different types are collected from different locations of Tebessa province situated in the northeast of Algeria.118 different samples are taken from different locations of Tebessa in order to investigate their geotechnical parameters namely dry unit weight $\boldsymbol{\gamma_d}(\mathbf{kN/m^3})$, wet unit weight $\boldsymbol{\gamma_h}(\mathbf{kN/m^3})$ water content **w** (%), fine fraction (%), Liquidity limits W_L (%), plasticity index $\mathbf{I_p}$ (%), void ratio e_0, Saturation degree $\mathbf{S_r}$ (%). [204]

In this strategy, experiments are conducted by simultaneously varying six factors over two levels (namely low level and high level). The two levels are so chosen that they cover the practical range of the parameters under consideration Tab1

In This case study the main objective is the modeling of compressibility index (C_c) and the analysis of results with ANOVA. For the presented implementation of DOE technique, Design-Expert13 software was employed to obtain the appropriate functional equations. The right tools at knowledge of research take in account mathematics and statistics to solve the problem considering each potential of the approximation.

The response surface methodology RSM in DOE techniques is widely used for machining processes. Experiments based on RSM technique relate to the determination of response surface based on the general equation **[205]:**

$$y = A0 + A1x1 + \cdots + Akxk + A12x1x2 + A13x1x3 + A11x1\,2 + Akkxk\,2 \qquad \text{(IV.3)}$$

Where A0, Ai, Aij are respectively interaction, linear, quadratic and intercept coefficients. xi input independent variables.

Continuous factors affect the quantitative response which is analyzed by response surface methodology (RSM), this later best fitting representative critical factors, commonly chosen in the screening phase of the experimental program. The final obtained results using RSM are polynomial models display the true response surface in the best approximation over a region of factors.

IV.6.5 Definition of the input variables and the output responses

In this case study, the effects of input parameters (dry unit weight $\boldsymbol{\gamma_d}(\mathbf{kN/m^3})$, wet unit weight $\boldsymbol{\gamma_h}(\mathbf{kN/m^3})$ water content **w (%)**, fine fraction **(%)**, Liquidity limits $\mathbf{W_L}$ (%), plasticity index $\mathbf{I_p}$ **(%)**, void ratio $\mathbf{e_0}$, Saturation degree $\mathbf{S_r}$ **(%),** on the output response the compressibility index (C_c), The levels for each factor are tabulated in Table IV.10.

Table IV.10: Factors for response surface study

Factor	Name	Level	Low Level	High Level	Std. Dev.	Coding
A	γ_d	17,15	14,10	20,20	0,0000	Actual
B	γ_h	19,60	17,30	21,90	0,0000	Actual
C	w	20,36	8,43	32,30	0,0000	Actual
D	F_f	79,85	61,20	98,50	0,0000	Actual
E	W_L	58,00	33,00	83,00	0,0000	Actual
F	I_P	38,00	16,00	60,00	0,0000	Actual
G	e_0	0,7050	0,3552	1,06	0,0000	Actual
H	S_r	76,00	52,00	100,00	0,0000	Actual

Factorial designs are widely used in experiments involving several factors where it is necessary to study the joint effect of the factors on a response.

Significant factors are identified using two-level factors as the first technique permit to compare the obtained results in full factorial design, where lower numbers of runs are required in this identification. The factorial design method is a general family of statistical methods, employed for the design of a scientific experiment. When an experiment is conducted using the factorial design method, the effect of various factors on one (like this case) or more response variables can be successfully investigated.

Each factor is generally considered as an independent variable and is studied at various discrete subdivisions or levels, namely discrete values that lie within a predefined range, appropriate for each experiment.

IV.6.6 DOE and response data implementation

Figure below shows the number of runs needed for the full factorial DOE where the two levels of factors variation are considered (as that used in this Example). If one runs more accurate, DOE using the rotatable central composite design with two levels, the number of tests will be even greater.

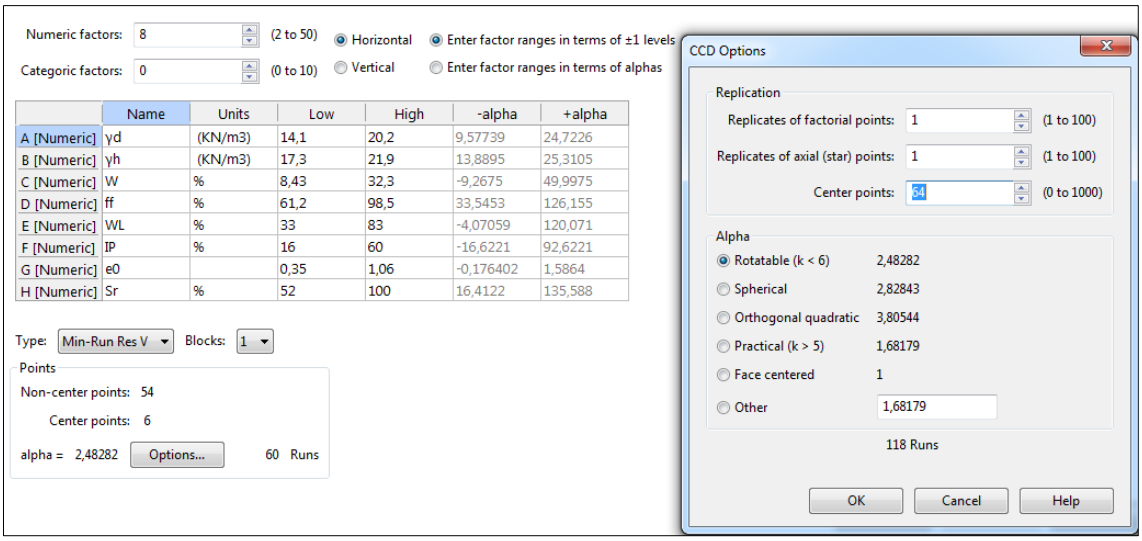

Figure IV.15: Definition of different parameters as numeric factors in Design-Expert

For the experiment design CCD-Rotatable was selected, in which standard error remains the same at all the points which are equidistant from the center of the region. The upper and lower limits and their levels of the parameters, as they are entered to the software.

CCD is composed of a core factorial that forms a cube with sides that are two coded units in length, from −1 to +1. The distance out of the cube, designated as distance "Alpha" and measured in terms of coded factor levels, is a matter for much discussion between statisticians. Design-Expert software offers a variety of options for Alpha.

IV.6.7 Statistical results analysis and the model properties

When start analyzing the responses numerically, Design-Expert provides a full array of response transformations via the Transform Option for now, accept the default transformation selection of None.

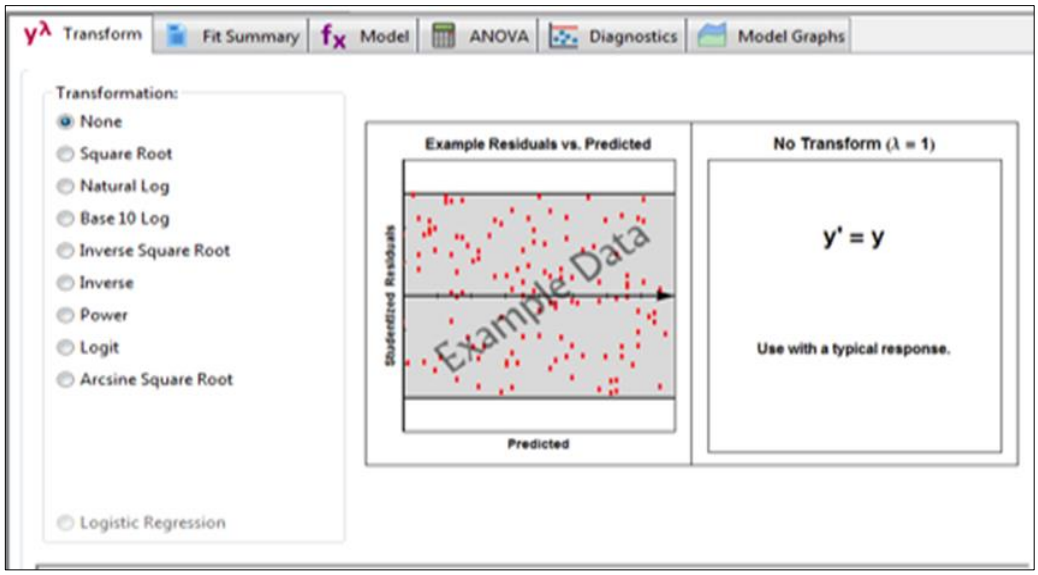

Figure IV.16: starting analysis

The Fit Summary tab. At this point Design-Expert fits linear, two-factor interaction (2FI), quadratic, and cubic polynomials to the response. At the top is the response identification, immediately followed below, in this case, by a warning: "The Cubic Model is aliased." Do not be alarmed. By design, the central composite matrix provides too few unique design points to determine all the terms in the cubic model. It's set up only for the quadratic model (or some subset).

Table IV.11: Model Fit Summary

Source	Model p-value	Lack of Fit p-value	Adjusted R^2	Predicted R^2	
Design Model	< 0.0001	< 0.0001	0,8543	0,7256	
Linear	**< 0.0001**	**< 0.0001**	**0,8122**	**0,7948**	**Suggested**
2FI	**0,0036**	**< 0.0001**	**0,8557**	**0,7465**	**Suggested**
Quadratic	0,3825	< 0.0001	0,8570	0,6238	
Cubic	< 0.0001		0,9943		Aliased

For each source of terms (linear, etc.), examine the probability ("Prob > F") to see if it falls below 0.05 (or whatever statistical significance level you choose). So far, Design-Expert is indicating (via bold highlighting) the quadratic model looks best – these terms are significant, but adding the cubic order terms will not significantly improve the fit, (even if they were significant, the cubic terms would be aliased, so they wouldn't be useful for modeling purposes.) Move down to the Lack of Fit Tests pane

for Lack of Fit tests on the various model orders.

The table of "Sequential Model Sum of Squares" (technically "Type I") shows how terms of increasing complexity contribute to the total model.

The Sequential Model Sum of Squares table: The model hierarchy is described below:

- "Linear vs Block": the significance of adding the linear terms to the mean and blocks,
- "2FI vs Linear": the significance of adding the two factor interaction terms to the mean, block, and linear terms already in the model,
- "Quadratic vs 2FI": the significance of adding the quadratic (squared) terms to the mean, block, linear, and two factor interaction terms already in the model, "Cubic vs Quadratic": the significance of the cubic terms beyond all other terms.

Table IV.12: Sequential Model Sum of Squares

Source	Sum of Squares	df	Mean Square	F-value	p-value	
Mean vs Total	4,42	1	4,42			
Linear vs Mean	**1,01**	**8**	**0,1262**	**64,23**	**< 0.0001**	**Suggested**
2FI vs Linear	**0,0919**	**28**	**0,0033**	**2,18**	**0,0036**	**Suggested**
Quadratic vs 2FI	0,0130	8	0,0016	1,09	0,3825	
Cubic vs Quadratic	0,1083	59	0,0018	30,58	< 0.0001	Aliased
Residual	0,0008	14	0,0001			
Total	5,64	118	0,0478			

On move right, the "Lack of Fit Tests" pane compares residual error with "Pure Error" from replicated design points. If there is significant lack of fit, as shown by a low probability value ("Prob > F"), then be careful about using the model as a response predictor. In this case, the linear model definitely can be ruled out, because its Prob > F falls below 0.05. The quadratic model, identified earlier as the likely model, does not show significant lack of fit. Remember that the cubic model is aliased, so it should not be chosen.

Table IV.13: Lack of Fit Tests

Source	Sum of Squares	df	Mean Square	F-value	p-value	
Linear	**0,2132**	**95**	**0,0022**	**37,39**	**< 0.0001**	**Suggested**
2FI	**0,1213**	**67**	**0,0018**	**30,16**	**< 0.0001**	**Suggested**
Quadratic	0,1083	59	0,0018	30,58	< 0.0001	
Cubic	0,0000	0				Aliased
Pure Error	0,0008	14	0,0001			

Look over the last pane in the Fit Summary report, which provides "Model Summary Statistics" for the 'bottom line' on comparing the options

The linear model and the 2FI comes out best: It exhibits low standard deviation ("Std. Dev."), high "R-Squared" values, and a low "PRESS."

The program automatically underlines at least one "Suggested" model. Always confirm this suggestion by viewing these tables.

IV.6.8 ANOVA for quadratic model

The ANOVA results are utilized to evaluate the effect of the built RSM model and its terms that are found to be statistically significant. **[206]**, The ANOVA analysis is performed via testing the hypothesis of equal variance, which is the test of a null hypothesis at a confidence level (95%) or significance level (0.05). For this purpose, the F-values in ANOVA table were calculated dividing the mean square of factor by the mean square of residual. Then, they were compared with the F-values from the Fisher distribution proposed for the significance level of 0.05. In the Fisher distribution, the F-values are determined according to the number of degree of freedom of the associated factors and residuals together with the significance (or probability) level

The contribution of each parameter in the built RSM model to the UCS performance of

mixture is determined dividing F-value of each parameter by the sum of F-values of all parameters and multiplying the obtained result by 100

ANOVA is commonly used to summarize the test for significance of the regression model and test for significance on individual model coefficients, the models summary statistics are shown in Table IV.14.

Table IV.14: ANOVA for response surface quadratic model for compressibility index

Source	Sum of Squares	df	Mean Square	F-value	p-value	
Model	1,11	44	0,0253	16,93	< 0.0001	significant
A-γd	0,0013	1	0,0013	0,8778	0,3519	
B-γh	0,0018	1	0,0018	1,17	0,2828	
C-W	0,0063	1	0,0063	4,22	0,0434	
D-ff	0,0004	1	0,0004	0,2386	0,6267	
E-WL	0,0007	1	0,0007	0,4705	0,4949	
F-IP	0,0002	1	0,0002	0,1457	0,7038	
G-e0	0,0002	1	0,0002	0,1050	0,7468	
H-Sr	0,0086	1	0,0086	5,76	0,0189	
AB	0,0041	1	0,0041	2,75	0,1014	
AC	0,0002	1	0,0002	0,1653	0,6855	
AD	0,0001	1	0,0001	0,0345	0,8531	
AE	0,0005	1	0,0005	0,3573	0,5519	
AF	5,433E-06	1	5,433E-06	0,0036	0,9521	
AG	1,561E-06	1	1,561E-06	0,0010	0,9743	
AH	0,0000	1	0,0000	0,0112	0,9160	
BC	0,0097	1	0,0097	6,50	0,0129	
BD	0,0028	1	0,0028	1,90	0,1726	
BE	0,0051	1	0,0051	3,43	0,0680	
BF	0,0017	1	0,0017	1,11	0,2963	
BG	0,0097	1	0,0097	6,48	0,0130	
BH	0,0104	1	0,0104	6,96	0,0102	
CD	0,0000	1	0,0000	0,0168	0,8972	
CE	0,0002	1	0,0002	0,1376	0,7117	
CF	0,0001	1	0,0001	0,0734	0,7872	
CG	0,0007	1	0,0007	0,4920	0,4853	
CH	0,0052	1	0,0052	3,49	0,0657	
DE	0,0053	1	0,0053	3,53	0,0643	
DF	0,0012	1	0,0012	0,7941	0,3758	
DG	0,0001	1	0,0001	0,0580	0,8104	
DH	0,0008	1	0,0008	0,5294	0,4692	
EF	0,0008	1	0,0008	0,5346	0,4670	
EG	0,0029	1	0,0029	1,94	0,1683	
EH	4,854E-08	1	4,854E-08	0,0000	0,9955	
FG	0,0037	1	0,0037	2,48	0,1193	
FH	0,0001	1	0,0001	0,0596	0,8078	
GH	0,0004	1	0,0004	0,2499	0,6187	
A^2	0,0011	1	0,0011	0,7635	0,3851	
B^2	0,0027	1	0,0027	1,81	0,1824	
C^2	0,0049	1	0,0049	3,25	0,0756	
D^2	0,0007	1	0,0007	0,4712	0,4946	
E^2	0,0005	1	0,0005	0,3614	0,5496	

F²	0,0012	1	0,0012	0,7977	0,3747	
G²	0,0028	1	0,0028	1,85	0,1785	
H²	0,0091	1	0,0091	6,05	0,0162	
Residual	0,1092	73	0,0015			
Lack of Fit	0,1083	59	0,0018	30,58	< 0.0001	significant
Pure Error	0,0008	14	0,0001			
Cor Total	1,22	117				

The sum of squares values given in Table IV.13 are used for the determination of the deviation from the mean. The total sum of squares (SST) is obtained by adding the sum of squares of model (SSM) and the sum of squares of residual (SSR).

Mean square of each factor is calculated through dividing their corresponding sum of squares by the associated degree of freedom

Model "F-value" of 16,93 implies that the model is significant. There is only a0.01 % chance that a model "F-value" this large could occur due to noise.

Values of "Prob > F" less than 0.05 indicate that model terms are significant; in this case A, B, C, D, E, F…to H² are significant model terms, values greater than 0.10 indicate the model terms are not significant. If there are many insignificant model terms, excluding those required to support hierarchy, model reduction may improve the model.

The "Lack of Fit" "F-value" of 30,58 implies the "Lack of Fit" is significant relative to the pure error. There is only a 0,01 % chance that a "Lack of Fit" "F-value" this large could occur due to noise; Significant lack of fit is bad we want the model to fit.

Table IV.15: Regression statistics for adopted reduced quadratic model

Std. Dev.	**0,0387**	R^2	**0,9108**
Mean	0,1936	**Adjusted R^2**	0,8570
C.V. %	19,98	**Predicted R^2**	0,6238
		Adeq Precision	18,3846

The analysis of the experimental data was performed to identify statistical significance of the physical parameters (dry unit weight $\boldsymbol{\gamma_d}(\mathbf{kN/m3})$, wet unit weight $\boldsymbol{\gamma_h}(\mathbf{kN/m3})$ water content **w** (%), fine fraction (%), Liquidity limits $\mathbf{W_L}$ (%), plasticity index $\mathbf{I_p}$ (%), void ratio $\mathbf{e_0}$, Saturation degree $\mathbf{S_r}$ (%), on the measured response compressibility index (C_c), The model was developed for 95 % confidence level and the results are summarized in the Table IV.15

The Predicted R^2 of 0,6238 is not as close to the Adjusted R^2 of 0,8570 as one might normally expect; the difference is more than 0.2. This may indicate a large block effect or a possible problem with your model and/or data. Things to consider are model reduction, response transformation, outliers, etc. All empirical models should be tested by doing confirmation runs.

Adeq Precision measures the signal to noise ratio. A ratio greater than 4 is desirable. Your ratio of 18,385 indicates an adequate signal. This model can be used to navigate the design space.

Table IV.15 shows the regression statistics. The coefficient of determination is high and close to 1, namely R-Squared equals to 0.9108, which is desirable. "Pred RSquared" of 0.6238 is in reasonable agreement with the "Adj R-Squared" of 0.8570.

The adequacy of the model should be checked by the examination of residuals. Residual analysis is necessary to confirm that the assumptions for the ANOVA are met. Other diagnostic plots may provide interesting information in some situations.

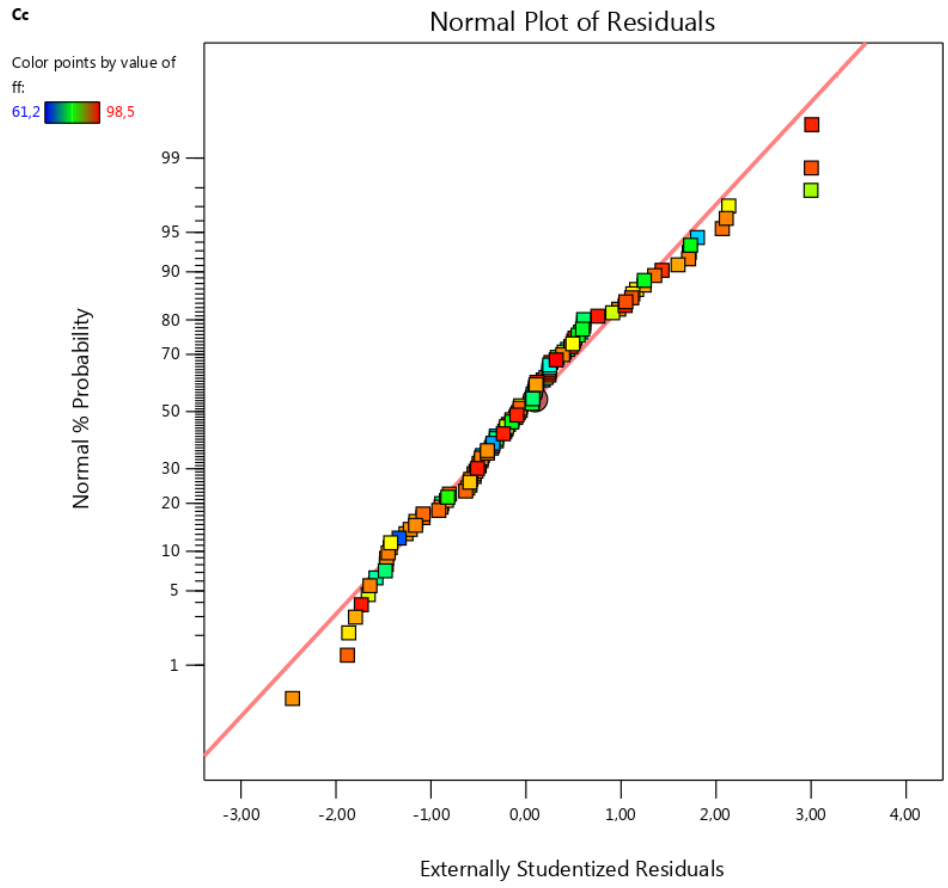

Figure IV.17: Normal probability plot of residuals for compressibility index (C_c)

The residuals are examined using the normal probability plots of the residuals and the plot of the residuals versus the predicted response. Normal plot of residuals, shown in Figure IV.18, should be in a straight line, the residuals generally fall on a straight line implying that the errors are distributed normally. Nonlinear patterns, such as an S-shaped curve, indicate non-normality in the error term, which may be corrected by a transformation.

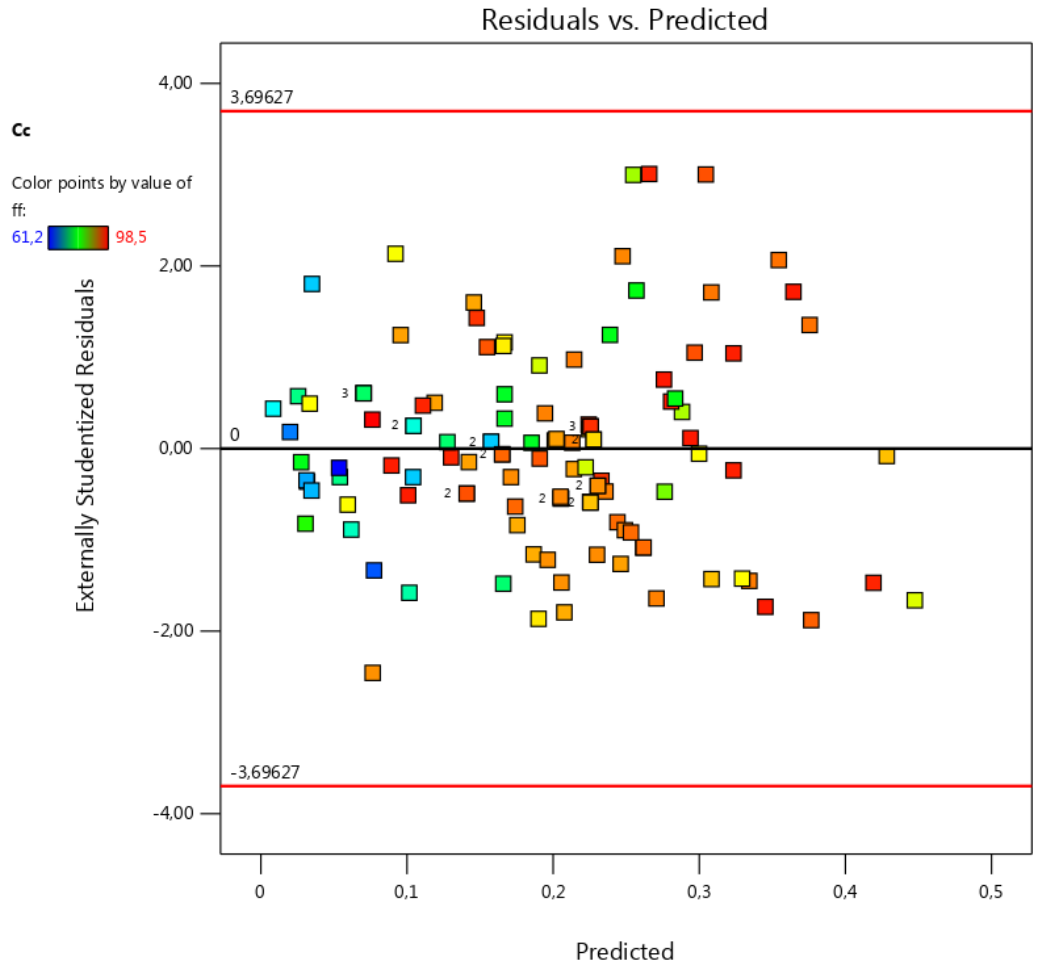

Figure IV.18: Residuals versus predicted response for compressibility index (C_c)

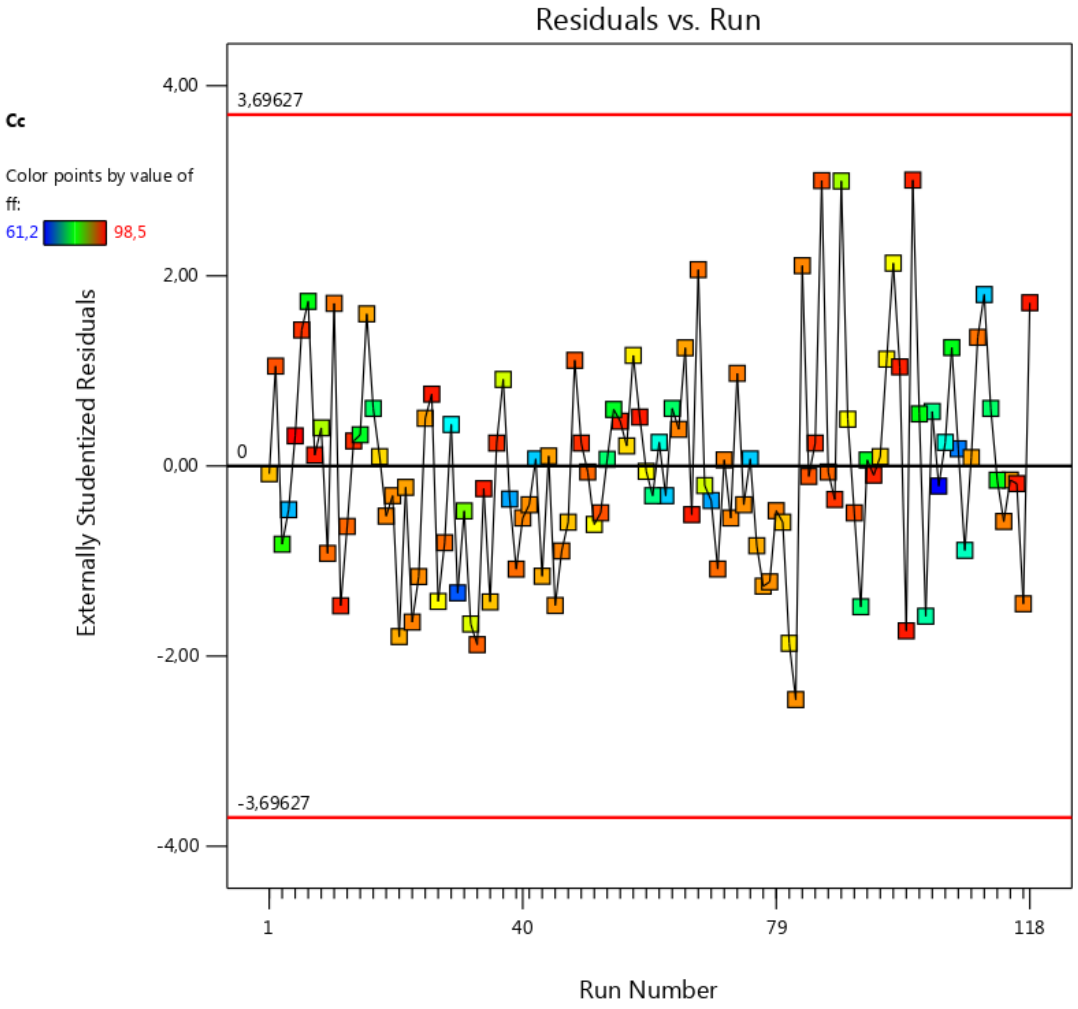

Figure IV.19: Residuals versus run for compressibility index (C_c)

Now you can see that, although the highlighted run does differ more from its predicted value than any other, there is really no cause for alarm due to it being within the red control limits.

Residuals versus run tests should be randomly scattered without trend this means that equal (constant) variance assumption of the least squares is satisfied. In this study, the externally standardized residuals versus run number is also plotted in (Figure IV.19) . 5 in order to check whether most of the externally residuals fall in the interval determined as -3.69 and 3.69 by the statistical software package (i.e., Design-Expert, released by Stat- Ease Inc.)

In DFBETAS, which breaks down the changes in the model to each coefficient, which statisticians symbolize with the Greek letter β, hence the acronym DFBETAS —

the difference in betas, for the Term click the down-list arrow and select A as shown in the following screen shot.

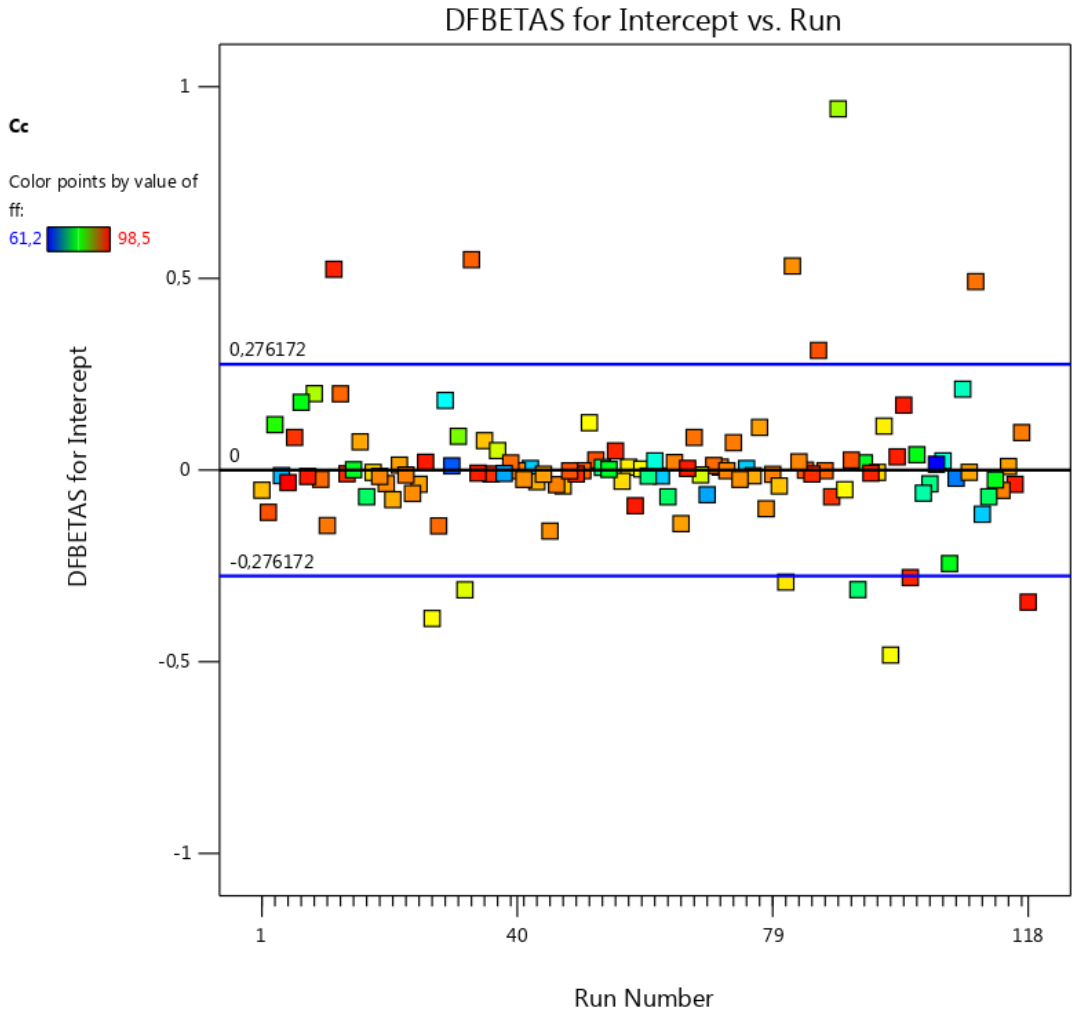

Figure IV.20: DFBETAS intercept versus run number

You can evaluate forty-five model terms (including the intercept) for this quadratic predictive model (see sidebar below for help).

In order to determine the quality of the adopted model, it needs to be checked whether points of predicted response versus actual values are randomly scattered along the 45° line like in Figure IV.20, this implies that the proposed model is adequate and there is no reason to suspect any violation of the independence or constant variance assumptions.

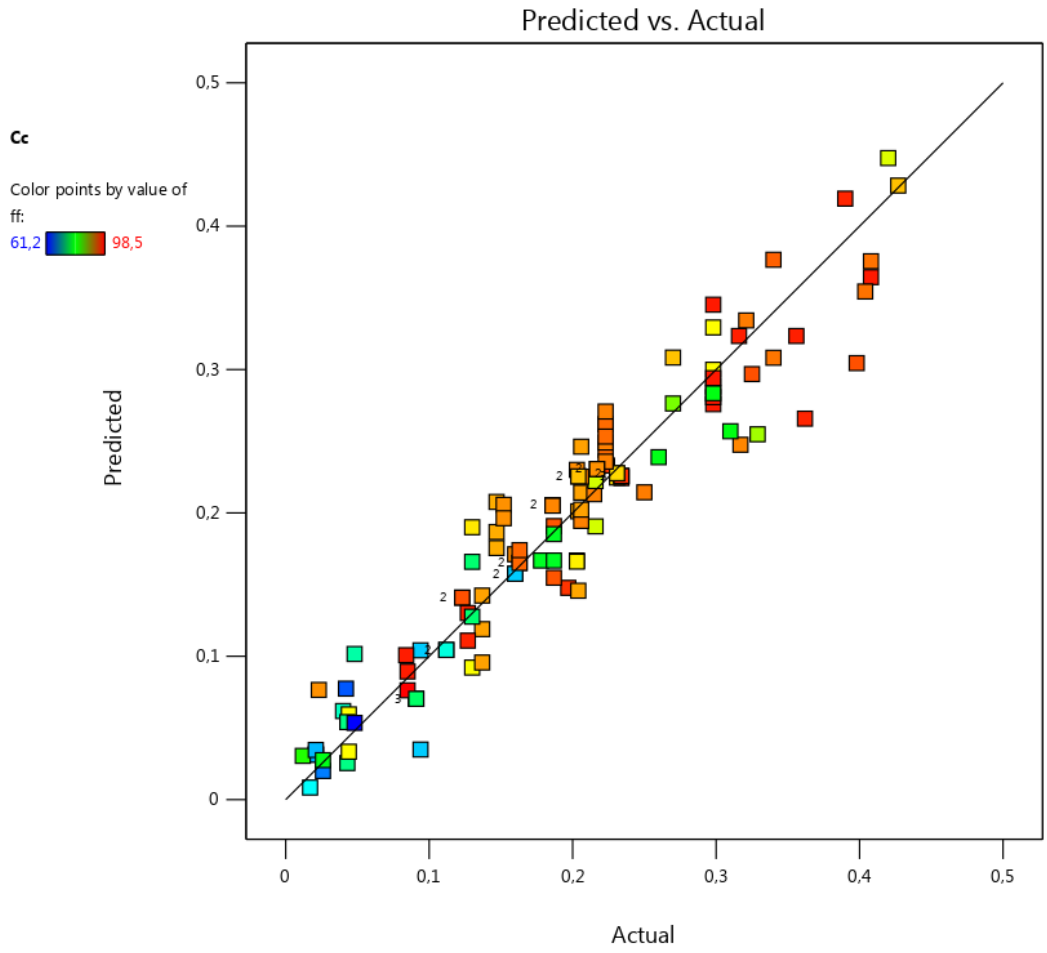

Figure IV.21 Predicted responses versus actual for compressibility index (C_c)

IV.6.9 Equations and models graphs

For the analyzed example the final equation in terms of actual factors was determined, which determines the compressibility index (C_c) from the input factors:

$$Cc = -0{,}14 + 0{,}016\gamma d - 0{,}0199\gamma h + 0{,}0049w + 0{,}0013Ff - 0{,}0012WL + 0{,}0056Ip + 0{,}29e0 - 0{,}0010Sr \quad \text{(IV.4)}$$

Figure IV.22 and IV.23 show the response surfaces describing the compressibility index (C_c) dependence on the dry and wet unit weight (kN/m^3) for this case study.

Next, the final equations and examples of response surfaces for the remaining measured responses are shown, the analysis was performed in analogy to the compressibility index (C_c).

As indicated by the color key on the left, the surface becomes ‘hot’ at higher response levels, yellow in the value 0,34 of compressibility index and red above 0,4.

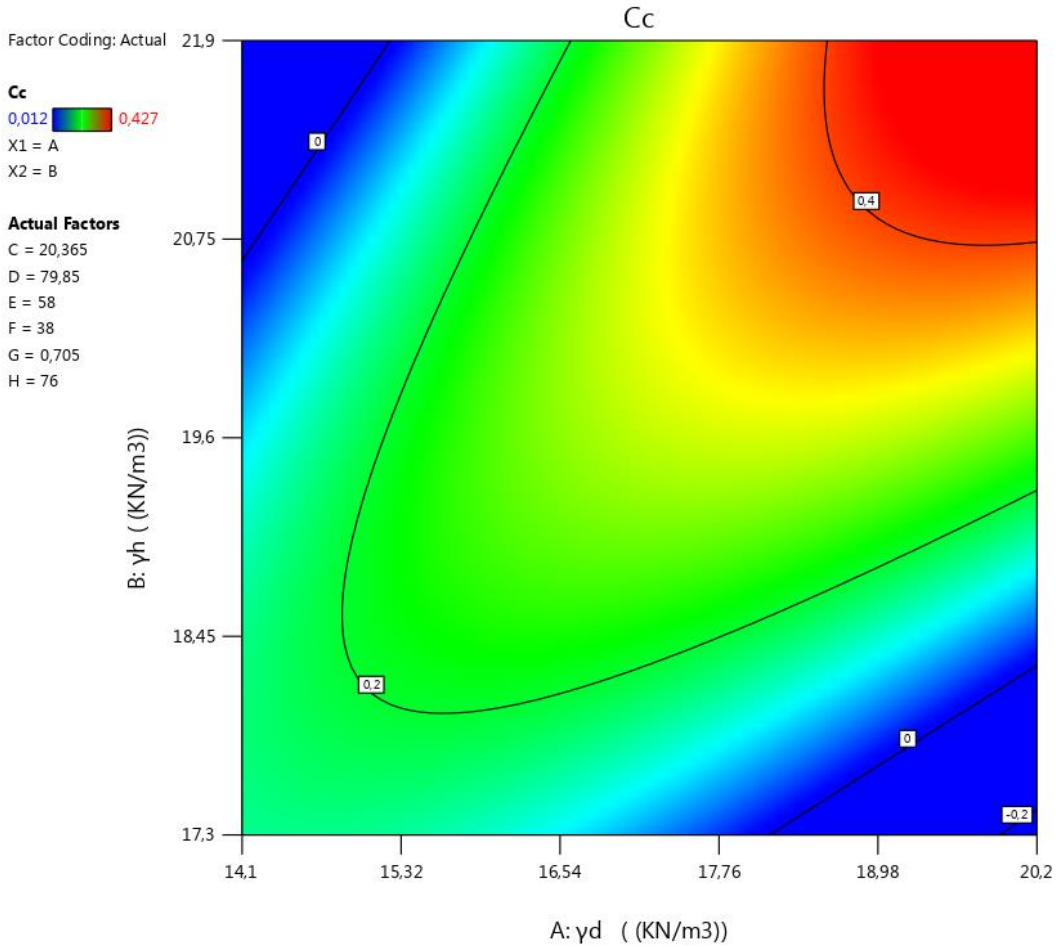

Figure IV.22: Response surface contour plot representing the compressibility index dependence on the dry and wet unit weight

Now to really get a feel for how the response varies as a function of the two factors chosen for display, you then will see three-dimensional display of the response surface.

The next figures (3D) show the response surfaces describing the compressibility index ($_{Cc}$) dependence on the dry unit weight (kN/m^3) and the water content w (%), then the plasticity index (%), respectively. Plasticity index (I_P), water content (w) and the compressibility index (C_c), the dry unite weight and the compressibility index for this case study.

The following figures shows the response surfaces describing the compressibility index (Cc) dependence on, the dry unit weight (kN/m^3) and the water content w (%), dry unit weight (kN/m^3) and the void ratio (%), the Dry unit weight (kN/m^3) and the wet unit weight (kN/m^3), the dry unit weight γ_d (kN/m^3) and the plasticity index (I_P), respectively.

So, they Shows the interaction between two process variables as function of factors

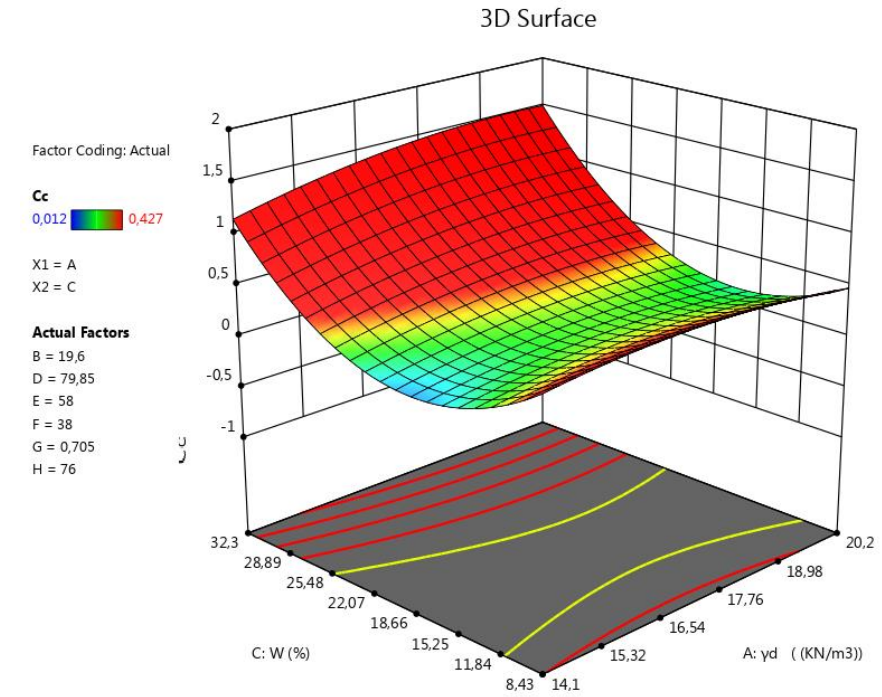

Figure IV.23: Response surface 3D representing the compressibility index (C_c) dependence on the dry unit weight γ_d (kN/m$_3$) and water content w (%)

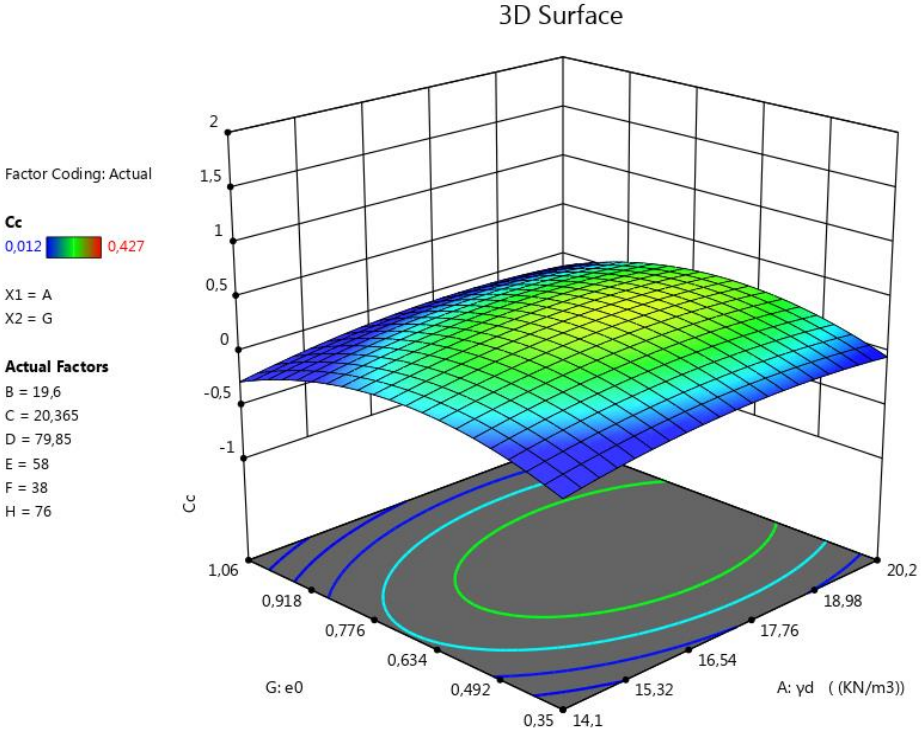

Figure IV.24: Response surface 3D representing the compressibility index (C_c) dependence on the dry unit weight γ_d (kN/m^3) and the void ratio e_0

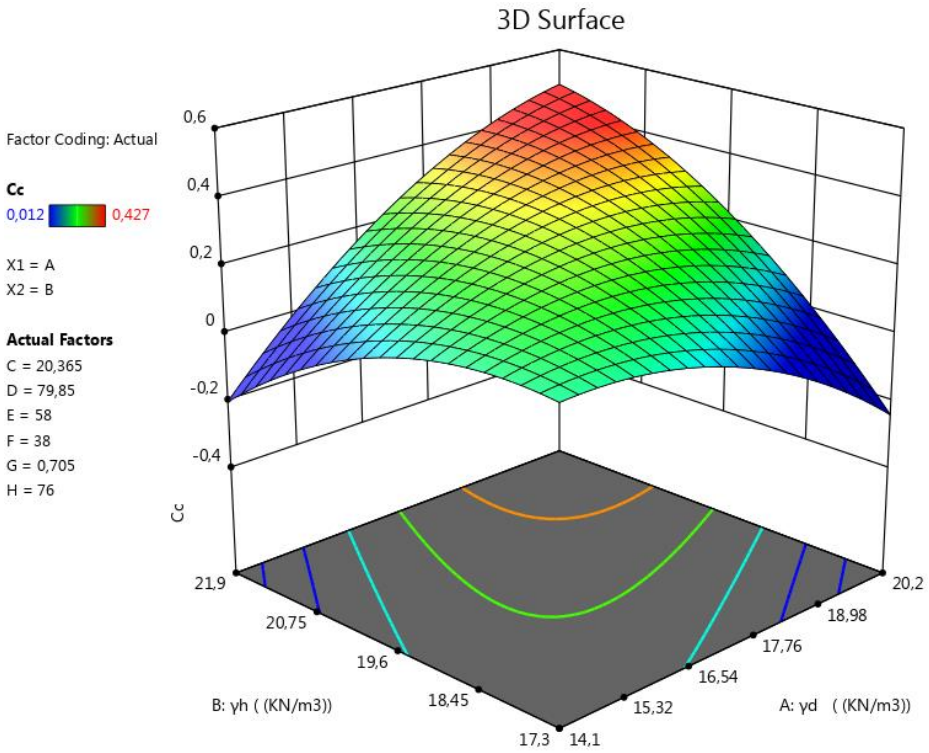

Figure IV.25: Response surface 3D representing the compressibility index (C_c) dependence on the dry unit weight γ_d (kN/m^3) and the wet unit weight γ_h (kN/m^3)

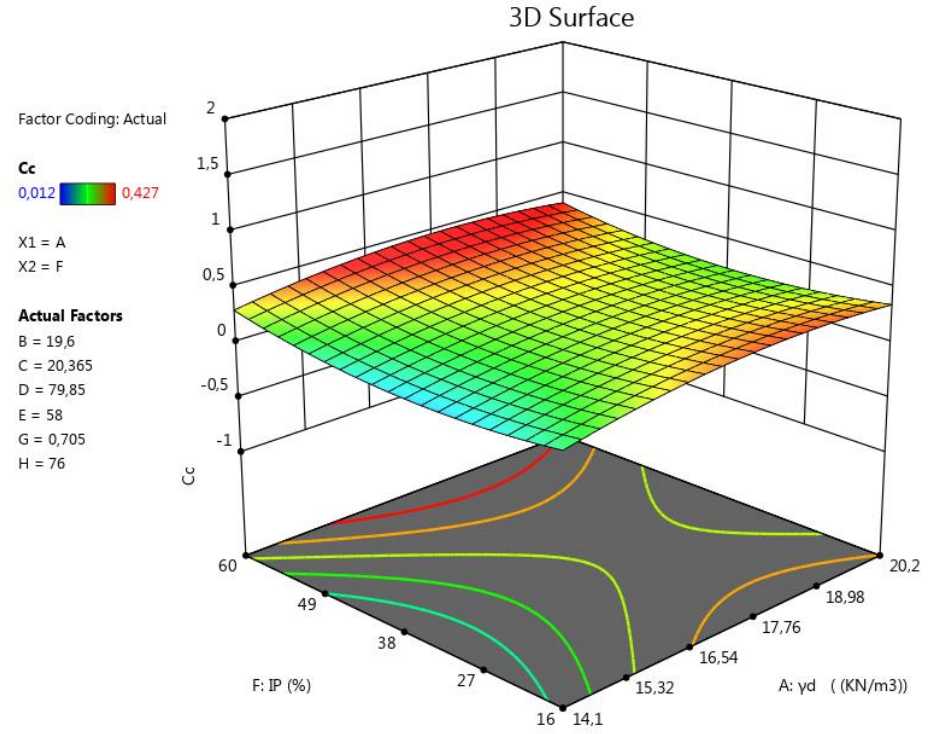

Figure IV.26: Response surface 3D representing the compressibility index (C_c) dependence on the dry unit weight γ_d (kN/m^3) and the plasticity index (I_P)

IV.6.10 Response surface methodology and optimization process

RSM is a group of mathematical and statistical techniques, often employed in engineering studies with regard to model problems, whose underlying structure is unknown and also optimize the desired output of these problems. The term Response Surface is employed to describe the surface that represents the output of a process when input parameter values vary within specified ranges. This method is of great importance specifically for machining problems, as it can be seen from the considerable amount of scientific works employing this method in the literature

Response Surface Methodology (RSM) is a collection of statistical and mathematical techniques useful for developing, improving, and optimizing processes **[207].**

The most extensive applications of RSM are in the particular situations where several input variables potentially influence some performance measure or quality characteristic of the process. Thus performance measure or quality characteristic is called the response, the input variables are sometimes called independent variables, and they are subject to the control of the scientist or engineer.

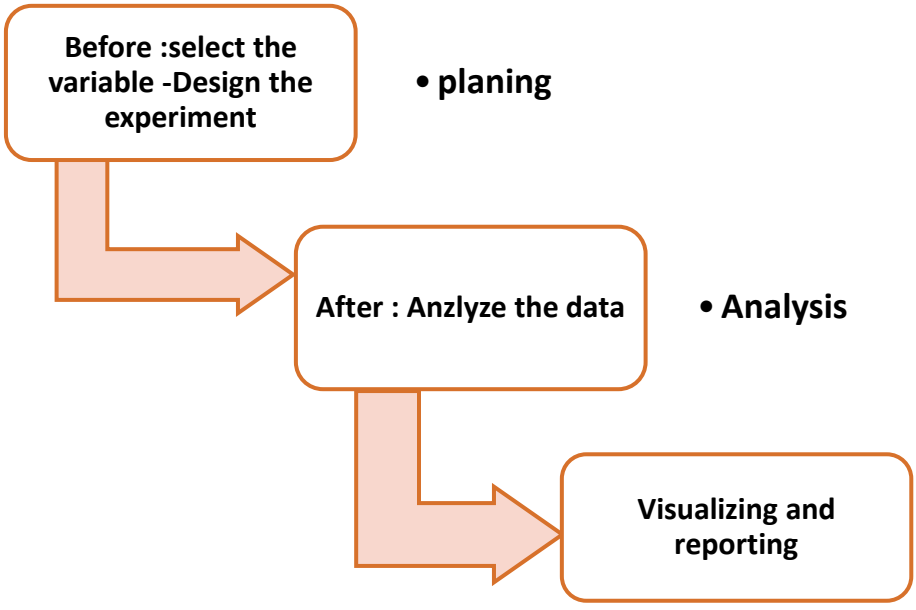

Figure IV.27: Steps in RSM study [207]

The field of response surface methodology consists of the experimental strategy for exploring the space of the process or independent variables, empirical statistical

modeling to develop an appropriate approximating relationship between the output response (Y) is the compressibility index (C_c), and the input variables (dry unit weight $\boldsymbol{\gamma_d}$ (**kN/m³**), wet unit weight $\boldsymbol{\gamma_h}$ (**kN/m³**) water content **w** (%), fine fraction $\mathbf{F_f}$**(%)**, Liquidity limits $\mathbf{W_L}$ **(%)**, plasticity index $\mathbf{I_p}$ **(%)**, void ratio $\mathbf{e_0}$, Saturation degree $\mathbf{S_r}$ (%)and optimization methods for finding the values of the process variables that produce desirable values of the response so the output can be written in the following form:

$$Cc = f(\gamma d.\gamma h.w.Ff.Wl.Ip.e0.Sr) \quad \text{(IV.5)}$$

Will identified the point on the quadratic response surface either it the minimum, maximum, of the surface, the critical values for the independent variables are the coordinates of the origin of the quadratic response surface.

Shown the predicted value of the dependent variable (response) at the critical values for each of the independent variables.

In most response surface designs, the problem is to find the optimum operating

conditions for a single response. However, in this case, the simplest method is a visual inspection, the surfaces can be investigated in order to find the design space that optimizes the entire response studies **[208, 210].**

The application of RSM to design optimization is aimed at reducing the cost of expensive analysis methods (e.g. finite element method or CFD analysis) and their associated numerical noise. because they reduce the effects of noise and they allow for the use of derivative-based algorithms.

For example, in this case, the optimization of the compressibility index (C_c) in terms of the different physicals parameters like dry unit weight $\boldsymbol{\gamma_d}$ (**kN/m³**), wet unit weight $\boldsymbol{\gamma_h}$ (**kN/m³**) water content **w** (%), fine fraction $\mathbf{F_f}$ (%), Liquidity limits $\mathbf{W_L}$ (%), plasticity index $\mathbf{I_p}$ (%), void ratio $\mathbf{e_0}$, Saturation degree $\mathbf{S_r}$ (%) **[25,].**

The program randomly picks a set of conditions from which to start its search for desirable results – your results may differ. Multiple cycles improve the odds of finding multiple local optimums, some of which are higher in desirability than others. Design-Expert then sorts the results from most desirable to least. Due to random starting conditions, your results are likely to be slightly different from those in the report above.

The ramp display combines individual graphs for easier interpretation. The colored dot on each ramp reflects the factor setting or response prediction for that solution, the height of the dot shows how desirable it is, view different solutions from

the Solutions drop-down menu on the factors tools; cycle through some of them and watch the dots. They may move only very slightly from one solution to the next.

The above optimal solution represents the formulation which best maximizes the compressibility coefficient and achieves a target value of 0.427, while at the same time finding the point with the minimum error transmitted to the responses. This should therefore represent process conditions that are robust to slight variations in factor parameters.

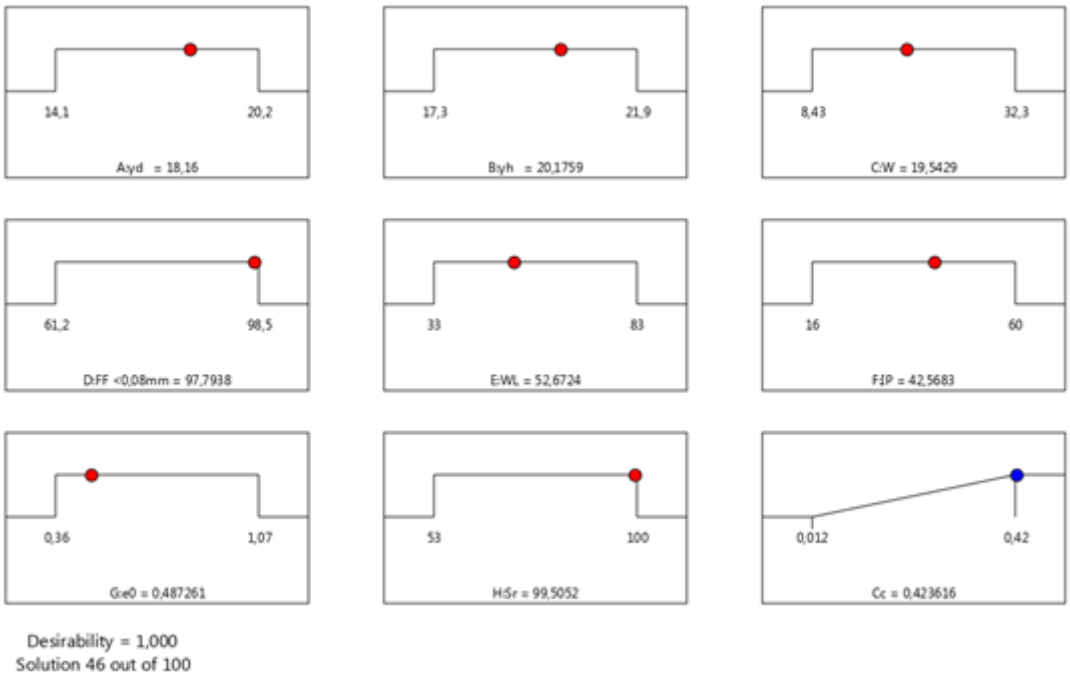

Figure IV.28: The maximization of the response

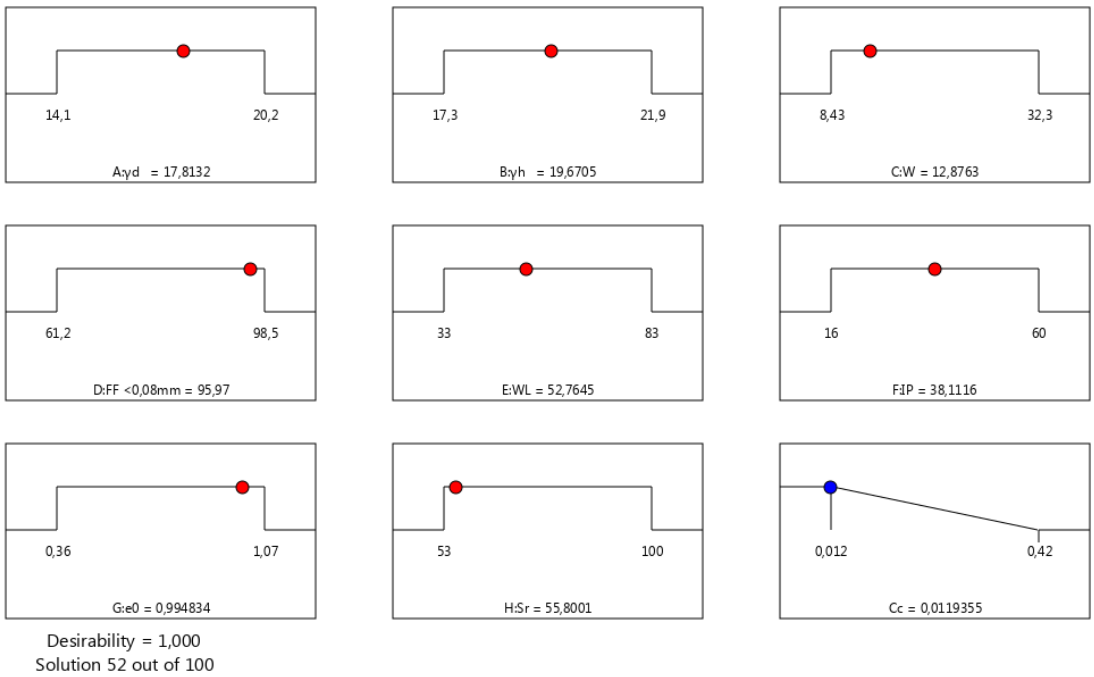

Figure IV.29: The minimization of the response

IV.6.11 Conclusion

Principal component analysis results using as input physical soil parameters show strong correlation on the first principal axes absorb about 75,04% of the total variance, the PCA allowed the grouping of the best correlated parameters as the first group composed of dry density, water content and the fines fraction with a high affection in the compressibility phenomenon, the second group constituted of soil indexes and pre-consolidation pressure with positive contribution.

PCA proved to be useful approaches to characterization of soils based on their properties, it helps to reveal some relationships between some soil parameters in the studied area, the results obtained from the use of the PCA tools were analyzed using the multiple regression analysis technique as it is known as a powerful and very practical method to predict and obtain possible correlation between geotechnical soil parameters.

The compression index parameter is taken as the output parameter and the different other variables proved from the PCA analysis that actually affect the output parameter were taken to be independent and correlated as input parameters; the multiple regression is established for developing empirical models to indicate reliable assessment of the compressibility of clayey soil, it indicates a best-fit correlation compared to all other empirical published model in literature with an R^2 of 0,87 in general, the model can be used for all soil conditions.

Combining the two considered tools PCA and multiple regression analysis the final obtained model allows to predict the compression index parameter from several physical and mechanical index, multiple regression analysis can validate the results and conclusions obtained from the application of PCA tool. This methodology to derive the model appear to be useful and powerful tool to estimate engineering properties of compressible soils and it can be applied to other investigation in different engineering parametric correlation problems.

Design of experiments (DOE) has been used in this work to the development and optimization of a processes. Typically for the present example case in geotechnical hazards is the optimization of the compressibility index (C_c) in terms of an important output parameter help engineers to calculate the settlement of fine grained soil, besides the methodology of DOE can provides different correlations of the input physical parameters, easily obtained from laboratory tests in order to found their effect on the response parameter.

Usually, an experimenter does not jump directly into an optimization problem; rather initial experimental screening designs are used in order to locate the most fruitful part of the experimental region in question. In our case the geotechnical parameters of the fine-grained soils compose the region of Tebessa basin has been collected from laboratory data base, then the statistically treated to obtain a complete matrix.

The present matrix which is based on the physical parameters dry unit weight $\boldsymbol{\gamma_d}$ (kN/m³), wet unit weight $\boldsymbol{\gamma_h}$ (kN/m³) water content w (%), fine fraction F_f (%), Liquidity limits W_L(%), plasticity index $\mathbf{I_p}$ (%), initial void ratio e_0, Saturation degree s_r (%) as input parameters and the response of the design is the compressibility index (C_c) parameter as the output parameter

So far, we find the main effects of the different factors on the compressibility of the clayey of Tebessa province. Fortunately, the present available general methods work satisfactorily in various situations when analyzing the problem. It uses a representative polynomial or regression model, by means of one or more methods under the DOE planning analysis and will depend of the user's goal, i.e. if users want a simple analysis, the statistical analysis using the ANOVA approaches can be the ideal method and for the present data base it gives an $R^2 = 0,91$ a very high correlation coefficient where the two factor interaction 2FI or quadratic suggested equation as detailed in this work.

The final step in the DOE is the optimization process used for the compressibility analysis is 'the response surface methodology 'RSM, which takes the (C_c) as the response factor and it concluded that is more influenced by $\boldsymbol{\gamma_h}$ ($\mathbf{kN/m^3}$), water content **w** (%), fine fraction $\mathbf{F_f}$ (%), plasticity index $\mathbf{I_p}$ (%), when the response is maximizing or minimize; at the same time all the contributed parameters are fixed (in range). the optimal values affecting the soil compressibility has been determined.

The process discussed in this research allows to find the best models that describe the studied soil compressibility compared to any other published models as well leads to coasts and time saving in predicting Cc output parameter.

Finally, the DOE is A popular and established technique for simultaneous determination of optimum settings of input variables that can determine optimum performance levels for one or more responses by Converting the estimated response model (Y) into individual desirability function (d) that are then aggregated into a composite function (D), This composite function is usually a geometric or an arithmetic, which will be maximized or minimized, respectively.

General conclusion

General conclusion

Compressibility of soil is known as the decrease in soil volume under compressive loads giving amount of settlement, the aim of the present work is to investigate the fine-grained soil compressibility that compose the major geological layers carrying the foundation's loads in Tebessa area (North-East of Algeria). Settlement of compressibility is depending on several parameters such as the nature of soil, geotechnical, physical, mechanical and mineralogical parameters. In this case study it has been collected a total 118 data sets from public earth works laboratory to analyze the compressibility of Tebessa soils. Many aspects of analysis and modeling has been presented in this master's memory, as first step it is used in the numerical modelisation plaxis and Sigma /w to estimate the settlement under the foundations and validate the different values of compressibility indices Cc and Cs obtained from the oedometer tests, it has been concluded that the results seems to be the same.

To help engineers in a rapid manner, to save coast and time, the main goal of this work is to generate an equation by indirect method to quantify the compression index Cc.

Consequently different statistical analysis methods have been suggested to study the compression index and geotechnical parameters correlations of the soil case study, the principal component analysis results using as input physical soil parameters show strong correlation on the first principal axes absorb about 75,13% of the total variance, the PCA allowed the grouping of the best correlated parameters as family of groups; the first one composed of dry and wet unit weight, the second group composed of water content, Atterberg limits and the fines fraction with a high contribution, the degree of saturation appears to be in single group and the fourth one is composed of compressibility index and initial void ration. PCA proved to be useful approaches to characterization of soils based on their properties, it helps to reveal some relationships between parameters in the studied area, the second method used in the present dissertation is the multiple regression analysis technique as it is known as a powerful and very practical method to predict and obtain possible correlation between geotechnical soil parameters.

The compression index parameter is taken as the output parameter and the different other variables proved from the PCA analysis that actually affect the output

parameter were taken to be independent and correlated as input parameters; the multiple regression is established for developing empirical models to
indicate reliable assessment of the compressibility of clayey soil, it indicates a best-fit correlation compared to all other empirical published model in literature with an R2 of 0.87.

Design of experiments (DOE) has been used in this work to the analysis, development and optimization of a processes. Typically for the present example case study in geotechnical hazards is the compressibility index (Cc) dependency and related to physical parameters of the fine-grained soil. Fortunately, the present available general methods work satisfactorily in various situations when analyzing the problem. It uses a representative polynomial or regression model, by means of one or more methods under the DOE planning analysis and depends of the user's goal, i.e. if users want a simple analysis, the statistical analysis using the ANOVA approaches can be the ideal method and for the present data base under the central composite design CCD method it gives an R2 = 0.91 a very high correlation coefficient where the suggested best fit model is two factor interaction 2FI or quadratic suggested equation as detailed in this work.

The final step in the DOE is the optimization process using the response surface methodology RSM which takes the compression index (Cc) as the response and the same eight physical parameters as input variables used in the mentioned proposed approaches, the obtained results allows to conclude that the compression index Cc is more influenced by **γh** (**kN/m3**), water content **w** (%), fine fraction Ff (%), plasticity index **Ip** (%), when the response is maximizing or minimize; at the same time all the contributed parameters are fixed (in range). the optimal values affecting the soil compressibility has been determined. The process discussed in this research allows to find the best models that describe the studied soil compressibility compared to any other published models as well leads to coasts and time saving in predicting Cc output parameter.

Bibliographic references

Bibliographic references

[1]: Faculty of Engineering – Cairo University Third Year Civil Soil Mechanics, Soil Compressibility & Settlement Spring 2015.

[2]: Dr. Mohammed Kadhum Fekheraldin, Foundation Engineering Lectures, University of Kufa\Civil Engineering Department \4th class 30 September 2019

[3]: Farzin Kalantary1 and Afshin Kordnaeij, Prediction of compression index using artificial neural network 6 June, 2012

[4]: Akayuli CFA, Ofosu B. Empirical model for estimating compression index from physical properties of weathered birimian phyllites. Electron J Geotech Eng. 2013; 18:6135–6144

[5]: V.Merrien-Soukatchoff, D. Amitrano, J. P. Piguet. Cours d'éléments de géotechnique, 2003-2004, Département Sciences de la Terre et Environnement. Ecole des mines de Nancy.

[6] : J.P. Mania, Déformabilité des sols tassements et consolidation, Technique de l'ingénieur, C214-2, 2000.

[7] : Robitaille V., Tremblay D., Mécanique des sols : théorie et pratique, Canada, Modulo éditeur, 1997.

[8] : L. Lagagna, A. A. Laimouche, Influence des tassements sur la stabilité des pacs de stockage énergétique. Mémoire de master, Université de Bejaïa, 2016, pages. 93

[9] : M. Cyr, Déformation des sols Cours de Mécaniques des sols I. Département de génie civil, INSA Toulouse.

[10] : V. Merrien-Soukatchoff, D. Amitrano, J. P. Piguet. Cours d'éléments de géotechnique, 2003-2004, Département Sciences de la Terre et Environnement. Ecole des mines de Nancy.

[11] : J.P. Mania, Déformabilité des sols tassements et consolidation, Technique de l'ingénieur, C214-2, 2000

[12]: Mohammed Kadum Fakhraldin , University Of Kufa | UOK · Department of Civil Engineering Asst. Prof. Dr. Civil Engineering septembre 2019

[13]: Moussa Amr Hussein ,Assr Mohamed, " Soil Mechanics "Consolidation of Soils 2017.

[14]: Marcel Dekker, Inc. 270 Madison Avenue, New York, New York 10016 compressibility and consolidation

[15]: Rendon-Herrero, O. (1980) "Universal Compression Index Equation" Jnl. Geot. Eng. Div, ASCE, Vol. 106, No. GT II pp 1179-1200.

[16]: Casagrande, A. (1936) "The Determination of the Pre-Consolidation Load and its Practical Significance" Proc. 1st Int. Conf. Soil Mechanics, 3, pp 60-64.

[17]: Das, B., M. (2014), " Principles of geotechnical Engineering " Eighth Edition, cengage Learning, ISBN-13: 978-0-495-41130-7.

[18]: Knappett, J. A. and Craig R. F. (2012), " Craig's Soil Mechanics" Eighth Edition, Spon Press, ISBN: 978-0-415-56125-9.

[19] : Chandra Bogireddy, Ganesh Sutar, Vasanwala. S. A Solanki. C. H, regional normalized empirical correlations for the compression index (Cc) OF SOIL – A CRITICAL OVERVIEW, India

[20]: Skempton A., W, Jones OT., Notes on the compressibility of clays. Quarterly Journal of the Geological Society. 1944 Jan 1;100(1-4):119-35.

[21]: Murayama, S., Akai, K., and Ueshita, K., Engineering properties of diluvial clays in Osaka. Soils and Foundations, 6(4):39–47, 1958.

[22]: Yamagutshi H.T., Characteristics of alluvial clay. Report of Kyushyu Agriculture Investigation Center of Japan. 1959;5(4):349-58.

[23]: Kyushu branch of JSSMFE, The ground around the Ariake sea, JSSMFE, Vol. 7, No. 4, pp. 31-36, 1959 (in Japanese).

[24]: Taniguchi H., Abe T.,and Goto M., Engineering properties of basement clay in ishikari peat layer, 5th Engineering Symposium of Hokkaido Development Bureau 1960 (In Japanese).

[25]: Cozzolino, V. M., Statistical forecasting of compression index. Proceedings of the fifth international conference on soil mechanics and foundation engineering, Paris. Vol. 1. 1961.

[26]: Taniguchi, H., Engineering properties of basement clay in rumoi harbor, Tsuch-to-Kisso, JSSMFE, No.49, 1962 pp. 19-27 (in Japanese).

[27]: Shouka H., Relationship of compression index and liquid limit of alluvial clay. In Proceedings of the 19th Japan Civil Engineering Conference. Touhoku 1964 May (pp. 30-31).

[28]: Terzaghi K and Peck RB, Soil mechanics in engineering practice, 2 ed., John Wiley and Sons, Inc., New York, 1967

[29]: Schofield A.N., and Wroth CP., Critical State Soil Mechanics. McGraw-Hill, London, UK.,1968.

[30]: Beverly, B. E., Consolidation Characteristics of Deep-Sea Sediments Recovered with a Giant Piston Corer: Blake-Bahama Outer Ridge Area, thesis presented to the Department of Civil Engineering, at Worchester Polytechnic Institute, in Worchester, Mass., in1975, in partial fulfillment of the requirements for the degree of Master of Science.

[31]: Azzouz, A. S., Krizek, R. J., & Corotis, R. B., Regression analysis of soil compressibility. Soils and Foundations, 16(2), 19-29, 1976.

[32]: Mayne, P.W., Cam-clay predictions of undrained strength. Journal of the Geotechnical Engineering Division, 1980, ASCE, 106(11): 1219–1242.

[33]: Burghignoli A, Scarpelli G., Properties of Italian clay soils. AGI Geotechnical Engineering in Italy. ISSMFE Golden Jubilee. 1985.

[34]: Bowles J., E., Physical and Geotechnical Properties of Soils. McGraw-Hill, New York, NY, USA. 1989.

[35]: Hirata S, Yao S, Nishida K., Multiple regression analysis between the mechanical and physical properties of cohesive soils. Soils and Foundations. 1990 Sep 15; 30(3):91-108.

[36]: Abdrabbo FM, Mahmoud MA., Correlations between index tests and compressibility of Egyptian clays. Soils and Foundations. 1990 Jun 15; 30(2):128-32.

[37]: Tsuchida T., A new concept of e-logp relationship for clays. In Proceedings of the 9th Asian regional conference on soil mechanics and foundation engineering, Bangkok, Thailand 1991 Dec (pp. 87-90).

[38]: Sridharan A, Nagaraj HB., Compressibility behaviour of remoulded, fine-grained soils and correlation with index properties. Canadian Geotechnical Journal. 2000 Jun 1;37(3):712-22.

[39]: Lav, M. A., and Ansal, A. M., Regression analysis of soil compressibility. Turkish Journal of Engineering and Environmental Sciences 25.2 (2001): 101-109.

[40]: Yoon GL, Kim BT, Jeon SS., Empirical correlations of compression index for marine clay from regression analysis. Canadian Geotechnical Journal. 2004 Dec 1;41 (6):1213-21.

[41]: Solanki, C. H., and J. A. Desai., Significance of Atterberg limits on compressibility parameters of alluvial deposits–new correlations. Proceedings of Indian Geotechnical Conference, Bangalore, India, p-20. Vol. 23, 2008.

[42]: Arpan Laskar and Sujit Kumar Pal, Geotechnical characteristics of two different soils and their mixture and relationship between parameters. Electronic Journal of Geotechnical Engineering. 2012;17: 2821-32.

[43]: Vinod, P., and Bindu. J., Compression index of highly plastic clays–an empirical correlation. Indian Geotechnical Journal 40.3 (2010): 174-180.

[44]: Park, H. I., and Lee, S. R., Evaluation of the compression index of soils using an artificial neural network. Computers and Geotechnics. 2011 Jun 30;38(4):472-81.

[45]: Widodo Slamet, and Abdelazim Ibrahim., Estimation of primary compression index (Cc) using physical properties of Pontianak soft clay. International Journal of Engineering Research and Applications (IJERA) 2.5 (2012): 2232-2236.

[46]: Nesamatha, R., and Dr Pd Arumairaj, Numerical Modeling for Prediction of Compression Index from Soil Index Properties. Electronic Journal of Geotechnical Engineering 20 (2015): 4369-34378.

[47]: Kumar R, Jain PK, Dwivedi P., Prediction of Compression Index (Cc) of Fine Grained Remolded Soils from Basic Soil Properties. International Journal of Applied Engineering Research. 2016;11(1):592-8.

[48]: Shiva Prashanth Kumar K. and Darga Kumar N., Evaluation of Coefficient of Consolidation in CH Soils. Jordan Journal of Civil Engineering. 2016, 10(4).

[49]: Nacci VA, Wang MC, Demars KR., Engineering behavior of calcareous soils. InProceedings of Civil Engineering in the Oceans III, ASCE Specialty Conference, Newark, Del 1975 Jun (pp. 9-12).

[50]: Wroth C P, Wood D M., The correlation of index properties with some basic engineering properties of soils. Canadian Geotechnical Journal. 1978 May 1;15(2):137-45.

[51]: Koppula, S. D., Statistical estimation of compression index. Geotechnical Testing Journal, GTJODJ, Vol.4, No.2, June 1981, pp.68-73.

[52]: Nakase A, Kamei T, Kusakabe O., Constitutive parameters estimated by plasticity index. Journal of Geotechnical Engineering. 1988 Jul;114(7):844-58.

[53]: Jain VK, Dixit M, Chitra R., Correlation of plasticity index and compression index of soil. International Journal of Innovations in Engineering and Technology (IJIET). 2015;5(3):263-70.

[54]: Peck RB, Reed WC., Engineering properties of Chicago subsoils. University of Illinois at Urbana Champaign, College of Engineering. Engineering Experiment Station.; 1954.

[55]: Nishida Y. A., brief note on compression index of soil. Journal of the Soil Mechanics and Foundations Division. 1956;82(3):1-4.

[56]: Hough BK., Basic Soils Engineering. The Ronald Press Company. New York pp.114-115, 1957. [41]

[57]: Osterberg, J. O, Personal Communication, 1972.

[58]: Azzouz, A. S., Krizek, R. J., & Corotis, R. B., Regression analysis of soil compressibility. Soils and Foundations, 16(2), 19-29, 1976.

[59]: Herrero Oswald Rendon., Universal compression index equation. Journal of Geotechnical and Geoenvironmental Engineering 106.ASCE 15829 (1980).

[60]: Serajuddin M. Universal compression index equation and Bangladesh soils. In Proceedings of the Ninth Southeast Asian Geotechnical Conference 1987 (pp. 61-72).

[61]: Kalantary Farzin, and Afshin Kordnaeij., Prediction of compression index using artificial neural network. Scientific Research and Essays 7.31 (2012): 2835-2848.

[62]: Widodo Slamet, and Abdelazim Ibrahim., Estimation of primary compression index (Cc) using physical properties of Pontianak soft clay. International Journal of Engineering Research and Applications (IJERA) 2.5 (2012): 2232-2236.

[63]: Sari PT, Firmansyah YK., The Empirical Correlation Using Linear Regression of Compression Index for Surabaya Soft Soil ASEM13 Sept.8-12, Korea 2013.

[64]: Bryan A. McCabe, Brian B. Sheil, Michael M. Long, Fintan J. Buggy, Eric R. Farrell, Empirical correlations for the compression index of Irish soft soils. Proceedings of ICE Geotechnical Engineering, Volume 167 Issue GE6, Pages 510–517 http://dx.doi.org/10.1680/geng.13.00116.

[65]: Nagaraj, T.S., and Srinivasa Murthy B.R., A critical reappraisal of compression index equations, Geotechnique, 36(1), 27-32, 1986.

[66]: Burland JB., On the compressibility and shear strength of natural clays. Géotechnique. 1990 Sep;40(3):329-78.

[67]: Nagaraj, T.S., and Srinivasa Murthy B.R., A critical reappraisal of compression index equations, Geotechnique, 36(1), 27-32, 1986.

[68]: Al-Khafaji AW, Andersland OB., Equations for compression index approximation.
Journal of geotechnical engineering. 1992 Jan;118(1):148-53.

[69]: Kosasih., A., Mochtar.,I.B., Pengaruh Kadar Air, Angka Pori, dan Batas Cair Tanah Lempung Terhadap Indeks Pemampatan Konsolidasi Cc dan Indeks Pengembangan Cs., Master Thesis, Program Pasca Sarjana, teknik Sipil ITS 1997.

[70]: Amardeep Singh, and Shahid Noor, Soil compression index prediction model for fine grained soils." Int. J. Innov. Eng. Technol. (IJIET) 1.4 (2012): 34-37.

[72]: Kalantary Farzin, and Afshin Kordnaeij., Prediction of compression index using artificial neural network. Scientific Research and Essays 7.31 (2012): 2835-2848.

[72]: Moran P., Mueser and Rutledge., Study of Deep Soil Stabilization by Vertical Sand Drains. Bureau of Yards and Docks, Department of the Navy, New York, NY, USA, 1958 contract No. NOY-88812.

[73]: Al-Jabban M.J.W.,Estimation of standard penetration test (SPT) of Hilla City-Iraq by using GPS coordination, Jordan Journal of Civil Engineering (JJCE), 2013, 7 (2), p. 133-145.

[74]: Salahudeen A.B., Sadeeq J.A., Evaluation of bearing capacity and settlement of foundations, Leonardo Electronic Journal of Practices and Technologies (LEJPT), 2016, 29, p. 93-114.

[75]: Tomlinson, M.J. and Boorman, R., 1995, Foundation Design and Construction, Longman Scientific and Technical, Brunthill, Harlow, England.

[76]: Akayuli CFA, Ofosu B. Empirical model for estimating compression index from physical properties of weathered birimian phyllites. Electron J Geotech Eng. 2013;18:6135–6144

[77]: Asadullah Khan Ghalib, type of foundation civil engineering, Apr 20, 2019

[78] Bowles , J.,E.,(1996) "Foundation Analysis and Design" -5th ed. McGraw-Hill, ISBN 0-07-912247-7.

[79]: Md. Rasel Sheikh, foundation of structure, fundamentals of infrastructure design and construction

[80]: Dr. Adnan A. Basma Foundation Engineering 1 / Chapter 1 Foundations: Types and Considerations

[81]: Das, B., M. (2012), "Principles of Foundation Engineering" Eighth Edition, CENGAGE Learning, ISBN-13: 978-1-305-08155-0.

[82]: floor Dr Mohamad Syazli Fathi Department of Civil Engineering UTM RAZAK School of Engineering & Advanced Technology UTM International Campus 2012

[83]: Poulos, H.G. (1999). Analysis and Design of Pile Foundations. Handouts from the Foundation Course – Univ. of Sydney

[84]: Schmertmann, J.H., 1991. discussion of "Settlement of Shallow Foundations on Granular Soils." Journal of Geotechnical Engineering, ASCE, Vol117, No. GTI, pp. 179-181.

[85]: Jeyepalan, J.K. and Boehm, R., 1986. "Procedures for Predicting Settlement in Sands." Settlement of Shallow Foundations on Cohesionless Soils: Design and Performance, ASCE, pp. 1-22.

[86]: Papadopoulos, B.P., 1992. "Settlement of Shallow Foundations on Cohesion!ess Soils." Journal of Geotechnical Engineering, ASCE, Vol. 118, No.3, pp. 377-393.

[87] : Morgan, J. R. & Poulos, H. G. (1968). Stability and settlement of deep foundations. In Soil mechanics selected topics (ed. I. K. Lee), pp. 528±609. New York: Elsevier

[88]: Poulos, H. G. (1968). Analysis of settlement of pile groups. GeÂotechnique 18, No. 3, 449±471

[89]: C. Wroth, D. Wood, The correlation of index properties with some basic engineering properties of soils, Canadian Geotechnical Journal, 15(2) (1978) 137-145.

[90]: S. Onyejekwe, X. Kang, L. Ge, Assessment of empirical equations for the compression index of fine-grained soils in Missouri, Bulletin of Engineering Geology and the Environment, 74(3) (2015) 705-716.

[91]: Gilboy, G. Soil Mechanics Research. Proc. ASCE, Vol. 57, No. 8, 1931, p. 1165

[92]: McCarthy, D. F., Jr., and Leonard, R. J. Compaction and Compression Characteristics of Micaceous Fine Sands and Silts. Highway Research Record 22, 1963, pp. 23-37

[93]: Wu, T. H. Relative Density and Shear Strength of Sands. Jour. Soil Mech. and Found. Div., Proc. ASCE, Vol. 83, No. SMl, Paper 1161, 195793. Paris, Vol. 1, 1961, pp. 527-532

[94]: L. J. LANGFELDER and V. R. NIVARGIKAR, Some Factors Influencing Shear Strength and Compressibility of Compacted Soils, Department of Civil Engineering, North Carolina State University, Raleigh

[95]: Jennings, J.E. B., and Burland, J.B. Limitation to the Use of Effective Stresses in Partly Saturated Soils. Geotechnique, Vol. 12, 1962, pp. 125-144

[96] :M.Dysli,recherche bibliographique et synthèse descorrélations entre les caractéristiques des sols département fédéral de l'environnement, des transports, de l'énergie et de la

[97]: Barden. (1965) consolidation of clay with nonlinear viscosity, Geotechnics 15,No,4

[98]: Dr. Roy E. Olson STRESS DISTRIBUTION Department of Construction Engineering Advanced Soil Mechanics Chaoyang University of Technology on Spring 1989

[99]: Das, B., M. (2014), " Principles of geotechnical Engineering " Eighth Edition, CENGAGE Learning, ISBN-13: 978-0-495-41130-7.

[100]: Knappett, J. A. and Craig R. F. (2012), " Craig's Soil Mechanics" Eighth Edition, Spon Press, ISBN: 978-0-415-56125-9

[101]: 4.Teferra, A. & Mesfin, L., Soil Mechanics, AAU

[102]: Dr. Abdulmannan Orabi. Stress Distribution in Soil CIVIL ENGINEERING AND ENVIRONMENTAL DEPARTMENT303322 - Soil Mechanics

[103]: Budhu M. (2000), Soil Mechanics and Foundations, Wiley and Sons.

[104]: Lambe, T. W., Whitman, R. V. (1999), Soil Mechanics, John Wiley & Sons Inc.

[105]: Widisinghe, S., and Sivakugan, N. (2014b). "Vertical stresses within gran-ular materials in containments."Int. J. Geotech. Eng., 8(4), 431–435.© ASCE

[105]: Ahlvin, R. G., and Ulery, H. H. 1962. Tabulated values for determining the complete pattern of stresses, strains, and deflections beneath a uniform circular load on a homogeneous half space. Highway Res. Board Bull. 342.

[106]: Barksdale, R., and Harr, M. E. 1966. An influence chart for vertical stress increase due to horizontal shear loadings. Highway Res. Board Rec. 108.

[107]: Egorov, K. E. 1940. Distribution of stresses in base under rigid strip footing. Mauchn. Issled, Stantsiya Fundamentstroya, no. 9.

[108]: Dr. Suhad Dawood Salman Mechanical Engineering Department Faculty of Engineering, Mustansiriyah University, Baghdad, Iraq

[109]: Leonards, G.A. and Girault, P. (1961). A Study of the One-Dimensional Consolidation Test, Proc. Fifth Int. Conf. on Soil Mechanics and Found. Eng., Paris, Vol. 1, 116-130.

[110]: Sandbækken, G., T. Berre and S. Lacasse (1986): Oedometer testing at the Norwegian Geotechnical Institute. Consolidation of soils: testing and evaluation: a symposium. ASTM, Special Technical Publication, 892, pp. 329-353.

[111]: Amar, S., and Jézéquel, J. "Pressuremeter test. Test method project." LCP. No. 15. (1985).

[112]: Combarieu, O. Bearing capacity of superficial foundations Pressuremeter and laboratory tests. Bulletin des laboratoires des ponts et chaussées - 211 - ref. 4134 - pp. 53-72. (1997)

[113]: Shad M. Sargand ,Teruhisa Masada, Evaluation of Cone Penetration Test-Based Settlement Prediction Methods for Shallow Foundations on Cohesionless Soils at Highway Bridge Construction Sites ,Ohio University

[114]: Robertson, P.K., 1991. "Estimation of Foundation Settlements in Sand from CPT." Geotechnical Engineering Congress, ASCE, Vol2, pp. 764-775

[115]: Skempton, A.W., 1986. "Standard Penetration Test Procedures and the Effects in Sands of Overburden Pressure, Relative Density, Particle Size, Ageing and Overconsolidation." Geotechnique, Vol. 36, No.3, pp. 425-447.

[116]: Schmertmann, J.H., 1986a. "Dilatometer to Compute Foundation Settlement." Use of Insitu Tests in Geotechnical Engineering, ASCE, pp. 303-321.

[117]: Parry, R.H.G., 1978. "Estimating Foundation Settlements in Sand from Plate Bearing Tests." Geotechnique, Vol. 28, No. I, pp. 107-118.

[118]: Dynamic Cone Probing Tests in Gravelly Soils." Proceedings of the 2nd European Symposium on Penetration Testing, Vol. I, pp. 337-344

[119]: AASHTO (1981). AASHTO T 222 – 94, Standard Method of Test for Non-Repetitive Static Plate Load Test of Soils and Flexible Pavement Components, for Use in Evaluation and Design of Airport and Highway Pavements, American Association of State Highways and Transport Officials

[120]: Salgado, R.; and Yoon, S. (2003). Dynamic Cone Penetration Test(DCPT) for Subgrade Assessment. FHWA/IN/JTRP-2002/30, Purdue University, West Lafayette, IN

[121] : Bendjeddou, A., Etude des glissements routiers Au Nord Est de l'Algérie. 2015, Université Mohamed Khider-Biskra. p. 68-69

[122]: Chan, D. H.-K., 1986. Finite Element Analysis of Strain Softening Material. Ph.D. Thesis, Civil Engineering Department, University of Alberta, Edmonton, Alberta, Canada.

[123] : Blés J. L. 1969 Contribution à l'étude des déformations cassantes de la feuille Morsott (SE Constantinois–Algérie). Les microfracturations et leurs relations avec les failles et les plis. Publications du Service Géologique de l'Algérie, (Série N° 11), Bulletin N° 39, pp. 7-17.

[124] : Aoudjehane M., Bouzenoune A, Rouvier H. et Thibiéroz J. (1992): Halocinèse et dispositifs d'extrusions du Trias dans l'Atlas saharien oriental (NE algérien). Gèol. Médit., Marseille, XIX, 273-287.

[125] : Dubourdieu G. 1956. Etude géologique de la région de l'Ouenza (Confis Algéro-tunnisie). Thèse. Sc. Paris Publ, serv. Cart géol, Algérie Beelt.№ 21.pp65.

[126] : Dubourdieu G. 1949. Carte géologique au 1/50 000, feuille de Djebel ouenza, № 125notice explicative, Pub. Serv. Carte géol, Algérie.

[127]: Al-Rawas, A. & Qamaruffin, M. (1998) Construction Problems of Engineering Structures Founded on Expansive Soils and Rocks in Northern Oman. *Building and Environment* . 33 **(**2-3), 159-171

[128] : Blés J. L. et Fleury 1970 Carte géologique1/50 000 Morsott et notice explicative. Publ. Serv. Geol. Algérie.

[129] : Djabri,L 1987 Contribution à l'étude hydrogéologique de la nappe alluviale de la plaine d'effondrement de Tébessa-Essai de modélisation. Thèse de Doc.Ing.Univ.Sci.Tech. de Franche-Comté, Besançon, 170p.

[130] : Smail B, Nouiri Z. (2015) Etude de la vulnérabilité a la pollution de la nappe de Tébessa par la méthode DRASTIC Mémoire de Master académique en Hydrogéologie, université de Tébessa.

[131] : Kowalski, W.M., Boudoukha A., Hemila M.L., Pharisat A.1997. Les stades d'éffondrement du graben de Tébessa (confines Algéro-Tunisiens) et la tectonique plicative Plio-Quaternaire. Pub. Soc.Hist.Nat.Montbéliard. PP 201-215.

[132]: Robert Reris and J. Paul Brooks Principal Component Analysis and Optimization: A Tutorial Virginia, January 11–13, 2015

[133]: Eric Xing Principal Components Analysis Machine Learning Lecture 24, April 16, 2008

[134]: I.T. Jolliffe, Prinicipal Component Analysis, 2nd Edition, Springer series in statistics 2002, page 1-3.

[135]: Lindsay I Smith, A tutorial on Principal Components Analysis, February 26, 2002, page 2-8

[136]: Jacobsson, Martin. "Forecasting commodity futures using Principal Component Analysis and Copula." (2015)

[137]: Face Recognition using Wavelet, PCA, and Neural Networks, Proceeding of the First International Conference on Modeling, Simulation and Applied Optimization, Sharjah, U.A.E. February 1-3, 2005

[138]: Novakovic, Jasmina, and Sinisa Rankov. "Classification Performance Using Principal Component Analysis and Different Value of the Ratio R." International Journal of Computers Communications & Control 6.2 (2011): 317-327.

[139]: Kiranjeet Kaur, Lalit Mann Singh. Heart Disease Prediction System Using PCA and SVM Classification, International Journal of Advance Research, Ideas and Innovations in Technology, www.ijariit.com

[140]: Smith, Lindsay I. "A tutorial on principal components analysis." Cornell University, USA 51 (2002): 52.

[141]: CHEN Bo, Ma Wu, "Research of Intrusion Detection based on Principal Components Analysis", Information Engineering Institute, Dalian University, China, Second International Conference on Information and Computing Science, 2009.

[142]: Varghese, Nebu, et al. "A survey of dimensionality reduction and classification methods.", International Journal of Computer Science and Engineering Survey (IJCSES) 3.3 (2012): 45.

[143]: George, Annie. "Anomaly detection based on machine learning: dimensionality reduction using PCA and classification using SVM." International Journal of Computer Applications 47.21 (2012).

[144]: HUANG, L., NGUYEN, X. L., GAROFALAKIS, M., JORDAN, M., JOSEPH, A.D., AND TAFT, N. In-network PCA and anomaly detection. In NIPS (2006)

[145]: Daniela Brauckho_, Kav_e Salamatian, Martin May. Applying PCA for Tra_c Anomaly Detection: Problems and Solutions. Proceeding of IEEE INFOCOM 2009,, Apr 2009, Rio de Janeiro,Brazil. pp.2866-2870, 2009.

[146]: P. Rameswara Anand,, Tulasi Krishna Kumar.K ,"PCA Based Anomaly Detection", International Journal of Research in Advent Technology, Vol.2, No.2, February 2014 E-ISSN: 2321-9637

[147]: K. S. Sodhi and M. Lal, "Face Recognition Using PCA, LDA and Various Distance Classifier," Journal of Global Research in Computer Science, Vol. 4, 2013, pp. 30-35.

[148]: P. J. Phillips, P. J. Flynn, T. Scruggs, K. W. Bowyer, J. Chang, K. Hoffman, J. Marques, J. Min and W. Worek, "Overview of the Face Recognition Grand Challenge," in Computer vision and pattern recognition, 2005. CVPR 2005. IEEE Computer Society Conference on, 2005, pp. 947-954.

[149]: D. Srinivasulu Asadi, Ch. DV Subba Rao and V. Saikrishna "A Comparative Study of Face Recognition with Principal Component Analysis and Cross-Correlation Technique," International Journal of Computer Applications Vol. 10, 2010

[150]: C. Li, Y. Diao, H. Ma and Y. Li, "A Statistical PCA Method for Face Recognition," in Intelligent Information Technology Application, 2008, pp. 376-380

[151] : Berrah, Y., Boumezbeur, A., Kherici, N., & Charef, N. (2018). Application of dimensional analysis and regression tools to estimate swell pressure of expansive soil in Tebessa (Algeria). Bulletin of Engineering Geology and the Environment, 77(3), 1155-1165.and regression tools to estimate swell pressure of expansive soil in Tebessa (Algeria). Bull. Eng. Geol. Environ. (2016)

[152]: (Barron, R. A. (1948). Consolidation of Fine-Grained Soils by Drain Wells by Drain Wells. Transactions of the American Society of Civil Engineers, 113(1), 718-742. Sivakugan, N., & Ameratunga, J. (2021). Basic soil mechanics. In Soft Clay Engineering and Ground Improvement (pp. 31-48). CRC Press..

[153]: MolaAbasi H, Shooshpasha I, Ebrahimi A. Prediction of Compression Index of Saturated Clays (Cc) Using polynomial models. Sci Iran 2016;23:500–7. doi:10.24200/sci.2016.2134

[154]: Gil Lim Yoon and Byung Tak Kim Regression Analysis of Compression Index for Kwangyang Marine Clay2006

[155]: Yasser Soltanpour and Hosam Salman 2019, Bayesian Probabilistic Approach to Assess the Compression and Recompression Indices of Over-Consolidated Expansive Clays March 2019

[156]: Lubos Boruvka andOldřich and Jan Jehlička, Principal component analysis as a tool to indicate the origin of potentially toxic elements in soils2005

[157]: Joliffe IT, Cadima J., Principal component analysis: a review and recent developments Jan 2016

[158]: SousaF.G.Martins, Multiple linear regression and artificial neural networks based on principal components to predict ozone concentrations Jan 2007

[159]: Esraa A. Mandhour, Prediction of Compression Index of the Soil of Al-Nasiriya City Using Simple Linear Regression Model 2020

[160]: Philipponnat, g, measurement of soil compressibility by means of an accelerated oedometer test1977

[161]: Laurence Wesley and Michael Pender, Soil stiffness measured in oedometer tests2008

[162]: XP P 94-090, French association for standardization, oedometric test

[163] r. David hammer, john w. Philpot, jon m. Maatta), applying principal component analysis to soil-landscape research-quantifying the subjective 1990

[164]: (Deeman Yousif Mahmood), Principal Component Analysis (PCA) MARCH 2018

[165]: Tadikonda Venkata Bharat1; Dhanesh Sing Das2; and Rakesh Kumar Sahu, Prediction of Compressibility Behavior of Clayey Soils of Different Plasticity for Containment Applications at Large Consolidation Pressures2019

[166]: ALTSCHAEFFL, A. G., the compressibility and sensitivity of an artificially sedimented clay soil: the grande-baleine marine clay, QUÉBEC, CANADA1960

[167]: DOUGLAS C. MONTGOMERY, ELIZABETH A. PECK, G. GEOFFREY VINING, INTRODUCTION TO LINEAR REGRESSION ANALYSIS 2012

[168]: Xin Yan, Xiao Gang Su), Linear Regression Analysis Theory and Computing2009

[169]: (Montgomery D C), Design and Analysis of Experiments2013

[170]: S. S. Garud, I. A. Karimi and M. Kraft, "Design of computer experiments: A review," Computers & Chemical Engineering, vol. 106, no. November, pp. 71-95, 2017.

[171]: J. K. Telford, "A Brief Introduction to Design of Experiments," Johns Hopkins APL Technical Digest, vol. 27, no. 3, pp. 224-232, 2007.

[172]:B. Durakovic, H. Bašić and H. Muhič, "The Interrelationships between quality managment practicies and their effects on innovation," in Trends in the Development of Machinery and Associated Technology, Budapest, 2014.

[173]:H. Guo and A. Mettas, "Design of Experiments and Data Analysis," in 2012 Annual Reliability and Maintainability Symposium

[174]: Bjerrum, L. (1973). Geotechnical problems involved in foundations of structures in the North Sea. Geotechnique, 23(3), 319-358.

[175]: Bowles JE (1979) Consolidation and consolidation settlements (Chap 11, Sect 11.8,). In: Physical and geotechnical properties of soils, 2nd edn, McGRAW-Hill, New York.

[176]: Carter, M., & Bentley, S. P. (1991). Correlations of soil properties. Pentech press publishers.

[177]: Dysli, M. Boccard, T., Escher, P.,. (1995). GEOBA: database of soil properties and probe logs. In International Journal of Rock Mechanics and Mining Sciences and Geomechanics Abstracts (Vol. 6, No. 32, p. 274A).

[178]: Widodo, S., & Ibrahim, A. (2012). Estimation of primary compression index (Cc) using physical properties of Pontianak soft clay. International Journal of Engineering Research and Applications, 2(5), 2231-2235.

[179]: Burland, J. B. (1990). On the compressibility and shear strength of natural clays. Géotechnique, 40(3), 329-378.

[180]: Terzaghi, K., Peck, R. B., & Mesri, G. (1996). Soil mechanics in engineering practice. John Wiley & Sons. SB

[181]: Shen, S. L., Wu, H. N., Cui, Y. J., & Yin, Z. Y. (2014). Long-term settlement behaviour of metro tunnels in the soft deposits of Shanghai. Tunnelling and Underground Space Technology, 40, 309-323.

[182]: Budhu, M. (2015). Soil mechanics fundamentals. John Wiley & Sons.

[183]: Das, R., Singh, P. K., Kainthola, A., Panthee, S., & Singh, T. N. (2017). Numerical analysis of surface subsidence in asymmetric parallel highway tunnels. Journal of Rock Mechanics and Geotechnical Engineering, 9(1), 170-179.

[184]: Yin, J. H., & Feng, W. Q. (2017). A new simplified method and its verification for calculation of consolidation settlement of a clayey soil with creep. Canadian Geotechnical Journal, 54(3), 333-347.

[185] : Yang, Q., Tang, Y., Yuan, B., & Zhou, J. (2019). Cyclic stress–strain behaviour of soft clay under traffic loading through hollow cylinder apparatus: effect of loading frequency. Road Materials and Pavement Design, 20(5), 1026-1058.

[186]: Kumar, R. & Chandrawanshi, S., (2021, April). Settlement Behaviour of Very Soft Soil Reinforced with Stone Columns. In Proceedings of the Indian Geotechnical Conference 2019: IGC-2019 Volume III (Vol. 136, p. 345). Springer Nature.

[187]: Ying-chun, Z., & Kang-he, X. (2005). Study on one-dimensional consolidation of soil under cyclic loading and with varied compressibility. journal of zhejiang university-science a, 6(2), 141-147.

[188]: Lav, M. A., & Ansal, A. M. (2001). Regression analysis of soil compressibility. Turkish Journal of Engineering and Environmental Sciences, 25(2), 101-109. [58]

[189]: Benbouras, M. A., Kettab Mitiche, R., Zedira, H., Petrisor, A. I., Mezouar, N., & Debiche, F. (2019). A new approach to predict the compression index using artificial intelligence methods. *Marine Georesources & Geotechnology*, *37*(6), 704-720. [51]

[190]: Park, T. S & Chang, D. M. (2011). A Study on the Planning of the Settlement Environment considering Survey in the Periphery of Local Industrial Park in Hongseong, Chungnam. Journal of the Korea Academia-Industrial Cooperation Society, 12(4), 1968-1975.

[191]: Ozer, M., Isik, N. S., & Orhan, M. (2008). Statistical and neural network assessment of the compression index of clay-bearing soils. Bulletin of Engineering Geology and the Environment, 67(4), 537-545.

[192]: Nath, A., & DeDalal, S. S. (2004). The role of plasticity index in predicting compression behavior of clays. Electronic Journal of Geotechnical Engineering.

[193]: Spagnoli, G., & Shimobe, S. (2020). Statistical analysis of some correlations between compression index and Atterberg limits. Environmental Earth Sciences, 79(24), 1-15. [65]

[194]: Tiwari, B., & Ajmera, B. (2012). New correlation equations for compression index of remolded clays. Journal of Geotechnical and Geoenvironmental Engineering, 138(6), 757-762.

[195]: Mohammadzadeh, D., Bazaz, J. B., & Alavi, A. H. (2014). An evolutionary computational approach for formulation of compression index of fine-grained soils. Engineering Applications of Artificial Intelligence, 33, 58-68.

[196]: Onyejekwe, S., Kang, X., & Ge, L. (2015). Assessment of empirical equations for the compression index of fine-grained soils in Missouri. Bulletin of Engineering Geology and the Environment, 74(3), 705-716.

[197]: Mohammadzadeh S, D., Kazemi, S. F., Mosavi, A., Nasseralshariati, E., & Tah, J. H. (2019). Prediction of compression index of fine-grained soils using a gene expression programming model. Infrastructures, 4(2), 26.

[198]: Zhang, P., Yin, Z. Y., Jin, Y. F., Chan, T. H., & Gao, F. P. (2021). Intelligent modelling of clay compressibility using hybrid meta-heuristic and machine learning algorithms. Geoscience Frontiers, 12(1), 441-452.

[199] : (Berrah, Y., Brahmi, S., Charef, N., & Boumezbeur, A. (2021). Swelling Clay Parameters Investigation Using Design of Experiments (A Case Study). Engineering Geology, 93.

[200]: McCabe BA, Sheil BB, Long MM, Buggy FJ, Farrell ER(2014) Empirical correlations for the compression index of Irish soft soils. Proc Inst Civ Eng Geotech Eng167(6):510–517

[201]: Mohammadzadeh S, D., Kazemi, S. F., Mosavi, A., Nasseralshariati, E., & Tah, J. H. (2019). Prediction of compression index of fine-grained soils using a gene expression programming model. *Infrastructures*, *4*(2), 26.

[202]: Jain VK, Dixit M, Chitra R (2015) Correlation of plasticity index and compression index of soil. Int J Innov Eng Technol 5(3):263–270

[203]: Myers, R., Khuri, A., & Carter, W. (1989). Response Surface Methodology: 1966-1988. Technometrics, 31(2), 137-157. doi:10.2307/1268813

[204]: Myers Raymond H. & D.C. Montgomery, 2002. "Response Surface Methodology: process and product optimization using designed experiment," A Wiley-Interscience Publication

[205]: Eskisar, T. (2021). Empirical Compressibility Index Equations for Artificial Remolded Clay Mixtures. Arabian Journal for Science and Engineering, 1-14.

[206]: Joshi., S., H.D. Sherali and J.D. Tew, 1998, "An Enhanced Response Surface Methodology

[207]: Sen, R. and Swaminathan, T. (1997). "Application of response-surface methodology to evaluate the optimum environmental conditions for the enhanced production surfactin." Applied Microbiology and Biotechnology, Vol. 47, No. 4, pp. 358-363.

[208]: Taguchi, G., 1987. "System of Experimental Design: Engineering Methods to Optimize Quality and Minimize Cost," UNIPUB/Kraus International, White Plains, NY.

[209]: Box, G. E. P. and N.R. Draper, 1987. "Empirical Model-Building and Response Surfaces," Jon Wiley & Sons, New York.

[210]: Khuri, A.I. and J.A. Cornell, 1996. "Response Surfaces," 2nd edition, Marcel Dekker. New York.